

AD 721688

Redesignated ALOS  
Tech Report 241,  
Vol II

(Oct. 1970)

~~AWSSR 105-413~~  
~~VOLUME II~~

AIR WEATHER SERVICE MANUAL

WEATHER

# THE PRACTICAL ASPECT OF TROPICAL METEOROLOGY

VOL. II. Notes on the  
Tropical Pacific and Southeast Asia



~~DDC  
RECEIVED  
JAN 25 1961  
RECEIVED  
A~~

26 JANUARY 1961

NATIONAL TECHNICAL  
INFORMATION SERVICE

UNITED STATES AIR FORCE

**Best  
Available  
Copy**

AWSM 105-48  
VOLUME II

AWS MANUAL  
NO. 105-48  
VOLUME II

Headquarters  
AIR WEATHER SERVICE (MATS)  
Scott Air Force Base, Illinois  
26 January 1961

FOREWORD

1. Designation. The attached copy of Air Force Surveys in Geophysics, No. 126, June 1960, entitled "Notes on the Meteorology of the Tropical Pacific and Southeast Asia," is hereby designated as AWSM 105-48, Volume II.

2. Purpose and Scope. This volume provides AWS personnel with information and guidance on certain phases of the descriptive meteorology and synoptic climatology of the tropical Pacific and southeast Asia, including sections on tropical cloud physics, local effects, and weather reconnaissance. As such, it supplements the material covered in Volume I. This volume is applicable to all AWS forecasting activities.

FOR THE COMMANDER:

JOHN C. HATTOX  
Lieutenant Colonel  
Director of Administrative Services



DISTRIBUTION: X  
Hq MATS . . . . . 3  
Hq AWS. . . . . 30  
Wings and Groups. . . . . 5  
Squadrons . . . . . 2  
Forecasting Detachments . . . . . 1  
Special . . . . . 176

OPT: AWSSS

AFCRC-TN-60-455

Air force surveys in geophysics

No. 126

Notes on the meteorology of the  
tropical pacific and southeast asia

Edited by  
C.S. Ramage

June 1960

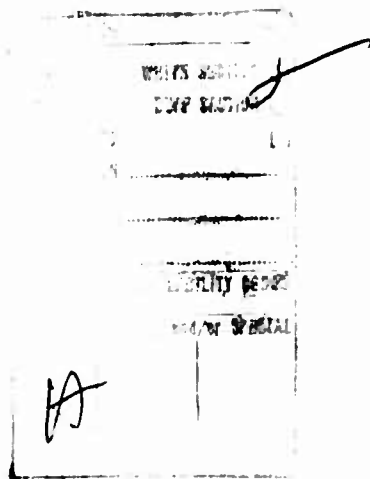


GRD

GEOPHYSICS RESEARCH DIRECTORATE  
AIR FORCE CAMBRIDGE RESEARCH CENTER  
AIR RESEARCH AND DEVELOPMENT COMMAND  
UNITED STATES AIR FORCE  
BEDFORD, MASSACHUSETTS

184

*The Air Force Surveys in Geophysics* is a publication series of the Geophysics Research Directorate, Air Force Cambridge Research Center, Air Research and Development Command. The sole purpose of this series is to satisfy, to the maximum possible extent, practical engineering or operational problems of the Department of Defense and especially those of the major commands of the United States Air Force.



Requests for additional copies by Agencies of the Department of Defense, their contractors, and other government agencies should be directed to the:

Armed Services Technical Information Agency  
Arlington Hall Station  
Arlington 12, Virginia

Department of Defense contractors must be established for ASTIA services, or have their 'need-to-know' certified by the cognizant military agency of their project or contract.

All other persons and organizations should apply to the:

U. S. DEPARTMENT OF COMMERCE  
OFFICE OF TECHNICAL SERVICES,  
WASHINGTON 25, D. C.

UNCL

Security Classification

DOCUMENT CONTROL DATA - R & D

(Security classification of title, body of abstract and indexing annotation must be entered when the overall report is classified)

1. ORIGINATING ACTIVITY (Corporate author)		2a. REPORT SECURITY CLASSIFICATION	
Hqs., Air Weather Service		Uncl	
2b. GROUP			
3. REPORT TITLE			
The Practical Aspect of Tropical Meteorology Vol II: Notes on the Meteorology of the Tropical Pacific and Southeast Asia			
4. DESCRIPTIVE NOTES (Type of report and inclusive dates)			
Technical Report			
5. AUTHOR(S) (First name, middle initial, last name)			
C.S. Ramage et al			
6. REPORT DATE		7a. TOTAL NO OF PAGES	7b. NO OF REFS
26 January 1961		175	
8a. CONTRACT OR GRANT NO.		9a. ORIGINATOR'S REPORT NUMBER(S)	
AF19(604)-1942		AWS Technical Report 241, Vol II	
b. PROJECT NO.		9b. OTHER REPORT NO(S) (Any other numbers that may be assigned this report)	
		AFCRC-TN-60-455; Air Force Surveys in Geophysics 126; AWS Manual 105-48, Vol-II	
10. DISTRIBUTION STATEMENT			
This document has been approved for public release and sale; its distribution is unlimited.			
11. SUPPLEMENTARY NOTES		SPONSORING MILITARY ACTIVITY	
Redesignated as AWS Technical Report 241, Vol. II, in Oct 1970		AF Cambridge Research Laboratories	
12. ABSTRACT			
<p>This report is designed to supplement other texts on tropical meteorology. It makes use of new observational material and accords the synoptic features of the monsoons more attention than they have received in the past.</p> <p>Hints on analysis, and the uses of auxiliary charts and continuity are followed by a chapter on the physical geography of the Pacific and a gazetteer describing the locations and environments of observing stations. Chapter 3 tabulates monthly mean resultant winds, steadiness and other derived data at standard pressure levels for 34 sounding stations. Chapter 4 which broadly considers the climatology of the region, leads to more detailed discussions of the synoptic climatology of the tropospheric field of motion in the central Pacific (Chapter 5) and of the synoptic climatology of the China Seas and southeast Asia (Chapter 6). Appendices amplify the topics covered in this chapter. The final chapters are devoted to tropical cloud physics, local effects and aerial weather reconnaissance.</p>			

AD

AFCRC-TN-60-455

Air Force Surveys in Geophysics  
No. 126

NOTES ON THE METEOROLOGY OF THE  
TROPICAL PACIFIC AND SOUTHEAST ASIA

Edited by  
C. S. Ramage

Meteorology Division  
Hawaii Institute of Geophysics  
University of Hawaii

Interim Report  
Contract No. AF 19(604)-1942  
December 1959

June 1960

Project 8641  
Task 86415

Prepared for

Meteorological Development Laboratory  
GEOPHYSICS RESEARCH DIRECTORATE  
AIR FORCE CAMBRIDGE RESEARCH CENTER  
AIR RESEARCH AND DEVELOPMENT COMMAND  
UNITED STATES AIR FORCE  
Bedford, Mass.

## FOREWORD

Shortly after Contract AF 19(604)-1942 was negotiated, Air Weather Service, Air Force Cambridge Research Center and the University of Hawaii agreed to include meteorology instruction in the contract, with the aim of intensively training Air Force meteorologists in the meteorology of the tropical Pacific and southeast Asia. The courses which were given at irregular intervals and lasted six weeks, consisted chiefly of laboratory work, supplemented by lectures, and depended heavily on material developed earlier in similar courses by Professor C. E. Palmer and his associates. "The Practical Aspect of Tropical Meteorology," written by the Palmer group and used as a text has served admirably except that in largely concentrating on the central Pacific it makes only sketchy references to the important typhoon and monsoon problems of the western Pacific and southeast Asia.

Although additional lectures, new laboratory series and lengthening the courses to eight weeks have contributed to remedy the deficiency, printed material has been so widely scattered that students have had to depend on note taking, a difficult task considering the concentrated nature of the instruction.

Now that the Air Force Institute of Technology has contracted for four eight-week courses in Advanced Tropical Meteorology to be given annually to Department of Defense, Weather Bureau and Southeast Asia Treaty Organization meteorologists, it becomes imperative to supplement "The Practical Aspect of Tropical Meteorology" with additional printed course material. To this end, copies of Contract scientific reports 2, 3 and 4 are distributed to each student, and typhoon reports embodying the most recent information and theories are being compiled. A gap remains, in the areas of descriptive and synoptic climatology of the Pacific and southeast Asia, tropical cloud physics, local effects, and weather reconnaissance. The present report is designed to fill the gap, but only temporarily, since a definitive publication must await more original research. Thus the report should be



considered as merely interim and likely to be amended, expanded or superseded by future investigation.

During the past three years, Air Weather Service officers seconded to the Meteorology Division have been responsible for all laboratory instruction in the Advanced Tropical Meteorology courses and for some of the lectures. Major James C. Sadler, Captain Forrest R. Miller and Captain Leighton E. Worthley developed much of the material used in Chapters 1, 2, 5, and 9. The present instructors, Captain Carl J. Wiederanders and Mr. Montie M. Orgill were responsible for Chapters 1, 3 and 5 and Chapters 2 and 9 respectively. Relevant published papers are reprinted as appendices.

Grateful acknowledgment is made to Joint Task Force Seven Meteorological Center, the Japan Meteorological Agency, the Australian Bureau of Meteorology, the New Zealand Meteorological Service and the Royal Observatory, Hong Kong, for their contributions to the contents of Chapter 3; to Dr. David I. Blumenstock for Eniwetok micrometeorological data; to Lt. Colonel Frank E. McCreary for opinions and advice on upper wind forecast techniques; to the Hickam Air Force Base Photographic Laboratory for reducing the diagrams to a standard size; and to the Clarendon Press for permission to draw on the excellent text, "The Physics of Clouds" by B. J. Mason, for much of the material in Chapter 7.

## ABSTRACT

This report is designed to supplement other texts on tropical meteorology. It makes use of new observational material and accords the synoptic features of the monsoons more attention than they have received in the past.

Hints on analysis, and the uses of auxiliary charts and continuity are followed by a chapter on the physical geography of the Pacific and a gazetteer describing the locations and environments of observing stations. Chapter 3 tabulates monthly mean resultant winds, steadiness and other derived data at standard pressure levels for 34 sounding stations. Chapter 4 which broadly considers the climatology of the region, leads to more detailed discussions of the synoptic climatology of the tropospheric field of motion in the central Pacific (Chapter 5) and of the synoptic climatology of the China Seas and southeast Asia (Chapter 6). Appendices amplify the topics covered in this chapter. The final chapters are devoted to tropical cloud physics, local effects and aerial weather reconnaissance.

## CONTENTS

	Page
1. Analytical hints, auxiliary charts and continuity	1 5
2. Geography of the Pacific	2 12
3. Upper wind climatology of sounding stations	3 42
4. Climatology of the Pacific and southeast Asia	4 80
5. Synoptic climatology of central Pacific tropospheric winds	5- 85
6. Synoptic climatology of the China Seas and southeast Asia south of 30°	6-101
A. The winter monsoon	6-101
B. The summer monsoon	6-113
7. Tropical cloud physics	7-121
8. Local effects	8-126
9. Weather Reconnaissance	9-131
APPENDICES	
I. Relationship of general circulation to normal weather over southern Asia and the western Pacific during the cool season	I-142
II. The cool season tropical disturbances of southeast Asia	II-148
III. Non-frontal crachin and the cool season clouds of the China Seas	III-159
IV. Variation of rainfall over south China through the wet season	IV-167
V. Diurnal variation of summer rainfall over east China, Korea and Japan	V-171

## ANALYTICAL HINTS, AUXILIARY CHARTS AND CONTINUITY

### 1. Introduction

The mid-latitude forecaster at a small weather station has many advantages over his counterpart serving in tropical regions. He receives via facsimile complete sets of analyses and prognostic charts, which assist him tremendously in solving his forecasting problems. The tropical forecaster generally receives no such help except for an occasional but usually inadequate facsimile analysis.

The adjustment from mid-latitude to tropical analysis and forecasting is not an easy one. Many of the techniques used previously, such as those which pertain to frontal analysis, slopes of systems, and particularly, application of the geostrophic wind assumption must be modified or be replaced by techniques which are applicable to the tropics.

In the tropics, where the tendency toward slow changes makes a correct forecast, over a short time interval, depend largely on correct analysis, good analysis programs are essential. A meteorologist in making the best possible analysis must constantly refer to auxiliary and continuity charts.

### 2. Streamline analysis

The procedures to be followed are well outlined in "The Practical Aspect of Tropical Meteorology"\* and need not be reiterated here. There are, however, additional items worthy of mention.

Order of analysis. It is suggested that one begin with the dominant features of the chart, the subtropical ridge axes of the Northern and Southern Hemispheres, which should be well defined by the previous analysis. Next, a large area of undisturbed wind flow, such as the trade winds, or a typhoon area with generally numerous reconnaissance reports and a center fix, might be analyzed.

Certain areas, exemplified by the Japan-Okinawa-Taiwan complex, the Marshall Islands, or reconnaissance routes, generally offer sufficient data for a good analysis with a minimum of interpolation. Since the objectivity of any analysis varies directly with the density of the reporting network, it is obvious that analyses made over maximum data areas should be completed prior to attempting analysis over minimum data areas where much subjective interpolation may be required.

#### Suggestions for improving technique

- (a) Look at the "big picture." On each chart the numerous

---

\*Henceforth shortened to "PA."

flow singularities are usually organized into systems of troughs and ridges, just as in mid-latitudes. Thus it is well to keep in mind the over-all pattern. Locate vortices before attempting to locate associated neutral points. If the vortices are accurately located, the neutral points will be readily found along the axes of troughs and ridges. For example, in fig 1-2, the 10,000 ft streamline chart for 28 July 1956, the subtropical ridge axis extends from central Japan eastward to just north of Weather Ship "Victor," thence eastnortheastward through the vortex at 50°N 155°W. One trough line extends from typhoon Wanda westnorthwestward to southern China; another extends from Wake Island eastnortheastward through the Midway Island area. These systems are also evident at 20,000 ft (fig 1-3); in fact the northeastward extension of the Wake-Midway trough is much more pronounced than at 10,000 ft. In addition a ridge line extends from Hawaii westward to the Marshall Islands. At 40,000 ft (fig 1-4), there is no difficulty in identifying the subtropical ridge axis nor the Wake-Midway trough. Each trough or ridge system contains at least two vortices as well as neutral points.

(b) Do not draw a streamline through every report. This certainly leads to a cluttered appearance, prohibits proper spacing of streamlines, and may result in poor analysis.

(c) Working outward from an anticyclonic and inward toward a cyclonic center ensures more rapid and elegant analysis, by guaranteeing that divergent flow around anticyclones and convergent flow around cyclones are readily and accurately depicted.

In the absence of strong evidence, cyclonic circulations should be analyzed as indrafts and anticyclonic circulations as outdrafts. PA states, "The experienced analyst will realize that, at low levels, the outdraft is more frequently combined with anticyclonic flow, while the indraft is most frequently combined with cyclonic flow. At upper levels, however, any of the combinations may appear." During meteorological operations supporting the 1958 nuclear test in the Marshall Islands, Commander D. F. Rex, Lt. Col. F. E. McCreary and Dr. R. R. Brownlee conducted experiments with mechanical wind analyses and forecasts for levels ranging from 10,000 to 50,000 ft. Using wind observations from more than 30 observing sites an IBM 704 computed east-west and north-south wind components at latitude-longitude intersections spaced two degrees apart. This was done by the method of inverse squares which weighted the contribution of each report to the interpolated value at the grid point according to its proximity to that point. The resultant wind at each grid point was then printed out by the computer and the charts analyzed. It is significant to note that neither anticyclonic indrafts nor cyclonic outdrafts could be detected on any of the charts.

Mid-tropospheric cyclonic outdrafts may develop and persist around typhoon cores. Air which has spiralled in toward the center (at low levels) at speeds determined by the low-level pressure gradients, tends to conserve its angular momentum as it rises within the core. Since a typhoon is warm-cored, pressure gradients decrease with height and in the middle troposphere the

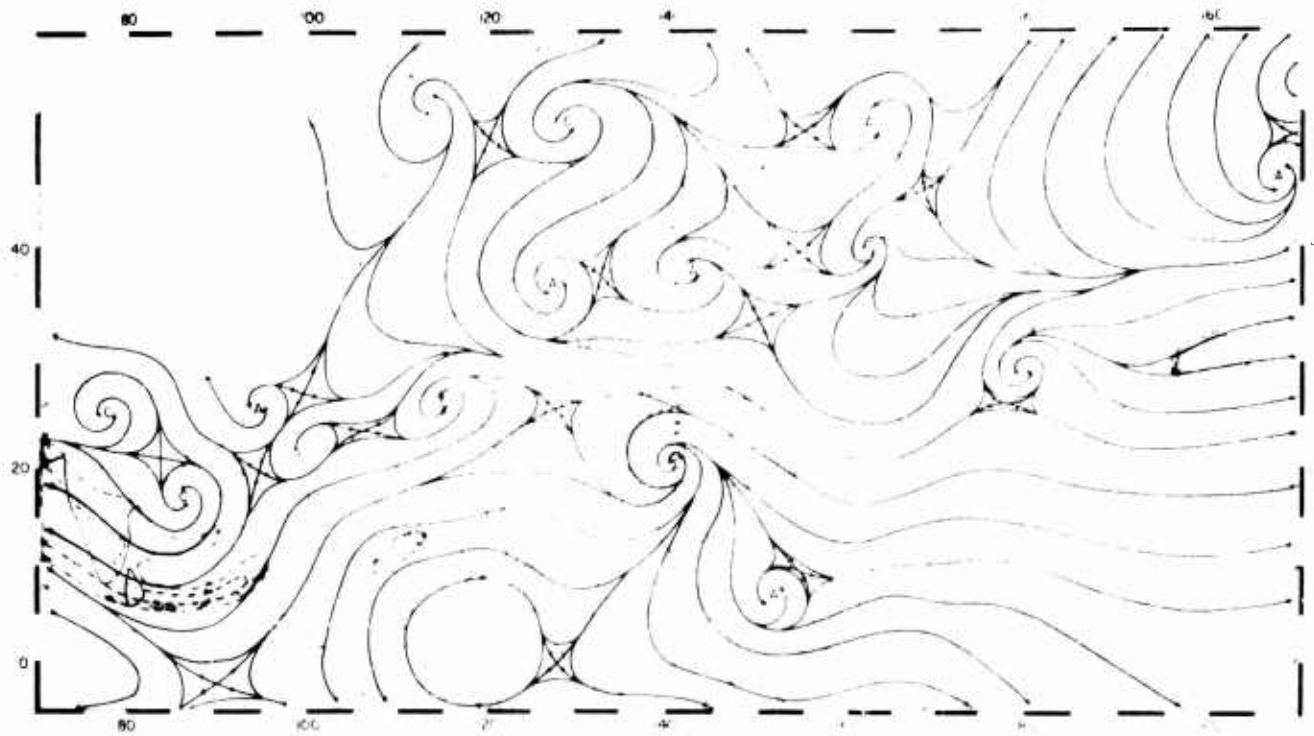


Figure 1-1. Surface streamline-isotach analysis for 00 GCT 28 July 1956. Isotachs are labelled in knots.

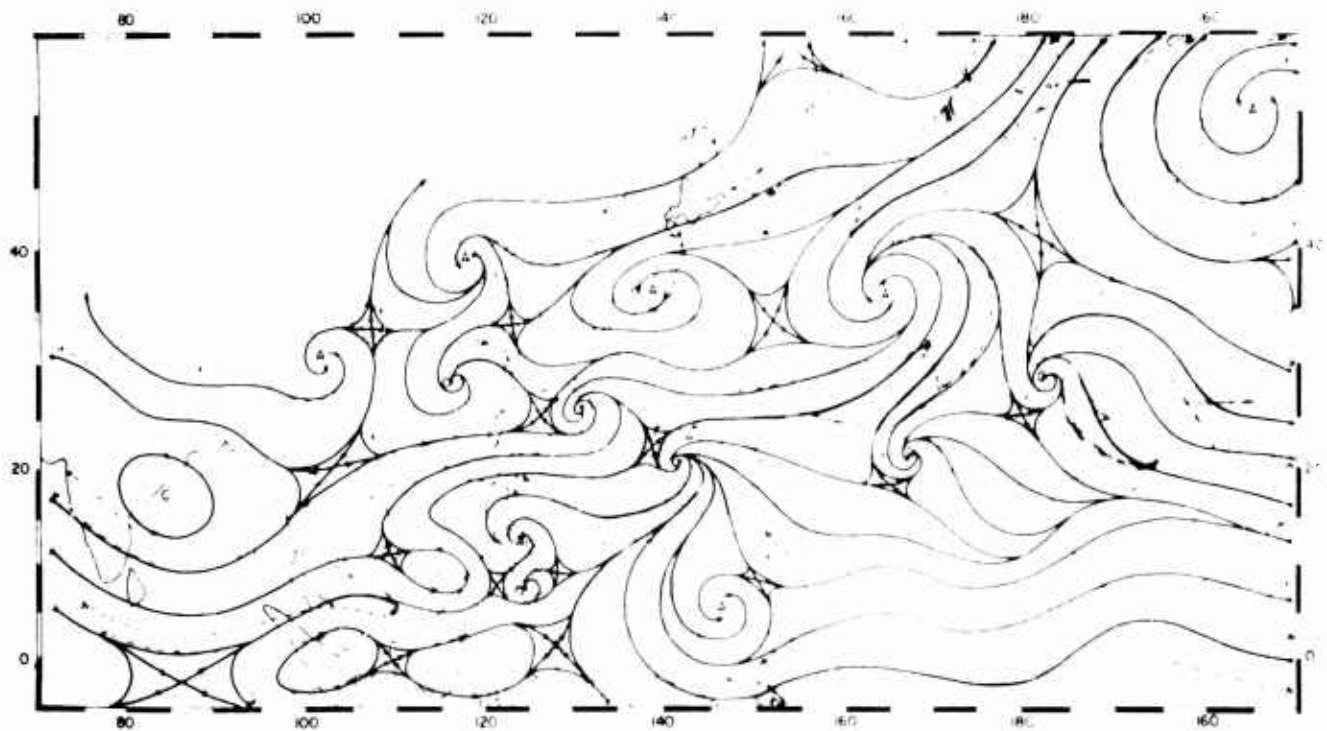


Figure 1-2. Same as fig 1-1 but for 10,000 ft.

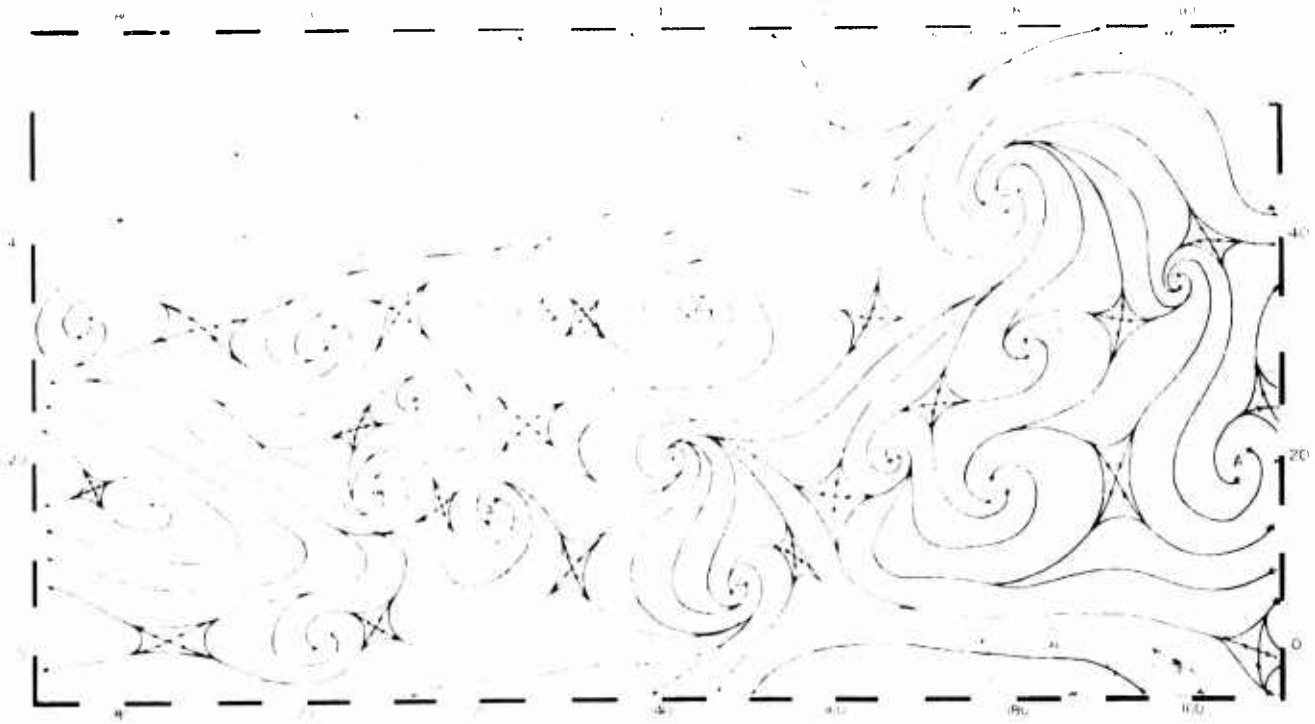


Figure 1-3. Same as fig 1-1 but for 20,000 ft.

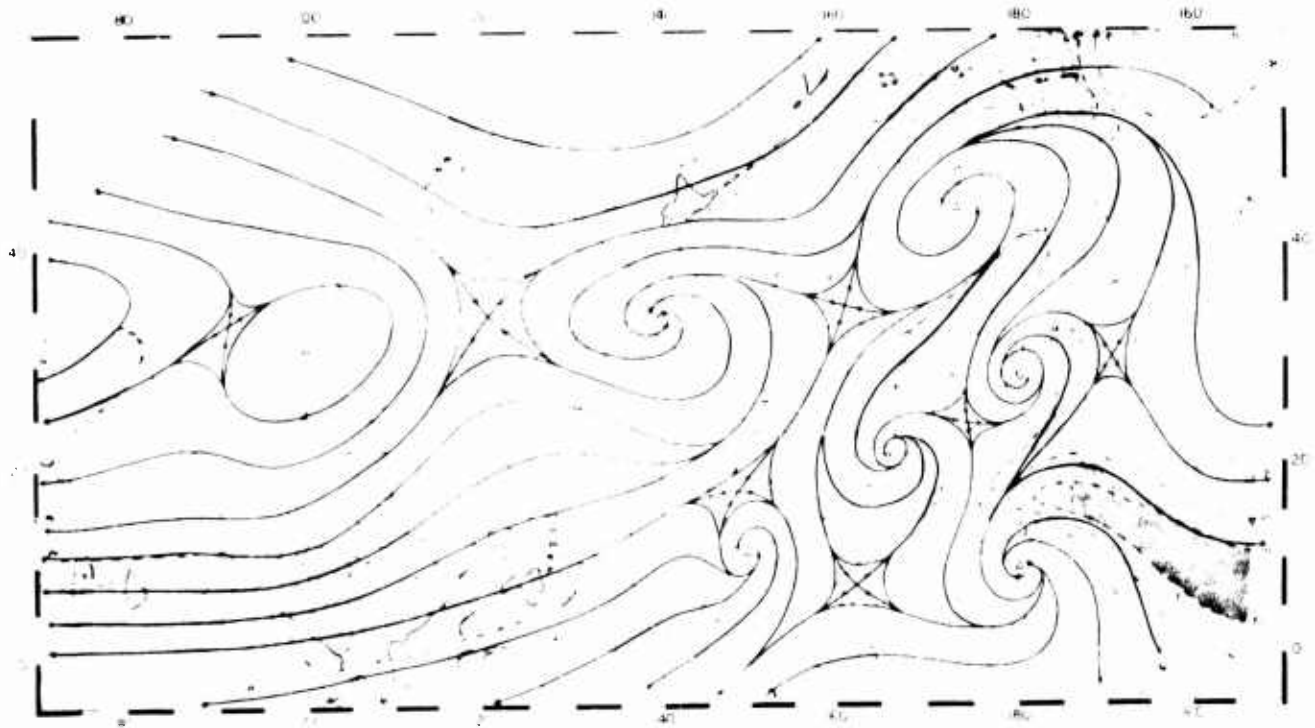


Figure 1-4. Same as fig 1-1 but for 40,000 ft.

centrifugal force begins to exceed the pressure-gradient force. The air is then accelerated outward toward higher pressure while still rotating cyclonically.

(d) Avoid distorting the analysis pattern over too large an area on the basis of one report, without substantiating data. On low-level charts of the trade wind region, analysis sometimes has shown a trough extending more than 1000 mi south of a reporting station whose observation is the only evidence that the trough exists. This procedure overtakes the use of single station analysis.

(e) Avoid depending too heavily on the pressure or contour analysis to determine the wind analysis. Despite the large deviations of geostrophic from measured winds in the tropics, some analysts unconsciously attempt to follow contours into tropical regions when drawing streamlines. Contours with arrow-heads and tails at opposite ends are still contours. Substituting an arrow for a pressure-height value does not magically convert a contour into a streamline.

(f) Remember that singularities may not extend through all levels of the troposphere. Many a high-level circulation does not penetrate down far enough to be detectable in the streamline analysis at 10,000 ft but may be reflected as a minimum speed area in the isotach analysis. Figs 1-2 and 1-3 contain an example. At 10,000 ft a speed minimum occurs between  $10^{\circ}$  and  $15^{\circ}$ N,  $170^{\circ}$ E and  $170^{\circ}$ W, almost directly beneath the 20,000 ft ridge axis.

(g) Beware of concluding that a light wind (less than 10 kn) is evidence of a singularity in the vicinity. Light steady flow is not uncommon and hence singularities should not appear in the analysis except where wind directions vary considerably in space or time.

### 3. The time-section

The time-section is invaluable as a tool for detecting data errors in either transmission or plotting. Table 1-1 shows the 19 July 1959 time-section for Wake Island during a period of deep, strong trade wind flow. It is obvious from a consideration of other levels and other times that the 700 mb wind of  $010^{\circ}$  31 kn reported on the 1200 GCT radiosonde message is wrong. Yet, one analyst blindly accepted it, and as a result his 700 mb analysis was erroneously distorted over several hundreds of miles in every direction from Wake Island. A brief glance at the time-section could easily have avoided this error.

Wind reports should be accepted as correct unless there is evidence to the contrary. The time-section is most likely to provide that evidence.

The wind reported at each level in a rawin or pibal message is determined by averaging the winds through a layer centered at the report level. This approximation to a single-level wind seldom seriously affects the representativeness of the reported



Table 1-1. Wake Island Time-section for 19 July 1959.

Wind directions are in tens of degrees and wind speeds in knots.

Height (thousands of ft)	0000 GCT	0600 GCT	1200 GCT	
40	0816		0723	
35	0721		0816	
30	0721		0815	
25	1219		0802	
20	1019		0611	
18	0918	0816	0713	wind at 700 mb
16	0916	0817	0911	
14	1017	0817	0821	on the 1200 GCT
12	1117	0818	0721	radiosonde report
10	0917	0822	<u>0731</u>	:- 0131
8	0916	0823	0920	
6	0821	0824	0923	
4	0822	0922	1019	
2	0822	0823	0919	

wind direction. However, the wind speed, which may undergo rapid fluctuations through the averaging layer, may not be accurately represented by the report. Analytical smoothing of the isotach field is therefore often needed. In pursuit of this end, time-sections, which depict both vertical and temporal wind distributions, can be effectively used.

#### 4. Continuity

In the tropics, circulation systems once established, tend to persist, either remaining quasi-stationary as does the subtropical ridge, or moving along fairly steadily as do typhoons. Thus, by carefully maintaining continuity an analyst greatly improves the quality of his analyses. Continuity charts, on which the successive positions of all circulation, ridge, or trough systems are plotted, enable the analyst to avoid unlikely movement velocities. The charts, by facilitating extrapolation, ensure that the analyst can, with some confidence, track moving circulations across areas bare of observations.

Frequently, a new circulation may be located. If it also

appears on the following synoptic chart, it can be accepted as in fact existing, and not being a spurious system reflecting incorrect or unrepresentative observations.

PA in emphasizing the importance of "vertical" continuity (pp 152-155) points out that circulations may best be located by locating the centers of relative vorticity maxima (cyclonic) and minima (anticyclonic) (see figs 1-1 to 1-4). However, it is also important to realize that a circulation which is vigorous at 40,000 ft may not be detectable in the vorticity field at 5000 or 10,000 ft, while a typhoon may well be overlain by an anticyclone in the high troposphere. Predominantly high-level circulations (cold lows) are best identified and followed on 40,000 ft charts. Conversely, surface charts are ideally suited to the location and tracking of predominantly low-level circulations (warm lows, cold highs). The circulations of warm highs often extend throughout the troposphere.

Time continuity should be relatively easy to maintain on upper or lower tropospheric charts. 500 mb (20,000 ft) charts however, rather poorly depict both high- and low-level circulations which may disconcertingly disappear and reappear as the systems weaken or intensify. Continuity can only be maintained with difficulty.

#### 5. Bibliography

Palmer, C. E., 1951: On high-level cyclones originating in the tropics. Trans. Amer. Geophys. Un., 32, 683-695.

Riehl, H., 1955: Weather analysis in tropical regions. NAVAER 50-1P-534, 99 pp.

## GEOGRAPHY OF THE PACIFIC

### 1. Introduction

Examination of a world map reveals that the Pacific Ocean constitutes the earth's largest single feature, comprising more than one-third of the earth's surface. The total area amounts to approximately 68,634,000 mi<sup>2</sup>. The Pacific Ocean is roughly elliptical in shape with the following boundaries:

- North - Bering Straits (56 mi wide)
- East - Coasts of North, Central and South America
- West - Asia, Indonesia, New Guinea and Australia
- South - Antarctica

The Pacific extends approximately 10,540 mi along the equator and roughly the same distance north-south. It is the deepest ocean (35,960 ft in the Marianas Trench), and has an average depth of 14,000 ft.

Excluding Australia, only a minute fraction of the Pacific is covered by land above sea level, predominantly in the form of small islands. The greatest concentration of islands exists in the region between 25°N and 25°S. This is indeed fortunate for the tropical meteorologist because each island is a potential weather observation post, and many have been so utilized for several years. On the other hand, the tropical meteorologist is at a distinct disadvantage when he looks at a weather chart, and is able to do no more than identify each observation station with a name and location. Only out-of-print publications describe the orography and locations of some of these weather stations. It is important that the forecaster, who must determine the present and future state of the atmosphere over the vast Pacific, be able to utilize accurately every jot of weather information. To do this properly he must familiarize himself with the Pacific Islands and their geography.

### 2. Divisions of the Pacific Ocean

Geographic. The ocean is divided into the North Pacific, north of the Tropic of Cancer (23°N), the Central Pacific, between the Tropic of Cancer and the Tropic of Capricorn (23°S), and the South Pacific, south of the Tropic of Capricorn.

Anthropological. There are three main divisions: Melanesia (dark or black islands) extending in an arc from western New Guinea to New Caledonia and Fiji, whose peoples are dark-skinned with heavy beards and frizzy hair; Micronesia (little islands) comprising the Carolines, Marianas, Marshalls and Gilbert and Ellice groups with inhabitants of mixed Melanesian, Polynesian and Malaysian stock; and Polynesia (many islands) which include New Zealand, Tonga and all other islands east of the International Date Line. The Polynesians, last migrants from Asia to the Pacific, are brown-skinned, straight-haired people.

Meteorological. Considering the lower atmosphere one might define the tropics as that envelope of air bounded by the axes of the subtropical anticyclones of both hemispheres. This definition implies that the tropical atmosphere is homogeneous and approximately barotropic. The atmosphere poleward of the subtropical ridges is generally non-homogeneous and baroclinic.

Geological. Islands which consist of granite and siliceous (40%  $\text{SiO}_2$ ) eruptive rock, called andesite, are labeled continental. These islands were probably joined to the mainland during some time in geologic history. They lie in general, west of a line extending from Japan through the Marshall Islands, Samoa and New Zealand. Islands which have primarily basalt or coral foundations are classified as oceanic and lie to the east of the line.

Bathymetric and seismic evidence gathered during the International Geophysical Year has prompted geologists to state that mid-ocean ridges form a continuous system about the earth. In the Pacific the main ridge extends from south of Australia and New Zealand to Easter Island. Here it is least known but branches probably extend to South America through Juan Fernandez and Galapagos Islands and perhaps to Mexico. The main ridge continues from Easter Island through the Line Islands and the Hawaiian chain to Kamchatka. Thus, it seems probable that a continuous ridge a few hundred miles wide, from 10,000 to 33,000 ft high, winds its way across the central ocean floor.

Earthquakes occur along most of this ridge which is the second most active seismic system on Earth. Where the ridge has been most closely studied, it has been found to have a central rift. Both rift and earthquakes suggest that the ridge follows a fault zone which geologists call the mid-ocean fracture system. The ridge is made up of basalt lava with some patches of ultrabasic rock, and the islands along it are basalt volcanoes. All this suggests that the ridge has been formed by the escape of basalt lava along a fracture zone and that basalt has been formed by partial melting of pockets in the ultrabasic rocks of the upper mantle at a depth of not more than 37 mi. The lack of abandoned ridges and the slow rate of the ridge's volcanism suggest that it has been in its present position for a very long time, perhaps for most of the Earth's history.

The mid-ocean ridge system divides the Pacific Ocean into eastern and western parts. The eastern Pacific is fairly uniform in depth and nearly devoid of islands except along the coasts of the Americas. Here an extension of the mid-ocean ridge system is defined as a broad submarine platform (about 13,000 ft below the surface) called the Albatross Plateau, branching north from South America toward Central America, and west through the Tuamotu Archipelago to Antarctica. From rifts or fissures along margins of the Plateau volcanic mountains have thrust out of the sea to form the islands of Sala-y-Gomez, Juan Fernandez, Galapagos, Easter and Cocos.

In contrast to the eastern section, many hundreds of islands dot the western Pacific between New Zealand and the Aleutians.

Mid-ocean island groups such as Hawaii, Samoa, Phoenix, Tokelau and Gilbert are extrusions of the mid-ocean ridge above sea level and have been formed either by volcanic activity or by the action of coral polyps around submerging old volcanoes (guyots).

Near the Asian continent certain other islands, exemplified by New Guinea, Solomons and New Hebrides are a complex volcanic, continental and coralline mixture. An intriguing aspect of certain continental margins is the volcanic island arc and associated deep trenches in the ocean floor. Great arcuate island festoons extend all the way from Alaska to Kamchatka and southward through the western Pacific to the Banda Sea of Indonesia. They are generally bowed outward toward the Pacific, and bounded on the Pacific side by deep narrow trenches whose depths exceed the elevation of Mount Everest. The islands of these arcs are mostly active volcanic cones rising from swells on the ocean floor to sea level and above. Some of the arcs, such as the Japanese Archipelago, consist of large islands with complex geologic foundations, but even these are replete with active volcanoes.

The island arcs of the western Pacific are most active earthquake belts and hence are considered belts of active deformation of the earth's crust. Within historical times, significant elevations and depressions of the land have been observed, at rates which if extrapolated backward into geologic time, allow geologists to account for the highest mountains or the most profound ocean depths.

Geologists have two theories regarding the formation of the deep oceanic trenches. The first theory states that oceanic trenches can be accounted for by the contracting of the earth's crust or by horizontal compressive forces acting over a limited area. The horizontal compressive forces cause the crust to down-buckle into the heavier material of the mantle, thus forming a trench. The second theory, which is more recent, states that trenches are due to overriding by the inner blocks of island arcs, which are thrust up at the surface and which bend down the ocean floor in front of them. The volcanoes which form adjacent to the deep oceanic trenches are believed to be caused by subsidiary faulting. This faulting provides channels along which lava and superheated solutions can rise from the depths.

Some of the deepest trenches found in the western Pacific are:

Cape Johnston (near Mindanao) 34,440 ft.

Horizon (Tonga Islands) 34,884 ft.

Vityaz (Kuril Islands) 34,044 ft.

Kamapo (southeast of Japan) 34,038 ft.

Nero (Tinian Island) 31,614 ft.

Aldrich (north of New Zealand) 31,080 ft.

Trenches have also formed in the eastern Pacific near the west coast of South America but they are somewhat shallower than the western trenches.

### 3. Tropical Pacific islands

Volcanic islands. These islands have been built up from the ocean floor by flow after flow of basaltic lava issuing from rifts. The flows thin out as they leave the center of eruption, until a gigantic dome is built above sea level. The dome may be ten to thirty miles wide at sea level and extend several thousand feet above sea level. As a final stage of volcanism several subsidiary volcanoes may break out on the slopes of the great dome and cinder cones be left as a result.

Volcanic islands vary in age and consequently in the degree to which the weather has affected them. The basalt weathers very easily, but where the flows are of recent origin, as in the case of Haleakala and Mauna Loa in the Hawaiian chain, the original dome-like profile is still preserved. Where erosion has gone further, and particularly in the case of ash cones, the old crater walls are broken down and sharply serrated. The dramatically jagged ridges of Kauai and Tahiti are the effects of severe erosion on extinct volcanoes.

Wind and weather observations taken from a volcanic island will be unrepresentative, particularly on the leeward side and below the level of the highest terrain. In fact, cloud formations show that peaks distort wind flow to about twice their height.

Diurnal effects produced by such large volcanoes as Mauna Loa may divert the normal northeast trade flow and at times completely overpower it.

#### Coral islands; Darwin's subsidence theory of atoll evolution.\*

Pre-Darwinian theories of coral reef formation had clouded rather than resolved the mystery of their existence. Voyagers and explorers of the 17th and 18th centuries fancied that coral animals erected their circular parapets for reasons of defense and compared them with beehives and the geometrical nests of wasps. One naturalist deduced that reefs were "built by fishes by means of their teeth." In prose and poetry nature writers eulogized the "skill" and "industry" of the "coral insect" in fabricating his "home."

Darwin was perfectly aware that coral formations consisted of the calcareous remains of small, static, colonial animals, and that their giant edifices were no more products of "skill" and "industry" than man's skeleton or the shells of clams. Yet the problem of process remained. Observations made by Darwin in the Cocos Isles revealed that the outer walls of coral of each reef and atoll plunged precipitously to enormous depths. Paradoxically he also ascertained that living corals existed only to a depth of 120 to 180 ft, a depth at which almost all the sunlight has been absorbed. The crucial question, therefore, as Darwin phrased it,

---

\*Based very largely on "Darwin's world of nature" by L. Barrett in Life Magazine, 20 July 1959, 54-68.

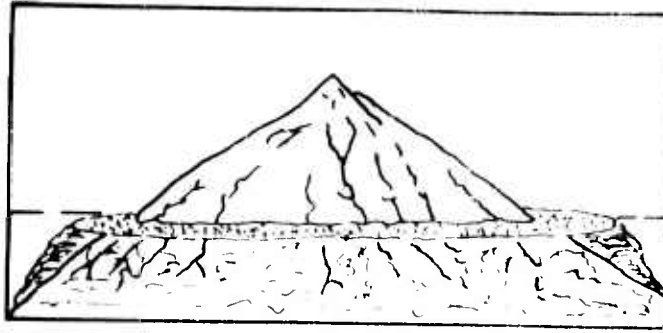
was "On what have the reef-building corals, which cannot live at great depth, based their massive structures?"

Darwin examined coral formations and separated them into three types: fringing reefs, barrier reefs and atolls. The fringing reef is a circular rampart of coral surrounding a volcanic island close to the island shore or contiguous with it. The barrier reef is similar to a fringing reef but separated from it by a channel of water. The atoll comprises a ring of coral surrounding a central, shallow lagoon (see figs 2-1, 2-2, 2-3, 2-4).

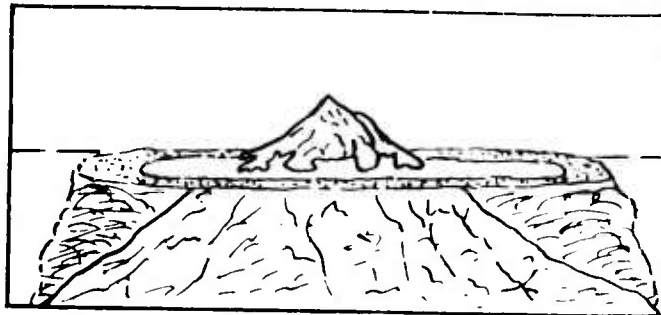
In these three types Darwin discerned a process of evolution. He concluded that coral formations were the end product of three processes: (1) the initial uplifting of an island by submarine volcanic action, (2) the gradual subsiding of the island into the sea, and (3) the colonizing of its subsiding slopes by myriad coral polyps which reproduced themselves in the sunlit upper strata of the sea and, as they perished, left behind their skeletons as foundations on which future generations continued to build. In Darwin's view the fringing reef came first, edging the shores of the newly created island. Then as the island subsided, the corals, ever building on the same foundations, became separated from the shore, and their structure assumed the form of a barrier reef. Finally the island disappeared completely, leaving only the circular atoll.

"From the fact of the reef-building corals not living at great depths," Darwin wrote, "it is absolutely certain that throughout these vast areas (of the ocean), wherever there is now an atoll, a foundation must have originally existed within a depth of 20 to 30 fathoms from the surface..." As island after island, slowly sank beneath the water, fresh bases would be successively afforded for the growth of the corals. In its essential outlines Darwin's theory is valid today. But as Darwin himself acknowledged, it is oversimplified and incomplete. Modern oceanographers agree that most atolls stand on volcanic foundations which have slowly subsided into the sea. During World War II the U. S. Navy discovered the existence of submerged flat-topped volcanic mountains, called guyots, scattered throughout the depths of the Pacific Ocean. Dredging produced pebbles that had obviously been sculptured by wave action, indicating that in the past these drowned flat-topped mountains had been islands protruding above the surface of the sea. Hence the fact of subsiding, as suggested by Darwin, was sustained. But subsidence is relative; it may result either from sinking of the island foundations or from a rise in sea level.

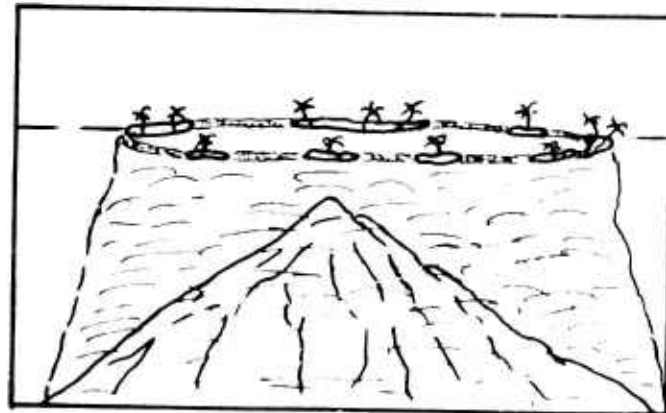
Fluctuations in ocean level have occurred repeatedly since prehistoric times as the result of alternate freezing and melting of the polar ice caps, causing sea levels to rise and fall. Recent studies of fossils and rock samples have revealed that the evolution of atolls is more complex than Darwin conceived in his vision of a forthright sequence from fringing reef to barrier reef to atoll. Deep borings have recently been made at three sites in the Pacific--in the Ellice Islands, the North Borodino Islands and



1. Fringing Reef



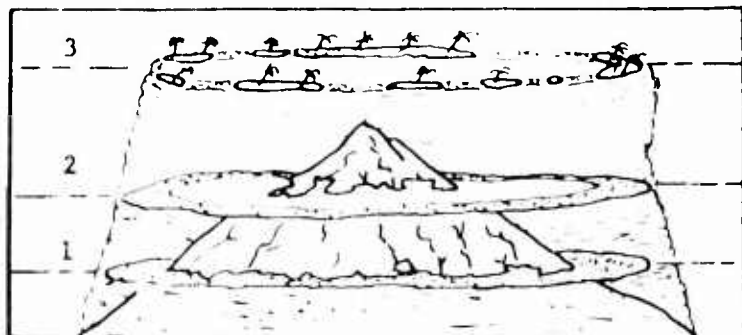
2. Barrier Reef



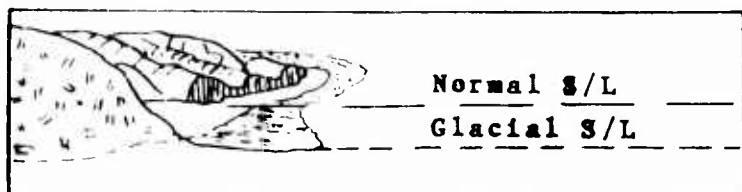
3. Atoll

Figure 2-1. Darwin subsidence theory of atoll formation.





farther off shore, until with the disappearance of the enclosed island, an atoll was formed. The three steps in the figure are: (1) a fringing reef, (2) a barrier reef, and (3) an atoll.



waves. Reefs began to grow on these submerged platforms as the water warmed and the sea level rose. He claims that the lagoon floor is uniform at 200-300 ft.



#### REIN THEORY

Rein suggested that organic deposits accumulated on still standing submarine summits, and that these deposits eventually built up to sea level. This does not effectively explain the lagoon.



#### MURRAY THEORY

Murray held a similar theory to Rein, but added that the lagoon of atolls resulted from solution while the reef grew outward; however, there is no real evidence to support this.

Figure 2-2. Atoll formation theories.

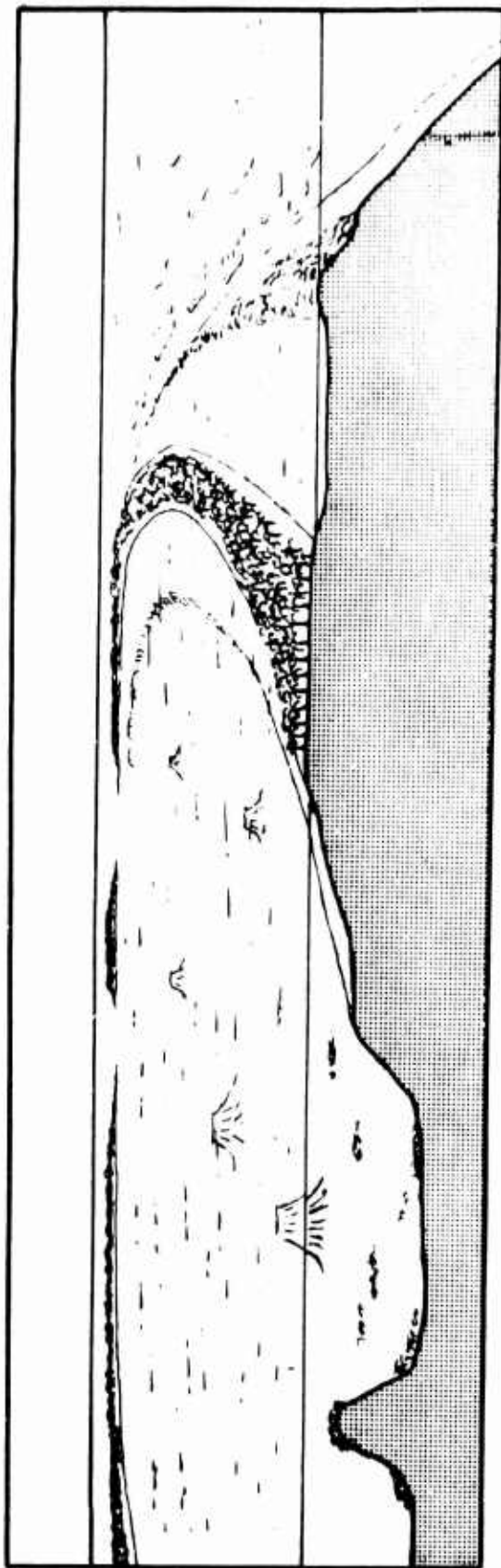


Figure 2-3. A typical coral atoll is circular, as shown in the vertical section above. To the far right the ocean washes across the shallow reef up to the high coral shore covered with palms. This shore encircles the inner lagoon, studded with pinnacles of coral thrusting upward from the bottom of the lagoon. In the foreground the cutaway shows the base of the atoll, layer upon layer of coral limestone skeletons built up through the ages on a submerged volcano.

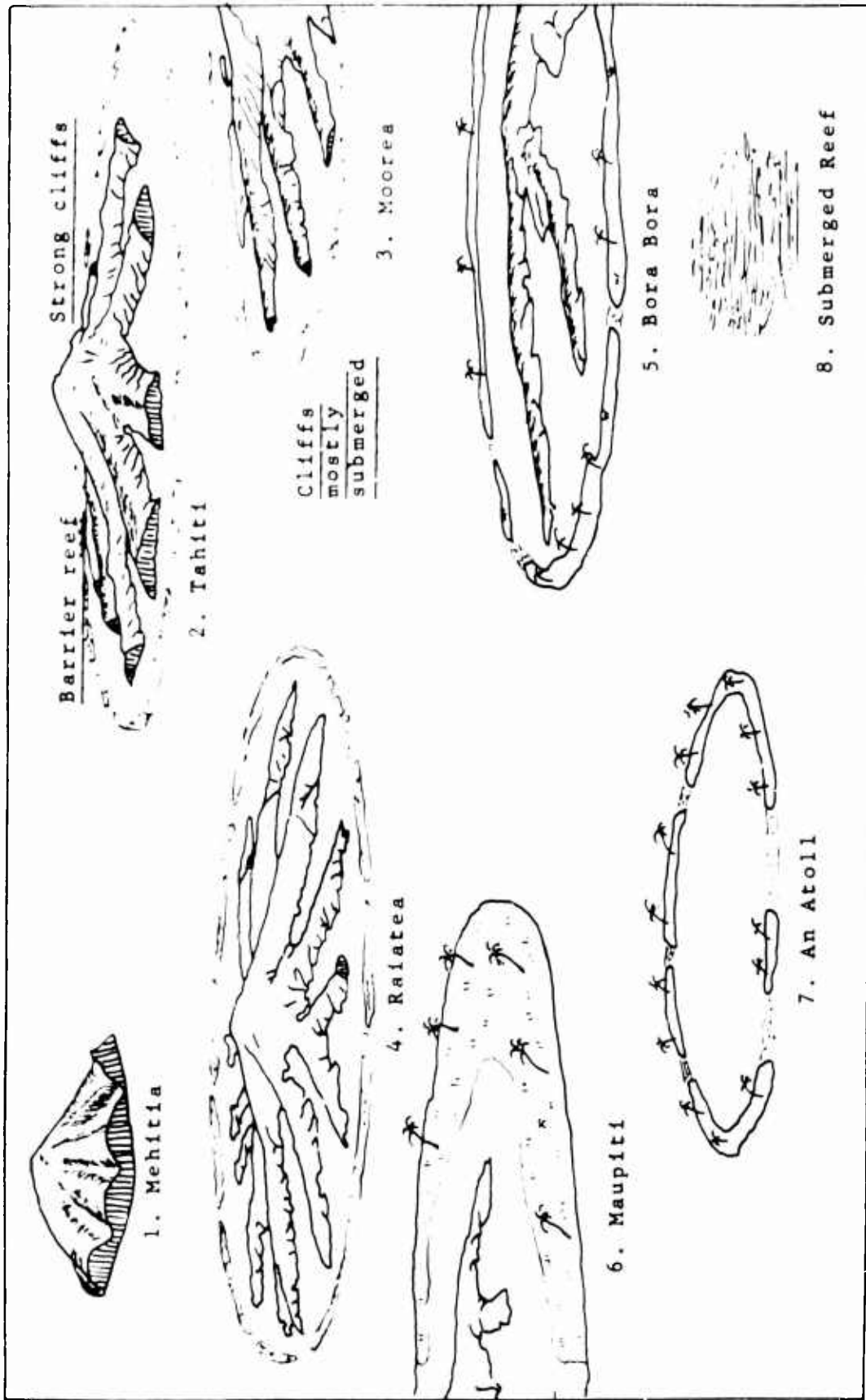


Figure 2-4. Society Islands stretch for approximately 200 miles in an almost east-west direction. They exhibit the complete cycle of Darwin's theory. The islands above are numbered from east to west, so it appears that there has been a strong tilting of the ocean floor to the west as the western islands show the most subsidence.

the Marshall Islands--and have provided important confirmations and revisions of Darwin's ideas. The deepest hole was bored in the Marshall group, at Eniwetok penetrating to 4600 ft and reaching the foundation on which the earliest substructure of the reef was laid down. It showed that the foundation of the Eniwetok atoll was indeed a submarine volcano, rising two miles from the ocean floor. The volcano at one time projected above sea level. Then, when volcanic action ceased, it slowly sank, and corals and their associated forms of life began building on the submerging slopes. The fossils of these organisms--found in the layers of sediment capping the volcanic foundation, date as far back as the Eocene Period, 60 million years ago. Oceanographers estimate that Eniwetok atoll has been subsiding at the rate of .03 in per century since that time.

Environment of growing coral. Coral lives in water with a salinity of between 27 and 40 parts per thousand (average open ocean salinity, 35 ppt). Water temperature is also critical, ranging from 65°F to 97°F; optimum growth occurs between 77 and 84°F. Most reef building takes place between the sea surface and 25 fathoms although reef coral may live as deep as 85 fathoms. Coral can withstand short periods of exposure to the air during low tide. It is dependent on sunshine and water circulation for food, oxygen and sediment removal. Reef corals are found in warm shallow tropical and subtropical waters between 35°N and 32°S.

Flat coral atolls consist of a group of small coral islands built on a large coral reef on top of a guyot. These islands are connected by a causeway and encompass a relatively shallow water area called a lagoon. They vary in size and shape with very few being completely circular. Jaluit, in the southern Marshalls is triangular. One of the smallest in the Pacific or elsewhere is Namorik which is less than one mile across. Kwajalein, one of the largest, is 100 mi along its longest axis.

Most flat atolls are named after the main inhabited island or the people of the atoll. Wake Atoll for example, is named after the largest of three islets.

Living conditions on flat atolls are difficult because fresh water is scarce and there is no fertile soil in which to plant crops. Inhabitants live on coconut products, breadfruit and sea food.

Flat coral atolls make excellent weather observation platforms since the wind over the atolls is undisturbed for most practical purposes. Tall palm or coconut trees which can rise to 100 ft may disturb the surface winds but have little effect on winds above the surface.

Raised coral atolls have been lifted sometime in geological history. The lagoon has disappeared leaving only a depression in most cases. Raised coral atolls have a greater supply of fresh water and better soil than the flat coral atolls.

Wind observations taken from these islands will generally be

representative for levels above the highest point on the island. However, surface observations are influenced to some extent by orography.

#### 4. Pacific island weather stations

Meteorologists in the Pacific, who must analyze and forecast the weather with the existing sparse network of reporting stations, are constantly striving to improve the data coverage. This is particularly true over the tropical Pacific where tropical cyclones can rapidly develop into typhoons.

Although the number of upper air wind observing stations in the Pacific is small compared to the area involved, there is a fairly good network of surface weather reporting stations over the central and western Pacific of both hemispheres. In any low level analysis of the wind field, pibal or rawin data can often be supplemented by surface winds and cloud directions. Although cloud directions can generally be considered representative, except over large mountainous islands, surface winds must be treated with caution.

Unless the analyst is familiar with the orography of Pacific islands, indiscriminate use of surface and low level winds (10,000 ft or lower) in streamline analyses can often lead to incorrect solutions. In the past there has never been one specific gazetteer or source which lists the exact location and topography of island weather stations. Because of this and the need for utilizing all available weather data in the tropical Pacific, the following table of Pacific island stations, their location, topography and type of weather reports has been compiled.

The listing has been restricted to those islands in both hemispheres which usually appear on a weather plotting chart as only a number. Stations on very large islands (with the exception of New Guinea) have been omitted.

For each weather reporting station, the following information is given:

1. The common name and international index number as it appears in HO 206, Vol. II or WMO No. 9 TP4, "Weather Reports, Vol. A, Nomenclature of Stations." The name of the island on which the station is located appears in brackets when the two names are different.

2. The geographical island group or chain designation.

3. Type of island, where

FA = Flat Coral Atoll with highest terrain below 30 ft msl.

RA = Raised Coral Island without volcanic peaks where terrain reaches 30 ft msl or higher.

SV = Small Volcanic Island whose mountain tops rise less than 3000 ft msl.

LV = Large Volcanic Island with volcanic peaks above  
3000 ft msl.

4. Height (ft above sea level) of the observing station and its general location on the island. This information aids the analyst in determining the representativeness of surface and upper wind data.

5. Highest point and its location on the island (for New Guinea, the highest point in the general area of the station). This information helps in estimating the lowest level at which pibal or rawin data are representative.

6. Type of weather reports transmitted, where

S - Surface synoptic

RW - Rawin

P - Pibal

W - Radio-wind

Recco - Aircraft reconnaissance

For detailed data on the frequency and times of reporting for each station consult, WMO No. 9, TP4, "Weather Reports, Vol. C, Transmissions."

In addition to the table, a locator chart showing the upper wind network for the Pacific region is included as fig 2-5. The names of stations which make rawin soundings at least once a day are underlined. Other stations are scheduled to make at least one pibal run per day.

#### 5. Bibliography

Freeman, O. W., 1951: Geography of the Pacific. New York, Wiley, 573 pp.

U. S. Navy, Hydrographic Office, 1954: Radio weather aids, Vol. 2. H. O. Pub. 206.

Wood, L. G., and P. R. McBride, 1955: The Pacific basin. Melbourne, Oxford Univ. Press, 393 pp.

World Meteorological Organization, 1953: Weather reports - Stations, codes and transmissions. Vol. A, Nomenclature of stations, W.M.O. No. 9, TP. 4.

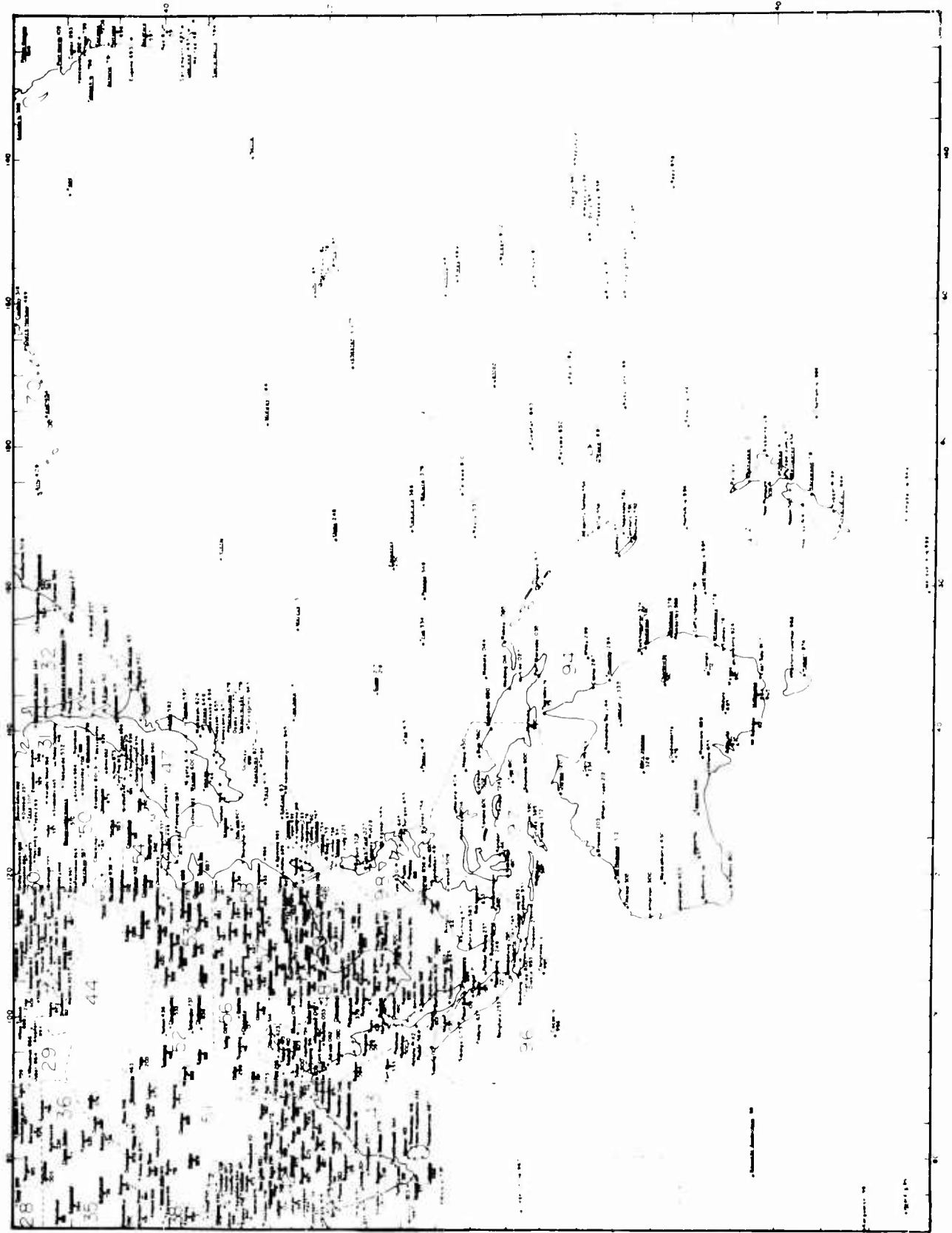


Figure 2-5. Upper wind stations of the Pacific and Far East. Rawin stations underlined.

Pacific island stations, their location, topography and type of weather reports

Name of reporting station, village or island	Intnl. Index No. 46	Island group or chain	Type of island	Height and general location of observing station on island	Highest point and location on island	Type of reports transmitted	Remarks
Matsu	639	Taiwan	S	Unknown (Unk)	200 ft, NE section	P(06, 18z)	
Penkiayu (Agincourt)	695	Taiwan	S	325 ft, W extremity	466 ft, E section	S	
Makung	734	Pescadores	S	Unk, W section of the biggest island	Less than 260 ft S section	RW(06, 18z)	
Kinmen (Quemoy)	736	Quemoy	S	Unk	Less than 400 ft	P(00, 12z)	
Lanyu	762	Taiwan	S	1059 ft, SW part	1798 ft, central section	S	
Pratas	810	Isolated island	FA	Unk	40 ft to the top of trees	S	
Nansha	902	Isolated island	FA	Unk	20 ft	S	
Hachijoizima	47	Nanpo Shoto	SV	267 ft, unk	2802 ft	S, W(06, 18z) RW (00, 12z)	
Murotomisaki	399	Ryukyu	SV	610 ft, NW section	846 ft	S	



Name of reporting station, village or island	Intnl. Index No. 47	Island group or chain	Type of island	Height and general location of observing station on island	Highest point and location on island	Type of reports transmitted	Remarks
Naze	909	Ryukyu	SV	13 ft, NW coast	2293 ft, SW part	S, W(06, 18z), RW (00, 12z)	Mountainous
Yonagunishima	912	"	SV	98 ft, N section	759 ft, E section	S	
Ishigakijima	918	"	SV	23 ft, SW side	1200 ft, NW part	S, P(00z)	
Miyakojima	927	"	SV	131 ft, unk	Less than 370 ft	S	
Kumejima	929	"	SV	Unk	1070 ft, N section	S	
Naha AB (Okinawa)	930	"	SV	16 ft, SW part	1650 ft, NE part	S, Radar storm detection	
Kadena AB (Okinawa)	931	"	SV	163 ft, approx. 15 mi NE of Naha	1650 ft, NE part	S, W(06, 18z), RW (00, 12z)	
Okinoerabushima	941	"	SV	98 ft, NE section	797 ft, SW section	S	
Minamio-agarijima	945	Daito	SV RA	52 ft, unk	Approx 200 ft	S, P(00z)	
Torishima	963	Nanpo Shoto	SV	272 ft, unk	1270 ft	S, W(06, 18z), RW (00, 12z)	

Name of reporting station, village or island	Intnl. Index No. 43	Island group or chain	Type of island	Height and general location of observing station on island	Highest point and location on island	Type of reports transmitted	Remarks
Pattler	860	Paracel	RA	23 ft, SW end	Approx 30 ft	S, P(08, 23z)	
Midway	91 066	Hawaiian chain	RA	43 ft, airfield in center	43 ft, central part	S, RW, P	
Iwo Jima	115	Volcano	SV	348 ft, N central part	554 ft, SW end	S, RW, P	
Marcus	131	Isolated island	RA	55 ft, central part	75 ft, central part	S, P, RW	
French Frigate Shoals	155	Hawaiian chain	RA	10 ft, one of the small atolls	221 ft, volcanic rock islet	S	
Kilauea Point (Kauai)	164	"	LV	186 ft, N part	5170 ft, central part	S	
Lihue (Kauai)	165	"	LV	148 ft, S coast	" " "	S, P, RW	
Makahuena Point (Kauai)	166	"	LV	Unk, S point	" " "	Irreg. synoptic	
Kaneohe Bay (Oahu)	176	"	LV	10 ft, E part	4046 ft ridge along W coast	P(00z)	Koolau range to the W 2500-3000 ft

Name of reporting station, village or island	Intnl. Index No.	Island group or chain	Type of island	Height and general location of observing station on island	Highest point and location on island	Type of reports transmitted	Remarks
Barbers Point NAS (Oahu)	178	Hawaiian chain	LV	50 ft, SW point	4046 ft ridge along W coast	P(00, 12z)	Waianae range to the N 4025 ft, Koolau range to E 2500-3000 ft
Honolulu (Oahu)	182	"	LV	15 ft, S coast	" " "	S, P	" " "
Makapuu Point (Oahu)	183	"	LV	540 ft, SE part	" " "	S	" " "
Puunene (Maui)	190	"	LV	104 ft, central part	10,025 ft volcano E section	S	" " "
Upolu Point (Hawaii)	195	"	LV	Unk, NW part	13,784 ft, central part	S	Loran station
Falalep (Ulithi)	203	Caroline	FA	Unk	Less than 30 ft	S	Trees to 82 ft
Agana/NAS (Guam)	212	Mariana	RA and SV	269 ft, W coast	1334 ft, SW corner	S, P (00z)	" " "
Anderson AFB (Guam)	218	"	RA and SV	530 ft, N central plateau	" " "	S, RW, P	" " "
Wake	245	Isolated island	FA	13 ft, SE part of atoll	21 ft, central part	S, RW, P	" " "
Eniwetok	250	Marshall	FA	11 ft, SE island of atoll	Less than 15 ft	S, RW, P	" " "

Name of reporting station, village or island	Intnl. Index No. 91	Island group or chain	Type of island	Height and general location of observing station on island	Highest point and location on island	Type of reports transmitted	Remarks
Rongerik	254	Marshall	FA	8-10 ft, SE part of atoll	10-15 ft	(AEC site, observations taken during AEC ops. only)	
Johnston	275	Isolated island	RA	8 ft, N side	70 ft, central part	S, RW, P	
Kailua (Hawaii)	281	Hawaiian chain	LV	Approx 6 ft, W central section	13,784 ft, central part	Irreg. synoptic	Volcano E of airport 8269 ft
Hilo (Hawaii)	285	Hawaiian chain	LV	36 ft, NE coast	"	S, RW, P	
Cape Kumukahi (Hawaii)	287	"	LV	41 ft, E point	"	S	
Truk (Moen)	334	Caroline	SV	8 ft, NW side	214 ft, W central part	S, RW, P	Surface observations taken between two 1000 ft hills
Kapinga-marangi	337	"	FA	10 ft, unk	Less than 30 ft	S, RW(00, 12z)Irreg	AEC site
Ponape	348	"	SV	151 ft, N side	2595 ft, central part	S, RW, P	
Kusaie	356	"	SV	Unk, E side	2064 ft, center	S	

Name of reporting station, village or island	Intnl. Index No. 91	Island group or chain	Type of island	Height and general location of observing station on island	Highest point and location on island	Type of reports transmitted	Remarks
Kwajalein	366	Marshall	FA	10 ft, SE side of atoll	10 ft, central part	S, RW, P	
Majuro	376	"	FA	10 ft, E side of atoll	16 ft, W part	S, RW, P	
Palmyra	385	Line	FA	6 ft, W side of atoll	Less than 10 ft	S	Special WEA MSC phoned to Honolulu
Koror (Palau)	408	Caroline	SV	109 ft, E side	420 ft central part	S, RW, P	
Yap	413	"	SV	56 ft, SE side	535 ft	S, RW, P	
Fanning	487	Line	FA	10 ft, W side	Approx 10 ft	S	Coconut trees 60 to 90 ft high
Christmas	489 490	Line	RA	5 to 10 ft, W side	40 ft, E central part	S, RW (03, 15z)	
Gizo	500	British Solomon	RA	10 ft, exact location unk	654 ft, S part	S	
Choiseul Bay (Choiseul)	501	"	LV	300 ft, NW end	3500 ft, center	S	NE side is mountainous, rugged, and steep. Thick - ly wooded

Name of reporting station, village or island	Intnl. Index No.	Island group or chain	Type of island	Height and general location of observing station on island	Highest point and location on island	Type of reports transmitted	Remarks
Roviana	503	British Solomon	RA	27 ft, exact location unk	376 ft, western part	S	Densely wooded
Honiara (Guadalcanal)	517	"	LV	30 ft, N coast	8000 ft, S coast	S, P(00, 06, 18z)	
Pawa (Ugi)	526	"	SV	Near sea level, W coast	670 ft, central part	S	
Nauru	530	Isolated island	RA	120 ft, W side	About 220 ft, central part	S, P(00, 18z)	
Ocean	533	"	RA	Near 215 ft, SW side	265 ft, central part	S	
Vanikoro	543	Santa Cruz	LV	Near sea level, SW side	3031 ft, central part	S	Active volcanic island with mts descending directly to the sea
Pt. Patterson (Vanua Lava)	551	Banks	SV	137 ft, E coast	2620 ft, two conical peaks on NE coast	S	300 ft volcanic ridge N-S
Luganville (Espiritu Santo)	554	New Hebrides	LV	50? ft, SE side	6169 W part	S, P(03z, 21z)	Numerous ranges extending to 6000 ft
N Vila (Efate)	558	"	RA	65 ft, SW side	2203 ft, NW side	S, P(00, 06, 12, 18z)	489 ft hill 1-1/2 mi NE of Vila

Name of reporting station, village or island	Intnl. Index No.	Island group or chain	Type of island	Height and general location of observing station on island	Highest point and location on island	Type of reports transmitted	Remarks
Erromanga	562	New Hebrides	LV	650 ft, exact location unk	3100 ft, M part	S	
Aneityum	568	"	SV	27 ft, SW side	2788 ft, W part	S	
Koumac	577	New Caledonia	LV	56 ft, NW coast	5380 ft, S end	S, P(03, 21z)	Two peaks to SE 5348 ft, 3589 ft
Fayoue (Ouvea)	579	"	RA	3 ft, S end	Less than 100 ft	S	
Chepenehe (Lifou)	582	"	RA	66 ft, N end	250 ft	S, P(21z)	
Tadine (Mare)	587	Loyalty	RA	66 ft, SW end	Less than 300 ft	S	
Tontouta	590	New Caledonia	LV	49 ft, SW end	5380 ft, S end	S, P(21z)	Mountain peaks to E 4500 ft
Yate	591	"	LV	1217 ft, SE end	5330 ft, S end	S	Mountain peaks to NW 7-5000 ft
Noumea	592	"	LV	228 ft, SW end	5380 ft, S end	S, P(03, 09, 21z)	Mountain peaks to N 4-5000 ft
Kuto (ile des Pins)	596	"	S	21 ft, SW side	873 ft, SW part	S	

Name of reporting station, village or island	Intnl. Index No.	Island group or chain	Type of island	Height and general location of observing station on island	Highest point and location on island	Type of reports transmitted	Remarks
Butaritari (Makin)	601	Gilbert	FA	5 ft, exact location unk	Less than 10 ft	S	Densely wooded with pandanus and coconut trees
Tarawa	610	"	FA	10 ft, SE side	10 ft	S, P(00, 06, 12, 18z)	
Beru	623	"	FA	10 ft, SW side	10-15 ft	S	
Arorae	629	"	FA	20 ft, center	20 ft, center	S	
Nanumea	631	Ellice	FA	5 ft, W side	Less than 10 ft	S	
Nui	636	"	FA	8 ft, E side	Less than 10 ft	S	
Funafuti	643	"	FA	13 ft, E side	10-15 ft	S, P(00, 06, 12, 18z)	
Nurakita	648	"	FA	10 ft, exact location unk	Approx 10 ft or more	S	Tops of coconut trees 60 to 80 ft
Rotuma	650	"	SV	90 ft, W side	840 ft center	S, P(00, 12z)	
Undu Point (Vanua Levu)	652	Fiji	LV	205 ft, NE point	3386 ft, S central part	S	Village on slope of 440 ft hill



Name of report- ing station, village or island	Intnl. Index No. 91	Island group or chain	Type of island	Height and general location of observ- ing station on island	Highest point and location on island	Type of reports trans- mitted	Remarks
Nasea (Vanua Levu)	657	Fiji	LV	49 ft, N coast	3386 ft, S central part	S	Town
Nambouwalu (Vanua Levu)	659	"	LV	117 ft, SW coast	" "	S	Peak 2763 ft, 10 mi to NE
Yasawa	660	"	SV	165 ft, SW coast	970 ft, near SW end	S	
Nathekoro (Vanua Levu)	663	"	LV	53 ft, S coast	3386 ft, S central part	S	
Matei (Taveuni)	665	"	LV	64 ft, N end	4076 ft, S central part	S	
Levuka (Ovalau)	678	"	SV	10 ft, E side	2050 ft, center	S	
Nandi (Viti Levu)	680	"	LV	51 ft, W side	4341 ft, N central part	S, RW (00z), W (06, 12, 18z)	Several peaks on Viti Levu over 3500 ft
Nausori (Viti Levu)	683	"	LV	12 ft, ten mi E of Suva	" "	S	
Lauthala Bay (Viti Levu)	690	"	LV	18 ft, SE coast	" "	S	Several high peaks to N and W, 3948 ft
Lakemba	691	"	SV	10 ft, SW coast	720 ft, center	S	

Name of reporting station, village or island	Intnl. Index No.	Island group or chain	Type of island	Height and general location of observing station on island	Highest point and location on island	Type of reports transmitted	Remarks
Vunisea (Kandavu)	693	Fiji	SV	109 ft, N central coast	2750 ft, center	S	
Matuku	697	"	SV	12 ft, middle of W side	1262 ft, center	S	
Ono-i-lau	699	"	SV	70 ft, probably on SW side	370 ft, NW part	S	Ono-i-lau consists of a cluster of 3 volcanic islands
Canton	700	Phoenix	FA	5 ft, NE side	Less than 10 ft	S, RW(00, 12z) P(06, 18z)	
Gardner	705	"	FA	5 ft, W side	Less than 10 ft	S	Palm trees reach 90 ft on NW end of atoll
Huli	710	"	FA	5 ft, W side	Less than 10 ft	S	
Atafu	720	Tokelau	FA	5 ft, NW end of atoll	Less than 10 ft	S	
Nukunono	724	"	FA	5 ft, S end of atoll	Less than 10 ft	S	
Fakaofu	728	"	FA	10 ft, W side	10 ft, center	S	Palm trees 80-90 ft

Name of reporting station, village or island	Intnl. Index No. 91	Island group or chain	Type of island	Height and general location of observing station on island	Highest point and location on island	Type of reports transmitted	Remarks
Mata-Utu (Wallis)	753	Isolated island	SV	10 ft, S side	475 ft, near center	S	
Faleolo (Upolu)	759	Samoa	LV	13 ft, W of Apia	3609 ft, center	S	
Apia (Upolu)	762	"	SV	5 ft, N coast	" " " " " "	S, P(00, 06, 12, 18z)	
Tafuna (Tutuila)	765	"	SV	10 ft, SW part	2141 ft, center	S	Weather reports irregular. Rugged, wooded mt ridge (EW) extends length of Tutuila
Keppel	776	Tonga or Friendly	SV	10 ft, SW side	350 ft, center	S	Fairly flat island
Vavau	780	"	SV	25 ft, W side	610 ft, SW end	S	Cliffs 200-600 ft high on NW, N and NE coasts
Haapai	784	"	Mixed	10 ft, exact location unk	Two islands 1600 ft 1700 ft	S	Consists of several small islands
Nukualofa (Tongatapu)	788	"	RA	5 ft, N coast	200 ft on S end	S, P(00, 06, 12, 18z)	Shallow lagoon in interior

Name of reporting station, village or island	Intnl. Index No. 91	Island group or chain	Type of island	Height and general location of observing station on island	Highest point and location on island	Type of reports transmitted	Remarks
Penrhyn (Tongareva)	800	Cook	FA	5 ft, easternmost island	Less than 10 ft	S, P(00, 06, 12, 18z)	50 ft palm trees
Rakahanga	804	"	FA	15 ft, location unk	Approx 15 ft	S	
Manihiki	808	"	FA	5 ft, W side atoll	Less than 10 ft	S	
Danger	811	"	FA	5 ft, northern island of atoll	Less than 10 ft	S	Palm trees to 30 ft
Niue	822	"	RA	65 ft, W side	200 ft, center	S	
Palmerston	826	"	FA	10 ft, westernmost island	10-15 ft	S	
Aitutaki	830	"	SV	15 ft, W coast	460 ft, N end	S, P(00, 06, 12, 18z)	200 ft N-S ridge through center of island
Mauke	840	"	RA	30 ft, center	30 ft, center	S	Trees reach 150 ft
Rarotonga	843	"	SV	15 ft, N side	2110 ft, center	S, P(00, 06, 12, 18z)	Precipitous volcanic peaks
Jarvis	901	Line	FA	18 ft, W side	Approx 20 ft	Irreg synoptic	

Name of reporting station, village or island	Intnl. Index No. 91	Island group or chain	Type of island	Height and general location of observing station on island	Highest point and location on island	Type of reports transmitted	Remarks
Malden	902	Line	RA	15 ft, W side	Approx 30 ft	S, RW(03z, 15z)	
Taiohae (Nuku Hiva)	920	Marquesas	LV	33ft, SE coast	3890 ft, NW part	S, P(18z)	
Atuona (Hiva Oa)	925	"	LV	16 ft, SE coast	3520 ft, W of center	S	Town on N side of bay
Napuka	927	"	FA	5 ft, exact location unk	Approx 5 ft	S, P(00z)	E and W sides are wooded but the S side is nearly bare
Puka-Puka	928	"	FA	7 ft, exact location unk	6 ft, central part	S	
Bora Bora	930	Society	SV	10 ft, SW coast	2386 ft, center	3, P(18z)	Surrounded by hills
Mopelia	931	"	FA	7 ft, exact location unk	Approx 7 ft	S	Coconut trees and brushwood on a number of islets
Uturoa (Raiatea)	934	"	LV	7 ft, N part	3389 ft, center	S	Mountainous character and covered with vegetation
Papeete (Tahiti)	938	"	LV	7 ft, NW coast, in bay	7339 ft, NW central	S, P(00z, 18z)	

Name of reporting station, village or island	Intnl. Index No. 91	Island group or chain	Type of island	Height and general location of observing station on island	Highest point and location on island	Type of reports transmitted	Remarks
Kaukura	939	Marquesas	RA	7 ft, N side	Approx 30 ft	S	
Makatea	940	Tuamotu	RA	174 ft, NW side	230 ft, center	S	Cliff along E coast
Rangiroa	941	"	FA	7 ft, N side of atoll	Approx 7 ft	S	
Hikueru	942	"	FA	7 ft, NW side of atoll	Less than 10 ft	S	
Takarao	943	"	FA	7 ft, SW side of atoll	Approx 7 ft	S, P(00z)	
Tureia	946	"	FA	5 ft, exact location unk	Approx 5 ft	S	Well wooded except on SE side
Anaa	947	"	FA	7 ft, NE side of atoll	Approx 7 ft	S	Partly wooded
Rikitea (Mangareva)	948	"	SV	13 ft, E side	1447 ft, SE point	S	
Reao	949	"	FA	7 ft, exact location unk	Approx 7 ft	S	Shrubs and coconut trees
Rurutu	950	Austral	SV	12 ft, NE side	1300 ft, N end	S, P(00z)	
Tubuai	954	"	SV	10 ft, N side	1309 ft, E side	S	

Name of reporting station, village or island	Intnl. Index No. 91	Island group or chain	Type of island	Height and general location of observing station on island	7 ft, W side	SV	30 ft, E side	2077 ft, W coast	1434 ft	S	Type of reports transmitted	Remarks
Raivavae	956	Austral	SV	7 ft, W side								Rugged hills, mostly covered with trees
Rapa	958	"	SV	30 ft, E side							S, P(00z)	Several 1000 ft peaks
Pitcairn	960	Isolated island	SV	870 ft, N side							S	E shore line has steep cliff
Lore Howe	91, 93 995	"	SV	35 ft, unk							P(22,04, 10,16z)	Mountainous and wooded
Norfolk	996	"	SV	360 ft, SW part							S, W(00z), RW(06z), P(06,12, 18z)	Mountainous
Raoul (Kermadec)	997	"	SV	160 ft, W side							S, RW(00z) P(00,06, 12z)	"
Madang (New Guinea)	94 014	New Guinea	LV	20 ft, NE coast								S, P(04, 16, 22z)
Lae (New Guinea)	027	"	LV	12 ft, E coast								S, P(04, 10, 16, 22z)

Name of reporting station, village or island	Intnl. Index No. 94	Island group or chain	Type of island	Height and general location of observing station on island	Highest point and location on island	Type of reports transmitted	Remarks
Port Moresby (New Guinea)	035	New Guinea	LV	100 ft, SE coast	13,363 ft, 40 mi NE	S,P(04, 10,16, 22z)	
Momote (Manus)	044	Admiralty	LV	17 ft, NE coast	3100 ft, S central part	S,P(01, 19z)	
Rabaul (New Britain)	085	Bismarck Archipelago	LV	20 ft, NE coast	8000 ft, 30 mi SW	S,P(04, 10,16, 22z)	
Willis	299	Isolated island	FA	26 ft, S islet	Less than 30 ft	S,P(02, 20z)	
Pitu (Morotai)	97 404	Indonesia	LV	50 ft, S coast	4101 ft, central part	S,P(00, 06,12z)	
Mapia	450	New Guinea	FA	10 ft, unk	Less than 30 ft	S,P(00, 06,18z)	Number of high coconut trees
Jefman (New Guinea)	502	"	LV	5 ft, NW coast of Vogelkop	9843 ft, N central Vogelkop	S,P(00, 06,12, 18z)	
Mokmer (Blak)	560	Schouten	SV	33 ft, S coast	3392 ft, NW part	S,P(00, 06,12, 18z)	



Name of reporting station, village or island	Intnl. Index No.	Island group or chain	Type of island	Height and general location of observing station on island	Highest point and location on island	Type of reports transmitted	Remarks
Sentani (New Guinea)	690	New Guinea	LV	324 ft, N coast	7000 ft, 5 mi W	S, P(00, 06, 12, 18z)	
Calayan	98 133	Babuyan (Philippines)	SV	43 ft, S coast	1780 ft, center	S	
Basco (Batan)	135	Batan (Philippines)	LV	36 ft, N section	3307 ft, N end	S, P(06, 18z)	

## UPPER WIND CLIMATOLOGY OF SOUNDING STATIONS

Middle and high latitude synoptic meteorologists, in furthering their understanding of day-to-day changes, refer constantly to mean pressure or pressure-height charts and are particularly concerned with anomalous departures from these mean charts. The low latitude synoptic meteorologist, on the other hand, seeking to relate daily patterns to long period averages, must perforce compare synoptic wind fields with analyzed charts of mean resultant winds and steadiness. Chapters 5 and 6 illustrate how useful such comparisons can be, enabling meteorologists to see reflected in seasonal changes, the trend in synoptic situations, and to apply intelligently the concepts of climatology and persistence to their forecasting.

Ideally, an atlas of charts depicting monthly mean resultant winds and steadiness over the tropical Pacific and Southeast Asia for the standard levels of 850 mb (5000 ft), 700 mb (10,000 ft), 500 mb (20,000 ft), 300 mb (30,000 ft), and 200 mb (40,000 ft) should be compiled and published. As a substitute for this commendable project, which is beyond the scope of the present report, monthly mean resultant winds, steadiness, mean zonal wind speeds and mean wind speeds have been tabulated on pages 3-46 to 3-79 for 24 sounding stations in the region.

Although periods of record vary, they are sufficiently long (with one exception) to provide stable averages. The exception is Christmas Island (91489). During the three years observations were made, the upper tropospheric winds in early summer were light variable or easterly. For the same months, winds from an easterly quarter prevailed further west at Canton Island (91700). However, the mean resultant high tropospheric winds for the latter station, encompassing more than eight years, are westerly in early summer. The discrepancy arises from the fact that in some summers high-level westerlies prevail at Canton Island. In these same years at the same levels, it is probable that Christmas Island experiences westerlies (see figs 5-8 to 5-13).

For some stations (e.g. Clark Air Base), means are derived from more than one ascent per day, but for others (e.g. the Australian and Fijian stations), from not more than one ascent per day. For Australian and Fijian stations, wind speed is tabulated to the nearest knot, and steadiness, since it was derived from the standard vector deviation, to the nearest 5 per cent.

In the table the stations are listed in International numerical order. The following listing, in alphabetical order, should facilitate reference.

<u>Station</u>	<u>Number</u>	<u>Latitude</u>	<u>Longitude</u>	<u>Page</u>
Broome, Australia	94203	17°57'S	122°13'E	3-73
Canton Island	91700	02°46'S	171°43'W	3-71
Christmas Island	91489	02°00'N	157°23'W	3-69
Clark Air Base, Philippines	98327	15°10'N	120°34'E	3-77

<u>Station</u>	<u>Number</u>	<u>Latitude</u>	<u>Longitude</u>	<u>Page</u>
Cloncurry, Australia	94335	20°40'S	140°30'E	3-76
Daly Waters, Australia	94234	16°16'S	133°23'E	3-74
Darwin, Australia	94120	12°26'S	130°52'E	3-72
Eniwetok Atoll	91250	11°20'N	162°20'E	3-60
Guam	91213	13°34'N	144°55'E	3-53
Hilo, Hawaii	91285	19°44'N	155°04'W	3-62
Hong Kong	45004	22°19'N	114°10'E	3-46
Iwo Jima	91115	24°47'N	141°20'E	3-55
Johnston Island	91275	16°44'N	169°31'W	3-61
Kadena, Okinawa	47931	26°21'N	127°45'E	3-51
Kagoshima, Japan	47827	31°38'N	130°36'E	3-49
Koror, Palau	91403	07°21'N	134°29'E	3-67
Kwajalein	91366	03°43'N	167°44'E	3-65
Lihue, Kauai	91165	21°59'N	159°21'W	3-57
Majuro	91376	07°06'N	171°24'E	3-66
Marcus Island	91131	24°17'N	153°53'E	3-56
Midway Island	91066	28°13'N	177°22'W	3-54
Nandi, Fiji	91630	17°45'S	177°27'E	3-70
Naze	47909	23°23'N	129°33'E	3-50
Ocean ship N		30° N	140° W	3-78
Ocean ship V		34° N	164° E	3-79
Ponape	91343	06°58'N	153°13'E	3-64
Port Hedland, Australia	94312	20°23'S	113°37'E	3-75
Singapore	48694	01°21'N	103°54'E	3-53
Tateno, Japan	47646	36°03'N	140°08'E	3-47
Torishima	47963	30°29'N	140°13'E	3-52
Truk	91334	07°27'N	151°50'E	3-63
Wake Island	91245	19°17'N	166°39'E	3-59
Yap	91413	09°31'N	133°03'E	3-68
Yonago, Japan	47744	35°26'N	133°21'E	3-48

(NOTE: Page numbers 3-44 and 3-45 inadvertently omitted)

850 mb							
Mean resultant winds and steady-	N	Ø	Vr	S	u	c	
ness at standard pressure levels.							
Station: Hong Kong (45004)	248	205	3.8	36	1.6	10.5	Jan
22°19'N, 114°10'E	223	220	9.7	68	6.2	14.2	Feb
Period: Sep. 1955-Aug. 1959	246	212	9.1	69	4.8	13.1	Mar
	236	211	7.5	65	3.7	11.5	Apr
	243	203	9.2	63	3.6	14.7	May
N = number of observations	227	215	10.3	68	5.9	15.1	Jun
Ø = mean resultant wind direction	245	181	6.2	45	0.1	13.7	Jul
Vr = mean resultant wind speed (kn)	240	128	7.7	47	-6.1	16.2	Aug
	222	069	7.2	52	-6.7	13.9	Sep
S = steadiness (percent)	240	062	10.5	78	-9.3	13.5	Oct
u = mean zonal wind speed (kn, E)	238	066	9.2	71	-8.4	13.0	Nov
c = mean wind speed (kn)	240	080	3.4	35	-3.3	9.7	Dec

700 mb						500 mb						
N	Ø	Vr	S	u	c	N	Ø	Vr	S	u	c	
248	258	20.6	91	20.1	22.5	248	261	44.2	92	43.7	47.9	Jan
223	260	25.6	94	25.2	27.1	223	262	51.5	95	51.0	54.1	Feb
246	247	16.2	76	14.9	21.4	246	258	38.6	97	37.8	40.0	Mar
235	253	14.5	82	13.8	17.7	233	261	24.9	90	24.6	27.6	Apr
242	234	13.6	82	11.0	16.6	242	245	15.9	85	14.4	18.6	May
223	231	12.2	73	9.5	16.5	214	234	7.7	54	6.2	14.4	Jun
244	174	7.2	54	-0.7	13.2	243	136	7.3	55	-5.1	13.4	Jul
235	136	7.8	47	-5.4	16.4	224	113	8.2	55	-7.5	15.1	Aug
219	085	4.4	35	-4.4	12.9	214	082	5.9	49	-5.8	12.0	Sep
235	358	5.5	50	0.2	11.0	238	276	7.9	57	7.9	13.9	Oct
238	282	3.9	31	3.8	12.1	237	266	23.4	91	23.3	25.6	Nov
229	260	12.2	75	12.0	16.4	213	263	36.2	94	35.9	38.6	Dec

300 mb						200 mb						
N	Ø	Vr	S	u	c	N	Ø	Vr	S	u	c	
210	256	66.2	93	64.3	71.2	120	253	75.0	93	71.7	81.0	Jan
200	263	77.5	98	77.0	79.7	104	259	82.5	96	81.0	85.7	Feb
230	258	62.5	96	61.1	65.2	115	257	72.5	99	70.6	73.2	Mar
222	264	41.1	94	40.9	43.5	112	264	51.2	95	50.8	54.0	Apr
223	267	15.2	74	15.2	20.5	116	282	21.4	78	20.9	27.2	May
204	350	2.4	16	0.4	15.0	103	023	10.7	46	-4.2	23.5	Jun
226	092	12.0	76	-0.4	15.7	112	082	22.4	86	-22.2	26.0	Jul
207	086	9.8	62	-9.8	15.7	110	069	15.0	66	-14.0	22.7	Aug
196	078	9.2	57	-9.0	16.2	91	081	7.5	44	-7.4	17.0	Sep
212	282	12.6	60	12.3	21.1	101	275	14.9	62	14.8	24.0	Oct
219	266	39.0	91	38.5	43.0	95	259	43.7	92	42.4	47.7	Nov
207	260	60.0	94	59.1	63.9	107	252	72.5	96	69.0	75.5	Dec

850 mb							
Mean resultant winds and steadiness at standard pressure levels.	N	θ	Vr	S	u	c	
Station: Tateno (47646)	372	268	16.3	75	16.3	21.8	Jan
36°03'N, 140°08'E	338	268	17.9	91	17.9	19.6	Feb
Period: Sept. 1952-Sept. 1956	372	257	11.3	64	11.3	17.7	Mar
Nov. 1956-Aug. 1958	360	243	10.1	60	9.2	16.7	Apr
N = number of observations	372	243	6.2	41	5.8	15.2	May
θ = mean resultant wind direction	360	221	4.3	36	2.9	11.9	Jun
Vr = mean resultant wind speed (kn)	372	230	4.3	38	3.3	11.3	Jul
S = steadiness (percent)	372	215	5.1	43	2.9	11.9	Aug
u = mean zonal wind speed (kn, E-)	329	211	7.2	47	3.7	15.2	Sep
c = mean wind speed (kn)	268	226	2.5	18	1.8	14.2	Oct
	330	256	8.0	50	8.0	15.9	Nov
	372	267	14.2	73	14.2	19.4	Dec

700 mb						500 mb						
N	θ	Vr	S	u	c	N	θ	Vr	S	u	c	
372	272	30.7	91	30.7	33.8	375	263	69.2	99	68.6	70.1	Jan
337	270	29.1	88	29.1	33.2	338	263	66.6	96	66.6	69.8	Feb
372	266	29.3	91	29.3	31.7	372	265	60.1	92	59.7	44.7	Mar
360	261	22.0	84	21.8	26.3	360	264	49.4	94	48.6	52.4	Apr
372	262	17.1	76	15.9	22.4	372	250	42.4	92	42.2	46.1	May
360	263	14.8	80	14.6	18.5	360	262	34.2	91	34.0	37.5	Jun
372	263	10.5	64	9.9	16.1	371	274	17.5	70	17.3	25.1	Jul
372	250	10.1	61	9.6	16.5	372	263	12.7	56	12.7	22.0	Aug
329	238	17.3	81	14.6	21.4	329	247	32.5	87	29.5	37.1	Sep
268	248	16.7	75	15.5	22.4	268	250	43.5	92	41.7	47.4	Oct
329	262	23.2	84	22.8	27.4	328	258	57.3	92	55.7	62.0	Nov
372	270	28.2	88	28.2	32.1	372	265	68.0	94	67.8	71.9	Dec

300 mb						200 mb						
N	θ	Vr	S	u	c	N	θ	Vr	S	u	c	
340	267	108.2	97	108.0	112.4	239	267	119.7	97	119.5	128.8	Jan
301	266	109.8	97	109.0	113.3	233	267	118.7	98	118.5	121.6	Feb
352	266	89.4	94	89.2	94.8	265	270	95.8	96	95.6	100.1	Mar
354	264	77.6	95	76.4	82.0	289	268	87.1	95	86.9	91.9	Apr
370	261	68.4	90	68.0	75.8	334	264	85.5	92	85.1	93.1	May
359	260	60.9	92	60.2	65.8	345	262	76.2	91	75.8	83.9	Jun
369	283	26.9	73	26.3	36.6	366	293	33.8	71	31.3	47.4	Jul
371	273	17.3	55	17.3	31.3	367	286	18.1	48	17.5	37.9	Aug
325	252	46.3	88	43.7	52.6	315	252	55.5	91	52.2	70.2	Sep
263	247	74.0	94	67.6	78.3	227	250	82.5	93	81.8	93.5	Oct
297	256	99.2	95	95.5	103.6	205	259	114.2	96	111.3	118.8	Nov
331	263	105.9	97	104.6	108.4	207	266	122.5	97	122.0	126.0	Dec

47744

850 mb						
Mean resultant winds and steadiness at standard pressure levels.	N	θ	Vr	S	u	c
Station: Yonago (47744)	372	278	20.2	89	20.0	22.8
35°26'N, 133°21'E	338	275	13.8	70	13.8	19.4
Period: Sept. 1952-Aug. 1958	372	272	10.6	57	10.6	18.5
	360	256	10.7	63	10.1	16.9
	370	247	9.0	53	6.8	16.9
N = number of observations	355	236	8.8	57	7.6	15.4
θ = mean resultant wind direction	372	239	12.7	73	11.1	17.3
Vr = mean resultant wind speed (kn)	372	224	5.7	42	4.1	13.6
	360	218	5.1	32	3.1	15.5
S = steadiness (percent)	372	274	4.3	30	4.3	14.2
u = mean zonal wind speed (kn, E-)	360	277	8.4	54	8.4	15.5
c = mean wind speed (kn)	372	275	16.9	80	16.9	21.2

700 mb						500 mb					
N	θ	Vr	S	u	c	N	θ	Vr	S	u	c
372	279	32.3	88	32.1	36.8	363	272	67.8	96	67.5	70.3
338	278	32.3	93	32.1	34.6	331	271	61.5	94	61.5	65.6
372	274	26.3	87	26.3	30.3	368	270	55.3	93	55.4	59.7
360	269	20.6	89	20.6	25.1	359	266	47.2	92	47.2	51.3
369	268	14.6	64	14.6	22.8	364	265	38.9	88	38.7	44.1
355	260	15.0	69	14.6	21.6	353	260	29.1	88	28.6	32.9
372	258	15.7	79	15.4	20.0	369	269	20.4	76	20.4	27.1
372	251	9.6	61	9.0	15.5	370	259	13.4	65	13.3	20.4
360	249	14.2	72	13.1	19.6	358	249	31.9	87	29.3	36.8
371	265	13.8	73	13.6	19.1	367	259	37.7	90	37.3	42.0
359	271	21.0	85	21.0	24.7	357	264	51.7	91	51.4	56.7
372	277	32.1	92	31.7	35.0	371	269	67.2	95	67.2	70.5

300 mb						200 mb					
N	θ	Vr	S	u	c	N	θ	Vr	S	u	c
269	266	100.8	95	100.4	105.1	160	262	117.5	97	116.2	120.5
274	267	93.8	94	93.6	99.8	158	263	111.9	96	111.1	116.5
311	270	83.7	93	83.7	89.7	181	269	98.4	98	98.4	100.4
302	265	70.5	94	70.1	74.8	100	269	77.7	95	77.2	82.2
340	263	65.8	93	65.8	70.8	173	267	80.6	97	80.2	83.1
311	263	53.0	89	52.8	65.8	201	267	63.8	88	56.1	73.2
349	273	27.4	76	27.2	36.0	286	284	31.9	70	31.1	45.7
358	267	17.7	65	17.7	27.2	292	282	17.9	51	17.5	34.8
331	253	47.0	89	44.7	52.8	221	255	55.3	91	52.8	60.9
317	255	62.2	91	59.7	68.0	200	252	76.7	92	72.3	83.5
297	257	85.1	97	80.6	88.0	150	257	110.9	98	105.9	112.8
288	265	96.1	95	95.7	100.6	153	265	112.1	97	111.8	114.8

850 mb							
Mean resultant winds and steady- ness at standard pressure levels.	N	θ	Vr	S	u	c	
Station: Kagoshima (47827)	372	293	19.1	81	17.1	23.3	Jan
31°38'N, 130°36'E	338	290	14.0	68	13.3	20.4	Feb
Period: Sept. 1952-Aug. 1958	371	278	10.9	52	10.7	21.0	Mar
	357	252	7.8	47	7.4	16.5	Apr
N = number of observations	370	233	5.1	29	3.9	17.7	May
θ = mean resultant wind direction	352	246	9.6	54	8.8	17.7	Jun
Vr = mean resultant wind speed (kn)	365	235	9.9	57	8.4	17.3	Jul
	368	171	3.7	27	-0.6	13.6	Aug
	342	191	3.3	22	0.6	14.2	Sep
S = steadiness (percent)	371	311	2.5	20	1.9	12.7	Oct
u = mean zonal wind speed (kn, E-)	357	302	4.5	32	3.7	14.0	Nov
c = mean wind speed (kn)	370	296	13.0	73	12.3	18.9	Dec

700 mb						500 mb						
N	θ	Vr	S	u	c	N	θ	Vr	S	u	c	
369	278	35.4	92	35.0	38.5	336	269	67.5	98	67.4	69.8	Jan
337	276	29.9	89	30.3	33.4	321	270	62.2	97	62.2	64.1	Feb
371	274	27.8	88	27.8	31.7	356	271	54.2	96	54.2	56.3	Mar
357	266	22.0	80	22.0	27.6	349	269	42.9	89	42.4	48.4	Apr
368	263	16.7	72	16.5	23.2	363	261	37.9	89	37.5	42.6	May
353	255	18.9	79	18.5	23.9	343	262	33.8	91	33.6	36.9	Jun
365	250	13.4	76	13.1	17.7	361	269	12.5	53	12.5	23.5	Jul
366	204	5.7	36	2.3	15.5	365	227	4.5	28	3.5	16.1	Aug
333	241	8.0	44	7.0	18.1	325	254	17.3	69	16.5	25.1	Sep
369	269	13.1	74	13.1	17.5	367	264	35.4	92	35.0	38.3	Oct
356	275	19.1	85	18.9	22.4	355	263	49.4	94	49.0	52.6	Nov
370	275	28.2	90	28.5	31.3	357	263	63.8	97	63.1	65.8	Dec

300 mb						200 mb						
N	θ	Vr	S	u	c	N	θ	Vr	S	u	c	
216	265	107.6	98	97.6	109.1	140	263	132.9	97	132.0	136.8	Jan
155	267	100.0	98	99.8	102.7	85	265	128.0	99	127.1	128.8	Feb
292	270	76.7	98	76.7	78.3	207	271	91.4	97	91.4	94.1	Mar
294	269	66.6	95	66.6	70.1	206	272	84.6	96	84.6	89.1	Apr
321	266	60.1	91	60.1	64.7	242	272	75.6	94	75.6	80.6	May
298	265	46.5	90	46.5	51.5	244	269	54.0	86	54.0	62.7	Jun
347	281	12.5	54	12.3	23.0	311	303	13.3	48	11.3	27.6	Jul
363	252	2.7	14	2.5	19.6	326	305	3.9	16	3.1	23.9	Aug
292	262	22.4	73	22.0	30.5	250	268	23.7	72	23.7	33.0	Sep
320	262	53.2	94	52.6	56.1	240	265	62.0	88	61.5	69.9	Oct
286	262	85.8	96	84.5	89.1	146	263	101.0	96	99.6	104.9	Nov
216	265	99.4	97	99.0	102.1	93	266	121.9	98	121.3	124.4	Dec

850 mb							
Mean resultant winds and steady- ness at standard pressure levels.	N	O	Vr	S	u	c	
Station: Naze (47909)	183	297	13.8	71	12.3	19.4	Jan
28°23'N, 129°33'E	170	300	12.9	68	11.1	18.9	Feb
Period: Mar. 1955-Aug. 1958	248	276	13.3	70	13.1	18.9	Mar
	211	268	9.7	53	8.0	18.5	Apr
N = number of observations	226	246	12.1	58	11.1	20.6	May
θ = mean resultant wind direction	236	230	14.8	74	8.8	20.0	Jun
Vr = mean resultant wind speed (kn)	246	209	7.6	31	3.9	24.3	Jul
	248	191	7.0	42	1.4	16.5	Aug
S = steadiness (percent)	171	129	2.5	15	-1.9	17.5	Sep
u = mean zonal wind speed (kn, E-)	184	357	5.8	39	0.4	14.8	Oct
c = mean wind speed (kn)	172	006	5.8	37	-0.6	15.9	Nov
	183	323	10.9	67	6.4	16.3	Dec

700 mb						500 mb						
N	θ	Vr	S	u	c	N	θ	Vr	S	u	c	
183	274	32.9	95	32.9	34.6	182	265	67.8	98	67.5	69.2	Jan
170	267	32.1	99	31.9	32.3	169	264	65.2	93	65.1	70.3	Feb
248	271	28.2	91	28.2	30.7	246	269	53.0	97	53.0	54.9	Mar
196	261	26.3	89	25.9	29.5	210	263	44.9	95	44.5	47.2	Apr
225	254	22.2	83	21.6	26.7	226	260	35.4	93	34.6	37.9	May
236	237	21.0	86	17.5	24.3	235	248	24.5	87	22.4	28.2	Jun
245	218	5.5	39	3.5	14.0	247	242	2.1	16	2.1	13.8	Jul
246	194	4.1	25	0.9	16.5	244	185	4.5	30	0.4	14.8	Aug
172	226	4.7	29	3.3	18.1	171	247	7.2	33	6.6	21.6	Sep
185	264	10.9	67	10.7	16.1	185	253	26.5	90	25.3	29.3	Oct
175	264	16.1	77	15.9	21.0	178	250	48.0	95	44.7	50.4	Nov
183	275	25.9	90	25.7	28.6	185	266	62.2	97	62.2	64.1	Dec

300 mb						200 mb						
N	θ	Vr	S	u	c	N	θ	Vr	S	u	c	
142	262	108.7	98	107.8	110.4	104	263	121.2	96	120.2	126.0	Jan
128	262	113.9	98	112.8	116.1	87	261	128.4	98	127.0	131.9	Feb
209	268	90.2	99	90.2	91.0	144	269	106.8	98	106.8	108.8	Mar
191	266	68.6	97	68.2	71.0	179	268	78.6	95	78.6	82.4	Apr
209	264	48.0	89	45.7	54.0	176	274	57.3	91	56.7	62.7	May
215	260	28.2	85	27.8	33.0	194	272	29.9	72	29.7	41.6	Jun
228	049	3.7	23	-2.7	16.1	206	036	9.9	48	-6.2	20.6	Jul
238	092	4.1	24	-4.1	17.1	213	052	6.6	32	-5.3	20.8	Aug
152	269	8.4	36	8.4	23.2	141	308	10.1	39	8.0	26.1	Sep
159	259	45.5	95	45.1	47.6	142	254	49.4	90	47.0	54.9	Oct
157	254	79.3	96	75.5	82.1	118	253	91.2	98	87.0	92.9	Nov
156	265	103.8	97	103.4	106.4	114	262	108.7	94	107.8	115.1	Dec



850 mb							
Mean resultant winds and steadiness at standard pressure levels,	N	θ	Vr	S	u	c	
Station: Kadena (47931)	236	301	7.3	46	6.2	15.7	Jan
26°21'N, 127°45'E	202	293	6.2	38	5.7	16.4	Feb
Period: July 1949-Feb. 1956;	228	276	10.0	61	9.9	16.3	Mar
May 1957-Dec. 1958; Feb.	217	245	9.0	56	8.2	16.0	Apr
1959-April 1959	225	238	11.3	68	9.5	16.7	May
	222	227	14.4	76	10.5	19.0	Jun
N = number of observations							
θ = mean resultant wind direction	240	203	6.0	41	2.3	14.6	Jul
Vr = mean resultant wind speed (kn)	225	168	4.4	31	0.9	14.4	Aug
S = steadiness (percent)	234	137	1.9	14	1.3	13.5	Sep
u = mean zonal wind speed (kn, E-)	251	048	3.8	33	2.8	11.4	Oct
c = mean wind speed (kn)	231	040	6.3	45	4.0	14.0	Nov
	270	352	4.2	30	0.6	13.8	Dec

700 mb						500 mb						
N	θ	Vr	S	u	c	N	θ	Vr	S	u	c	
236	274	29.2	92	29.1	31.6	216	267	56.7	96	56.6	59.0	Jan
202	273	27.9	90	27.9	31.1	192	269	57.2	97	57.2	59.1	Feb
225	272	27.8	94	27.8	29.5	211	272	47.7	96	47.7	49.5	Mar
215	262	20.9	87	20.7	23.9	207	267	34.4	92	34.3	37.2	Apr
225	254	18.8	90	18.1	20.9	220	264	25.6	93	25.5	27.6	May
220	236	16.9	83	14.0	20.4	215	249	18.0	81	16.8	22.1	Jun
237	193	4.5	32	1.0	13.9	234	159	1.9	16	0.7	12.2	Jul
225	171	3.9	27	0.6	14.4	221	135	3.4	24	2.4	14.3	Aug
233	208	2.5	17	1.2	14.3	230	227	2.9	18	2.1	15.8	Sep
252	54	7.7	57	7.4	13.5	251	256	18.3	82	17.8	22.2	Oct
229	4	13.7	72	13.6	18.9	230	259	33.7	91	33.1	37.0	Nov
270	272	21.8	87	21.8	25.0	262	264	50.5	96	50.3	52.7	Dec

300 mb						200 mb						
N	θ	Vr	S	u	c	N	θ	Vr	S	u	c	
140	264	93.8	98	93.3	95.6	111	263	103.7	98	102.9	105.8	Jan
129	265	103.1	98	102.6	105.6	86	263	105.9	98	105.2	108.5	Feb
161	270	88.2	98	88.2	90.3	116	270	96.3	96	96.3	100.4	Mar
181	270	59.1	96	59.1	61.6	164	270	70.5	96	70.5	73.3	Apr
208	270	35.7	93	35.7	38.2	203	278	42.8	89	42.3	47.9	May
197	263	17.1	71	17.0	24.1	194	283	17.4	57	16.9	30.3	Jun
213	082	7.4	47	7.3	15.9	208	065	13.8	58	12.5	23.8	Jul
209	092	7.8	46	7.7	17.0	208	074	9.6	43	9.2	22.2	Aug
224	294	1.4	08	1.3	16.7	221	307	4.3	19	3.4	22.1	Sep
236	264	30.4	86	30.2	35.4	230	262	34.8	85	34.5	41.1	Oct
204	260	58.5	95	57.6	61.5	184	257	62.2	94	60.6	66.0	Nov
220	263	81.9	97	81.3	84.2	164	263	90.9	97	90.3	93.8	Dec

850 mb							
Mean resultant winds and steadiness at standard pressure levels.	N	O	Vr	S	u	c	
Station: Torishima (47963)	89	275	18.5	90	18.3	21.6	Jan
30°29'N, 140°18'E	79	270	15.9	74	15.9	21.6	Feb
Period: Aug.-Sept. 1954, May-Aug. 1956; Oct. 1956-Apr. 1958; Jun-Aug 1958	93	266	16.1	73	16.1	22.0	Mar
	98	262	11.9	72	11.7	16.5	Apr
	91	243	12.9	66	10.7	15.4	May
	147	250	14.0	69	13.6	20.2	Jun
N = number of observations							
O = mean resultant wind direction	154	255	10.6	67	10.1	15.7	Jul
	185	195	4.5	39	1.2	11.9	Aug
Vr = mean resultant wind speed (kn)	88	188	11.3	62	1.6	18.1	Sep
S = steadiness (percent)	88	225	6.3	45	4.9	15.0	Oct
u = mean zonal wind speed (kn, E-)	89	246	6.0	35	5.5	17.1	Nov
c = mean wind speed (kn)	87	263	16.1	84	15.9	19.3	Dec

700 mb						500 mb						
N	O	Vr	S	u	c	N	O	Vr	S	u	c	
89	270	32.7	94	32.7	34.8	89	271	58.3	97	58.3	59.9	Jan
79	264	30.7	93	30.5	32.9	80	265	56.1	98	55.9	57.5	Feb
93	269	28.8	90	28.8	32.1	93	267	53.2	99	53.0	54.2	Mar
98	265	22.4	87	22.4	25.7	95	266	36.9	96	36.8	38.5	Apr
91	251	18.5	77	18.1	23.9	87	254	28.6	80	28.2	32.7	May
147	251	23.0	87	21.8	26.2	146	252	30.7	92	29.1	33.4	Jun
154	258	10.6	63	10.5	16.7	153	276	11.3	61	11.1	18.5	Jul
185	187	6.2	53	.8	11.7	181	165	2.3	21	.4	10.9	Aug
87	204	13.1	64	5.3	20.4	86	217	15.7	68	9.4	23.2	Sep
88	237	14.6	74	12.3	19.8	88	246	29.3	90	26.5	32.7	Oct
88	251	20.6	85	19.4	24.1	75	250	37.5	85	35.0	43.7	Nov
87	266	29.9	94	29.9	31.7	87	264	60.4	97	60.1	62.4	Dec

300 mb						200 mb						
N	O	Vr	S	u	c	N	O	Vr	S	u	c	
62	264	97.8	97	97.2	100.5	88	266	112.0	97	111.8	115.4	Jan
80	262	100.5	97	99.5	103.0	79	262	116.4	98	115.0	118.4	Feb
93	267	83.8	97	83.8	86.1	93	268	101.5	97	101.5	104.2	Mar
92	268	54.0	94	53.6	57.3	92	270	70.1	94	70.1	74.4	Apr
85	263	38.3	91	37.9	42.0	79	269	45.5	91	45.5	49.6	May
144	256	34.4	91	33.6	37.7	141	262	36.8	83	36.6	44.3	Jun
152	305	10.9	51	8.8	21.2	150	337	14.0	50	5.7	27.8	Jul
182	060	3.9	20	-3.3	19.1	178	052	8.2	34	-6.2	24.1	Aug
85	241	14.6	64	12.7	22.8	85	281	14.4	54	14.0	26.9	Sep
87	251	42.7	88	40.1	48.4	84	253	46.5	80	45.7	57.7	Oct
69	250	67.8	91	62.9	74.8	66	253	82.3	98	78.2	84.0	Nov
87	261	91.4	93	90.2	98.2	85	263	107.9	97	107.1	111.0	Dec

650 mb							
Mean resultant winds and steadiness at standard pressure levels	N	Ø	Vr	S	u	c	
Station: Singapore (48674)	119	023	6.6	55	-2.6	12.0	Jan
01°21'N, 103°54'E	111	005	7.6	70	-0.7	10.6	Feb
Period: Feb. 1955-Jan. 1959	120	007	4.1	51	-0.5	8.1	Mar
	115	298	3.3	76	3.0	20.2	Apr
N = number of observations	113	249	6.5	63	6.1	10.3	May
Ø = mean resultant wind direction	113	243	6.4	62	5.7	10.3	Jun
Vr = mean resultant wind speed (kn)	116	242	10.2	80	9.0	12.7	Jul
	112	257	6.2	50	6.1	12.5	Aug
S = steadiness (percent)	90	207	7.1	70	3.2	10.2	Sep
u = mean zonal wind speed (kn, E-)	102	213	6.9	65	3.7	10.6	Oct
	113	280	7.0	57	6.9	12.3	Nov
c = mean wind speed (kn)	116	345	7.2	57	1.9	12.7	Dec

700 mb						500 mb						
N	Ø	Vr	S	u	c	N	Ø	Vr	S	u	c	
121	043	2.8	27	-1.9	10.2	122	055	4.7	39	-3.6	11.9	Jan
112	353	3.3	35	0.4	9.5	113	077	6.2	51	-6.0	12.2	Feb
121	060	2.9	34	-2.5	8.5	119	092	7.0	55	-6.9	10.8	Mar
115	287	1.5	18	1.4	8.4	115	089	5.0	53	-5.0	9.5	Apr
113	265	4.9	50	4.9	9.8	119	102	4.0	40	-3.9	9.9	May
110	262	5.4	51	5.4	10.6	113	101	7.8	68	-7.7	11.5	Jun
117	266	8.3	66	8.2	12.6	114	101	8.3	60	-8.1	12.5	Jul
114	254	7.7	62	7.7	12.5	115	107	8.7	71	-8.3	12.3	Aug
91	195	2.1	21	0.5	9.8	91	090	10.3	82	-10.3	12.5	Sep
108	206	3.7	34	1.6	10.8	106	090	6.5	61	-6.5	10.6	Oct
115	274	7.6	59	7.6	12.8	112	215	0.9	09	0.5	9.8	Nov
118	310	4.3	45	3.3	9.6	118	051	2.2	23	-1.7	9.4	Dec

300 mb						200 mb						
N	Ø	Vr	S	u	c	N	Ø	Vr	S	u	c	
122	098	6.5	50	-6.4	13.0	120	117	15.9	76	-14.2	20.9	Jan
113	095	14.7	83	-14.6	17.6	112	118	28.6	93	-25.2	31.0	Feb
118	104	10.7	74	-10.4	14.4	119	120	15.7	76	-13.6	20.2	Mar
115	090	8.1	72	-8.1	11.3	116	108	12.9	77	-12.3	16.7	Apr
115	089	11.4	80	-11.4	14.3	112	078	19.4	86	-19.0	22.5	May
112	086	18.7	94	-18.7	19.9	110	073	31.5	93	-30.1	33.9	Jun
115	087	22.2	96	-22.2	23.1	112	077	39.1	95	-38.2	41.0	Jul
114	090	23.1	96	-23.1	24.1	113	075	39.3	96	-38.1	41.0	Aug
85	084	18.1	93	-18.0	19.5	81	072	36.5	97	-34.8	37.8	Sep
103	083	13.4	88	-13.3	15.3	103	076	22.3	90	-21.7	24.8	Oct
112	083	8.3	70	-8.3	11.8	109	086	16.5	80	-16.5	20.5	Nov
118	100	9.6	70	-9.5	13.7	117	108	20.6	86	-19.8	23.9	Dec

850 mb							
Mean resultant winds and steadiness at standard pressure levels.	N	O	Vr	S	u	c	
Station: Midway Island (91066)	637	269	12.3	54	12.3	23.0	Jan
28°13'N, 177°22'W	633	251	9.5	47	9.0	20.1	Feb
Period: July 1949-Nov. 1957	678	221	0.4	02	0.3	16.4	Mar
	671	189	0.4	03	0.1	12.9	Apr
N = number of observations	568	178	1.3	11	0.0	12.0	May
O = mean resultant wind direction	561	196	4.0	34	1.1	11.9	Jun
Vr = mean resultant wind speed (kn)	707	104	9.8	73	-9.5	12.6	Jul
S = steadiness (percent)	710	116	6.9	62	-6.2	11.1	Aug
u = mean zonal wind speed (kn, E-)	689	109	1.7	15	-1.6	11.3	Sep
	745	074	3.7	30	-3.6	12.3	Oct
	738	247	2.6	17	2.4	15.4	Nov
c = mean wind speed (kn)	626	250	5.6	28	5.2	20.1	Dec

700 mb						500 mb						
N	O	Vr	S	u	c	N	O	Vr	S	u	c	
637	271	22.2	70	22.2	31.5	480	273	33.3	76	33.3	43.8	Jan
624	263	19.5	73	19.3	26.6	566	272	35.7	86	35.7	41.7	Feb
672	273	7.5	40	7.5	18.7	651	280	17.3	66	17.1	26.4	Mar
666	276	6.3	39	6.3	16.1	633	279	15.5	65	15.3	23.7	Apr
561	274	3.8	28	3.8	13.4	511	306	13.4	53	10.9	25.3	May
562	232	3.1	24	2.5	12.9	549	289	5.8	37	5.5	15.5	Jun
701	094	8.2	67	-8.2	12.3	678	076	5.2	41	-5.1	12.6	Jul
712	103	4.7	45	-4.6	10.4	694	079	2.4	20	-2.3	11.9	Aug
679	047	1.2	09	-0.9	12.7	645	354	2.7	18	0.3	15.3	Sep
734	014	2.5	18	-0.6	14.1	712	318	6.1	32	4.1	19.3	Oct
740	276	9.1	47	9.1	19.4	705	279	19.0	67	18.7	28.4	Nov
612	267	15.8	61	15.8	25.9	564	271	29.3	74	29.3	39.6	Dec

300 mb						200 mb						
N	O	Vr	S	u	c	N	O	Vr	S	u	c	
360	282	56.8	81	55.6	70.1	280	289	62.5	86	59.3	72.6	Jan
423	286	55.6	85	53.6	65.6	297	291	72.8	86	67.8	84.4	Feb
583	287	31.1	74	29.8	42.3	499	293	55.1	86	50.7	64.1	Mar
561	287	23.3	68	22.3	34.3	427	294	30.8	71	28.1	43.3	Apr
551	288	9.3	52	8.8	18.0	444	320	14.8	44	9.6	33.3	May
519	326	11.2	48	6.2	23.1	484	341	15.7	52	5.2	30.1	Jun
631	037	6.6	34	-4.0	19.2	560	023	10.0	37	-3.9	26.9	Jul
644	024	4.9	25	-2.0	19.7	585	007	8.5	33	-1.0	26.1	Aug
576	018	4.7	21	-1.4	22.2	511	025	6.6	24	-2.8	28.0	Sep
639	330	10.0	36	5.0	28.1	557	333	12.7	38	5.8	33.7	Oct
616	291	28.9	72	27.1	40.3	502	298	32.4	71	28.7	45.6	Nov
398	282	43.3	76	42.1	56.7	281	279	47.6	76	47.0	62.4	Dec

450 mb							
Mean resultant winds and steadiness at standard pressure levels.	N	O	Vr	S	u	c	
Station: Iwo Jima (91115)	217	286	8.7	56	8.4	15.5	Jan
24°47'N, 141°25'E	186	263	8.2	49	8.1	16.0	Feb
Period: July 1949-April 1951;	186	249	6.2	44	5.7	14.2	Mar
Aug. 1951-Feb. 1952; Apr. 1952-May	197	213	5.3	45	3.2	11.6	Apr
1953; Aug. 1953-Dec. 1953; Feb. 1959-	189	212	7.8	51	4.2	12.7	May
Apr. 1959	162	201	8.3	51	2.9	13.6	Jun
N = number of observations	185	168	4.2	36	0.8	11.7	Jul
O = mean resultant wind direction	202	157	5.5	42	2.2	13.2	Aug
Vr = mean resultant wind speed (kn)	20	48	8.3	53	4.4	14.2	Sep
S = steadiness (percent)	212	227	5.2	46	4.1	11.5	Oct
u = mean zonal wind speed (kn, E-)	215	159	4.0	32	1.4	12.6	Nov
c = mean wind speed (kn)	250	272	2.6	19	2.6	13.9	Dec

700 mb						500 mb						
N	O	Vr	S	u	c	N	O	Vr	S	u	c	
217	274	27.5	88	27.4	31.1	197	273	50.8	94	50.7	54.1	Jan
186	269	24.8	86	24.8	28.8	168	269	53.1	95	53.1	55.9	Feb
189	267	20.5	86	20.5	23.7	186	271	42.8	97	42.8	44.3	Mar
197	257	12.1	75	11.8	15.9	191	272	25.4	90	25.4	28.2	Apr
194	239	9.0	69	7.7	13.1	190	260	13.2	77	13.1	17.2	May
164	210	7.5	55	3.7	13.7	157	220	5.9	41	3.8	14.3	Jun
185	164	2.6	21	0.7	12.1	179	102	2.4	20	2.4	12.2	Jul
210	157	4.3	33	1.7	13.1	206	128	4.1	30	3.2	13.8	Aug
202	152	7.6	52	3.5	14.7	198	138	6.8	47	4.5	14.4	Sep
213	182	3.5	31	0.1	11.2	211	227	4.9	38	3.6	12.8	Oct
221	244	8.1	54	7.3	15.1	216	253	19.8	80	18.9	24.6	Nov
250	264	16.7	79	16.6	21.2	238	266	36.7	90	36.6	40.7	Dec

300 mb						200 mb						
N	O	Vr	S	u	c	N	O	Vr	S	u	c	
155	272	72.1	95	72.0	76.1	138	271	81.5	96	81.5	85.2	Jan
126	273	80.9	96	80.8	84.5	112	269	88.3	96	88.3	92.2	Feb
160	274	70.5	96	70.3	73.8	152	274	83.1	96	82.9	86.6	Mar
180	274	45.5	95	45.4	48.1	145	281	57.3	94	56.3	60.9	Apr
182	276	18.5	76	18.4	24.4	178	291	21.8	69	20.3	31.8	May
149	238	0.9	05	0.8	17.6	148	025	5.5	24	2.3	23.3	Jun
166	059	5.1	30	4.4	16.9	156	054	10.5	40	8.5	26.3	Jul
198	096	5.1	31	5.1	16.7	187	066	7.1	29	6.5	24.8	Aug
194	119	5.2	28	4.5	18.7	185	078	6.1	26	6.0	23.3	Sep
204	267	7.2	40	7.2	17.9	199	290	11.3	50	10.6	22.4	Oct
203	265	29.6	85	29.5	34.7	192	271	35.8	87	35.8	41.2	Nov
207	269	53.8	90	53.8	59.9	180	270	65.5	93	65.5	70.7	Dec

850 mb							
Mean resultant winds and steadiness at standard pressure levels.	N	Ø	Vr	S	u	c	
Station: Marcus Island (91131)	371	266	8.8	66	8.8	13.3	Jan
24°17'N, 153°58'E	332	255	6.2	39	6.0	15.9	Feb
Period: Sept. 1952-Aug. 1956;	368	168	1.9	14	-0.8	14.0	Mar
Oct. 1956-Aug. 1958	358	150	5.3	44	-2.5	11.9	Apr
	370	141	5.7	53	-3.5	10.7	May
N = number of observations	358	142	4.1	40	-2.3	10.1	Jun
Ø = mean resultant wind direction	371	147	5.0	49	-2.3	11.9	Jul
Vr = mean resultant wind speed (kn)	351	121	7.7	57	-6.4	11.7	Aug
S = steadiness (percent)	284	107	9.9	73	-9.4	13.6	Sep
u = mean zonal wind speed (kn, E-)	368	119	8.4	61	-7.2	13.6	Oct
c = mean wind speed (kn)	350	123	6.0	47	-5.1	12.9	Nov
	363	155	0.9	07	0.0	14.8	Dec

700 mb						500 mb						
N	Ø	Vr	S	u	c	N	Ø	Vr	S	u	c	
363	271	23.0	92	23.0	24.9	354	270	48.2	96	48.2	50.5	Jan
330	265	20.6	83	20.6	24.9	328	269	48.2	95	40.2	50.9	Feb
371	262	12.7	70	11.9	18.1	368	270	31.7	90	31.7	35.4	Mar
358	238	5.5	41	4.5	13.3	359	269	17.3	77	17.3	22.4	Apr
372	263	3.1	31	-0.9	10.1	367	264	4.1	31	3.9	13.3	May
356	133	2.5	25	-1.9	10.5	357	160	0.9	08	-0.6	12.3	Jun
372	126	5.1	43	-2.7	11.7	369	080	2.7	23	-2.5	11.9	Jul
351	114	6.0	47	-5.5	12.9	348	092	4.9	40	-4.9	12.3	Aug
284	107	9.0	69	-8.6	13.1	286	095	9.6	65	-9.4	14.8	Sep
370	121	5.1	40	-4.3	12.7	366	101	3.9	28	-3.9	13.8	Oct
355	192	3.1	25	+0.4	12.5	353	249	9.4	52	8.8	17.9	Nov
359	263	10.9	60	10.7	18.1	359	271	30.1	88	30.1	34.0	Dec

300 mb						200 mb						
N	Ø	Vr	S	u	c	N	Ø	Vr	S	u	c	
265	278	68.4	99	67.8	69.2	180	278	68.0	98	67.4	69.2	Jan
254	275	68.8	96	68.6	69.8	205	273	72.7	94	72.5	77.4	Feb
337	276	53.4	84	53.0	63.8	299	275	71.5	94	70.5	76.4	Mar
354	271	32.7	85	32.7	38.3	312	287	43.3	84	42.6	51.5	Apr
357	293	9.2	47	8.0	19.3	345	304	12.3	45	10.7	27.2	May
350	074	2.9	18	-2.3	16.1	337	050	8.4	36	-6.8	23.3	Jun
353	047	55.1	33	-2.3	15.4	338	034	10.9	45	-6.0	24.3	Jul
328	049	7.0	46	-5.3	14.4	316	023	10.9	42	-4.3	26.3	Aug
258	075	9.7	52	-9.4	18.6	231	050	11.9	42	-9.0	27.8	Sep
341	091	1.9	11	-1.9	18.1	310	347	0.9	04	0.2	23.3	Oct
338	269	13.4	60	13.4	22.2	310	292	19.1	67	17.5	28.6	Nov
301	275	41.8	91	41.6	45.7	245	284	44.1	91	42.9	48.2	Dec

850 mb							
Mean resultant winds and steadiness at standard pressure levels.	N	O	Vr	S	u	c	
Station: Lihue (91165)	235	154	2.3	17	1.0	13.9	Jan
21°59'N, 159°21'W	216	073	3.8	26	3.6	14.7	Feb
Period: Feb. 1950-Dec. 1950	238	064	4.7	36	4.2	13.0	Mar
	236	061	9.0	68	7.9	13.2	Apr
N = number of observations	238	063	10.5	83	9.4	12.6	May
O = mean resultant wind direction	264	072	13.0	92	12.3	14.2	Jun
Vr = mean resultant wind speed (kn)	268	071	14.1	95	13.4	14.9	Jul
S = steadiness (percent)	269	068	13.4	90	12.5	14.9	Aug
u = mean zonal wind speed (kn, E-)	264	069	10.8	84	10.1	12.9	Sep
c = mean wind speed (kn)	276	069	9.3	70	9.1	14.1	Oct
	288	068	7.7	56	7.2	13.7	Nov
	263	068	8.1	54	7.5	14.9	Dec

700 mb						500 mb						
N	O	Vr	S	u	c	N	O	Vr	S	u	c	
235	244	4.8	30	4.3	15.8	231	273	16.0	65	16.0	24.5	Jan
216	256	2.1	13	2.0	16.6	213	277	13.4	57	13.3	23.6	Feb
238	255	2.1	14	2.1	14.7	236	273	13.0	59	13.0	21.9	Mar
236	072	3.6	28	3.4	12.7	233	285	6.4	40	6.2	16.1	Apr
238	068	5.6	52	5.1	10.8	238	291	3.1	25	2.9	12.6	May
263	085	9.7	82	9.7	11.9	263	098	3.6	27	3.6	13.3	Jun
268	087	9.0	76	9.0	11.9	267	212	1.9	16	1.0	12.0	Jul
268	084	6.1	58	6.1	10.5	267	254	3.9	35	3.7	11.3	Aug
263	071	6.8	62	6.5	10.9	264	261	1.9	17	1.9	11.3	Sep
275	080	5.6	43	5.6	12.9	275	013	0.4	03	0.1	13.8	Oct
287	064	3.1	24	2.8	13.0	281	321	4.6	29	2.9	15.9	Nov
258	071	2.3	15	2.1	14.9	255	295	10.0	44	9.1	22.5	Dec

300 mb						200 mb						
N	O	Vr	S	u	c	N	O	Vr	S	u	c	
211	289	37.0	78	35.1	47.7	166	289	49.6	86	46.9	57.9	Jan
184	284	35.3	76	34.3	46.5	155	284	53.6	83	52.0	64.2	Feb
216	272	36.8	83	36.7	44.6	173	275	58.2	87	58.0	66.8	Mar
231	273	24.9	73	24.8	34.3	215	274	46.3	86	46.2	54.1	Apr
232	267	17.4	63	17.3	27.8	224	266	32.6	77	32.5	42.3	May
263	266	8.0	32	8.0	25.7	258	264	21.8	59	21.7	36.9	Jun
265	256	21.1	75	20.5	28.0	257	259	34.6	84	33.9	41.0	Jul
266	259	22.9	85	22.5	27.1	267	262	35.7	87	35.4	41.1	Aug
261	257	14.3	57	14.0	25.0	259	262	24.4	70	24.2	34.9	Sep
271	271	10.5	42	10.5	24.8	259	271	21.1	63	21.1	33.6	Oct
271	290	15.0	53	14.5	28.4	233	291	23.0	61	21.5	37.7	Nov
239	290	28.0	64	28.3	40.4	213	291	40.1	79	37.4	50.8	Dec

850 mb							
Mean resultant winds and steadiness at standard pressure levels.	N	O	Vr	S	u	c	
Station: Guam (91218)	654	088	19.1	92	-19.7	21.5	Jan
13°34'N, 144°55'E	694	093	17.5	91	-18.5	20.4	Feb
Period: July 1949-Feb. 1958	732	091	18.3	94	-13.8	20.1	Mar
	695	097	18.7	94	-18.6	20.0	Apr
N = number of observations	734	098	16.2	91	-16.1	17.8	May
O = mean resultant wind direction	690	101	16.5	91	-16.1	18.0	Jun
Vr = mean resultant wind speed (kn)	675	108	10.7	78	-10.2	13.6	Jul
S = steadiness (percent)	664	127	3.6	58	- 6.9	14.8	Aug
u = mean zonal wind speed (kn, E-)	679	116	7.6	53	- 6.8	14.3	Sep
	748	107	9.9	69	- 9.4	14.3	Oct
	742	099	18.7	88	-13.4	21.3	Nov
c = mean wind speed (kn)	749	090	20.0	87	-20.0	23.0	Dec

700 mb						500 mb						
N	O	Vr	S	u	c	N	O	Vr	S	u	c	
651	091	14.2	87	-14.2	16.4	640	101	11.8	77	-11.6	15.3	Jan
654	096	12.0	79	-12.0	15.3	661	099	9.9	67	- 9.3	14.7	Feb
724	089	11.8	83	-11.8	14.2	708	082	8.8	64	- 8.7	13.7	Mar
688	094	11.8	83	-11.7	14.2	681	085	8.3	63	- 8.2	13.0	Apr
735	097	9.6	79	- 9.6	12.2	726	077	6.2	54	- 6.1	11.5	May
696	102	12.9	87	-12.6	14.8	695	099	11.5	79	-11.4	14.5	Jun
670	107	9.6	75	- 9.1	12.8	660	100	8.4	66	- 8.3	12.8	Jul
656	121	9.0	61	- 7.7	14.6	634	112	9.9	65	- 9.2	15.2	Aug
682	112	8.1	58	- 7.5	13.9	665	107	8.3	59	- 8.0	14.0	Sep
746	109	9.4	69	- 8.9	13.7	730	101	9.2	65	- 9.1	14.2	Oct
737	099	16.6	85	-16.4	19.4	722	095	17.8	84	-17.7	21.1	Nov
737	092	16.5	84	-16.5	19.7	721	095	15.7	80	-15.7	19.7	Dec

300 mb						200 mb						
N	O	Vr	S	u	c	N	O	Vr	S	u	c	
611	105	5.1	42	- 4.9	11.9	578	181	3.7	29	0.0	13.0	Jan
636	113	1.7	14	- 1.5	11.9	617	214	5.4	36	3.0	14.9	Feb
678	310	3.3	24	2.5	13.4	645	247	9.2	51	8.4	17.9	Mar
644	306	6.4	37	5.2	17.3	608	286	11.9	55	11.5	21.7	Apr
709	319	5.0	31	3.3	16.1	682	282	14.8	58	14.5	25.5	May
664	074	2.3	15	- 2.2	15.4	647	274	5.0	24	5.0	20.8	Jun
634	074	5.0	36	- 4.8	13.9	611	062	5.6	29	- 5.0	19.5	Jul
591	092	7.0	48	- 6.9	14.5	563	057	8.1	38	- 6.9	21.2	Aug
640	076	4.7	36	- 4.5	13.0	606	036	5.5	30	- 3.2	18.6	Sep
680	091	4.4	29	- 4.4	15.0	650	051	2.6	13	- 2.1	20.2	Oct
679	084	12.5	65	-12.4	19.2	616	078	7.7	38	- 7.5	20.2	Nov
676	088	10.0	61	-10.0	16.5	639	090	5.2	33	- 5.2	15.7	Dec



350 mb						
Mean resultant winds and steadiness at standard pressure levels.						
	N	θ	Vr	S	u	c
Station: Wake Island (91245)	235	087	6.9	49	6.8	14.1
19°17'N, 166°39'E	219	095	7.0	56	7.0	12.5
Period: July 1949-Dec. 1958	239	098	11.1	77	-11.0	14.5
	250	092	14.3	90	-14.2	15.9
N = number of observations	277	096	14.6	94	-14.5	15.6
θ = mean resultant wind direction	264	094	12.6	91	-12.8	14.1
Vr = mean resultant wind speed (kn)	307	100	12.4	92	-12.2	13.5
S = steadiness (percent)	304	100	11.9	90	-11.7	13.2
u = mean zonal wind speed (kn, E-)	284	097	11.4	85	-11.3	13.4
c = mean wind speed (kn)	269	100	11.9	78	-11.7	15.2
	267	091	14.2	85	-14.2	16.7
	275	089	10.2	71	-10.2	14.4

700 mb						500 mb					
N	θ	Vr	S	u	c	N	θ	Vr	S	u	c
235	321	2.9	20	1.9	14.7	224	298	14.0	63	12.3	22.3
218	307	2.9	21	2.3	13.6	220	289	15.5	74	14.6	21.0
243	070	4.7	39	-4.5	11.9	239	304	11.9	61	9.8	19.5
252	084	9.5	73	-9.4	13.1	248	359	3.9	31	0.1	12.7
277	090	10.9	81	-10.9	13.4	271	073	6.2	50	6.4	13.3
264	090	11.8	86	-11.8	13.8	260	084	9.3	72	9.8	13.6
306	097	9.4	79	-9.4	11.9	300	089	3.2	23	-3.2	11.5
298	099	8.7	79	-8.6	11.0	290	092	3.5	34	-3.5	10.2
283	092	9.2	76	-9.2	12.1	274	039	7.4	62	-7.4	11.9
268	098	9.7	68	-9.6	14.3	269	087	6.6	43	-6.6	15.3
267	089	11.1	72	-11.1	15.5	263	072	9.9	56	-9.4	17.8
272	069	5.0	36	-4.7	13.9	268	324	5.7	31	3.4	18.2

300 mb						200 mb					
N	θ	Vr	S	u	c	N	θ	Vr	S	u	c
196	292	29.5	89	27.4	33.3	169	286	31.6	87	30.4	36.2
198	293	34.4	88	31.7	38.9	163	286	37.8	89	36.4	42.7
206	288	38.2	84	36.4	45.6	166	280	48.5	92	47.7	52.9
232	300	21.5	72	18.6	29.8	218	284	33.5	81	37.6	47.3
262	298	8.3	38	7.3	21.8	254	278	24.5	66	24.2	37.4
252	070	8.0	41	-1.5	19.5	246	009	4.9	19	-0.8	26.1
288	299	5.8	31	5.1	18.9	285	297	13.2	43	11.8	30.6
271	300	5.0	31	4.3	16.2	261	292	12.2	46	11.3	26.6
264	017	2.9	16	-0.9	18.0	257	308	8.4	32	6.6	26.3
258	360	3.6	17	0.0	20.9	250	312	9.0	33	6.7	27.1
255	026	5.4	24	-2.4	22.9	247	333	7.0	27	3.1	25.7
240	310	14.4	56	11.1	25.6	224	299	18.7	66	16.4	28.3

## 850 mb

Mean resultant winds and steadiness at standard pressure levels.	N	O	Vr	S	u	c	
Station: Eniwetok Atoll (91250)	521	084	19.0	93	-18.5	20.5	Jan
11°20'N, 162°20'E	540	087	18.6	95	-18.5	19.6	Feb
Period: Nov. 1949-Dec. 1949;	508	085	17.0	91	-17.0	18.7	Mar
Apr. 1950-Dec. 1955; Jan.-Feb.	505	089	16.6	96	-16.6	17.4	Apr
1956; Jan. 1957-Feb. 1958	547	096	15.8	90	-15.7	17.6	May
	408	094	16.5	94	-16.4	17.6	Jun
N = number of observations							
O = mean resultant wind direction	606	098	15.0	89	-14.9	16.2	Jul
	636	100	13.7	89	-13.5	15.3	Aug
Vr = mean resultant wind speed (kn)	556	099	11.8	86	-11.7	13.7	Sep
S = steadiness (percent)	599	100	12.1	84	-11.9	14.3	Oct
u = mean zonal wind speed (kn, E-)	590	096	18.2	93	-18.2	19.7	Nov
c = mean wind speed (kn)	587	089	16.8	88	-16.8	19.1	Dec

## 700 mb

## 500 mb

N	O	Vr	S	u	c	N	O	Vr	S	u	c	
512	088	14.4	86	-14.4	16.7	505	084	16.7	82	-16.6	20.4	Jan
537	091	12.5	84	-12.5	14.9	533	086	14.0	77	-14.0	18.1	Feb
509	084	8.9	67	- 8.9	13.2	489	061	6.8	45	- 6.0	15.2	Mar
504	088	7.3	66	- 7.3	11.0	491	076	4.4	39	- 4.3	11.4	Apr
546	101	8.2	72	- 8.1	11.4	517	109	1.9	18	- 1.8	10.7	May
399	097	13.1	88	-13.0	14.8	362	092	10.1	77	-10.0	13.0	Jun
604	099	12.1	89	-12.0	13.6	523	095	9.1	74	- 9.1	11.3	Jul
637	101	13.4	91	-13.2	14.8	598	099	12.9	89	-12.7	14.5	Aug
552	102	11.2	84	-10.9	13.3	521	096	9.7	74	- 9.7	13.1	Sep
597	099	11.2	83	-11.0	13.5	572	095	10.0	71	-10.0	14.0	Oct
590	096	15.0	88	-14.9	17.0	573	092	13.9	74	-13.9	18.9	Nov
580	088	12.2	75	-12.1	16.3	558	082	13.1	64	-13.0	20.6	Dec

## 300 mb

## 200 mb

N	O	Vr	S	u	c	N	O	Vr	S	u	c	
494	069	6.7	42	- 6.3	15.8	479	111	1.4	08	- 1.3	16.9	Jan
522	050	3.6	26	- 2.7	13.8	503	252	2.0	13	1.9	15.4	Feb
467	297	6.7	43	5.9	15.5	435	260	12.4	65	12.1	19.2	Mar
468	273	13.6	57	13.6	23.8	445	266	20.5	72	20.5	28.5	Apr
464	264	15.1	70	15.0	21.5	426	263	24.5	81	24.3	30.3	May
317	292	2.8	17	2.6	16.4	296	264	12.2	54	12.2	22.7	Jun
463	284	4.5	34	4.4	13.2	427	264	10.9	54	10.8	20.1	Jul
548	120	3.6	29	- 3.1	12.4	512	247	1.3	08	1.2	16.6	Aug
479	109	0.7	06	- 0.7	11.6	454	269	4.1	24	4.1	17.3	Sep
531	017	1.7	11	- 0.5	15.4	512	299	5.5	26	4.8	21.0	Oct
552	055	0.7	04	- 0.6	17.4	523	268	6.9	34	6.9	20.5	Nov
527	034	3.5	19	- 2.0	18.4	495	271	4.8	26	4.8	18.5	Dec

850 mb							
Mean resultant winds and steadiness at standard pressure levels	N	θ	Vr	S	u	c	
Station: Johnston Island (91275)	585	108	8.2	54	-7.8	15.1	Jan
16°44'N, 169°31'W	630	089	10.9	73	-10.9	14.9	Feb
Period: Jan. 1950-Aug. 1958	709	083	10.6	70	-10.6	15.2	Mar
	720	089	14.8	89	-14.8	16.7	Apr
N = number of observations	771	086	15.7	94	-15.6	16.7	May
θ = mean resultant wind direction	661	088	17.4	95	-17.3	18.3	Jun
	772	089	16.4	95	-16.4	17.3	Jul
Vr = mean resultant wind speed (kn)	743	089	16.9	95	-16.9	17.8	Aug
S = steadiness (percent)	625	086	13.6	92	-13.6	14.8	Sep
u = mean zonal wind speed (kn, E-)	633	087	14.1	89	-14.1	15.9	Oct
	620	090	15.1	87	-15.1	17.3	Nov
c = mean wind speed (kn)	622	097	13.0	73	-12.9	17.9	Dec

700 mb						500 mb						
N	θ	Vr	S	u	c	N	θ	Vr	S	u	c	
589	147	1.4	09	-0.8	14.8	570	284	9.3	41	9.0	22.6	Jan
632	065	4.6	36	-4.1	12.8	620	315	10.9	54	7.7	20.2	Feb
704	043	2.8	24	-1.9	12.0	685	297	12.7	62	11.4	20.6	Mar
724	089	5.5	47	-5.5	11.7	702	283	5.6	35	5.4	15.8	Apr
773	087	5.6	55	-5.6	10.1	750	291	3.7	30	3.5	12.6	May
662	090	3.6	74	-8.6	11.6	653	092	2.5	20	-2.5	12.4	Jun
769	089	9.0	78	-9.0	11.6	748	149	0.9	09	-0.5	9.9	Jul
746	091	10.3	87	-10.2	12.4	717	100	5.0	49	-4.9	10.2	Aug
627	088	7.1	67	-7.1	10.5	583	093	5.3	49	-5.3	10.7	Sep
640	087	8.3	67	-8.3	12.4	611	068	3.5	27	-3.3	12.5	Oct
622	087	9.7	67	-9.7	14.5	614	066	7.6	48	-6.9	16.0	Nov
621	096	6.7	45	-6.7	14.8	595	355	4.2	23	0.4	18.7	Dec

300 mb						200 mb						
N	θ	Vr	S	u	c	N	θ	Vr	S	u	c	
538	292	26.1	67	24.2	38.8	480	287	34.6	79	33.0	43.9	Jan
566	298	33.0	71	29.2	46.3	491	294	40.9	76	37.5	52.5	Feb
600	283	44.2	85	43.0	52.2	520	284	54.9	37	53.3	63.4	Mar
669	273	34.7	81	34.6	42.7	628	275	53.8	86	53.6	62.5	Apr
720	275	26.5	79	26.4	33.7	672	273	44.5	88	44.4	50.6	May
631	272	13.9	58	13.9	24.1	585	265	28.0	77	28.0	36.4	Jun
686	265	18.3	76	18.3	24.2	629	268	32.1	84	32.1	38.0	Jul
673	257	12.4	67	12.1	18.5	618	260	22.7	79	22.4	28.7	Aug
543	257	9.1	51	8.8	17.1	517	263	19.4	70	19.2	27.8	Sep
564	275	12.3	52	12.2	23.7	538	268	22.8	70	22.8	32.6	Oct
583	314	7.8	33	5.7	23.9	547	288	17.2	56	16.4	30.9	Nov
566	300	18.4	61	15.9	30.2	531	294	25.0	65	22.8	38.5	Dec

850 mb							
Mean resultant winds and steadiness at standard pressure levels.	N	O	Vr	S	u	c	
Station: Hilo (91235)	555	135	5.5	52	- 3.9	10.6	Jan
19°44'N, 155°04'W	514	112	4.2	41	- 3.9	10.3	Feb
Period: Feb. 1950-May 1958	596	121	4.0	38	- 3.5	10.6	Mar
n = number of observations	538	078	4.5	54	- 4.4	8.3	Apr
o = mean resultant wind direction	614	075	5.4	67	- 5.2	8.1	May
v = mean resultant wind speed (kn)	537	081	5.8	75	- 5.7	7.7	Jun
s = steadiness (percent)	553	070	6.1	77	- 5.8	7.9	Jul
u = mean zonal wind speed (kn, E-)	553	073	5.9	72	- 5.6	8.2	Aug
	543	070	5.2	71	- 4.9	7.3	Sep
	640	079	5.6	63	- 5.5	8.9	Oct
	653	100	5.0	52	- 5.0	9.6	Nov
	603	091	5.0	45	- 5.0	11.0	Dec

700 mb						500 mb						
N	O	Vr	S	u	c	N	O	Vr	S	u	c	
553	126	3.0	22	- 2.4	13.9	544	288	10.0	48	9.5	20.8	Jan
513	165	1.0	07	- 0.3	13.8	500	278	12.1	57	12.0	21.2	Feb
592	220	2.6	21	1.7	12.6	577	267	14.5	67	14.5	21.7	Mar
587	080	3.4	31	- 3.3	11.0	583	278	7.8	47	7.8	16.5	Apr
615	031	3.1	30	- 3.0	10.4	609	268	6.3	42	6.3	14.9	May
538	090	8.4	74	- 8.4	11.3	530	140	1.8	14	- 1.2	13.2	Jun
551	089	8.7	73	- 8.7	12.0	540	110	2.3	20	- 2.2	11.6	Jul
554	086	5.9	59	- 5.9	10.0	557	139	0.3	03	- 0.2	9.9	Aug
543	070	4.2	48	- 4.0	8.8	538	082	0.3	03	- 0.3	10.7	Sep
638	083	5.3	49	- 5.2	10.8	635	088	0.7	05	- 0.7	12.9	Oct
651	092	5.7	47	- 5.7	12.1	647	343	1.9	13	9.6	14.4	Nov
604	089	5.0	37	- 5.0	13.4	589	305	5.2	26	4.3	19.8	Dec

300 mb						200 mb						
N	O	Vr	S	u	c	N	O	Vr	S	u	c	
508	292	35.1	78	32.5	45.2	417	291	48.3	86	45.2	56.0	Jan
438	279	35.0	74	34.5	47.3	348	283	53.1	81	51.7	65.3	Feb
497	271	43.0	85	43.0	50.8	362	277	61.5	87	61.0	70.3	Mar
535	273	33.7	84	33.7	39.9	461	273	57.3	92	57.2	62.3	Apr
586	264	26.1	78	26.0	33.6	526	267	41.6	85	41.5	48.9	May
519	257	17.9	63	17.4	28.5	493	264	34.0	79	33.8	42.9	Jun
531	260	16.6	69	16.4	23.9	511	259	26.2	78	25.8	33.5	Jul
538	264	15.7	77	16.6	21.6	531	262	26.6	84	26.4	31.7	Aug
527	255	14.5	67	14.0	21.6	508	260	23.4	78	23.0	30.1	Sep
627	265	15.9	60	15.9	26.6	605	265	30.0	78	30.0	38.5	Oct
639	281	15.4	55	15.2	28.1	608	275	27.4	71	27.3	38.6	Nov
550	287	23.4	65	22.4	36.2	491	290	36.4	76	34.1	47.8	Dec

## 850 mb

Mean resultant winds and steadiness at standard pressure levels.							N	θ	Vr	S	u	c	
Station: Truk (91334)							220	082	16.6	93	-16.4	17.9	Jan
07°27'N, 151°50'E							240	084	16.8	93	-16.7	18.1	Feb
Period: July 1951-Feb. 1958							244	083	14.5	91	-14.4	15.9	Mar
							229	092	13.9	91	-13.9	15.2	Apr
N = number of observations							242	097	10.7	81	-10.7	13.2	May
θ = mean resultant wind direction							232	098	12.2	87	-12.1	14.1	Jun
Vr = mean resultant wind speed (kn)							251	105	9.2	83	- 8.8	11.1	Jul
S = steadiness (percent)							222	120	5.7	49	- 5.0	11.6	Aug
u = mean zonal wind speed (kn, E-)							219	124	4.6	47	- 3.9	9.8	Sep
							232	116	3.9	36	- 3.5	10.8	Oct
c = mean wind speed (kn)							227	100	9.5	69	- 9.4	13.7	Nov
							216	089	12.2	75	-12.2	16.2	Dec

## 700 mb

## 500 mb

N	θ	Vr	S	u	c	N	θ	Vr	S	u	c	
210	093	13.3	85	-13.3	15.6	207	093	19.8	92	-19.7	21.5	Jan
232	089	13.9	90	-13.8	15.4	224	089	17.4	88	-17.4	19.7	Feb
233	087	10.7	80	-10.6	13.3	216	088	11.6	70	-11.6	16.5	Mar
225	097	10.4	84	-10.3	12.4	217	096	7.0	55	- 7.0	12.7	Apr
241	097	8.6	72	- 8.5	11.9	231	095	4.9	44	- 4.9	11.2	May
229	098	13.4	90	-13.2	14.9	220	098	10.8	78	-10.7	13.8	Jun
243	103	11.4	87	-11.2	13.1	233	099	12.1	86	-11.9	14.1	Jul
219	106	9.4	71	- 9.1	13.3	217	102	13.3	83	-13.0	16.1	Aug
209	107	7.5	67	- 7.2	11.2	199	105	10.2	76	- 9.9	13.4	Sep
223	105	6.7	59	- 6.4	11.4	213	099	9.0	71	- 8.9	12.7	Oct
215	095	10.1	73	-10.0	13.8	206	099	9.7	64	- 9.6	15.2	Nov
214	096	10.2	66	-10.2	15.4	205	093	15.6	80	-15.6	19.5	Dec

## 300 mb

## 200 mb

N	θ	Vr	S	u	c	N	θ	Vr	S	u	c	
200	098	15.3	87	-15.1	17.5	197	122	15.3	77	-13.0	20.0	Jan
213	095	11.5	76	-11.4	15.2	206	124	13.2	68	-11.0	19.5	Feb
203	106	7.7	51	- 7.4	15.2	196	152	10.9	53	- 6.0	20.4	Mar
209	148	2.0	14	- 1.1	14.1	199	215	6.8	36	3.9	18.8	Apr
217	223	1.7	13	1.1	12.8	206	247	6.4	34	5.9	18.8	May
207	126	4.2	32	- 3.4	13.0	204	218	3.8	23	2.3	16.3	Jun
225	104	9.2	67	- 8.9	13.7	217	091	8.1	47	- 8.1	17.4	Jul
204	099	10.6	74	-10.7	14.4	197	074	10.4	55	-10.0	19.0	Aug
192	091	9.8	74	- 9.8	13.3	188	063	10.3	58	- 9.6	17.8	Sep
211	094	7.2	58	- 7.2	12.4	204	070	5.7	33	- 6.4	17.1	Oct
203	108	4.2	26	- 4.1	16.3	201	119	8.2	41	- 8.8	20.1	Nov
195	094	10.0	61	-10.0	16.3	191	102	9.5	56	- 9.3	17.1	Dec

## 850 mb

Mean resultant winds and steadiness at standard pressure levels.						
	N	θ	Vr	S	u	c
Station: Ponape (91343)	181	076	17.4	93	-16.9	18.7
06°58'N, 158°13'E	296	080	18.3	93	-18.0	19.6
Period: July 1951-Feb. 1958	302	083	15.4	91	-15.3	16.9
	308	088	16.7	94	-16.7	17.8
N = number of observations	250	091	13.7	88	-13.7	15.6
θ = mean resultant wind direction	259	091	14.0	91	-14.0	15.4
Vr = mean resultant wind speed (kn)	279	096	11.7	91	-11.7	12.8
S = steadiness (percent)	210	101	9.1	76	- 8.9	12.0
u = mean zonal wind speed (kn, E-)	204	098	7.3	69	- 7.3	10.6
	305	102	6.6	58	- 6.4	11.3
c = mean wind speed (kn)	188	093	10.7	77	-10.6	13.9
	201	082	13.8	88	-13.6	15.6

## 700 mb

## 500 mb

700 mb						500 mb					
N	θ	Vr	S	u	c	N	θ	Vr	S	u	c
165	087	11.3	81	-11.3	14.0	162	082	19.1	87	-18.9	22.0
289	087	12.0	86	-11.9	13.9	283	084	15.9	87	-15.8	18.2
287	093	7.9	67	- 7.9	11.8	281	086	12.3	70	-12.3	17.5
294	091	9.2	75	- 9.1	12.2	280	089	5.1	41	- 5.1	12.3
238	094	8.1	70	- 8.1	11.6	232	103	3.4	30	- 3.4	11.4
242	094	12.1	89	-12.1	13.6	222	089	10.3	79	-10.3	13.1
272	096	12.1	90	-12.1	13.4	256	098	12.2	87	-12.1	14.0
199	096	12.0	88	-12.0	13.6	171	093	14.6	92	-14.6	15.9
191	097	10.3	83	-10.2	12.4	166	094	11.5	79	-11.5	14.6
307	103	7.0	63	- 6.8	11.2	291	096	3.0	65	- 7.9	12.4
175	090	9.4	70	- 9.4	13.4	160	085	10.5	69	-10.5	15.3
185	088	9.7	82	- 9.7	11.9	172	081	14.9	83	-14.7	18.0

## 300 mb

## 200 mb

300 mb						200 mb					
N	θ	Vr	S	u	c	N	θ	Vr	S	u	c
161	089	12.1	75	-12.1	16.2	162	126	10.8	60	- 8.8	17.9
275	092	10.4	67	-10.4	15.5	276	122	10.1	61	- 8.5	16.6
276	097	6.9	44	- 6.9	15.6	274	155	8.8	45	- 3.7	19.4
271	235	8.2	51	- 6.7	16.0	269	240	15.1	71	13.1	21.4
214	229	6.4	46	- 4.8	13.8	208	246	13.9	66	12.7	21.0
214	116	3.9	33	- 3.5	11.8	201	249	4.0	26	- 3.7	15.4
248	098	6.3	49	- 6.3	12.8	239	074	2.5	15	- 2.4	16.3
166	095	12.5	83	-12.4	15.0	161	080	8.4	51	- 8.2	16.4
155	094	8.0	60	- 7.9	13.4	152	070	6.4	38	- 6.0	16.8
291	083	4.7	38	- 4.7	12.5	284	030	3.0	18	- 1.5	16.7
152	103	2.0	13	- 1.9	15.6	147	228	2.8	14	- 2.0	19.7
161	087	8.0	54	- 8.0	14.9	160	129	4.9	29	- 3.8	16.9

## 850 mb

Mean resultant winds and steadiness at standard pressure levels.							
	N	θ	Vr	S	u	c	
Station: Kwajalein (91366)	552	085	15.8	91	-15.7	17.3	Jan
08°43'N, 167°44'E	525	088	18.3	92	-18.3	19.8	Feb
Period: July 1949-Nov. 1957	550	093	14.7	84	-14.7	17.5	Mar
	556	089	16.9	94	-16.9	18.0	Apr
N = number of observations	553	093	16.3	91	-16.3	17.9	May
θ = mean resultant wind direction	489	092	16.5	93	-16.5	17.7	Jun
Vr = mean resultant wind speed (kn)	677	096	14.5	92	-14.4	15.8	Jul
S = steadiness (percent)	646	098	12.1	90	-12.0	13.5	Aug
u = mean zonal wind speed (kn, E-)	536	097	10.0	85	-9.9	11.8	Sep
	569	098	10.0	80	-9.9	12.5	Oct
c = mean wind speed (kn)	624	092	14.6	89	-14.6	16.4	Nov
	489	091	15.6	85	-15.5	18.3	Dec

## 700 mb

## 500 mb

700 mb						500 mb						
N	θ	Vr	S	u	c	N	θ	Vr	S	u	c	
553	091	11.7	81	-11.7	14.4	542	082	16.7	84	-16.5	20.0	Jan
526	090	12.2	82	-12.2	14.8	502	086	15.3	77	-15.3	20.0	Feb
551	106	6.2	52	-5.9	12.0	548	076	6.6	42	-6.4	15.7	Mar
567	098	6.9	64	-6.8	10.7	557	032	2.3	11	-0.7	11.5	Apr
551	098	10.6	81	-10.5	13.1	517	098	3.2	34	-3.2	9.5	May
490	095	14.1	92	-14.1	15.4	461	090	7.6	69	-7.6	11.0	Jun
683	096	13.9	91	-13.8	15.3	637	098	11.9	82	-11.7	14.6	Jul
649	096	14.0	91	-13.9	15.4	612	095	14.4	91	-14.3	15.8	Aug
534	094	11.3	88	-11.3	12.9	518	094	10.6	81	-10.6	13.1	Sep
567	096	10.2	79	-10.2	12.9	558	095	8.7	67	-8.7	13.0	Oct
627	093	12.0	83	-11.9	14.4	600	087	11.1	67	-11.1	16.6	Nov
494	096	11.3	75	-11.2	15.1	475	089	12.4	64	-12.4	19.3	Dec

## 300 mb

## 200 mb

300 mb						200 mb						
N	θ	Vr	S	u	c	N	θ	Vr	S	u	c	
513	076	4.1	23	-3.9	14.4	477	186	1.3	08	0.1	15.7	Jan
460	044	4.0	25	-2.8	16.1	407	219	2.7	14	1.7	18.7	Feb
498	289	6.4	37	6.1	17.1	441	255	11.9	53	11.5	22.4	Mar
494	262	15.0	67	14.9	22.3	438	258	25.2	82	24.6	30.6	Apr
466	260	9.4	57	9.2	16.5	416	265	19.0	75	18.9	25.2	May
413	241	3.3	22	2.9	14.9	366	262	10.9	53	10.8	20.6	Jun
565	125	3.1	25	-2.5	12.3	493	227	5.1	31	3.7	16.3	Jul
522	101	9.2	67	-9.1	13.8	440	093	4.5	31	-4.5	14.4	Aug
481	091	6.5	52	-6.5	12.4	425	079	2.3	15	-2.2	15.3	Sep
511	096	1.6	13	-1.6	12.6	437	287	5.2	31	5.0	17.0	Oct
546	294	1.2	07	1.1	16.1	502	264	9.3	45	9.2	20.8	Nov
441	275	1.4	08	1.4	16.9	408	250	7.3	37	6.9	19.5	Dec

							350 mb						
Mean resultant winds and steadiness at standard pressure levels.							N	O	Vr	S	u	c	
Station:	Majuro (91376)						154	078	14.9	91	-14.5	16.3	Jan
	07°06'N, 171°24'E						234	075	15.3	89	-14.8	17.2	Feb
Period:	Sept. 1952-Nov. 1952;						242	083	13.5	37	-13.4	15.6	Mar
	Feb. 1955-Feb. 1958						254	081	15.8	93	-15.6	16.9	Apr
							256	089	16.5	93	-16.5	17.8	May
N =	number of observations						195	093	15.3	92	-15.3	16.6	Jun
O =	mean resultant wind direction						209	094	14.1	93	-14.1	15.1	Jul
Vr =	mean resultant wind speed (kn)						111	096	12.8	91	-12.7	14.0	Aug
S =	steadiness (percent)						122	096	11.0	85	-11.0	12.9	Sep
u =	mean zonal wind speed (kn, E-)						227	102	10.6	82	-10.4	12.9	Oct
c =	mean wind speed (kn)						194	099	12.0	79	-11.8	15.2	Nov
							117	081	10.8	71	-10.7	15.2	Dec

700 mb						500 mb						
N	O	Vr	S	u	c	N	O	Vr	S	u	c	
153	083	8.9	70	-8.9	12.7	145	064	12.6	75	-11.3	16.9	Jan
233	079	10.5	78	-10.4	13.5	228	078	13.1	73	-12.8	18.0	Feb
233	098	5.3	50	-5.2	10.6	231	067	6.5	40	-6.0	16.1	Mar
251	092	8.9	75	-8.9	11.8	243	305	1.1	12	0.9	9.5	Apr
251	093	11.6	83	-11.6	14.0	242	080	2.8	31	-2.8	9.1	May
198	090	14.0	91	-14.0	15.4	191	089	7.6	68	-7.6	11.2	Jun
207	093	15.5	95	-15.5	16.4	200	096	13.9	89	-13.8	15.6	Jul
114	091	14.1	95	-14.1	14.8	110	088	13.4	85	-13.4	15.7	Aug
126	096	12.2	86	-12.1	14.2	120	091	13.2	88	-13.2	15.0	Sep
228	097	10.1	76	-10.1	13.3	227	107	8.2	65	-7.8	12.7	Oct
195	103	10.0	74	-9.8	13.6	194	095	9.6	58	-9.5	16.5	Nov
123	096	5.2	44	-5.2	11.8	119	066	9.2	59	-8.4	15.7	Dec

300 mb						200 mb						
N	O	Vr	S	u	c	N	O	Vr	S	u	c	
139	028	2.4	17	-1.1	14.0	139	194	3.1	16	0.7	19.5	Jan
224	054	6.2	37	-5.0	16.9	218	145	4.1	21	-2.4	19.7	Feb
224	267	4.8	30	4.8	16.0	220	234	11.5	52	9.2	22.2	Mar
233	252	16.6	78	15.7	21.3	230	251	26.7	87	25.3	30.7	Apr
229	246	9.2	56	8.4	16.5	220	263	20.0	80	19.9	24.9	May
183	170	2.5	22	-0.4	11.5	178	261	10.9	61	10.7	17.9	Jun
195	114	7.4	60	-6.8	12.4	189	183	3.2	20	0.1	15.8	Jul
112	094	9.4	70	-9.4	13.4	109	078	5.2	38	-5.1	13.6	Aug
119	090	6.6	49	-6.6	13.5	116	065	1.1	07	-1.0	16.7	Sep
220	216	1.5	11	0.9	14.1	216	273	11.0	53	11.0	20.8	Oct
190	279	3.8	24	3.7	15.7	187	267	11.1	50	11.0	22.0	Nov
118	281	4.4	30	4.3	14.9	117	251	7.9	45	7.4	17.6	Dec



850 mb						
Mean resultant winds and steadiness at standard pressure levels.						
	N	0	Vr	S	u	c
Station: Koror (91408)	210	079	15.3	86	-15.0	17.7
07°21'N, 134°29'E	200	080	15.5	89	-15.3	17.4
Period: Sept. 1950-Apr. 1951;	199	072	13.5	83	-12.8	15.4
July 1951-Feb. 1958	207	081	8.7	65	-8.6	13.4
	230	100	7.4	67	-7.3	11.0
	226	102	6.4	55	-6.3	11.6
N = number of observations						
θ = mean resultant wind direction	259	151	2.9	28	-1.4	10.5
Vr = mean resultant wind speed (kn)	213	238	5.8	41	4.9	14.1
S = steadiness (percent)	208	219	3.8	35	2.4	10.9
u = mean zonal wind speed (kn, E-)	229	251	3.3	26	3.1	12.8
c = mean wind speed (kn)	195	007	0.6	06	-0.1	10.6
	219	078	8.0	52	-7.9	15.2

700 mb						500 mb					
N	θ	Vr	S	u	c	N	θ	Vr	S	u	c
194	089	14.1	88	-14.1	16.1	168	095	17.0	90	-16.9	18.8
186	085	13.4	83	-13.3	16.1	169	095	17.2	88	-17.1	19.6
184	081	11.2	81	-11.0	13.8	163	087	15.3	85	-15.2	17.9
195	085	7.7	62	-7.6	12.5	186	078	8.9	66	-8.8	13.5
219	100	7.0	67	-6.9	10.4	197	087	7.3	70	-7.3	10.4
216	097	8.4	65	-8.3	12.9	193	096	10.2	79	-10.1	12.9
242	102	6.7	56	-6.6	12.0	216	101	12.1	81	-11.9	15.0
187	159	1.8	13	-0.7	13.8	150	110	9.9	68	-9.3	14.6
194	127	3.5	33	-2.8	10.6	158	108	8.5	66	-8.1	12.9
205	152	1.7	14	-0.8	11.9	179	102	5.8	50	-5.7	11.5
174	087	1.8	13	-1.8	14.4	154	091	7.2	50	-7.2	14.3
197	083	8.4	55	-8.4	15.2	171	097	13.9	75	-13.9	18.5

300 mb						200 mb					
N	θ	Vr	S	u	c	N	θ	Vr	S	u	c
150	101	16.0	86	-15.7	18.6	132	116	21.4	90	-19.3	23.8
	103	14.3	88	-14.0	16.3	140	122	22.3	90	-19.0	24.8
	097	11.8	78	-11.7	15.2	142	125	16.9	80	-13.9	21.0
161	099	10.8	69	-10.6	15.6	141	111	12.5	63	-11.7	19.8
180	111	3.5	32	-3.3	10.8	170	135	2.4	17	-1.7	14.5
186	096	7.7	59	-7.7	13.0	175	078	6.3	40	-6.2	15.8
197	092	14.7	88	-14.7	16.8	182	071	18.6	81	-17.6	23.0
126	088	18.5	90	-18.5	20.5	116	070	24.1	83	-22.7	29.2
131	087	13.0	84	-13.0	15.5	115	067	20.4	80	-18.8	25.6
155	084	8.7	63	-8.6	13.8	137	075	13.4	67	-12.9	20.0
136	093	8.2	54	-8.2	15.3	125	088	11.8	58	-11.8	20.5
148	098	14.8	81	-14.7	18.2	136	108	18.0	83	-17.1	21.7

350 mb							
Mean resultant winds and steadiness at standard pressure levels							
	N	θ	Vr	S	u	c	
Station: Yap (91413)	303	082	19.6	92	-19.4	21.4	Jan
09°31'N, 133°08'E	305	084	17.8	93	-17.7	19.2	Feb
Period: Jan. 1950-Apr. 1951;	321	075	16.6	91	-16.0	18.2	Mar
June 1951; Aug. 1951-Feb. 1953	338	036	14.7	85	-14.6	17.3	Apr
	235	095	12.1	86	-12.1	14.0	May
N = number of observations	229	092	11.0	81	-10.9	13.5	Jun
θ = mean resultant wind direction	232	117	5.5	51	-4.9	10.9	Jul
Vr = mean resultant wind speed (kn)	236	172	2.8	22	-0.4	13.0	Aug
S = steadiness (percent)	254	171	3.3	31	-0.5	10.7	Sep
u = mean zonal wind speed (kn, E-)	274	150	2.0	17	-1.0	11.6	Oct
c = mean wind speed (kn)	257	088	8.9	57	-8.9	15.5	Nov
	257	084	14.2	76	-14.1	18.7	Dec

700 mb						500 mb						
N	θ	Vr	S	u	c	N	θ	Vr	S	u	c	
303	036	17.5	89	-17.4	19.6	273	091	19.2	90	-19.2	21.4	Jan
305	087	13.9	87	-13.9	15.9	292	095	16.4	86	-16.4	19.0	Feb
321	074	13.5	87	-13.0	15.6	314	081	16.2	87	-16.0	18.7	Mar
341	085	10.9	79	-10.9	13.8	338	085	9.8	71	-9.7	13.8	Apr
231	094	10.0	81	-10.0	12.3	220	085	8.3	72	-8.2	11.5	May
231	094	11.2	81	-11.2	13.8	220	094	10.9	82	-10.9	13.3	Jun
232	102	9.2	73	-9.0	12.6	229	098	12.1	82	-12.0	14.7	Jul
234	129	4.6	32	-3.5	14.4	227	104	9.7	61	-9.4	15.8	Aug
257	122	5.1	41	-4.3	12.3	244	106	8.0	62	-7.7	13.0	Sep
266	105	4.1	34	-4.0	11.9	251	096	6.3	53	-6.7	12.8	Oct
252	089	9.9	63	-9.9	15.7	234	087	13.0	76	-13.0	17.0	Nov
253	090	12.7	77	-12.7	16.5	213	093	16.0	84	-16.0	19.0	Dec

300 mb						200 mb						
N	θ	Vr	S	u	c	N	θ	Vr	S	u	c	
237	099	14.4	82	-14.3	17.5	226	123	15.2	76	-12.8	19.9	Jan
273	099	11.2	77	-11.1	14.5	261	134	15.2	76	-10.9	19.9	Feb
290	099	9.2	61	-9.1	15.2	257	143	15.2	75	-9.2	20.4	Mar
307	111	5.4	39	-5.0	14.0	271	136	8.0	43	-5.6	18.6	Apr
207	154	0.5	04	-0.2	11.4	198	235	5.3	34	4.4	15.4	May
216	096	6.2	45	-6.2	13.8	206	131	1.0	06	-0.8	17.0	Jun
224	090	10.8	74	-10.8	14.6	219	069	11.9	62	-11.2	19.2	Jul
209	090	13.1	76	-13.1	17.3	201	064	17.9	71	-16.1	25.3	Aug
233	084	10.3	71	-10.2	14.6	222	067	14.8	69	-13.6	21.6	Sep
239	083	6.7	49	-6.6	13.7	230	062	7.7	40	-6.3	19.1	Oct
214	082	12.5	68	-12.4	18.3	206	088	12.3	59	-12.2	20.9	Nov
191	091	14.3	78	-14.3	18.3	190	104	14.7	73	-14.2	20.2	Dec

## 850 mb

Mean resultant winds and steadiness at standard pressure levels.		N	θ	Vr	S	u	c	
Station: Christmas Island		145	093	14.1	86	-14.1	16.4	Jan
(91489)		130	092	16.5	92	-16.5	17.9	Feb
02°00'N, 157°23'W		156	090	13.6	96	-13.6	14.2	Mar
Period: Oct. 1956-Sept. 1959		176	094	14.2	95	-14.1	15.0	Apr
		174	094	14.6	95	-14.5	15.4	May
N = number of observations		170	095	12.5	38	-12.5	14.2	Jun
θ = mean resultant wind direction		167	097	15.1	90	-15.0	16.7	Jul
		101	098	16.8	95	-16.6	17.6	Aug
Vr = mean resultant wind speed (kn)		96	096	13.1	89	-13.1	14.7	Sep
S = steadiness (percent)		125	093	12.8	86	-12.8	14.8	Oct
u = mean zonal wind speed (kn, E-)		149	090	9.7	58	-9.7	16.6	Nov
c = mean wind speed (kn)		145	093	12.1	82	-12.1	14.8	Dec

## 700 mb

## 500 mb

N	θ	Vr	S	u	c	N	θ	Vr	S	u	c	
145	084	3.3	33	-3.3	10.0	149	319	1.8	09	1.1	12.2	Jan
130	096	7.1	64	-7.1	11.1	130	098	2.0	15	-1.9	13.6	Feb
156	094	8.8	72	-8.8	12.2	155	217	2.9	22	1.7	13.2	Mar
176	093	13.5	96	-13.5	14.0	176	111	7.1	60	-6.6	11.9	Apr
176	090	15.3	94	-15.3	16.2	176	094	12.3	83	-12.3	14.9	May
169	089	14.0	91	-14.0	15.4	166	089	14.6	87	-14.6	16.7	Jun
167	090	15.3	93	-15.3	16.4	167	084	15.3	91	-15.2	16.9	Jul
101	090	17.2	97	-17.2	17.8	102	085	17.7	94	-17.6	18.3	Aug
96	087	14.4	94	-14.4	15.3	96	088	16.3	89	-16.3	18.3	Sep
125	092	12.6	91	-12.6	13.9	125	087	11.5	73	-11.4	15.7	Oct
149	080	4.0	34	-4.0	11.8	149	007	0.3	03	0.0	10.7	Nov
145	086	4.1	39	-4.1	10.6	145	130	1.9	15	-1.5	12.3	Dec

## 300 mb

## 200 mb

N	θ	Vr	S	u	c	N	θ	Vr	S	u	c	
149	259	14.0	64	13.7	21.3	149	261	19.3	63	19.1	30.3	Jan
130	260	7.9	39	7.8	20.1	130	257	12.9	49	12.5	26.1	Feb
155	251	15.6	75	14.7	20.8	155	264	23.9	77	23.7	31.2	Mar
176	251	2.1	12	2.2	16.9	176	274	15.0	57	15.0	26.1	Apr
174	210	1.3	10	0.6	13.6	174	286	7.6	46	7.3	16.5	May
167	104	6.6	41	-6.4	16.2	168	340	3.1	16	1.1	19.5	Jun
167	090	13.6	72	-13.6	18.8	167	062	11.9	59	-10.6	20.1	Jul
102	088	13.4	76	-13.4	17.7	102	068	10.5	45	-9.7	23.3	Aug
96	185	2.8	15	0.3	19.1	96	265	1.8	08	1.8	22.2	Sep
124	100	2.7	17	-2.6	15.8	124	321	5.1	23	3.3	22.4	Oct
149	253	8.3	45	8.0	18.5	149	255	15.3	62	15.2	25.4	Nov
145	264	5.6	32	5.6	17.3	145	244	14.5	66	13.1	22.0	Dec

---

 Mean resultant winds and steadiness at standard pressure levels.
 

---

Station: Nandi (91680)

17°45'S, 177°27'E

Period: Aug. 1945-Jan. 1946;

Nov. 1948-Nov. 1950; Jan.

1951-Aug. 1952

N = number of observations

O = mean resultant wind direction

Vr = mean resultant wind speed (kn)

S = steadiness (percent)

u = mean zonal wind speed (kn, E-)

c = mean wind speed (kn)

---

700 mb						500 mb						
N	θ	Vr	S	u	c	N	θ	Vr	S	u	c	
521	327	3	25	2	12	514	287	6	40	6	15	Jan
420	018	4	30	-1	13	403	301	2	15	2	13	Feb
449	346	7	40	2	18	439	319	6	40	4	15	Mar
405	309	5	40	4	12	377	290	8	55	7	15	Apr
401	317	5	35	3	14	362	282	13	70	13	19	May
409	030	2	15	-1	13	391	311	6	40	5	15	Jun
389	281	5	35	5	14	347	266	15	70	15	21	Jul
395	285	10	65	10	15	381	278	21	85	21	25	Aug
349	287	11	65	11	17	315	284	25	85	24	29	Sep
357	289	8	60	8	13	331	280	17	75	17	23	Oct
404	305	4	35	3	11	389	289	11	65	10	17	Nov
353	015	2	20	-1	10	353	295	5	40	5	12	Dec

---

300 mb						200 mb						
N	θ	Vr	S	u	c	N	θ	Vr	S	u	c	
482	270	14	60	14	23	425	273	19	60	19	32	Jan
368	238	6	30	5	20	301	235	15	50	12	30	Feb
413	248	8	40	7	20	370	250	15	55	14	27	Mar
319	265	16	70	16	23	282	250	23	75	22	31	Apr
306	270	25	85	25	29	267	274	37	85	37	44	May
360	270	19	75	19	25	320	256	29	85	28	34	Jun
317	267	31	85	31	36	290	265	41	85	41	48	Jul
	271	33	90	33	37	297	262	39	90	39	43	Aug
	280	42	95	41	44	246	271	52	95	52	55	Sep
	273	33	90	33	37	237	272	44	90	44	49	Oct
	280	27	85	27	32	345	276	39	90	39	43	Nov
	290	17	75	16	23	324	281	31	90	30	34	Dec

---

850 mb							
Mean resultant winds and steady- ness at standard pressure levels.	N	θ	Vr	S	u	c	
Station: Canton Island (91700)	504	081	9.8	62	- 9.7	15.8	Jan
02°46'S, 171°43'W	442	083	15.1	86	-15.0	17.5	Feb
Period: Aug. 1949-Feb. 1958	441	082	17.8	93	-17.6	19.2	Mar
	416	089	15.9	95	-15.9	16.8	Apr
N = number of observations	424	093	14.9	92	-14.9	16.2	May
θ = mean resultant wind direction	411	094	16.9	95	-16.8	17.7	Jun
Vr = mean resultant wind speed (kn)	416	095	16.9	96	-16.9	17.7	Jul
S = steadiness (percent)	445	098	18.0	95	-17.8	18.9	Aug
u = mean zonal wind speed (kn, E-)	468	098	16.7	94	-16.5	17.7	Sep
c = mean wind speed (kn)	510	095	15.5	92	-15.5	16.9	Oct
	488	093	9.5	65	- 9.5	14.7	Nov
	496	086	9.8	66	- 9.8	14.8	Dec

700 mb						500 mb						
N	θ	Vr	S	u	c	N	θ	Vr	S	u	c	
466	068	2.7	22	- 2.5	12.3	381	190	1.8	15	0.3	12.4	Jan
408	087	3.2	33	- 3.2	9.8	350	150	1.9	16	- 1.0	12.0	Feb
404	091	8.0	62	- 8.0	12.9	325	168	2.2	20	- 0.5	11.2	Mar
386	089	11.5	88	-11.5	13.1	312	117	2.5	24	- 2.2	10.5	Apr
392	091	13.0	92	-13.0	14.1	315	100	8.0	59	- 7.8	13.4	May
385	091	15.2	92	-15.2	16.4	310	086	14.0	78	-13.9	17.9	Jun
394	088	16.0	94	-16.0	17.0	353	092	18.1	92	-18.1	19.7	Jul
421	091	16.7	94	-16.7	17.7	362	090	17.3	91	-17.3	18.9	Aug
435	087	16.3	94	-16.3	17.3	382	091	17.5	91	-17.5	19.4	Sep
494	089	13.1	89	-13.1	14.7	426	088	11.7	76	-11.7	15.3	Oct
462	100	3.9	36	- 3.3	10.8	388	222	1.1	09	0.7	12.4	Nov
456	075	2.4	25	- 2.3	9.7	375	273	3.0	25	3.0	12.1	Dec

300 mb						200 mb						
N	θ	Vr	S	u	c	N	θ	Vr	S	u	c	
330	206	6.3	43	2.8	14.7	313	198	13.5	55	4.2	24.5	Jan
295	223	9.7	50	6.7	19.3	279	212	16.5	52	8.7	31.5	Feb
266	202	8.7	49	3.2	17.6	256	206	17.1	57	7.6	29.8	Mar
254	258	9.3	44	2.0	21.1	238	264	18.8	60	18.7	31.2	Apr
254	263	8.0	38	7.9	20.8	246	271	16.4	56	16.4	29.4	May
258	099	2.7	16	- 2.6	16.3	248	267	6.5	34	6.5	19.0	Jun
320	094	10.8	68	-10.8	16.0	296	087	4.1	22	- 4.1	18.9	Jul
322	094	6.4	44	- 6.4	14.4	306	003	0.9	06	0.0	16.3	Aug
338	133	3.4	20	- 2.5	16.7	326	283	4.4	23	4.3	19.2	Sep
370	216	1.0	06	0.6	16.5	346	263	7.6	34	7.5	22.2	Oct
328	246	8.9	49	8.2	18.3	304	243	15.4	62	13.8	25.1	Nov
311	235	9.0	50	7.4	18.1	287	238	14.6	55	12.4	26.7	Dec

850 mb							
Mean resultant winds and steady- ness at standard pressure levels.	N	θ	Vr	S	u	c	
Station: Darwin (94120)	86	180	4	35	0	11	Jan
12°26'S; 130°52'E	77	180	5	45	0	11	Feb
Period: 1 Aug. 1952-31 Dec. 1955	81	153	7	55	- 3	13	Mar
	70	112	11	80	-10	14	Apr
N = number of observations	86	101	10	80	-10	13	May
θ = mean resultant wind directions	87	111	9	80	- 8	11	Jun
Vr = mean resultant wind speed (kn)	92	122	5	55	- 4	9	Jul
S = steadiness (percent)	113	121	12	85	-10	14	Aug
u = mean zonal wind speed (kn, E-)	103	121	12	85	-10	14	Sep
	112	119	10	80	- 9	13	Oct
c = mean wind speed (kn)	101	117	9	75	- 8	12	Nov
	112	121	6	55	- 5	11	Dec

700 mb						500 mb						
N	θ	Vr	S	u	c	N	θ	Vr	S	u	c	
78	127	5	40	- 4	13	74	225	1	05	1	20	Jan
77	143	5	40	- 3	13	76	180	2	15	0	13	Feb
70	130	8	55	- 6	15	69	135	3	25	- 2	12	Mar
68	111	8	65	- 7	12	53	090	2	15	- 2	13	Apr
76	099	6	50	- 6	12	67	090	1	10	- 1	10	May
84	104	4	40	- 4	10	71	326	4	30	2	13	Jun
76	112	5	45	- 5	11	74	333	2	15	1	13	Jul
110	124	7	60	- 6	12	99	360	1	05	0	20	Aug
96	119	10	75	- 9	13	70	117	2	15	- 2	13	Sep
112	107	14	85	-13	16	105	112	5	40	- 5	13	Oct
106	101	15	85	-15	18	109	108	6	50	- 6	12	Nov
112	099	12	75	-12	16	109	101	5	40	- 5	13	Dec

300 mb						200 mb						
N	θ	Vr	S	u	c	N	θ	Vr	S	u	c	
71	---	Calm	0	0	---	64	043	7	40	- 5	18	Jan
71	090	3	25	- 3	12	65	046	12	65	- 9	18	Feb
60	072	3	25	- 3	12	50	054	9	50	- 8	18	Mar
44	045	1	05	- 1	20	32	027	2	10	- 1	20	Apr
60	301	6	40	5	15	50	287	10	50	10	20	May
69	301	12	65	10	18	59	298	15	65	14	23	Jun
67	304	7	40	6	18	62	300	8	40	7	20	Jul
93	292	5	30	5	17	79	288	6	30	6	20	Aug
78	270	5	30	5	17	70	276	10	45	10	22	Sep
104	270	5	30	5	17	95	276	10	45	10	22	Oct
102	270	1	05	1	20	98	284	4	20	4	20	Nov
108	---	Calm	0	0	---	100	360	4	20	0	20	Dec

Mean resultant winds and steadiness at standard pressure levels.

Station: Broome (94203)  
 17°57'S; 122°13'E  
 Period: 1 Jan. 1955-31 Dec. 1955

N = number of observations  
 O = mean resultant wind direction  
 Vr = mean resultant wind speed (kn)  
 S = steadiness (percent)  
 u = mean zonal wind speed (kn, E-)  
 c = mean wind speed (kn)

700 mb						500 mb						
N	O	Vr	S	u	c	N	O	Vr	S	u	c	
110	100	14	80	-14	18	79	105	8	55	- 8	15	Jan
88	106	15	85	-14	18	62	105	9	65	- 9	14	Feb
115	102	11	70	-11	16	88	122	5	40	- 4	13	Mar
112	080	6	50	- 6	12	91	259	5	30	5	17	Apr
117	322	2	15	1	13	102	272	13	55	13	24	May
114	296	3	20	3	15	97	270	16	65	16	25	Jun
123	296	3	20	3	15	108	266	15	65	15	23	Jul
123	315	4	30	3	13	104	264	15	65	15	23	Aug
148	330	4	30	2	13	138	266	15	65	15	23	Sep
152	360	5	40	0	13	136	270	11	55	11	20	Oct
148	040	5	40	- 3	13	129	278	7	40	7	18	Nov
136	084	9	65	- 9	14	126	C A L M		0	0	--	Dec

300 mb						200 mb						
N	O	Vr	S	u	c	N	O	Vr	S	u	c	
73	260	3	20	3	15	68	279	10	55	10	18	Jan
85	090	2	15	- 2	13	81	302	5	35	4	14	Feb
100	263	8	45	8	18	88	272	18	85	18	21	Mar
86	261	22	75	22	29	79	265	34	85	34	40	Apr
89	264	31	80	31	39	83	265	44	90	44	49	May
110	266	30	75	30	40	106	266	38	85	38	45	Jun
112	266	30	80	30	38	107	266	32	80	32	40	Jul
109	260	29	75	29	39	109	264	28	75	28	37	Aug
138	257	31	80	30	39	128	261	35	80	35	44	Sep
127	259	26	75	26	34	122	262	30	80	30	38	Oct
125	262	20	75	20	27	110	265	26	75	26	35	Nov
113	264	13	60	13	22	101	270	21	75	21	28	Dec

Near resultant winds and steadiness at standard pressure levels.

Station: Daly Waters (94234)  
 16°16'S, 133°23'E  
 Period: 1 June 1951-31 Aug. 1955

N = number of observations  
 Ø = mean resultant wind direction  
 Vr = mean resultant wind speed (kn)  
 S = steadiness (percent)  
 u = mean zonal wind speed (kn, E-)  
 c = mean wind speed (kn)

700 mb						500 mb						
N	Ø	Vr	S	u	c	N	Ø	Vr	S	u	c	
110	126	15	75	-12	20	78	113	8	50	-7	16	Jan
88	129	16	80	-12	20	83	120	8	55	-7	15	Feb
108	134	14	80	-10	18	82	147	5	40	-3	13	Mar
104	131	9	65	-7	14	76	193	5	40	1	13	Apr
115	150	4	30	-2	13	103	262	8	45	8	18	May
144	207	2	15	1	13	131	270	11	55	11	20	Jun
153	234	4	30	3	13	146	275	13	60	13	22	Jul
153	199	3	20	1	15	144	275	13	65	13	20	Aug
140	169	5	40	-1	13	101	270	11	55	11	20	Sep
140	145	7	55	-4	13	105	236	7	40	4	18	Oct
128	124	11	70	-9	16	111	180	4	30	0	13	Nov
140	119	13	80	-11	16	95	135	4	35	-3	11	Dec

300 mb						200 mb						
N	Ø	Vr	S	u	c	N	Ø	Vr	S	u	c	
64	279	3	20	3	15	50	286	10	50	10	20	Jan
80	270	1	05	1	20	72	307	5	30	4	17	Feb
77	253	8	55	8	14	64	275	10	55	10	18	Mar
73	255	17	70	16	24	65	259	21	80	21	26	Apr
104	263	23	80	23	29	104	258	33	85	32	39	May
143	270	25	75	25	33	104	265	32	80	32	40	Jun
136	275	23	75	23	31	140	270	27	75	27	36	Jul
135	280	22	75	22	29	126	276	24	75	24	32	Aug
98	275	24	80	24	30	74	275	29	80	29	36	Sep
87	267	20	75	20	27	91	268	28	80	28	35	Oct
104	270	13	60	13	22	75	273	20	75	20	27	Nov
79	273	9	50	9	18	96	281	15	65	15	23	Dec



850 mb							
Mean resultant winds and steadiness at standard pressure levels,	N	θ	Vr	S	u	c	
Station: Port Hedland (94312)	36	074	7	35	- 7	20	Jan
20°23'S, 118°37'E	32	077	9	55	- 9	16	Feb
Period: 1 Oct. 1951-2 Dec. 1952;	37	085	11	70	-11	16	Mar
24 June 1953-31 Dec. 1955 (700 mb	39	056	4	30	- 3	13	Apr
below); 1 Jan. 1954-30 Sept. 1958	38	333	4	25	2	16	May
(above 700 mb)	30	076	8	60	- 8	13	Jun
N = number of observations	45	360	2	15	0	13	Jul
O = mean resultant wind direction	41	360	1	10	0	10	Aug
Vr = mean resultant wind speed (kn)	36	270	1	05	1	20	Sep
S = steadiness (percent)	75	261	6	40	6	15	Oct
u = mean zonal wind speed (kn, E-)	66	135	2	15	- 1	13	Nov
c = mean wind speed (kn)	77	117	2	15	- 2	13	Dec

700 mb						500 mb						
N	θ	Vr	S	u	c	N	θ	Vr	S	u	c	
46	066	12	60	-12	20	141	109	3	20	- 3	15	Jan
40	067	13	75	-13	17	129	111	9	60	- 9	15	Feb
38	090	8	55	- 8	15	141	143	5	35	- 3	14	Mar
42	360	1	05	0	20	135	253	10	60	10	17	Apr
45	301	12	60	10	20	138	272	31	85	31	37	May
30	360	3	20	0	15	134	263	32	85	32	38	Jun
45	287	10	60	10	17	141	277	41	90	41	46	Jul
40	287	10	60	10	17	148	268	31	90	31	34	Aug
39	308	11	60	9	18	146	259	25	85	25	29	Sep
68	270	30	85	30	35	148	284	21	80	20	26	Oct
68	337	8	50	3	16	142	290	9	55	8	16	Nov
78	009	6	40	- 1	15	117	243	2	15	2	13	Dec

300 mb						200 mb						
N	θ	Vr	S	u	c	N	θ	Vr	S	u	c	
129	252	6	35	6	17	120	270	17	65	17	25	Jan
114	233	5	30	4	17	102	270	10	50	10	20	Feb
137	257	9	45	9	20	129	270	21	75	21	28	Mar
122	264	27	80	27	34	116	263	50	90	50	56	Apr
123	270	48	90	48	53	110	267	63	90	63	70	May
122	266	49	90	49	54	110	264	57	90	57	63	Jun
138	270	58	95	58	61	131	267	65	95	65	68	Jul
137	270	49	95	49	52	123	270	52	95	52	55	Aug
132	265	48	95	48	51	126	263	52	90	52	58	Sep
114	270	43	85	43	51	107	270	48	90	48	53	Oct
108	266	30	85	30	35	103	273	51	95	51	54	Nov
113	270	20	75	20	27	107	273	35	90	35	39	Dec

850 mb							
Mean resultant winds and steadiness at standard pressure levels	N	θ	Vr	S	u	c	
Station: Cloncurry (94335)	81	090	7	50	- 7	14	Jan
20°40'S, 140°30'E	71	090	11	75	-11	15	Feb
Period: 14 Aug. 1952-31 Dec. 1955	79	107	17	90	-16	19	Mar
	82	090	10	70	-10	14	Apr
	88	108	6	50	- 6	12	May
N = number of observations	88	127	5	40	- 4	13	Jun
θ = mean resultant wind direction	92	135	4	30	- 3	13	Jul
Vr = mean resultant wind speed (kn)	107	108	3	25	- 3	12	Aug
S = steadiness (percent)	120	090	3	25	- 3	12	Sep
u = mean zonal wind speed (kn, E-)	107	063	4	30	- 4	13	Oct
c = mean wind speed (kn)	107	090	1	10	- 1	10	Nov
	104	090	2	15	- 2	13	Dec

700 mb						500 mb						
N	θ	Vr	S	u	c	N	θ	Vr	S	u	c	
85	124	4	35	- 3	11	84	211	6	40	3	15	Jan
72	111	9	65	- 8	14	71	180	2	15	0	13	Feb
81	114	12	75	-11	16	81	166	4	25	- 1	16	Mar
82	090	4	35	- 4	11	82	245	14	65	13	22	Apr
86	217	5	35	3	14	87	265	26	80	26	33	May
90	225	7	40	5	18	88	270	29	80	29	36	Jun
93	234	9	55	7	16	93	257	18	65	18	28	Jul
111	254	7	45	7	16	98	264	30	85	30	35	Aug
120	259	5	40	5	13	120	264	27	85	27	32	Sep
109	270	3	25	3	12	109	256	21	80	20	26	Oct
112	---	Calm	0	0	--	112	249	14	65	13	22	Nov
105	153	2	15	- 1	13	104	229	9	55	8	16	Dec

300 mb						200 mb						
N	θ	Vr	S	u	c	N	θ	Vr	S	u	c	
76	265	12	55	12	22	57	270	18	60	18	30	Jan
78	281	10	50	10	20	68	290	15	55	14	27	Feb
75	270	12	55	12	22	68	284	21	70	20	30	Mar
80	262	34	85	34	40	66	266	52	95	52	55	Apr
80	259	50	90	49	56	49	260	65	95	64	72	May
82	271	51	90	51	57	47	270	63	90	63	70	Jun
78	264	51	90	51	57	43	261	56	90	55	62	Jul
100	265	51	90	51	57	72	262	53	90	52	59	Aug
110	264	50	90	50	56	79	265	63	95	63	66	Sep
97	262	42	90	42	47	76	263	58	90	58	64	Oct
100	255	31	85	30	37	76	255	42	85	42	49	Nov
97	248	22	75	20	29	73	250	33	80	32	41	Dec

## 850 mb

Mean resultant winds and steadiness at standard pressure levels		N	θ	Vr	S	u	c	
Station:	Clark Air Base (98327)	686	075	11.5	85	-11.1	13.3	Jan
	15°10'N, 120°34'E	591	078	8.9	81	-8.7	11.0	Feb
Period:	July 1949-April 1958	637	086	7.3	79	-7.3	9.3	Mar
		593	096	5.8	74	-5.7	7.8	Apr
N =	number of observations	546	122	3.5	47	-3.0	7.5	May
θ =	mean resultant wind direction	535	180	4.8	41	0.0	11.6	Jun
Vr =	mean resultant wind speed (kn)	599	182	2.7	26	0.1	10.5	Jul
S =	steadiness (percent)	654	242	7.2	55	6.3	13.1	Aug
u =	mean zonal wind speed (kn, E-)	613	198	2.7	27	0.9	10.9	Sep
		628	077	5.8	49	-5.7	11.8	Oct
c =	mean wind speed (kn)	652	065	9.1	63	-8.2	14.5	Nov
		686	072	13.6	86	-12.9	15.7	Dec

## 700 mb

## 500 mb

N	θ	Vr	S	u	c	N	θ	Vr	S	u	c	
678	117	6.9	64	-6.3	10.8	622	197	3.2	28	0.9	11.5	Jan
583	112	4.8	43	-4.4	11.1	567	218	2.1	18	1.3	11.5	Feb
634	099	5.7	64	-5.6	8.9	616	192	2.7	29	0.5	9.1	Mar
590	091	6.2	71	-6.2	8.7	576	096	1.2	15	-1.2	8.4	Apr
539	118	4.4	46	-3.9	9.5	530	112	3.0	32	-2.8	9.5	May
536	162	4.8	36	-1.5	13.4	503	134	5.9	45	-4.3	13.2	Jun
595	150	3.4	28	-1.7	12.4	571	112	5.9	47	-5.5	12.7	Jul
648	237	5.6	37	4.7	15.1	597	158	3.1	21	-1.2	14.7	Aug
619	146	2.9	23	-1.6	12.7	595	116	5.6	42	-5.0	13.4	Sep
627	092	7.5	56	-7.5	13.5	604	094	7.4	57	-7.4	13.1	Oct
652	091	8.2	51	-8.2	16.5	628	087	6.2	41	-6.2	15.3	Nov
683	097	10.4	71	-10.3	14.1	678	127	6.5	53	-5.2	12.3	Dec

## 300 mb

## 200 mb

N	θ	Vr	S	u	c	N	θ	Vr	S	u	c	
636	245	10.1	62	9.1	16.4	610	228	15.7	72	11.6	21.7	Jan
531	242	8.4	58	7.4	14.5	500	223	13.2	65	9.0	19.1	Feb
594	253	10.9	71	10.5	15.4	553	237	16.7	78	14.0	21.4	Mar
561	278	6.9	53	6.8	13.1	535	266	9.6	60	9.5	16.0	Apr
500	059	3.8	32	-3.2	11.2	457	042	7.3	47	-4.9	15.7	May
470	082	8.0	57	-7.9	14.0	433	063	14.4	69	-12.8	20.9	Jun
544	082	8.1	63	-8.0	12.8	500	076	14.3	72	-13.9	19.9	Jul
557	087	9.4	65	-9.3	14.4	528	073	16.3	75	-15.7	21.7	Aug
581	083	7.7	56	-7.7	13.7	553	070	13.0	65	-12.3	20.1	Sep
565	085	7.8	57	-7.8	13.7	539	082	9.0	55	-8.9	16.2	Oct
592	097	5.3	36	-5.3	14.8	549	116	6.1	37	-5.5	16.6	Nov
650	191	3.8	31	0.7	12.3	627	202	8.9	53	3.4	16.7	Dec

## Ship N

850 mb							
Mean resultant winds and steadiness at standard pressure levels.	N	θ	Vr	S	u	c	
Station: Ocean Ship N	402	252	6.6	36	6.3	18.3	Jan
30°N, 140°W	404	288	2.9	16	2.7	18.0	Feb
Period: July 1949-June 1950;	418	022	4.8	28	-1.8	16.9	Mar
July 1952-June 1957	413	355	3.4	21	0.3	16.1	Apr
	438	358	4.0	28	0.1	14.3	May
N = number of observations	440	036	10.2	72	-6.0	14.2	Jun
θ = mean resultant wind direction	438	050	11.5	80	-8.8	14.3	Jul
Vr = mean resultant wind speed (kn)	445	042	8.7	70	-5.9	12.4	Aug
S = steadiness (percent)	413	028	7.2	60	-3.4	12.1	Sep
u = mean zonal wind speed (kn, E-)	389	013	3.7	29	-0.8	12.8	Oct
c = mean wind speed (kn)	407	278	2.9	18	2.9	16.0	Nov
	421	264	5.1	25	5.1	19.7	Dec

700 mb						500 mb						
N	θ	Vr	S	u	c	N	θ	Vr	S	u	c	
420	269	12.7	54	12.7	23.5	390	271	23.0	69	23.0	33.5	Jan
421	280	6.7	30	6.6	22.4	412	280	15.4	51	15.2	30.1	Feb
429	342	5.9	30	1.8	19.4	400	300	12.9	49	11.1	26.2	Mar
453	303	6.8	40	5.7	20.0	438	290	16.4	59	15.5	27.9	Apr
450	309	6.7	36	5.1	18.6	423	281	15.1	59	14.8	25.8	May
455	018	9.4	60	2.9	15.6	442	328	8.3	49	4.4	17.1	Jun
447	046	7.4	57	5.3	12.9	417	307	1.8	14	1.5	13.1	Jul
467	020	4.7	39	1.6	12.1	447	272	7.6	49	7.6	15.6	Aug
420	009	4.9	36	0.8	13.6	405	278	7.3	41	7.2	17.6	Sep
422	345	4.3	28	1.1	15.5	414	296	7.5	38	6.8	19.5	Oct
432	282	6.3	32	6.1	19.8	438	271	13.7	51	13.7	26.7	Nov
441	268	9.3	38	9.3	24.7	419	269	18.9	58	18.9	32.4	Dec

300 mb						200 mb						
N	θ	Vr	S	u	c	N	θ	Vr	S	u	c	
323	275	34.4	74	34.2	46.6	238	282	41.4	77	40.4	54.0	Jan
371	283	25.5	57	24.9	44.9	305	279	36.5	70	36.1	51.9	Feb
342	293	24.1	59	22.1	40.7	275	288	32.9	68	31.3	48.1	Mar
388	281	27.3	66	26.8	41.6	305	280	34.0	71	33.4	48.1	Apr
364	274	24.9	65	24.8	38.2	293	277	30.5	68	30.3	45.1	May
390	299	11.6	44	10.2	26.2	305	289	13.4	42	12.7	32.1	Jun
353	247	12.3	54	11.3	22.7	272	244	20.6	69	18.5	30.0	Jul
376	255	20.7	70	20.0	29.6	314	250	32.2	80	30.4	40.4	Aug
337	260	22.1	62	21.8	35.5	272	250	35.1	78	33.0	45.0	Sep
332	286	15.5	48	14.9	32.2	261	282	19.8	52	19.4	38.4	Oct
394	281	21.5	56	21.2	38.1	332	286	24.3	57	23.4	42.6	Nov
348	275	33.0	69	32.9	47.6	290	280	38.2	69	37.7	55.1	Dec

850 mb						
Mean resultant winds and steadiness at standard pressure levels.	N	θ	Vr	S	u	c
Station: Ocean Ship V	332	259	21.2	72	20.8	29.3
34°N, 164°E	331	262	22.0	76	21.7	28.8
Period: Feb. 1951-June 1957	350	247	16.2	66	14.8	24.4
	323	242	11.1	53	9.8	20.9
	354	246	14.0	73	12.8	19.3
N = number of observations	339	260	16.5	77	16.3	21.5
θ = mean resultant wind direction	304	197	9.6	57	2.8	16.7
Vr = mean resultant wind speed (kn)	300	197	6.4	43	1.9	14.8
S = steadiness (percent)	304	269	2.2	16	2.2	14.1
u = mean zonal wind speed (kn, E-)	341	218	5.6	33	3.4	17.0
c = mean wind speed (kn)	320	259	11.9	51	11.7	23.2
	322	265	15.1	61	15.1	24.9

700 mb						500 mb					
N	θ	Vr	S	u	c	N	θ	Vr	S	u	c
343	264	34.4	87	34.2	39.5	336	266	61.2	91	61.1	67.0
340	263	38.4	90	38.1	42.7	328	265	64.4	94	64.1	68.8
354	257	28.4	84	27.6	33.8	334	262	43.9	90	43.5	48.8
335	255	20.7	74	20.0	27.8	328	262	36.9	87	36.5	42.5
357	255	21.1	82	20.4	25.6	350	261	31.1	88	30.7	35.5
341	267	25.5	88	25.5	29.1	333	268	35.4	89	35.3	39.7
316	209	8.8	50	4.3	17.5	302	226	7.2	41	5.2	17.6
307	206	5.2	34	2.3	15.4	295	234	3.4	24	2.8	14.3
312	287	4.7	27	4.5	17.1	295	296	8.2	39	7.4	21.2
349	246	8.8	45	8.0	19.7	341	261	14.1	56	13.9	25.0
311	264	26.4	80	26.2	32.8	314	263	46.1	90	45.8	51.3
329	269	28.6	81	28.6	35.3	311	267	52.8	89	52.7	59.3

300 mb						200 mb					
N	θ	Vr	S	u	c	N	θ	Vr	S	u	c
253	272	97.3	94	97.2	103.3	153	273	99.6	94	99.5	105.8
242	269	99.0	94	99.0	105.6	116	274	104.9	94	104.6	112.6
281	268	65.2	91	65.2	71.6	219	272	79.2	90	79.2	88.4
289	268	54.4	89	54.3	61.3	254	275	61.2	85	61.0	71.7
314	268	39.6	86	39.5	45.9	288	274	41.9	80	41.8	52.3
304	271	44.0	89	44.0	49.6	263	279	47.3	85	46.8	55.8
264	277	5.2	24	5.2	21.6	201	337	7.7	26	3.1	29.3
264	322	2.3	13	1.4	17.7	237	015	4.5	18	-1.2	24.9
267	318	11.1	39	7.4	28.5	237	334	14.2	40	6.1	35.5
313	271	20.0	58	20.0	34.3	287	281	21.5	54	21.1	39.6
258	267	61.3	90	61.2	68.0	195	273	68.2	91	68.2	75.2
243	272	84.7	91	84.7	93.5	143	277	90.7	91	90.1	99.9

## 1. Introduction

Over this region it is convenient to identify two seasons, Winter and Summer, each of about four months' duration, separated by two shorter transition seasons, Spring and Autumn, of about two months each. The Northern Hemisphere winter (Southern Hemisphere summer) lasts from November through February, the summer (Southern Hemisphere winter) from May through August with transition seasons occupying March, April and September, October. In a normal year weather during the transition months alternately resembles summer and winter conditions. However, in abnormal years, which are far from infrequent, a transition period may have weather indistinguishable from one of the major seasons.

This introduction contains a warning; namely that averages for individual months, except possibly for midwinter or midsummer months, often differ from the climatic normals for those months.

The climatic picture of the Pacific and southeast Asia is dominated by the Pacific anticyclone and the Asiatic monsoons. Seasonal variations in all the surface elements (winds, pressure, temperature, sea temperature, cloudiness and rainfall) are least over the eastern and central Pacific and in general (except near the equator) increase steadily westward, reaching a maximum over southeast Asia in the far west of the region. This is of course to be expected since the transition is from an oceanic to a continentally dominated climate. Honolulu and Hong Kong are both stations near sea level at about the same latitude. Table 4-1, comparing the two stations, shows that a wide variety of climates can occur in the tropics and that one would be most unwise to generalize on the basis of only one part of the region. The comparison between Honolulu and Hong Kong suggests an important axiom, namely, that over the oceanic tropics far removed from

Table 4-1. Summer and winter at Honolulu and Hong Kong.

Mean	Honolulu			Hong Kong		
	Jan	July	Range	Jan	July	Range
Air Temperature (°F)	71	78	7	60	82	22
Sea Temperature (°F)	74	78	4	63	77	14
Pressure (mb)	1016	1017	1	1020	1005	15
Rainfall (mm)	95	31	64	32	386	354

major land masses, winter and summer climatological charts are recognizably similar to one another, whereas over and near the continents, there is no resemblance.

## 2. Surface air temperatures

Although most treatments of climatology start with the pressure and wind fields, it is in fact the field of temperature, deriving directly from the march in latitude of the sun at its zenith, which determines the distribution of pressure and winds. However, the effect of the sun's variation in latitude is by no means uniform, since the ocean's heat capacity is very much greater than the land's. In the transition from winter to summer, the land heats more rapidly, and in the transition from summer to winter, cools more rapidly than the ocean. In this we find an explanation for a greater range of air temperature at Hong Kong where the land effect dominates, than at Honolulu which has an oceanic climate.

Over the eastern and central Pacific the thermal equator moves probably less than  $5^{\circ}$  latitude away from the geographical equator throughout the year, whereas further west it lies over central Australia in January and over central China in July, a range of more than  $50^{\circ}$  latitude.

## 3. Surface winds and pressures

A cursory glance reveals that the mean fields of surface temperature, pressure and winds are closely related (fig 2-2 of PA). The thermal equator coincides with a pressure trough, called by some meteorologists the intertropical trough. This designation is usually erroneous for the trough is seldom the meeting zone of air from opposite hemispheres. High pressure centers are displaced poleward in summer and equatorward in winter. Again the greatest displacement occurs in the western part of our region. For example, along the meridian of  $130^{\circ}\text{E}$ , highest pressure in January is found at  $65^{\circ}\text{N}$  and in July at  $30^{\circ}\text{S}$ , whereas along  $170^{\circ}\text{W}$  two maxima exist throughout the year, ranging from  $28^{\circ}\text{N}$  in January to  $35^{\circ}\text{N}$  in July in the Northern Hemisphere, and from  $32^{\circ}\text{S}$  to  $20^{\circ}\text{S}$  in the Southern Hemisphere. This seasonal variation in pressure distribution is reflected in the wind regimes. Over the open oceans the trade winds and doldrums shift poleward in the summer and equatorward in the winter. Over southeast Asia the strong and persistent winter monsoon flowing around the intense Asiatic anticyclone gives way in summer to weak and fitful southerlies. A corresponding but less marked reversal occurs over eastern Australia.

## 4. Sea temperatures

Open ocean surface temperatures vary only slightly with the seasons. However, over the western ocean, great seasonal changes in the wind regime produce corresponding changes in ocean currents and in sea temperatures. In winter, the strong northeast monsoon transports cold water along the China coast setting up a steep northwest directed sea temperature gradient. This distribution, as later chapters show, exerts a profound effect on weather processes over southeast Asia and the western Pacific during winter and spring, so much so that of all the climatic charts, that of winter mean sea surface temperature is the most important (fig

III-1)\*. The winter anticyclone centered over Australia produces a similar effect: winter sea temperatures off the east coast are 10 to 12°F below those of summer.

#### 5. Clouds and rainfall

Normal cloud and rainfall distributions are less simply explained than distributions of the variables already dealt with. To be properly useful, cloud classification must include types as well as amounts, and any explanations of the charts must take account of the interrelationships of air and surface temperatures, wind directions and humidity distribution.

In other words, one should discuss the climatology of clouds and rain synoptically. Thus winter distributions can be better described and explained at the end of the section on the winter monsoon and summer distributions at the end of the section on the summer monsoon.

#### 6. The large-scale features of the monsoons

Low levels. Geography and climatology texts often give the impression that, in the Asia-Australia monsoon regions, air at low levels flows massively across the equator, from north to south in the northern winter and from south to north in the northern summer. This notion is probably valid for the equatorial Indian Ocean west of 65°E where mean southward flow in January amounts to 10 kn, and mean northward flow in July to 13 kn.

Further east, however, the Asian and Australian "branches" of the monsoons are essentially confined to their own hemispheres and are not associated with large-scale persistent trans-equatorial flow. A small net flow crosses the equator from the winter to the summer hemisphere (means for January and July = 5 kn) through the agency of equatorial eddies.

In January, eddies over the Indian Ocean between a weak northeast monsoon and the southeast trades are ill-defined and ephemeral. Further east, counterclockwise eddies between the northeast trades and the Australian summer monsoon may be readily identified.

In July, the southwest monsoon and the circulation around the South Indian Ocean and Australian highs are separated, east of 65°E, by clockwise equatorial eddies.

The change in sense of eddy rotation between January and July would appear to favor the theory that the eddies are turbulent derivatives of the major circulations to north and south. However, other equally plausible and equally untested theories have been advanced to account for their existence.

There is some evidence that the bold and extensive orography of Indonesia may favor eddy development to the west of Sumatra,

---

\*Figure 1 of Appendix III.



over Borneo and to the north of New Guinea.\*

Upper levels. In the upper troposphere the heat low of the summer hemisphere is overlain by an anticyclone while the high pressure ridge of the winter hemisphere is displaced toward the equator. Thus it is not surprising to find easterlies predominating over the equatorial portions of the Indian and west Pacific Oceans and little evidence of eddies.

#### 7. The large-scale features of the central Pacific circulation

The major synoptic features which are readily evident on any mean resultant wind chart, are the semi-permanent subtropical ridge and steady wind regimes. Migratory ridges or troughs, typhoons or tropical cyclones, do not appear. During the typhoon season, a persistent upper tropospheric trough usually extends eastnortheast-west southwest across the central North Pacific.

Low levels. The trades blow the year round on the equatorial sides of the subtropical ridges, directed from north of east in the Northern Hemisphere and from south of east in the Southern Hemisphere. Over the western part of the central ocean, in the summer hemisphere, the trades are displaced by low latitude westerlies which form part of the summer monsoon circulations.

Upper levels. Above the trades, and separated from them by the subtropical ridge, lie the antitrades, the low latitude extension of the polar westerlies. The antitrades are the strongest steady winds in the tropics, often reaching speeds of more than 100 kn at the poleward fringes of the tropics in winter. The equatorial easterlies of the western Pacific may occasionally extend as far eastward as 160°E.

#### 8. Bibliography

Gherzi, E., 1951: The meteorology of China (2 vols.). Macau, Imprensa Nacional, 423 pp, 23 tables.

India Meteorological Department, 1945: Climatological charts of the Indian monsoon area. Poona, Govt. Photozinc Office, 72 charts.

Landsberg, H., 1945: Climatology. Handb. of Met., 928-997. New York, McGraw-Hill Co.

McDonald, W. F., 1938: Atlas of the climatic charts of the oceans. Washington, U. S. Govt. Printing Office, 130 charts.

---

\* H. Riehl in "On the formation of typhoons," (J. Meteor., 5, 247-264. 1948) and B. W. Thompson in "An essay on the general circulation of the atmosphere over southeast Asia and the west Pacific," (Q. J. Roy. Meteor. Soc., 77, 569-597. 1951) describe the clockwise equatorial eddies of the northern summer and mention preferred formation areas north of New Guinea and over Borneo.

Meteorological Office, London, 1937: Weather in the China Seas and in the western part of the North Pacific Ocean. Vol. I, 1, MO 404a, General information, Vol. II, MO 404b, Local information. London, H. M. Stationery Office, 164 pp, 771 pp.

\_\_\_\_\_, 1943: Weather in the Indian Ocean, Vol. I. MO 451a, General information, Vol. II, Location information. London, H. M. Stationery Office, 52 pp, 1123 pp.

\_\_\_\_\_, 1947: Monthly meteorological charts of the western Pacific Ocean. MO 484. London, H. M. Stationery Office, 120 pp.

\_\_\_\_\_, 1949: Monthly meteorological charts of the Indian Ocean. MO 519. London, H. M. Stationery Office, 98 pp.

\_\_\_\_\_, 1956: Monthly meteorological charts of the eastern Pacific Ocean. MO 515. London, H. M. Stationery Office, 122 pp.

Royal Dutch Meteorological Institute, 1935: Oceanographic and meteorological observations in the China Seas and in the western part of the North Pacific Ocean. 'S-Gravenhage, Rijksuitgeverij, 94 pp.

U. S. Navy, 1956: Marine climatic atlas of the World. Vol. II, North Pacific Ocean. NAVAER 50-1C-529. Washington, Supt. of Documents, 275 charts.

\_\_\_\_\_, 1957: Marine climatic atlas of the World. Vol. III, Indian Ocean. NAVAER 50-1C-530. Washington, Supt. of Documents, 267 charts.

# SYNOPTIC CLIMATOLOGY OF CENTRAL PACIFIC

## TROPOSPHERIC WINDS

### 1. Introduction

Over much of the central Pacific, large-scale circulation features persist for several days without undergoing significant changes in position or intensity. Thus a mean resultant wind chart for a period of up to one month is recognizably similar to a synoptic wind chart for any individual observing time during that month.

A mean chart at any given horizontal or pressure level presents a picture of supposedly normal conditions. Very often, however, if the time period over which the parameters are averaged is too long, some of the significant features which should be disclosed are lost in the averaging process. The usual mid-latitude procedure of presenting mean seasonal charts cannot be followed in the tropics because the major changes in tropical synoptic patterns do not coincide with the calendar changes of seasons. A month is probably the longest period for which mean charts can be meaningful without damping out all significant features. Although this period of time is in many cases longer than optimum, data for shorter periods are usually unavailable. Consequently, throughout this chapter, calendar month averages will be used (with the exception of figs 5-1 to 5-6).

Steadiness, the ratio of mean resultant wind to mean wind X 100, provides a good basis for estimating how often synoptic patterns resemble mean patterns. Over areas where steadiness exceeds 90 per cent, wind directions on most days are unlikely to deviate much from the mean, whereas a steadiness of 10 per cent indicates that the synoptic pattern may only fortuitously resemble the mean.

On a succession of monthly mean resultant wind charts one may easily follow seasonal changes which in turn are related to slow changes in the frequencies of various synoptic patterns. Mean charts for particular months often vary considerably from year to year thus revealing important inter-annual dissimilarities in synoptic patterns.

The relationships of mean flow patterns to synoptic patterns is discussed in the remainder of this chapter under the following headings: firstly, normal intra-annual changes, secondly, inter-annual variability, and thirdly, short-period forecasting.

### 2. Intra-annual circulation changes

A series of six semi-monthly mean cross-sections between Nauru ( $0^{\circ}32'S$ ,  $166^{\circ}55'E$ ) and Ocean Ship Victor ( $34^{\circ}N$ ,  $164^{\circ}E$ ) (figs 5-1 to 5-6) shows the transition from winter to summer in

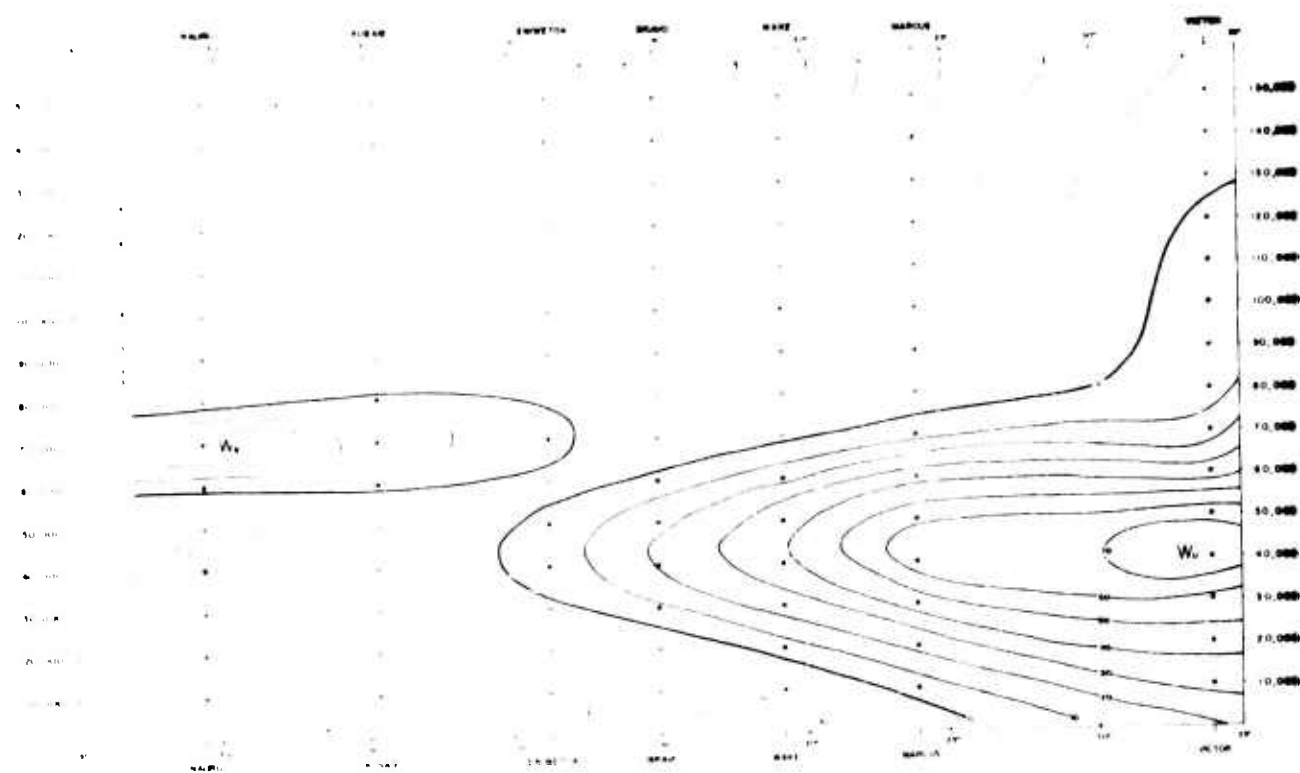


Figure 5-1. Mean zonal winds (knots) near 165°E, 1-15 April 1958. (From "A study of the mean vertical wind structure over the Eniwetok Proving Ground area" by F. E. McCreary, Joint Task Force Seven Met. Cent., TP-15, 65 pp. 1959).

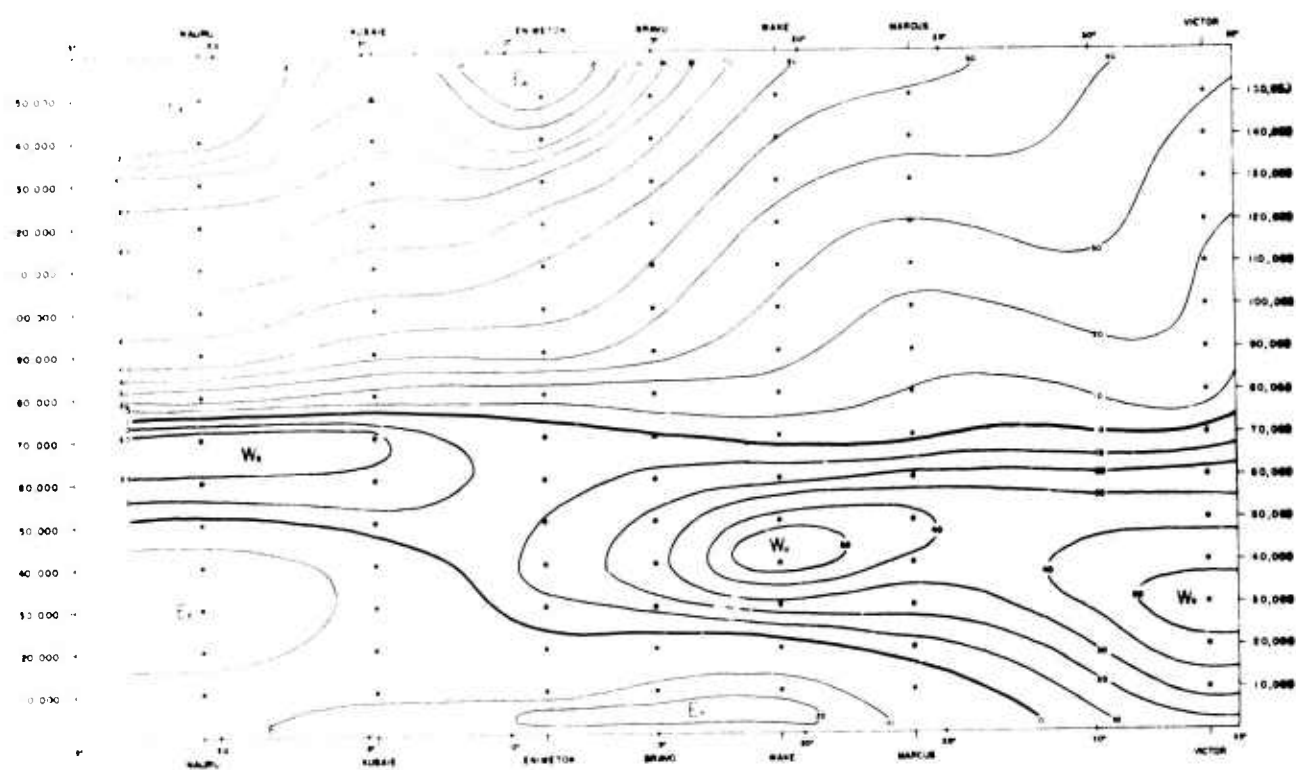


Figure 5-2. Same as fig 5-1 but for 16-30 April 1958.

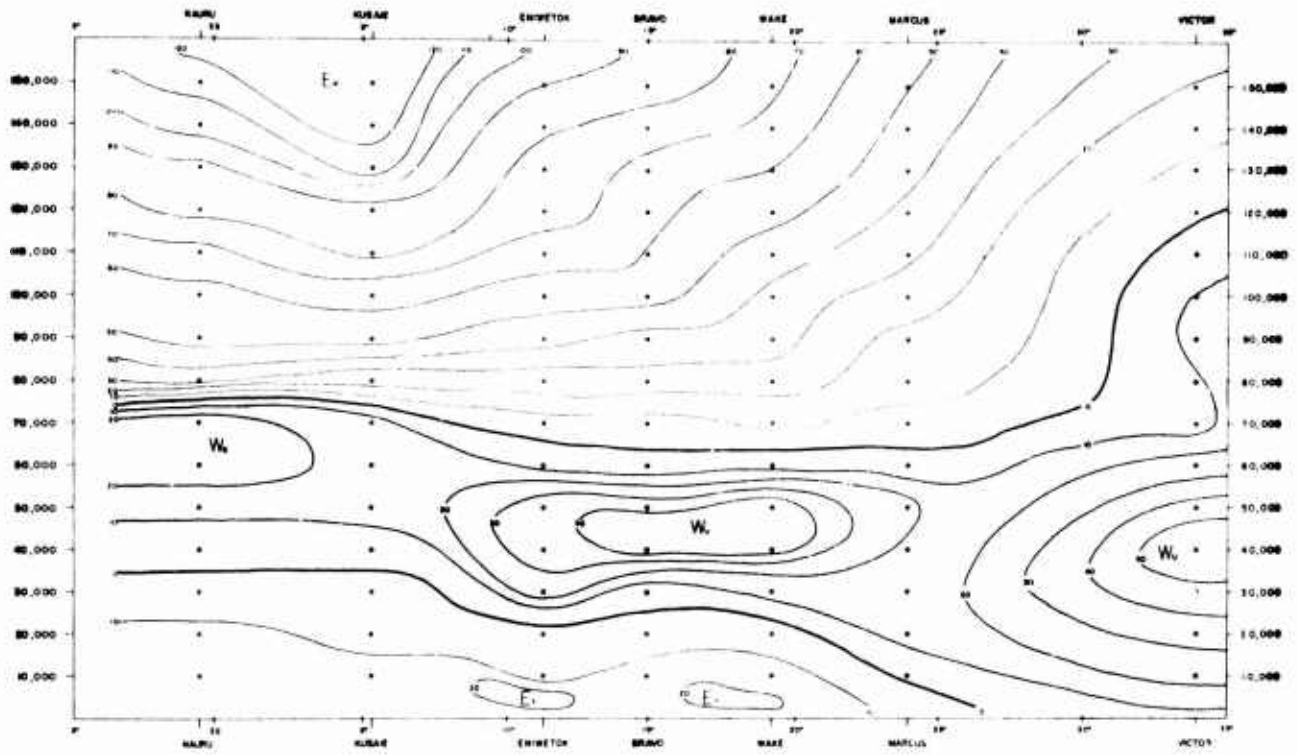


Figure 5-3. Same as fig 5-1 but for 1-15 May 1958.

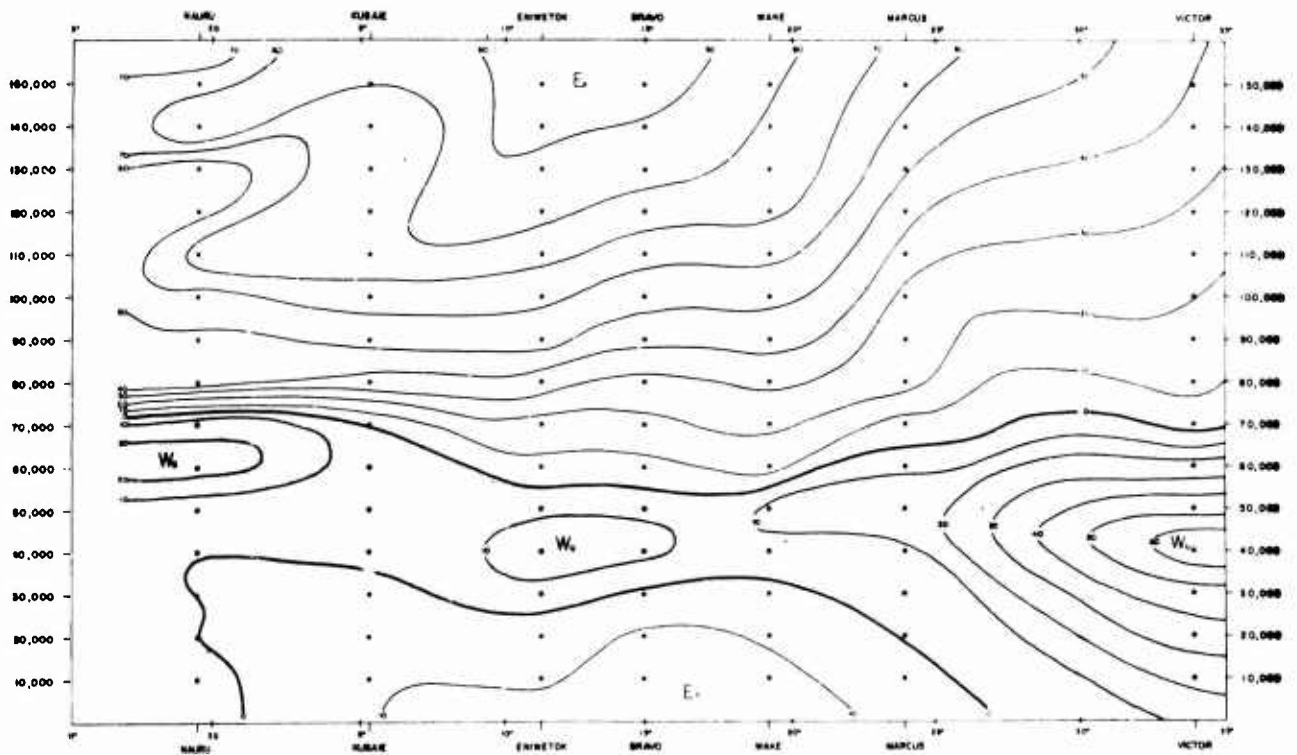


Figure 5-4. Same as fig 5-1 but for 16-31 May 1958.

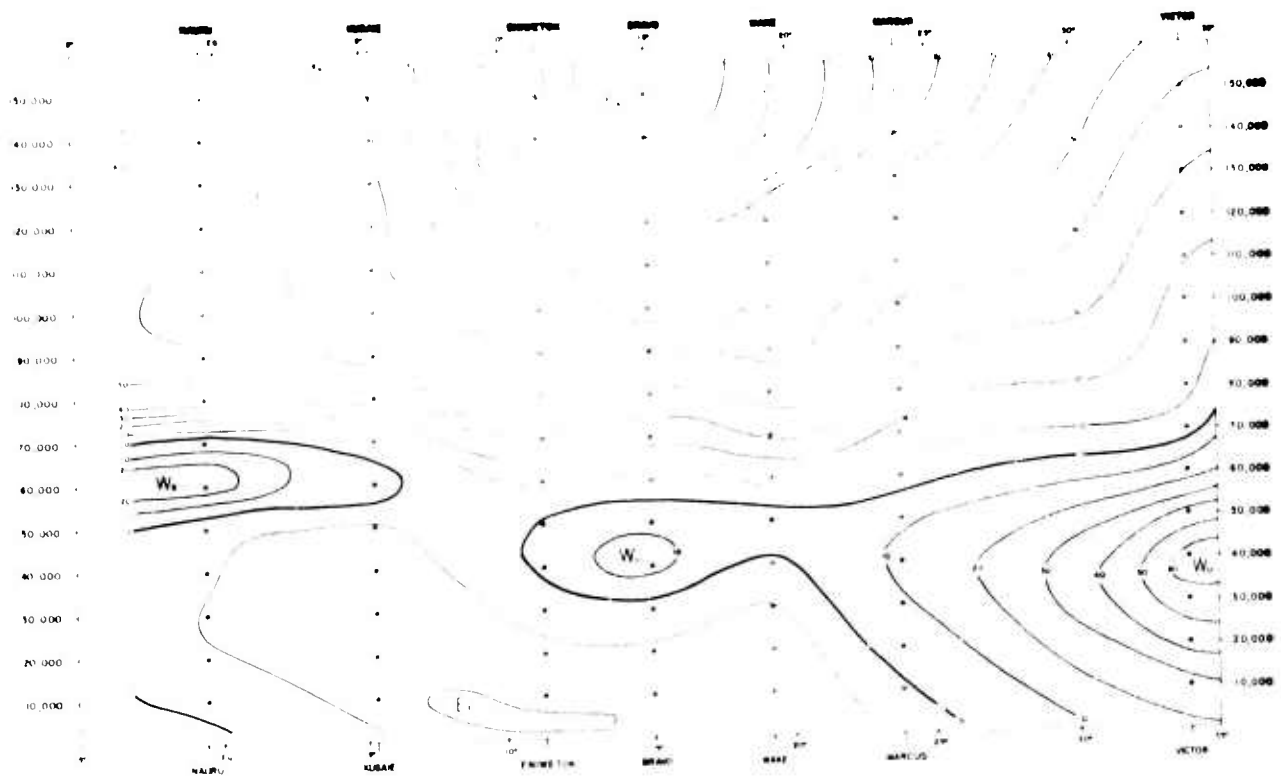


Figure 5-5. Same as fig 5-1 but for 1-15 June 1958.

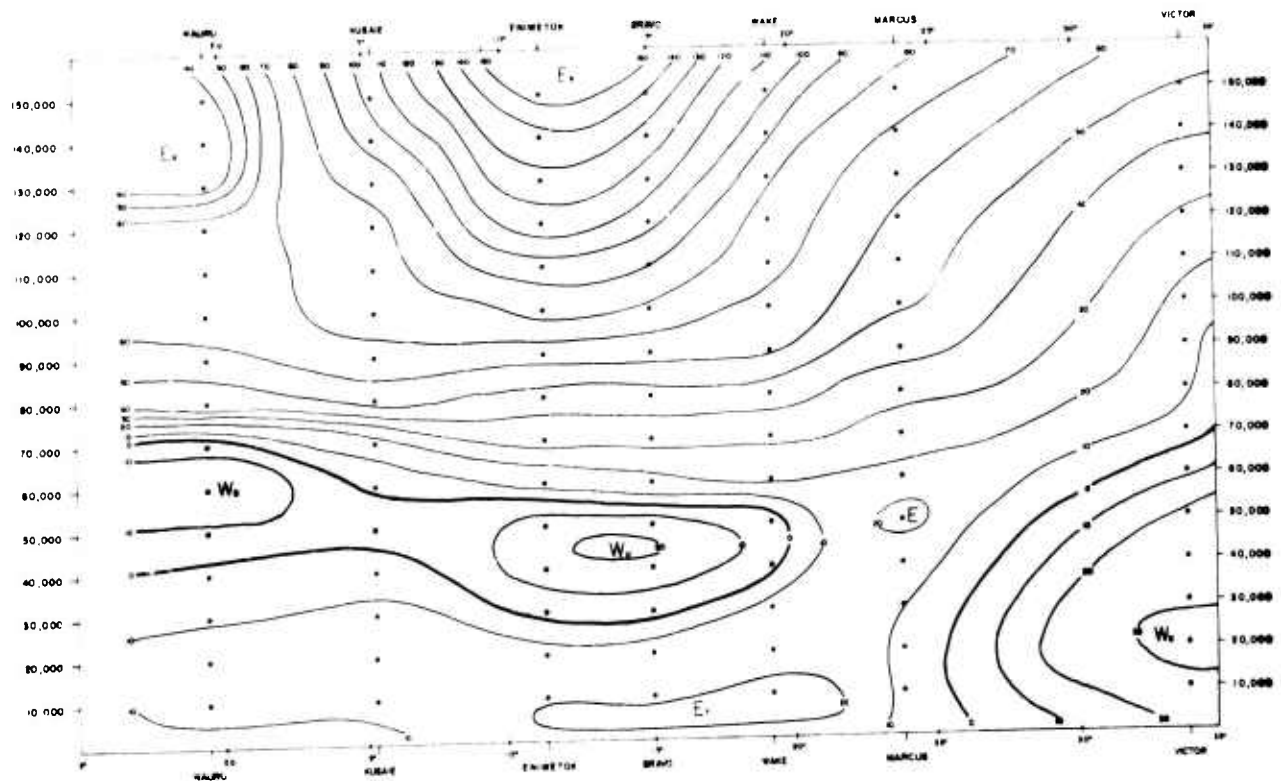


Figure 5-6. Same as fig 5-1 but for 16-30 June 1958.

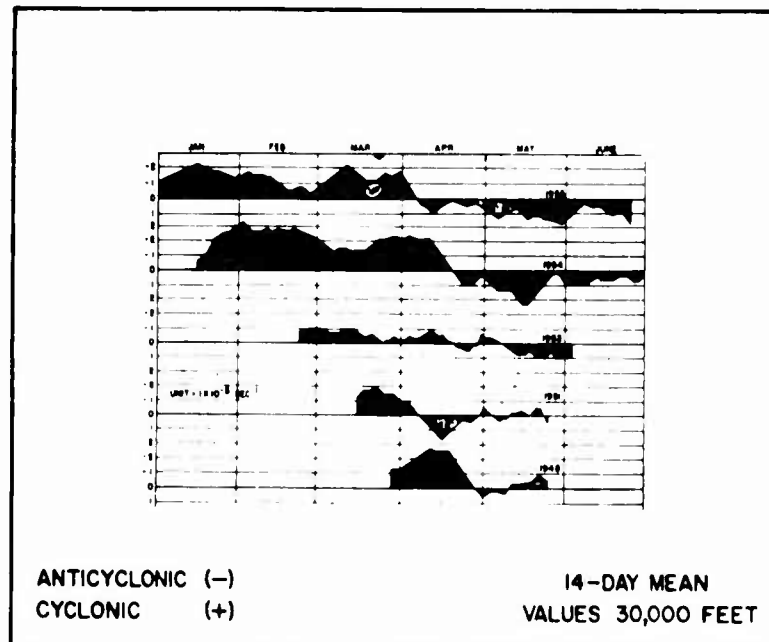
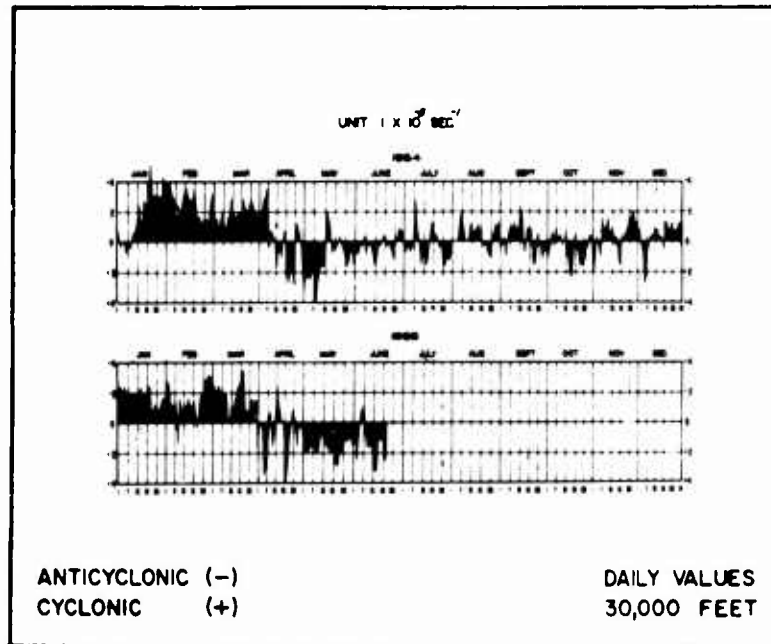


Figure 5-7. Time charts of wind shear at 30,000 ft between Wake Island and Eniwetok Atoll. (From "A study of the 30,000 ft wind field over the west central Pacific" by F. E. McCreary and J. B. Wharton, Joint Task Force Seven Met. Cent., TP-5, 19 pp. 1957).

1958\*. In early April the antitrades are very strong, the trades shallow, in the Wake Island area. By late May the trades, although weaker, extend to 30,000 ft from Wake southward. The changing slope of the subtropical ridge accompanies development of the mid-Pacific trough, which by May is well defined at 30,000 ft between Wake and Eniwetok. In early June the trough extends to 40,000 ft, being most pronounced slightly farther north in late June.

Fig 5-7, time charts of the wind shear at 30,000 ft between Wake and Eniwetok, confirms that as the subtropical ridge weakens and the mid-Pacific trough develops, transition from winter to summer in the upper troposphere usually occurs quite rapidly, but that probably the return to winter conditions is more gradual.

Seasonal characteristics at 30,000 ft are also illustrated by figs 5-8 and 5-9. In January 1955 (fig 5-8), the Northern Hemisphere subtropical ridge lies along 15°N and circulation is anticyclonic west of the Date Line. East of the Date Line a trough stretching northeast-southwest through Hawaii derives from frequent winter "Kona" storms in that area.

In May 1955 (fig 5-9), the subtropical ridges of both hemispheres are further north and the mid-Pacific trough is well defined, extending from north of Johnston Island, south of Wake Island to the area southwest of Guam.

### 3. Inter-annual circulation changes

Circulation patterns, especially during transition months, may vary markedly from year to year. For example, fig 5-7 shows that the change from anticyclonic to cyclonic wind shear at 30,000 ft between Wake and Eniwetok took place during April in 1954 and 1955 but not until late May in 1948 and 1951.

Inspection of the 30,000 ft mean resultant wind charts for May 1955, 1956, 1957 and 1958 (figs 5-9 to 5-12), reveals that in 1955, 1956, and 1958, Northern Hemisphere summer patterns predominated. Among these months, however, differences can be detected. The mid-Pacific trough of 1955 and 1958 is replaced by two troughs in 1956, one extending from Ocean Ship Victor to Truk and the other from Midway to the vicinity of Wake.

In contrast to the pronounced ridge-trough systems of these Mays, the circulation of May 1957, with strong zonal flow north of 20°N resembles Northern Hemisphere winter conditions (c.f. fig 5-8).

The most persistent inter-annual feature, an anticyclonic cell east of the Philippines, appears on the mean chart of the four Mays (fig 5-13). The mid-Pacific trough is also evident.

---

\* The changes observed along this cross-section, which is in the region of the mid-Pacific trough, may not be representative of changes to the east and west.





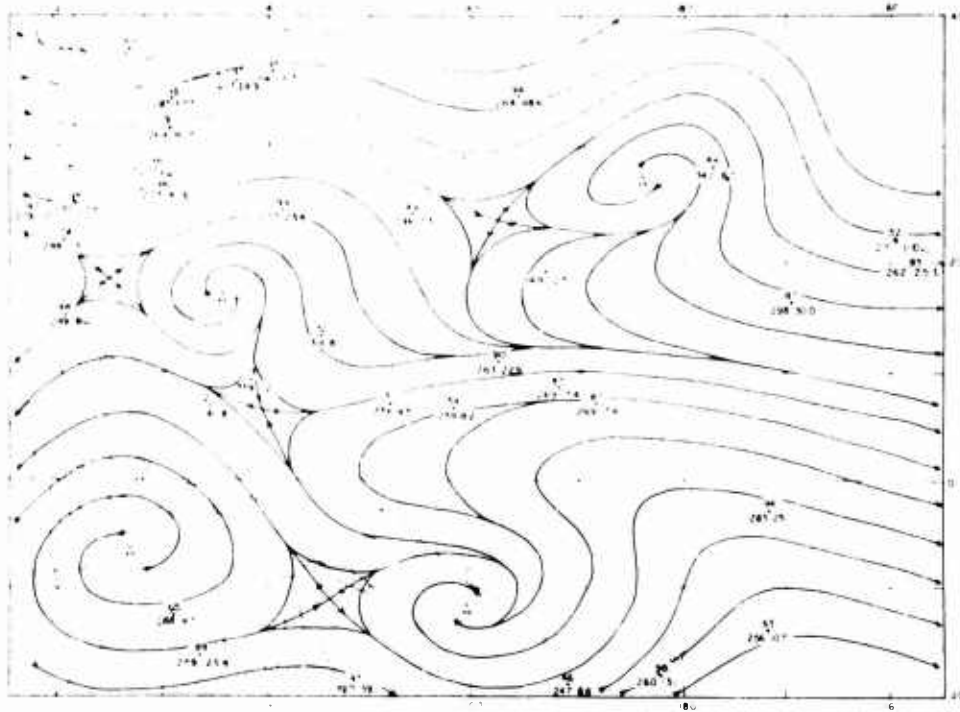


**Figure 5-9.** As for fig 5-8 but for May 1955.

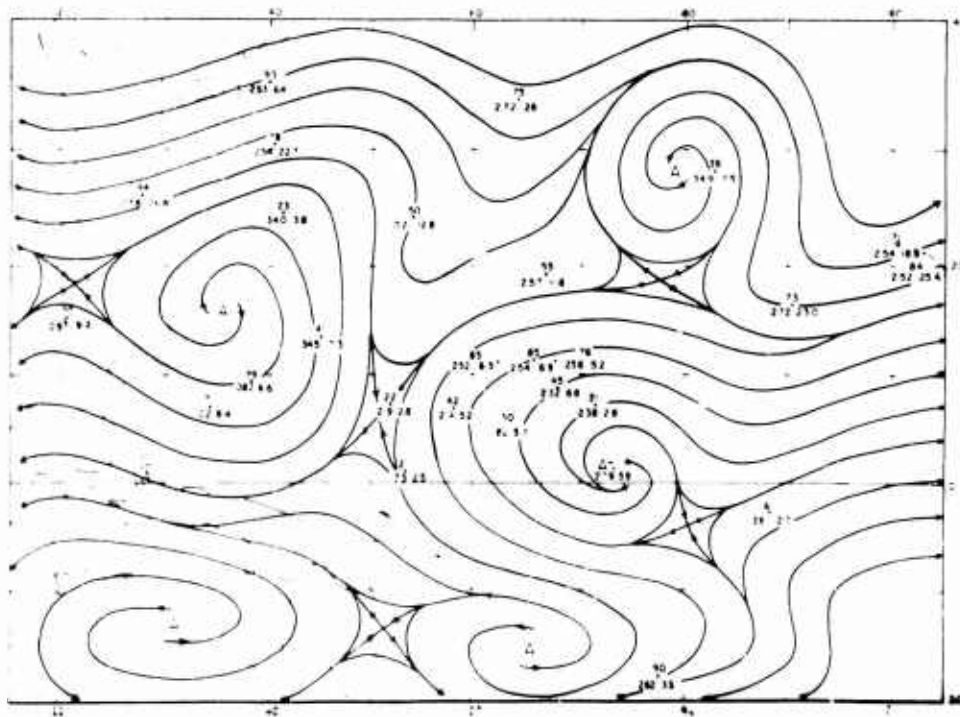


**Figure 5-10.** As for fig 5-8 but for May 1956.

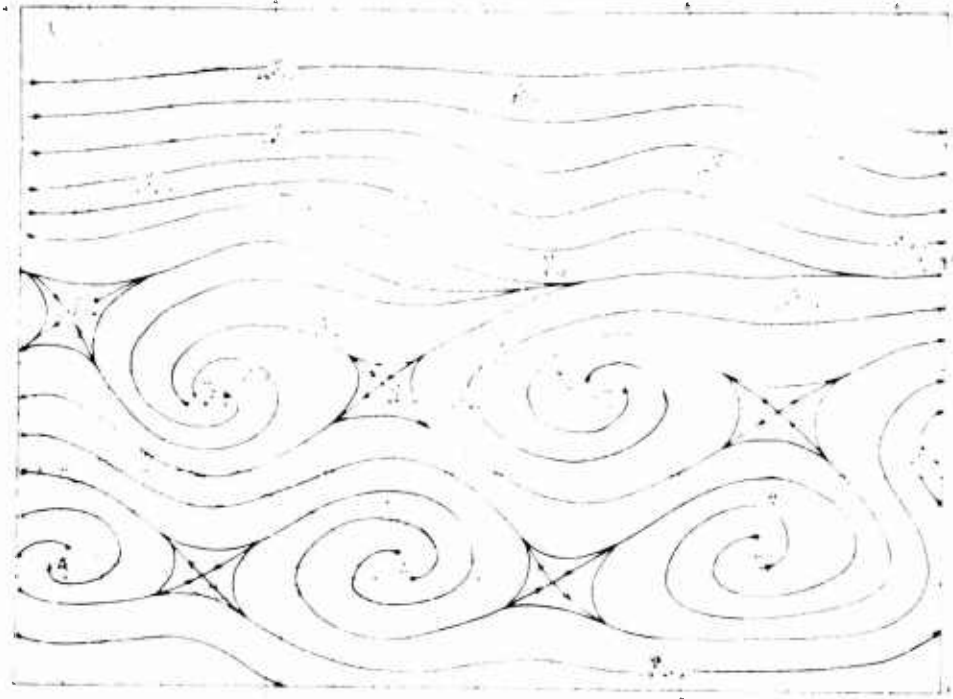


Figure 5-11. As for fig 5-8 but for May 1957.

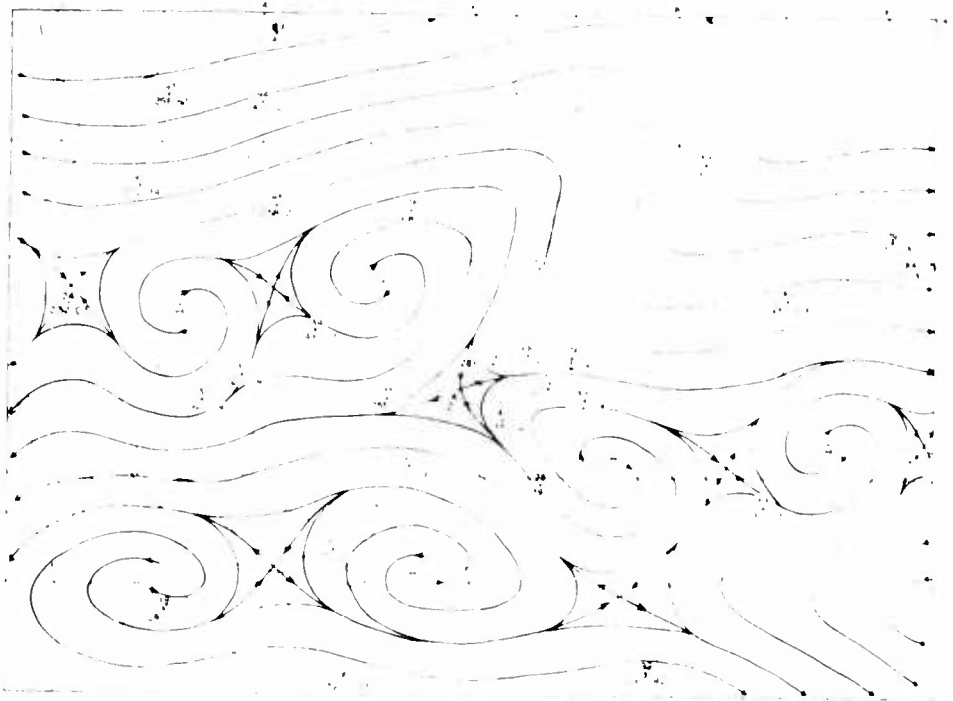
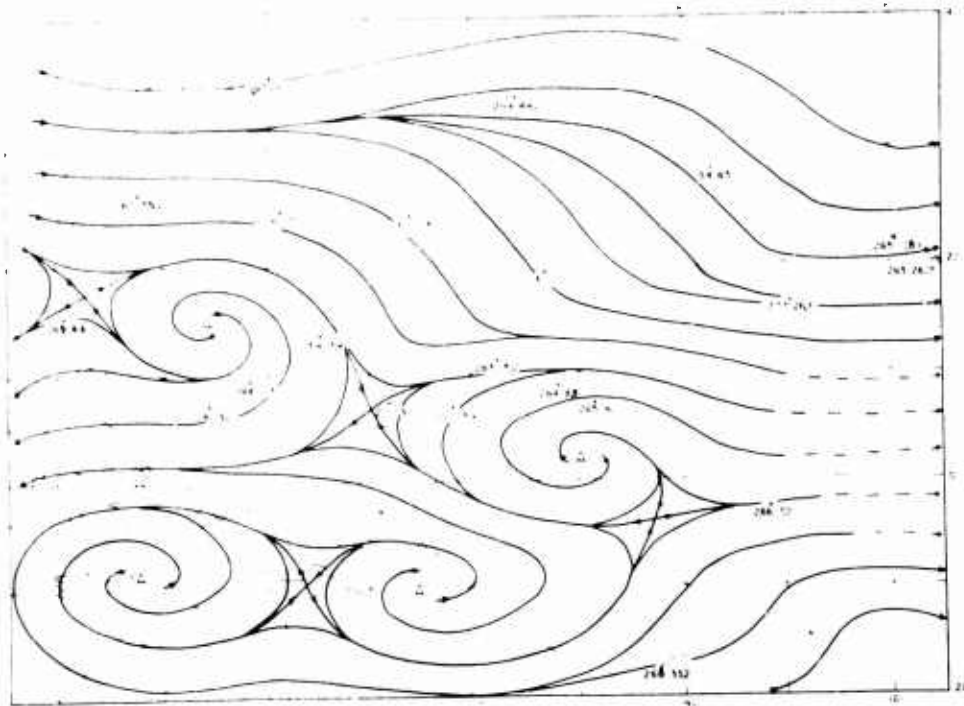


Figure 5-12. As for fig 5-8 but for May 1958.



Although the mean chart combines only four years, reference to the data tabulated in Chapter 3 uncovers insignificant differences between the 4-year and long period means. One concludes that a 4-year record should be sufficient to define the mean monthly resultant patterns.

Since the mid-Pacific trough is an upper-tropospheric phenomenon, it is not surprising that intra-annual variability of May circulations at 10,000 ft (figs 5-16 to 5-18) is less than at 30,000 ft. However, scanty evidence suggests that during May 1957 (the winter-like month at 30,000 ft), the Northern Hemisphere subtropical ridge at 10,000 ft lay closer to the equator than in 1954, 1956 or 1958. Although the mean resultant direction of the trades at 10,000 ft varies little from year to year, steadiness does. In May 1954, steadiness in the Marshalls ranged from 80 to 90 per cent and in 1958 from 35 to 70 per cent, possibly because of greater wave activity in the latter year. Longer term 10,000 ft normals resemble the 1958 means and steadiness more than those of 1954 and 1956.

Mean resultant 30,000 ft wind charts for October 1954 and 1955 (figs 5-14 and 5-15) are alike in that the mid-Pacific trough appears on both. Apart from this, October 1954 is similar to a Northern Hemisphere winter, and October 1955 to a summer configuration.

#### 4. Application of circulation climatology to short-period forecasting

Large-scale tropical circulation features are often long lived and move slowly. Thus persistence "forecasts" of tropospheric wind fields for periods of up to 24 hours are often better than subjective forecasts made by experienced meteorologists. That persistence combined with climatology may further improve forecasts, is borne out by two recent tests.

J. W. Reed of the Sandia Corporation used Eniwetok upper wind measurements made during the 1956 nuclear tests to derive regression equations relating the current and mean resultant winds to the future winds. The equations, when tested on the independent data of the 1958 nuclear tests, bettered both the official forecasts and persistence, throughout the troposphere. The average margin of superiority was about 15 per cent.

The Joint Task Force Seven Meteorological Center conducted a simpler test. They computed daily, a mean resultant of the current wind and the climatological mean for Midway Island, over a two-month period for each mandatory level from 850 to 200 mb. The "forecasts" thus obtained, on being compared with routine 24-hour subjective forecasts made in a weather station, proved superior in 90 per cent of cases. Superiority margins sometimes exceeded 20 per cent.

This procedure can be applied to area wind forecasting. A carefully analyzed (streamlines and isotachs) synoptic wind chart is superimposed on a monthly mean resultant wind chart of the same

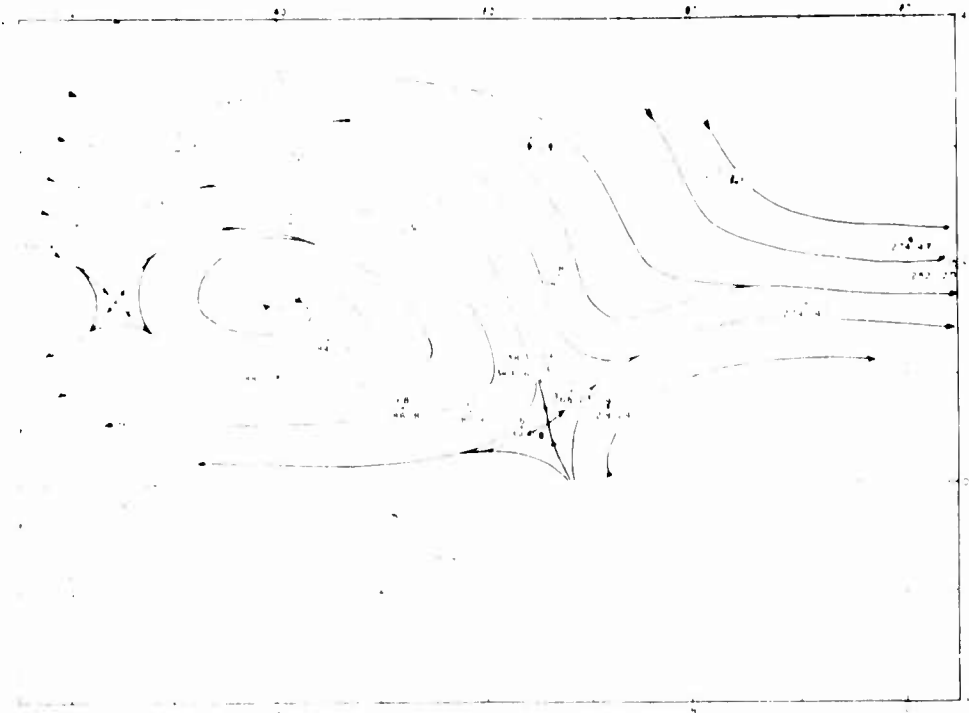


Figure 5-14. As for fig 5-8 but for October 1954.

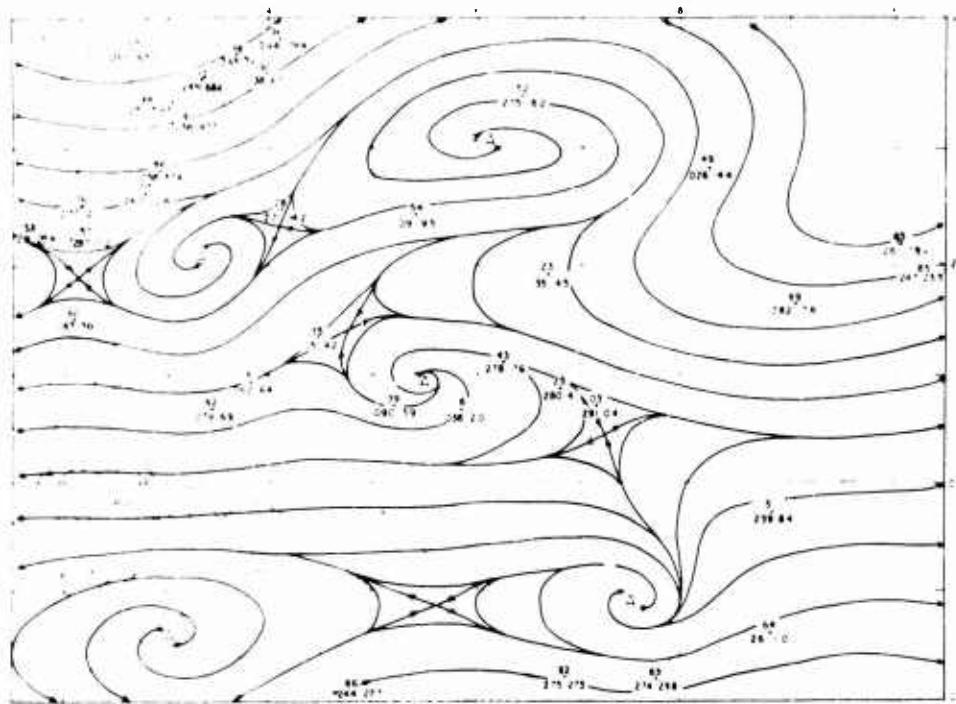


Figure 5-15. As for fig 5-8 but for October 1955.



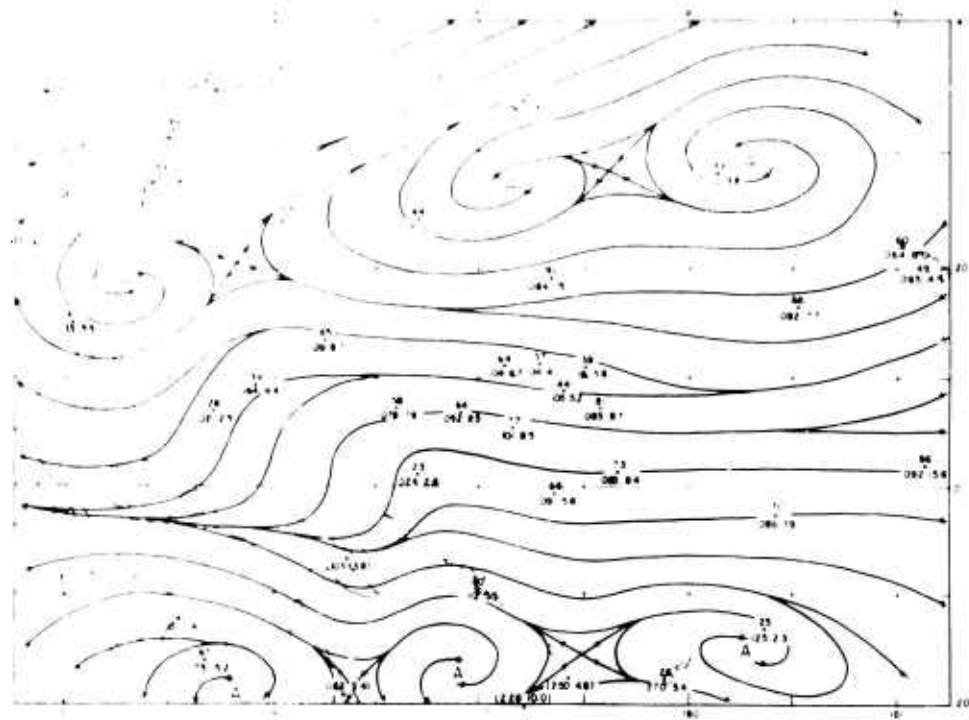


Figure 5-18. As for fig 5-8 but at 10,000 ft for May 1958.



scale for the corresponding month and for the same area. Mean resultant wind vectors are readily determined at suitable intervals (say five degrees) by straightforward graphical methods and then analyzed to provide the prognostic wind chart. Forecasts prepared this way were encouragingly better than subjective forecasts. Because long-period mean monthly resultant wind distribution may damp out significant features of particular years (c.f. figs 5-9 and 5-13), better results may stem from the forecaster selecting the mean chart for an individual month most like the current synoptic chart. In a brief inconclusive test of this technique, students in the Advanced Tropical Meteorology course, after analyzing a few days of May 1951 30,000 ft synoptic charts, all selected the May 1955 mean resultant chart (fig 5-9) as the best analogue. They prepared their prognostic charts in about 30 minutes and were then told to apply any amendments they thought necessary. It is significant to note that not only did the application of persistence-climatology lead to good 24-hour prognoses, but that every subjective amendment increased the errors.

Although such results are encouraging, it is well to realize that the persistence-climatology method has limitations. Because mean charts present smoothed pictures of the dominant circulation features only, the method may be primarily applicable to upper levels with simple synoptic patterns. If a synoptic chart includes a cyclone, the cyclone will be weakened in the forecast unless it lies close to a mean trough axis. High steadiness indicates a strong predisposition for the wind to blow in the mean resultant direction or to shift toward that direction. Low steadiness can not be so simply interpreted. Fig 5-19 compares the mean frequency distributions of 700 mb wind directions at Johnston Island during August, a month of high steadiness and January, a month of low steadiness. Obviously, large deviation from easterly flow is most unlikely in August. The January mean resultant wind direction of southsoutheast and low steadiness stems from a nearly symmetrical bimodal frequency distribution. The median 24-hour wind shift during January 1958 was 20° and during August 1958, 26°. Thus a persistence-climatology forecast for Johnston Island in January should give more weight to persistence than to climatology. Summing up, the method is promising and necessary additional work on it seems justified.

##### 5. Bibliography

Dean, G. A., 1956: The 1955 mean monthly wind circulation over the tropical central Pacific area. Institute of Geophysics, U. of California, 16 pp.

McCreary, F. E., 1959: A Christmas Island climatology study. Joint Task Force 7, Meteor. Center, TP-11, 23 pp.

\_\_\_\_\_, 1959: A study of the mean vertical wind structure over the Eniwetok Proving Ground area. Joint Task Force 7, Meteor. Center, TP-15, 65 pp.

\_\_\_\_\_, 1959: A Johnston Island climatology study. Joint Task Force 7, Meteor. Center, TP-17, 21 pp.

\_\_\_\_\_ and J. B. Wharton, 1957: A study of the 30,000 foot wind field over the west central Pacific. Joint Task Force 7, Meteor. Center, TP-5, 19 pp.

Oahu Research Center, 1954-55: Scientific reports 1-13, Contract AF 19(604)-546.

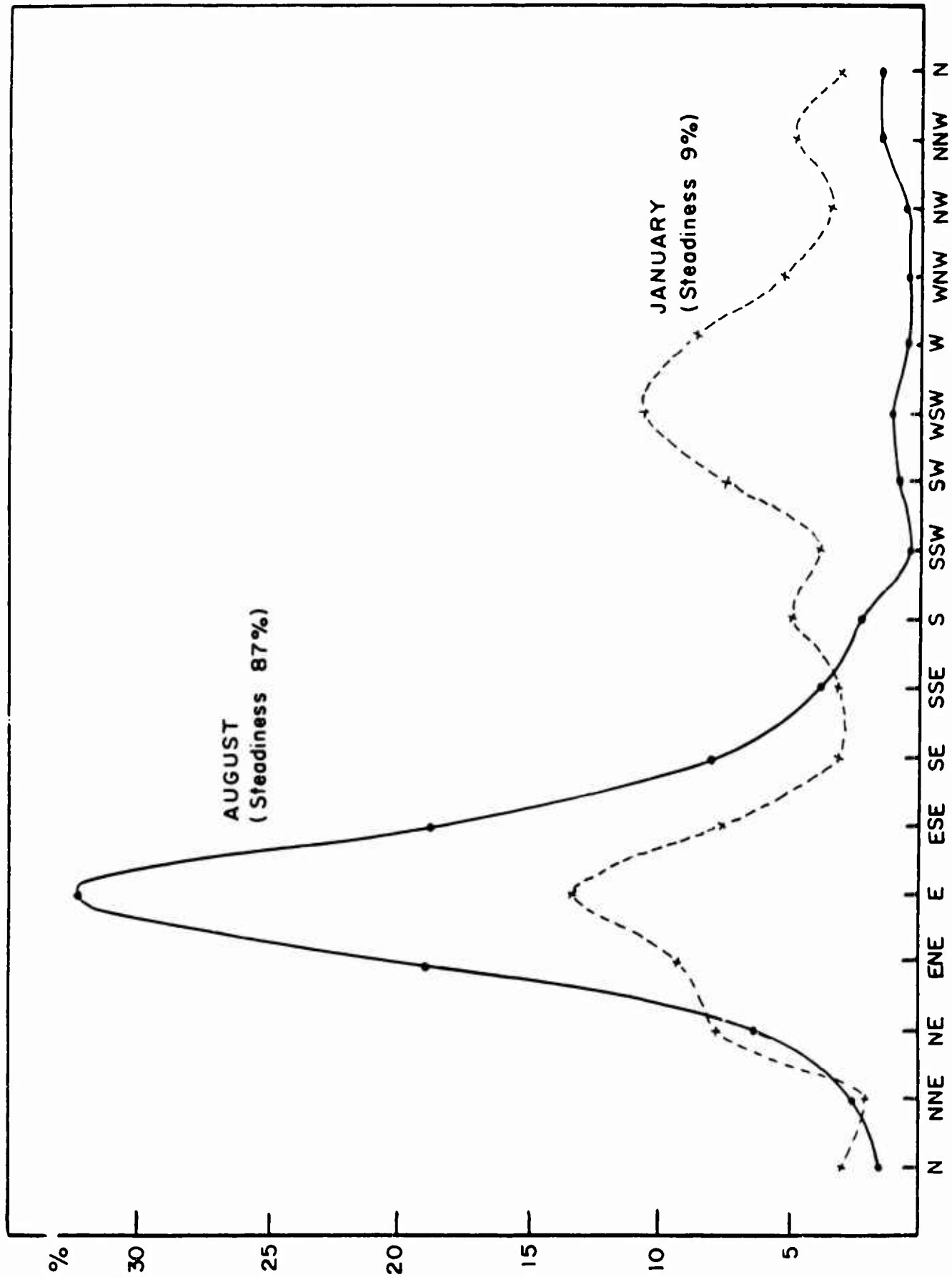


Figure 5-19. Frequency distributions of 700 mb wind directions during January and August at Johnston Island. Period of record: nine years.

THE SYNOPTIC CLIMATOLOGY OF THE CHINA  
SEAS AND SOUTHEAST ASIA SOUTH OF 30°

(A) THE WINTER MONSOON

1. Introduction

The winter monsoon, climatologically speaking, is part of the circulation around the intense Siberian anticyclone. It generally reaches tropical southeast Asia early in October as a burst of dry cold air from north or northeast. Within a month the monsoon has attained full strength except over the China Sea south of 10°N where the maximum occurs in January. The monsoon may in this month extend as far south as Singapore.

Although the monsoon is astonishingly steady (table 6-1), especially in November and December, it possesses a definite rhythm, dying away and strengthening in a series of surges with a period of about 10-12 days.

Table 6-1. Percentage frequency of N or NE winds at  
Pratas Reef (46810), 20° 42'N; 116° 42'E.

	Oct	Nov	Dec	Jan	Feb
	88	83	80	78	71
>25 kn	50	63	52	50	38

To trace the origins of monsoon surges and of the region's winter weather we must first consider the situation at higher levels. During winter a strong northward directed temperature gradient exists over the continent and west Pacific. Hence the Siberian anticyclone in which central surface pressures may reach 1065 mb can scarcely be found at 10,000 ft, for at and above that level polar westerlies prevail everywhere north of 18°N (fig 6-1). The Himalayan-Tibetan massif channels these winds into an intense quasi-stationary jet-stream lying along the southern boundary of the mountains, the Yangtze Valley and south Japan. To the north of the mountains weak and ephemeral jet streams occur between 45 and 70°N (fig I-1).

South of the southern jet stream and probably intimately associated with it is a zone of subsidence with a sharp inversion as its lower boundary at between 7000 and 12,000 ft (fig I-4). So great is the subsidence that it produces a thermal equator in the middle troposphere between 14° and 18°N. The near-vertical subtropical ridge aloft coincides with the thermal equator and separates baroclinic westerlies in the north from slightly baroclinic easterlies further south (fig I-5). To the west, persistent upper tropospheric southwesterlies converge with the circum-

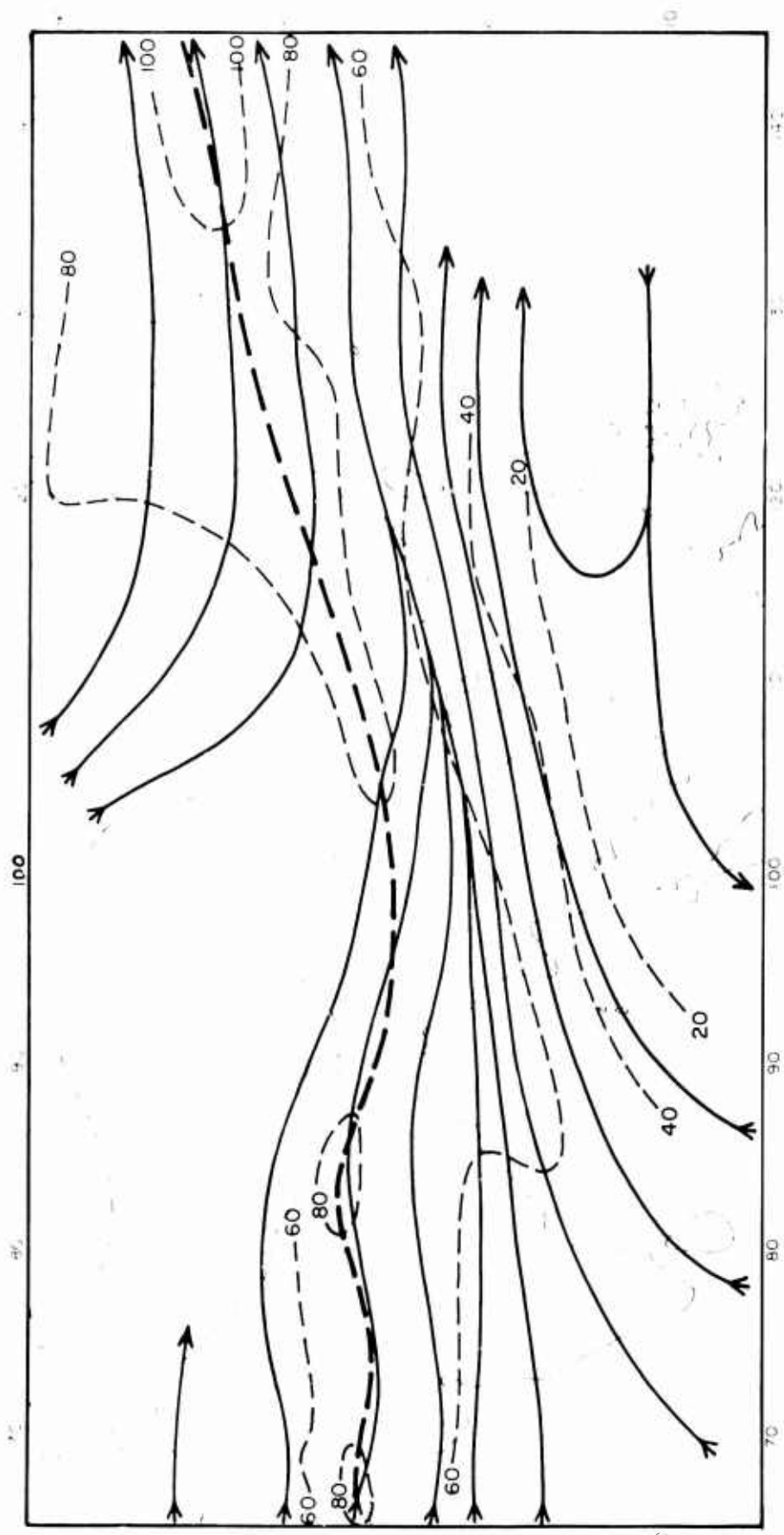


Figure 6-1. Mean resultant 30,000 ft winds for winter (December-February). Isotachs in knots, axis of southern jet stream shown by heavy dashed line.

Himalayan westerlies near  $110^{\circ}\text{E}$  and probably contribute significantly to the subsidence.

Cyclogenesis is associated with jet streams. However, except when it breaks down completely, the Siberian anticyclone inhibits surface cyclogenesis over the southern part of the continent. Often, only when disturbances reach the strongly frontogenetic China and Japan Seas do surface cyclones form with almost explosive suddenness. A deepening cyclone accelerates the northerly flow west of its center and causes a "surge" of the monsoon. As the cyclone passes away to the east, the monsoon gradually weakens until the next depression develops. Surface cyclogenesis gives far too little warning of a surge, for the monsoon freshens almost simultaneously, especially over the Ryukyus and south Japan. However, the triggering wave disturbance in the polar westerlies can usually be tracked over China for some days previous.

The major region of cyclogenesis lies beneath the southern jet stream at about latitude  $30^{\circ}\text{N}$  (fig I-6). First signs of development are usually given by the sudden appearance of high and medium cloud and then in the space of 24 hours a fully fledged cyclone with marked warm and cold fronts may spring into being.

Warm fronts seldom develop within the tropics or if they do, quickly move north. However, cold fronts, the leading edges of monsoon surges, may move far into the tropics.

The quasi-stationary jet stream, anchored by the Himalayas significantly modifies cold fronts. Whereas over North America a vigorous cold front is often accompanied southward by a jet stream aloft and does not undergo too much intensity change, over south-east Asia fronts move under the jet stream and then leave it behind. While beneath it, they are vigorous, but as they pass further south and move beneath the subsidence layer, cloud depth rapidly decreases and rainfall becomes insignificant (fig I-3). Despite this change in cloud and precipitation, surface changes in temperature, pressure and wind at the fronts often remain marked and may be detected well east and south of the mainland.

Over the China Seas, cold fronts retain their identities at the surface as long as the air behind them flows across the sea surface isotherms from cold to warm. Then, as heat and moisture are rapidly added from below, thick cumuloform or turbulent stratocumulus cloud forms and light showers (particularly common over the warm Kuroshio current) may develop. Away from the jet stream, the subsidence inversion sharply limits cloud tops, which rarely exceed 10,000 ft. When, after a sea passage, the monsoon air strikes exposed and often mountainous coasts, such as north Formosa, east Philippines and Annam, lifting releases considerable and persistent rain. Ahead of the advancing front, air is generally in thermal equilibrium with the sea surface and contains little low cloud.

Eventually, as air behind a southward moving front begins to flow parallel to the sea surface isotherms, convective processes

die out and the clouds dissipate. Horizontal density discontinuities vanish and the front ceases to be a front. However, shear and sometimes convergence may persist and be reflected in a line of cloud near where the old front would be expected to lie.

## 2. Early winter (mid-October to mid-January)

During October the subtropical ridge aloft, now moving southward reaches the same average latitude it occupied in June (fig 6-2). By January it has reached its normal winter latitude along about  $15^{\circ}\text{N}$ .

North of the ridge, eastward moving disturbances or recurred tropical storms account for most of the precipitation; south of the ridge, typhoons or easterly waves follow west or sometimes westsouthwest tracks.

From this superficial description one would expect the weather patterns of October and November to resemble those of May and June but this is not so. Whereas in early summer west Pacific typhoons are few and ill-developed, in autumn they are numerous and may reach their greatest intensity.

This period, south of  $30^{\circ}\text{N}$ , is one of ebb and flow between the northeast monsoon and typhoons; the latter dominate at first, but by January only feeble storm remnants or weak easterly waves penetrate west of  $125^{\circ}\text{E}$ .

Monsoon bursts are generally from north or northeast, giving fine weather along the continental coast but considerable convection cloud and some showers offshore where heating and moisture addition reach their maxima for the year. Onset of the monsoon coincides with establishment of the normal winter flow pattern aloft. South of the jet stream subsidence flattens the cumuloform clouds of summer into the stratiform clouds of winter.

The China coast north of Amoy is typhoon-free during this period, but typhoons, especially in October, frequently pass across the South China Sea. They present a difficult forecast problem. If a storm heads across the northern part of the South China Sea during a monsoon lull, it may give the coast prolonged battering (the two longest typhoon gales at Hong Kong occurred in October) and may even recurve nearby. On the other hand, storms approaching the south China coast frequently lose intensity and occasionally completely fill. This occurs when comparatively cold dry air from China enters the storm, causing the air circulating around the center to lose potential energy.

For a source of cold dry air to exist over China, the Siberian anticyclone must already have spread south into north China and become fairly well established. Thus one would expect an approaching storm to lose intensity if pressure over central China were above normal. This usually happens, but occasionally when central China pressure is well above normal, an approaching typhoon shows no sign of weakening. Surface pressure indications are therefore not always reliable.

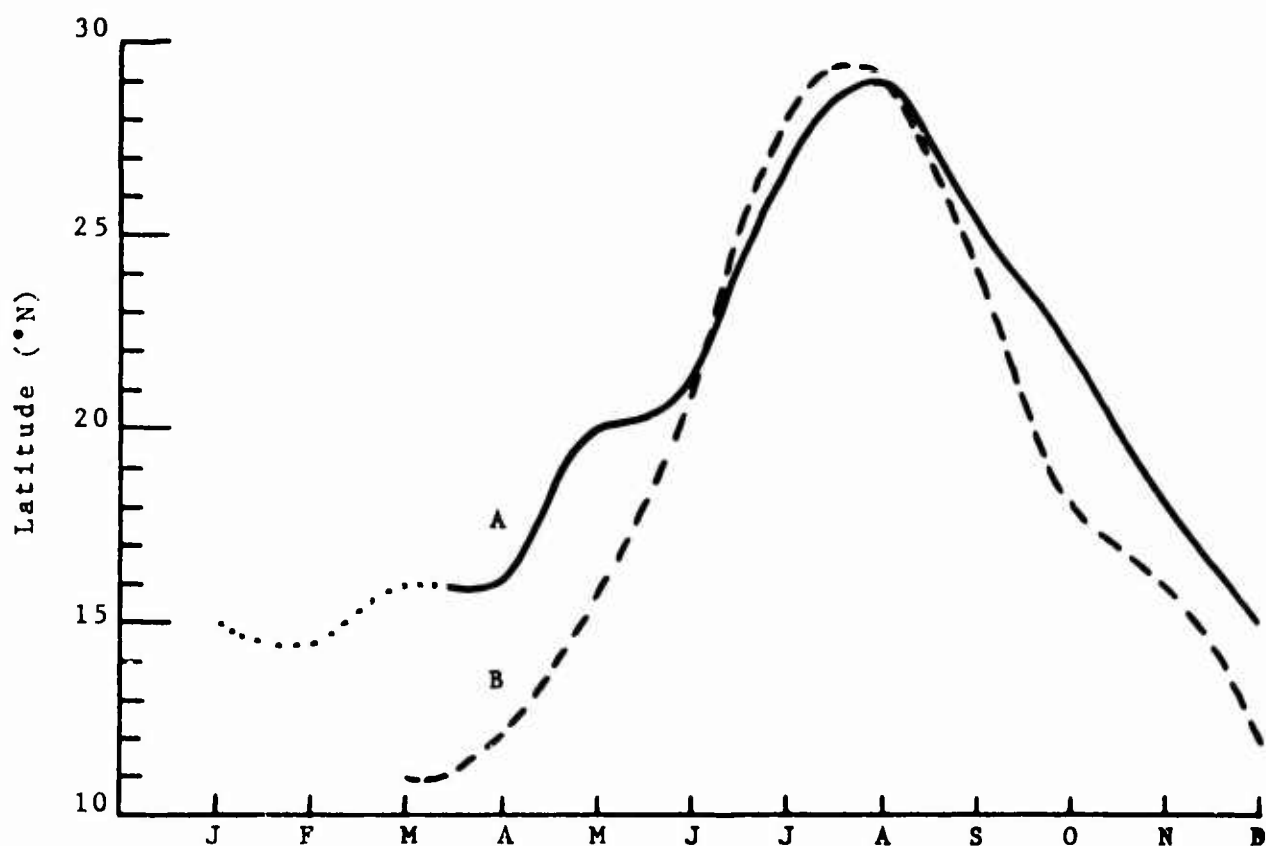


Figure 6-2. The subtropical ridge aloft in the Far East and western Pacific.

A. Median monthly recurvature latitudes of tropical disturbances. (From "Tropical cyclones in the western Pacific and China Sea area" by P. C. Chin, Royal Observatory, Hong Kong, Tech. Mem. 7. 1958).

B. Maximum northerly latitudes to which easterlies extend at 8 km along the meridian of 78°E. (From "The general circulation of the atmosphere over India and its neighbourhood" by K. R. Ramanathan and K. P. Ramakrishnan in Mem. India Meteor. Dept., 26, 189-245. 1939).

In this period, low level flow across the China Seas has a dual character. In the north it forms part of the circulation around the continental anticyclone, in the south it is part of the deep easterly stream of tropical maritime air south of the subtropical ridge. Easterly waves, often the remnants of storms move in this stream. In the south, weather is typically fine ahead of a wave and unsettled to the rear; in the north, particularly if a disturbance in the polar westerlies is present, weather may become unsettled some distance ahead of the trough line and worsen somewhat after its passage (figs II-2, 3, 4). Tropical storms heading west to the south of the subtropical ridge aloft may influence weather north of the ridge in the manner of a vigorous easterly wave.

Over the South China Sea the subtropical ridge aloft seldom possesses a marked cellular structure and storms moving westward on its southern side normally do not recurve. Should they do so, weakening is usually so rapid that there is little chance of their retaining destructive winds. Because of the generally steady movement of storms and waves, extrapolation based on previous tracks gives adequate results. However, storms in December or January may have their westward progress across the South China Sea suddenly checked by a surge of the northeast monsoon. Movement is then slow and erratic and filling often ensues.

By mid-January (except rarely, south of 10°N) the winter monsoon is so dominant that westward moving tropical disturbances never affect the region.

### 3. Late winter and spring (mid-January to end of April)

This period is one of steadily increasing rainfall over most land areas. Exceptions are the east coast areas of Annam and the northern Philippine Islands. There, orographic rain diminishes as the winter monsoon weakens.

Aloft, the polar westerlies, the southern jet stream and the subtropical ridge dominate the circulation, particularly in January and February.

More and more often from February onward this well defined distribution breaks down and divisions between dry and wet areas become increasingly blurred. The westerlies weaken and the subtropical ridge fluctuates considerably, sometimes moving well south of 15°N, sometimes jumping north of 25°N. Its axis often slopes equatorward with height. Although "normal" conditions occur on a high proportion of days in January and February, the norm in April, is one of rapid weather changes.

All precipitation-producing disturbances north of the subtropical ridge move eastward.

Monsoon surges. During late winter, surges of the monsoon alternate with lulls. A northerly surge, which develops behind a cold front when the center of high pressure remains stationary over Siberia, may be dry and free of low cloud along the coast of



China and inland, south of the jet stream. As the air moves out across much warmer seas convection clouds rapidly form.

When, in rear of a cold front, a high cell moves eastward from China, the monsoon surge reaches the tropics as an east-north-east wind. The air having first been warmed and moistened by the Kuroshio Current is then cooled as it moves over cold coastal waters; should turbulence be sufficient, stratiform cloud which may give drizzle, quickly forms above the lifting condensation level (fig III-2). Further at sea, of course, convection is less vigorous than in northerly surges and clouds are scattered.

Most surges fall somewhere between these two extreme examples. A knowledge of trajectories and normal sea surface temperature distribution will help foretell cloud and weather distribution.

Lulls between surges occur when the continental anticyclone, or a cell split off from it, moves eastward. Winds south of the high pressure center veer, convection clouds over the warm seas decrease and cooling along the coast may produce stratiform clouds. Little change occurs in short lulls but when they are prolonged, high pressure over China may break down altogether and a wedge from the Pacific anticyclone extend across the area and on to the mainland. Weather over the sea areas becomes almost cloudless, but in the cold coastal water zone, rapid cooling may lead to the development of low stratus cloud and drizzle, or even sea fog, the crachin of south China.

The longer a lull in the monsoon persists the warmer and moister the air reaching the continent becomes. Cloud base steadily lowers and eventually sea fog forms. At Hong Kong (and in the rest of the crachin zone) dew point rises steadily during a lull. If the air is moving around a high centered near Japan, the rise averages 3°F/24 hours; should it be moving around a wedge from the Pacific high, (more common in March and April) the rise averages 4°F/24 hours. Since sea temperature tends to remain steady over such intervals, one can often estimate the time dew point and sea temperature will coincide and sea fog form.

The trend in surges and lulls is toward an increasing number of easterly surges, increasingly long lulls between surges and more persistent crachin, as the year advances. Turbulence, topography, diurnal heating and dew point/sea temperature differences, all play important parts in determining when and where crachin will develop and what form it will take. The interrelations of these factors along the coast may be extremely complex. For example, if wind speed decreases 5 kn as the temperature maximum approaches, an apparently permanent layer of thick stratus may dissipate. A slight change in wind direction and a previously fog-free bay is rapidly enveloped. A range of hills more than 1000 ft high can greatly modify stratus distribution while even lower lying land can hold up advancing sea fog. Each area has its local peculiarities. Since vigorous crachin usually occurs in the col or trough region west of a surface high, it is associated with local winds veering with height. Conversely it is unlikely when winds back with height. Surges of the

northeast monsoon may be important crachin modifiers. However, from February onward even moderate surges may not dissipate crachin, for the air behind the front can still be undergoing surface cooling along the coast. A temporary lifting in cloud base but no break in cover is usual. Particularly in the Formosa Strait - south China area - crachin can be modified without any surge at all. With eastnortheast flow, air reaching the south China coast has usually passed down the Formosa channel over a heating surface; however with general easterly flow, the air reaching south China may previously have swung around south Formosa and have crossed a cooling surface. Thus, when general flow direction is critical, minute disturbances can switch the air from one track to another and coastal weather from cloudy to fog.

Sometimes in January and February, general high pressure over China breaks down. Frontal systems extend from west to east across north China and south of the Yangtze and small high cells move eastward across south China. Apart from some Ac when troughs between the cells pass, coastal weather stays fine and westerlies occasionally reach the surface. Marked lowering of the base of the westerlies and general weakening of low level winds presage this development. Coastal areas south and southeast of a cell center may have moderate or fresh southeast winds but with the air having so recently passed over land, no significant dew point rises or low cloud occur.

#### 4. Interruptions of the normal winter monsoon cycle

Tropical trough (figs II-3 to 18). "Tropical trough" is a name given to a cold-core disturbance which may first appear around mid-January over southern India at and above 30,000 ft. The trough, moving eastward, sharply interrupts the prevailing upper tropospheric southwesterlies. The lower troposphere is little affected until the trough reaches the Andamans but from there on it intensifies and colder air moves in from north. Bangkok rawins provide a good warning. High level winds there turn westerly, veer and strengthen as the trough passes.

Rarely, the trough continues eastward at more than 20 kn having little effect on surface weather until it reaches the strongly fronto-genetic region east of Formosa.

Tropical troughs generally intensify, slow and stop over Thailand or Indo China. When this happens, weather to the east deteriorates, usually along the line of a previously quiescent polar front marking the southern limit of the most recent north-east monsoon surge. As long as the trough remains stationary, wave disturbances move along the polar front, producing highly variable and unsettled weather to the north. Eventually, as the upper southwesterlies re-establish over India and the Bay of Bengal, the tropical trough weakens. It may then move east but usually dies in situ. India observations are essential for one to detect onset of this phase.

Tropical troughs become more frequent as the year advances.

Most of the rainfall of March and April, south and west of the Ryukyus, can be attributed to them, and their activity largely determines the precipitation pattern of these months. In April, and at times in March, the polar front usually lies over the northern part of the South China Sea and through the southern Ryukyus with true Tm instead of modified Pm air to the south. Then, when the front is activated, thunderstorms are common. Tropical troughs originate and intensify in the tropics and seem to exert little effect on the mid-latitude westerlies.

West China trough. In winter the major Far Eastern long wave mid-latitude westerly trough lies along about 125°E and surface cyclones usually develop east of this longitude. However, a few times every cool season (rarely more than four) the trough along 125°E dissipates or moves rapidly eastward. A warm wedge extends westward from the Pacific anticyclone bringing fine weather to the Ryukyus and China and sea fog to the China coast. The Siberian anticyclone retreats northward and westward and over south China dew point and temperature rise and pressure falls. At this state, a trough in the westerlies moving east from India will intensify over west China. This results in the region of surface cyclogenesis being displaced about 20 degrees westward. As long as the trough remains over west China, central China and sea areas from the Formosa strait northward experience extremely unsettled weather.

When hemispheric flow returns to normal the west China trough moves eastward. The wedge from the Pacific anticyclone has earlier brought tropical maritime air far inland and warm front and cold front thunderstorms are common. West of the trough line there is vigorous subsidence, an intense anticyclone builds behind the surface cold front and normal conditions return. Just ahead of and at the trough the surface front and depression system may travel sufficiently far south to give rain to south China and northern Indochina although weather stays fair south of 20°N.

Occasionally (fig 6-3) a west China trough situation lasts from ten to twenty days. The trough and its associated depression may move eastward. However, there is no rapid anticyclogenesis west of the trough line. Instead, pressure falls again over China and upper winds back from northwest to southwest. The eastward moving trough weakens as a new deep cold trough intensifies over west China. While it remains stationary it is a source of shallow disturbances travelling eastnortheast. South of the disturbance track, south China experiences persistent southerly winds and unseasonably warm and humid weather. When the trough finally moves eastward the continental anticyclone is restored to its usual position.

Toward the end of April, heating of the continent flattens temperature gradients and the west China trough ceases to be of significance.

Major displacement of the subtropical ridge. Only one type of situation seems capable of giving prolonged clear weather

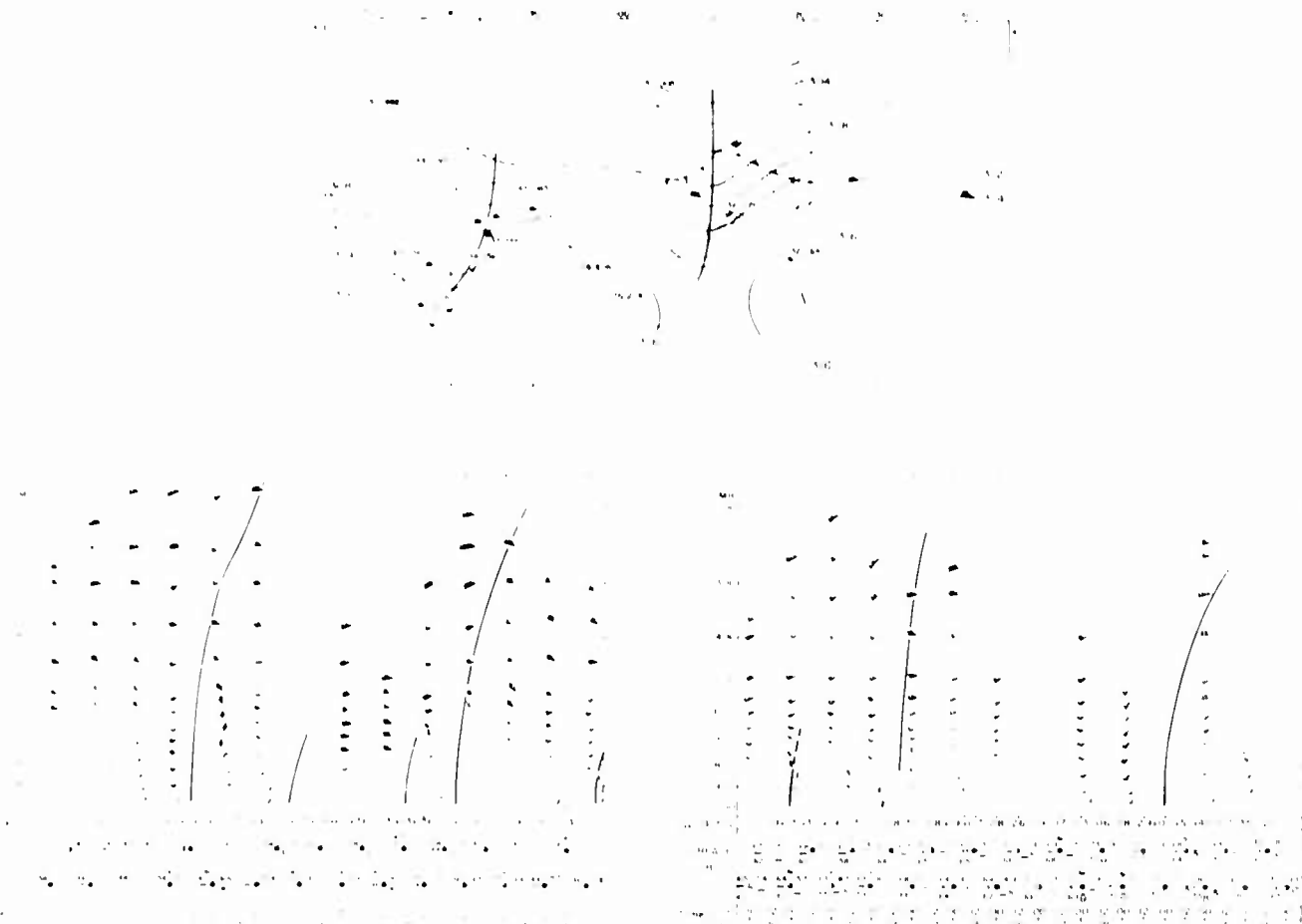


Figure 6-3. The West China Trough.

Top: 300 mb chart for 03 GCT 23 February 1946 (pressure-height contours labelled in hundreds of feet). Indian observations are for 1030 GCT.

400 mb wind arrows are dashed. Surface fronts and areas where rain fell in the previous 24 hours (stippled) are also shown.

Left: Hankow (30°25'N, 114°17'E) time section for 20 February to 4 March 1946.

Right: Canton (23°10'N, 113°20'E) (upper winds) and Hong Kong (22°18'N, 114°10'E) (surface observations) time section for 20 February to 4 March 1946. Measurable rain fell at Hong Kong on: 22nd 1.5 mm; 2nd 35.1 mm; 3rd 21.2 mm; 4th 7.6 mm.

A trough after moving eastward from India, intensified over west China, generated a surface depression and rain area by 23 February, and also crossed Hankow and Canton on that day. A second trough developed shortly over West China and renewed vigorous wave activity on the polar front. Weather at Hankow, north of the front was very unsettled, while Hong Kong, south of the front experienced persistent drizzle or fog. The second west China trough moved east on 1 March and gave thunderstorms at Hong Kong. The sequence was repeated when a third trough intensified over west China. Not until 7 March did a burst of the winter monsoon accompany re-establishment of the Siberian anticyclone and normal conditions.

over south China and the Ryukyus in March or April. On an average, once every two or three years (in response probably to a sharp change in the hemispheric circulation), the southern jet stream disappears and the subtropical ridge aloft shifts several degrees northward. The eastern part of a ridge cell overlies south China where northwest winds at all heights bring in phenomenally dry air liberally laced with Tibetan dust and possibly Burma smoke. This situation may last a week with southward moving fronts rapidly dissipating over southern Japan. It breaks down gradually and without rain.

#### 5. Cloud and rainfall

The foregoing discussion helps explain the distribution of winter cloud (fig 6-4) and rainfall. Cloud amounts are greatest along the axis of the southern jet stream and along windward coasts. At sea, skies are cloudier in December with heat and moisture being added to vigorous monsoon bursts, than in March when air-sea temperature differences are less. Along the China coast, however, the crachin causes March cloudiness to exceed December's (see also fig III-C).

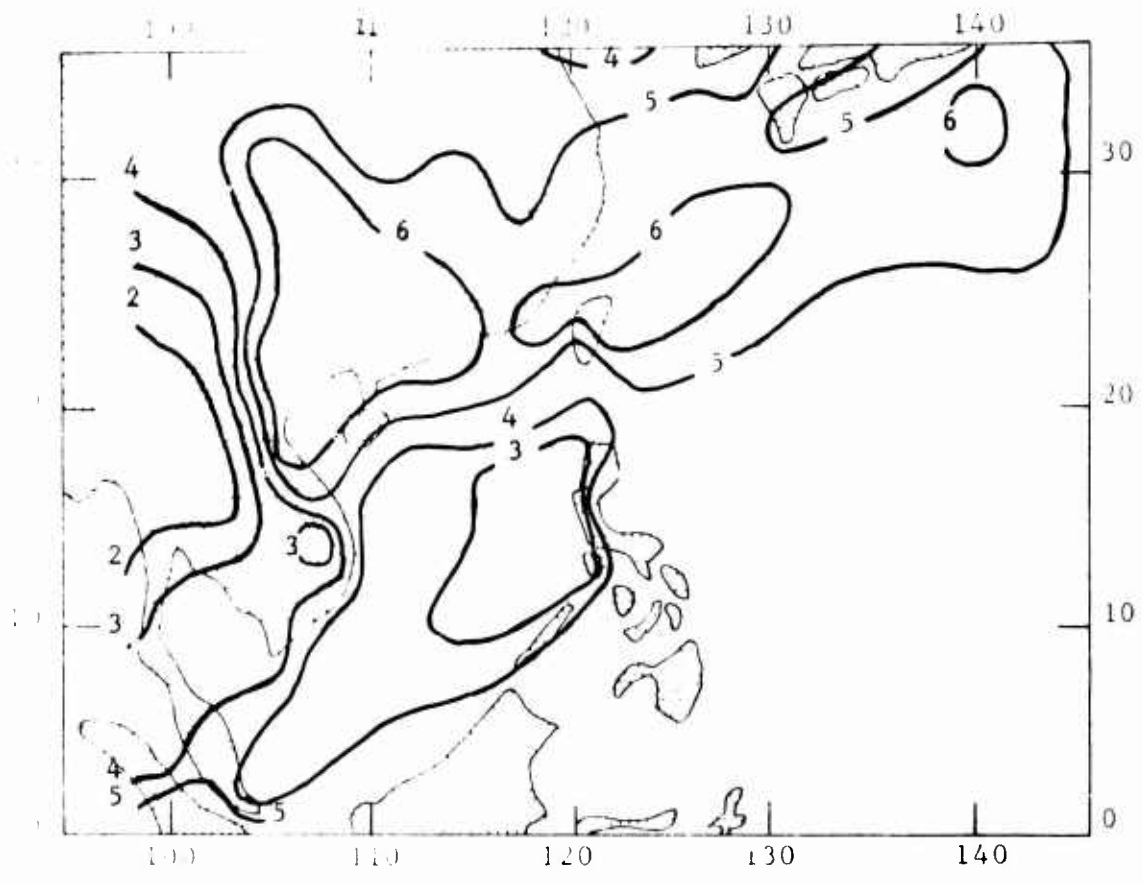
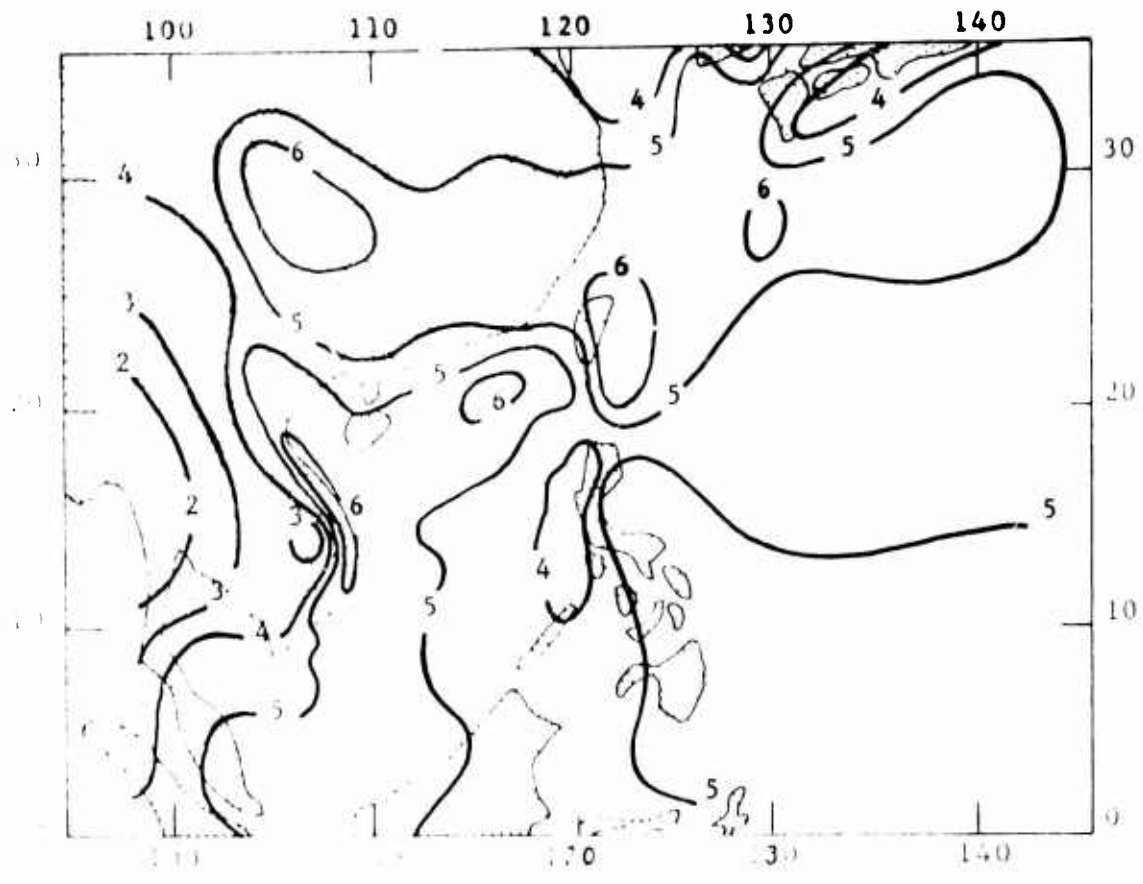


Figure 6.4. Mean monthly cloudiness for December (top) and March (bottom) in oktas.

6. Introduction

Everyone in southeast Asia knows what the winter monsoon is, and its surges feature in casual conversation and in the press. No such recognition is accorded the summer monsoon. Whereas in India people treat it as a topic of life and death and follow its "bursts" with anxious concern, east of Burma, the summer monsoon is a rather negative phenomenon and might almost be defined as absence of the winter monsoon.

7. Early summer (May through late June or early July)

As spring merges into early summer, a heat low begins to develop over south and southeast Asia, and at low levels gradually extends its circulation east and south, eventually displacing the ridge of the Pacific anticyclone from the China Sea (although at 10,000 ft and higher the ridge is frequently found to extend to south Viet Nam). One consequence is the extension of south and southwest flow across the south China Sea, reaching during May to the island of Luzon. At this time the prolonged dry spell experienced by the western Philippines, which have lain beneath the subtropical ridge aloft and on the lee side of the mountains, comes to an end and orographically reinforced precipitation develops (table 6-2).

During early summer, surface air mass discontinuities disappear. Diminishing temperature differences between coastal waters and the open sea spread steadily northward. Crachin is almost unknown south of 25°N after early May. However, the strong southerly flow over relatively cold coastal waters in rear of a May tropical storm moving westward across the south China Sea can bring dense fog to the south China coast.

Over the oceans, air and water are generally in temperature equilibrium with one another and scattered cumuloform cloud is the rule in undisturbed conditions.

In May, over coastal and inland areas of China, Korea, and Japan, there first appears the peculiar early morning rainfall maximum typical of all the summer months (fig V-2). Usually the morning maximum occurs about dawn inland, but sometime later along the coast, where it probably coincides with onshore movement of a sea breeze convergence zone. Inland, a second maximum, which occurs in the afternoon and evening, reflects convection resulting from intense surface heating.

8. Early summer disturbances

Tropical trough. During early summer the region of tropical trough intensification shifts from Thailand-Indo China to the Bay of Bengal. The transition occurs most often in either the first or third weeks of May. Thus when the first trough intensifies in

the Bay, Burma, instead of lying beneath subsiding air west of a trough axis, experiences the effects of massive convergence east of the axis. Its dry season abruptly ends as the summer monsoon 'bursts' over the country.

Further east, weather develops in response to tropical trough activity as in earlier months. Consequently, rainfall increases steadily (fig IV-2), and not abruptly as in Burma. Although surface temperature gradients flatten as summer advances, a cold water remnant persists along the China coast which becomes a preferred region for the polar front. Thus when the front is activated, south China often experiences heavy rain. Development of rain and thick altostratus sheets over southwest Burma and Thailand indicates subsequent (not too long after) deterioration further east, the "spring" or "plum" rains of China and Japan.

By June, surface frontal discontinuity along the polar front is hard to find, but at higher levels, temperature contrasts may still exist. Disturbances on the front can be more easily located at 5000 or 10,000 ft than at sea level. Properties of the polar front at this time of year are not well understood.

Occasionally in May or June the polar front lies across south China. The coastal region then suffers from the hot humid but relatively rain-free "southwest monsoon."

Active tropical troughs displace the subtropical ridge aloft well south and east of its normal position over the South China Sea. When this happens in May and June, true tropical storms neither form in nor move into the South China Sea. When tropical troughs are absent, the ridge moves west and north and tropical disturbances have room to form in or to move into South China Sea. Often these disturbances have no surface closed isobar but one can sometimes trace a rain area and a wind-shift line around the subtropical high cell and onto the China coast. Tracking a rain area is not too hard, for at this time of year weather over the China Seas is usually very fine and rain shows up well.

It is instructive to compare mean monthly rainfall amounts for Hong Kong and Manila listed in table 6-2, for these reveal that although the southerly monsoon reaches Manila before Hong

Table 6-2. Mean monthly rainfalls for Hong Kong and Manila (mm).

	Jan	Feb	Mar	Apr	May	Jun	Jly	Aug	Sep	Oct	Nov	Dec
HK	32	45	73	136	236	333	386	363	264	110	43	26
M	21	11	21	33	113	234	439	406	360	170	133	77

Kong, precipitation at the northern station increases significantly, more than two or three months earlier. The reason is that Hong Kong is affected by disturbances stemming from tropical



trough activity while Manila in early summer, although experiencing low-level cyclonic southwesterly flow, is often overlain by the rain-inhibiting subtropical ridge.

Hybrid storms of the South China Sea (usually in June but occasionally in July, August or September). By June the south-north temperature gradient has weakened sufficiently for easterlies to appear just below the tropopause south of  $25^{\circ}\text{N}$ . During this month, tropical troughs often activate the polar front or its remnant shear line across the northern part of the South China Sea. Rather meager evidence suggests that at such times, a high-level westward moving cyclone may slowly extend its circulation to the surface, where strong winds are first confined to the eastern semicircle and then spread around the center. The winds seldom exceed 45 kn possibly because of the considerable initial shearing between layers and proximity to the coast. During development the storm is stationary or moves slowly and erratically; when finally the circulation extends throughout the troposphere, the center moves westward. On an average one such "hybrid" storm with characteristics of both warm- and cold-cored lows, develops every June.

A similar initial distribution of westerlies in the lower and middle troposphere and easterlies above is found over the South China Sea when a typhoon is filling over south or southeast China. Thus hybrid storms may form (although rarely) in July, August or September.

9. Mid-summer (late June or early July to mid-July)

In June, the subtropical ridge aloft tends to move north. At times during the month the ridge axis may move north of  $20^{\circ}\text{N}$ . South China then lies in the western part of a ridge cell and experiences fine weather and light winds. However, such a temporary axis shift exposes the coast to westward moving storms. Statistics show that the risk is slight; only two June storms moving from east have given gales in Hong Kong in 70 years.

Available evidence indicates that early in July in most years the Northern Hemisphere subtropical ridge aloft "jumps" northward (fig 6-2). Over southeast Asia the shift occurs so regularly that it produces the most important weather singularity of the year.

In June, the ridge axis usually lies near  $21^{\circ}\text{N}$ . By mid-July, however, the ridge is usually found along  $23^{\circ}\text{N}$  and all the areas to the south are overlain by deep easterlies.

As the ridge moves north, weather over south China becomes fine and the land dries out as it passes (fig IV-2). The season of westward moving disturbances begins and the region lies open to the great typhoons of the western Pacific. (Note the sharp increase in Manila rainfall).

10. Late summer and fall (mid-July to early or mid-October)

This is the typhoon season. Storms forming anywhere east of

the Philippines may now move steadily westnorthwest and eventually reach up on the coasts of China and Indo China. Rain comes from typhoons, tropical storms and easterly waves.

Generally, rainfall is more concentrated than in early summer, although totals stay about the same. There may be more rainless days for there is always a fine clear day or two in the divergent zone ahead of the right front quadrant of an advancing storm. This means that valuable upper wind observations can often be made and preliminary storm precautions carried out with minor inconvenience.

#### 11. Easterly waves (usually in early summer and fall)

South of the subtropical ridge line, in the region of deep easterly flow, disturbances may move westward. Easterly waves as they are known have had about as frantic a vogue in the tropics as fronts before them, being used by many meteorologists to account for every piece of otherwise inexplicable bad weather. Disillusionment has of course set in but the waves should not disappear from charts for they are one of the most useful tropical models yet devised.

As the name implies an easterly wave is a wave distortion of easterly flow. It moves westward in the general stream but rather more slowly. The classical model seldom closely resembles actual waves but one should become familiar with its characteristics (fig 6-5).

There may be little temperature or pressure variation across the wave, in fact temperatures or pressures are as likely to rise as fall with its passage. It can most readily be detected in the wind field for winds back ahead of the wave and veer behind it. The wave is generally most intense at around 10,000 ft but can seldom be detected above 25,000 ft.

Using the following definitions,

$q$  = relative vorticity

$f$  = coriolis parameter

$\Delta p$  = depth of a column of air

Let us consider the dynamics of an easterly wave. The Rossby vorticity theorem states that  $\frac{q + f}{\Delta p} = \text{const.}$ , if one makes the important assumption that the atmosphere is an ideal, frictionless homogeneous, incompressible gas in purely horizontal motion. Surprisingly, considering these assumptions, the theorem seems to be generally valid for many tropical disturbances. In an easterly wave moving more slowly than its surrounding flow, air east of the wave axis moves into an area of increasing  $f$  and increasing  $q$ . This means that individual air columns stretch and convergence with upward motion takes place. Ahead of the axis, air moves into an area of decreasing  $f$  and decreasing  $q$ , individual air columns shrink and divergence with sinking takes place. Thus the moist layer is deeper east of the axis and precipitation tends to be



concentrated there.

If a wave were to move faster than the general winds, changes in  $q$  and  $f$  would have opposite signs and distribution of convergence and divergence would depend on the relative magnitudes of  $f$  and  $q$ . In the Pacific, bad weather appears to be as frequently observed ahead of as in the rear of easterly waves.

Easterly waves crossing the Philippines may curve around the ridge from the Pacific anticyclone and eventually appear as waves on the polar front. During the period of recurvature they are hard to detect in the wind field but their associated bad weather area usually persists.

Although some easterly waves may give severe rains, particularly over mountainous islands, many, especially over the open ocean are accompanied by nothing more troublesome than a few showers. Nevertheless they should all be carefully watched for some may be nascent typhoons, phenomena no one ignores.

In July, August and September a well-marked surface low pressure trough extends from just west of Guam to central China. Easterly waves moving into the trough rapidly change into vortices and no longer resemble the model.

12. Typhoons. (these are the subject of separate reports)

13. Cloud and rainfall

The cloud and rainfall patterns of May (early summer) differ from those of August (late summer) (fig 6-6). Considering only cloudiness, since the rainfall charts exhibit similar features, we find that in May a minimum occurs along the subtropical ridge and a maximum in the region of the polar front beneath the jet stream remnant.

In August, the northern location of the subtropical ridge is reflected by a cloud minimum along about  $30^{\circ}\text{N}$ , while south of  $20^{\circ}\text{N}$  clouds have increased with the increase in tropical disturbances. Orographic effects due to a predominance of south or southwest surface flow show over Indo China, the Philippines, Formosa and Japan.

14. Bibliography

Koteswaram, P., 1958: The easterly jet stream in the tropics. Tellus, 10, 43-57.

Murakami, T., 1959: The general circulation and water-vapor balance over the Far East during the rainy season. Geophys. Mag., 29, 131-171.

Staff Members, Academia Sinica, Peking, 1957-58: On the general circulation over eastern Asia. Tellus, 9, 432-446; 10, 58-75; 10, 299-312.

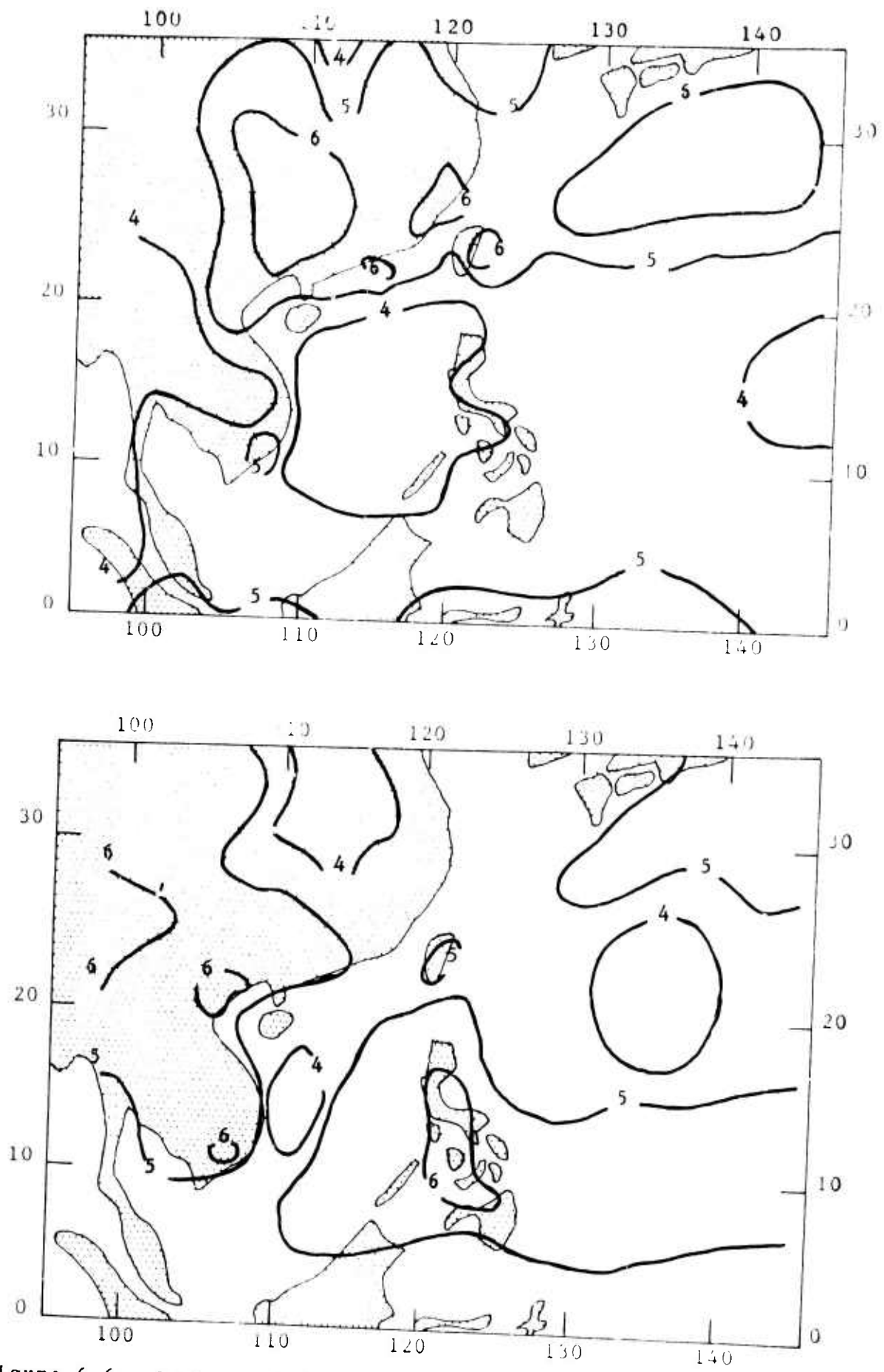


Figure 6-6. Mean monthly cloudiness for May (top) and August (bottom) in oktas.

Thompson, W. W., 1941: An essay on the general circulation of  
the atmosphere over Southeast Asia and the West Pacific.  
*J. Roy. Meteor. Soc.*, 77, 569-597.

## TROPICAL CLOUD PHYSICS

### 1. Introduction

Condensation, growth and precipitation usually occur simultaneously in clouds, with each process continually merging with and transforming into the others. Although in this short discussion of tropical cloud physics it will be convenient to treat them separately, one should remember that the separation has merely pedagogic and not physical justification.

### 2. Condensation

In air free of aerosols and ions, condensation of water vapor occurs only if the supersaturation reaches several hundred percent. In the atmosphere, abundant foreign particles serve as ready-made nuclei for condensation and prevent these large supersaturations from being achieved.

Ionized particles (not filterable by ordinary methods) can act as condensation nuclei if the ratio of the vapor pressure to the saturation vapor pressure (saturation ratio) = 4 for negative ions; = 6 for positive ions; i.e., relative humidities of 400 percent or 600 percent. Except in the laboratory, these degrees of supersaturation are never observed and hence one must conclude that ions are not important nuclei and that much more effective nucleating agents are always to be found in the atmosphere.

Consider a droplet of pure water introduced into a just saturated atmosphere. Since the equilibrium vapor pressure over the drop exceeds that over a plane water surface, the drop will evaporate.

A nucleus of an insoluble particle serves to facilitate condensation at a degree of supersaturation which diminishes with increasing nucleus size. If the nucleus is porous or contains recesses, capillary condensation will be able to set in at relative humidities below 100 percent.

If a droplet nucleus is wholly or partly soluble, condensation will begin at a lower supersaturation than on an insoluble particle of the same size. This arises from the fact that at the soluble surface, equilibrium vapor pressure is reduced by an amount depending upon the nature and concentration of the solute.

There are thus two effects. The equilibrium vapor pressure is inversely proportional to the drop radius and to the solute concentration. Hence nucleus droplets must be larger than a critical size for a certain supersaturation if they are to grow to form water (cloud) droplets.

It has been found that all sodium chloride (NaCl) nuclei with mass  $> 10$ - $15$  gm and nonsoluble nuclei with radius  $> 1$  micron ( $1/1000$  mm) require supersaturations of less than 0.1 percent for them to act as centers of continued condensation.

In addition to solid insoluble particles, and soluble matter giving rise to pure solution droplets, aerosols may also consist of mixed nuclei which are partly soluble, partly insoluble. The latter two groups being hygroscopic will obviously be preferred as centers of condensation.

Whether or not non-hygroscopic particles play a significant role in cloud formation depends largely on the number and sizes of the hygroscopic nuclei present, since in general these will be favored. Moreover, in view of the fact that insoluble particles may obtain a hygroscopic film, either by capturing small solution droplets or by acting as condensation surfaces for trace impurities, it may be that non-hygroscopic particles are rare in the free atmosphere. They can certainly be ignored over and near all the tropic oceans and probably elsewhere as well.

Generally, nuclei are most heavily concentrated over cities (approx.  $140,000 \text{ cm}^{-3}$ ) and least over oceans (approx.  $900 \text{ cm}^{-3}$ ).

Hygroscopic nuclei, which are among the largest and most efficient, are believed to originate from sea salts and from combustion processes. There is no doubt that condensation nuclei are produced by the disintegration of sea water. Sea-salt particles have been found in the air over the sea up to heights of 10,000 ft, their numbers increasing in strong winds, and they are also advected over land.

However, sea salt nuclei are only a minor constituent of atmospheric aerosol. Even over the ocean where spray is being produced, their concentration may not greatly exceed  $100 \text{ cm}^{-3}$ . Of the nuclei involved in cloud droplet formation, perhaps one tenth consist of sea salt, and the rest of mixed nuclei and the products of natural or man-made fires.

### 3. Growth

There are two conceivable processes by which nucleus droplets may attain radii of several microns and so form cloud or fog:

- a) diffusion of water vapor to and its condensation on their surfaces,
- b) growth by the coalescence of droplets moving relative to one another.

Since the rate of increase of droplet radius by diffusion is inversely proportional to the radius itself and since coalescence rates depend upon droplet size we should expect diffusion processes to contribute most to the growth of very small cloud droplets and collision processes to contribute most to the growth of large cloud droplets.

Obviously, both processes operate at once and their contributions cannot be measured or separated outside the laboratory. However, many theoretical computations indicate that collisions contribute very little to the growth of droplets with radii of



less than 15 to 20 microns.

The size distribution of cloud droplets is controlled not only by the micro-physical processes of droplet growth on nuclei, but also by the larger scale processes of cloud dynamics which will determine the cloud dimensions, the degree of mixing with the environment, the distribution of vertical velocity, the scale and intensity of turbulence, and the period for which individual droplets will remain in the cloud.

#### 4. Precipitation

Since we are considering tropical clouds, we can restrict ourselves to only one form of precipitation - rain. Although hail does occur in the tropics it is sufficiently rare not to warrant treatment in the space of a single lecture.

Droplets moving downward from the base of a cloud immediately begin to evaporate and of course the evaporation is proportional both to the height of the cloud base and to the dryness of the air beneath. As a rough rule a radius of about 100 microns may be regarded as a lower limit to the size of precipitation elements. The condensation process alone cannot produce droplets of average radius  $> 30$  microns and since these evaporate completely after falling a few feet in unsaturated air they cannot reach the ground as precipitation.

What then is the mechanism operating to increase cloud particle sizes?

a) Bergeron in 1935 (supported later by Findeisen) was quite positive he had the correct answer. Having concluded that hydrodynamic attraction forces, differences of capillary and hygroscopic forces, temperature differences and collisions resulting from turbulence were all inefficient or much too slow, he announced categorically that the only factor which could account for the release of precipitation was the appearance of a few ice crystals among a much larger population of supercooled droplets in those parts of the cloud where the temperature was below  $-10^{\circ}\text{C}$ . Since water saturation represents supersaturation with respect to ice, condensation would take place continuously on the ice, liquid water at the same time evaporating from the droplets until the liquid phase was entirely consumed. Bergeron therefore claimed that almost all raindrops originate as ice particles which grow copiously in this way and hence, that all rain clouds must extend well above the level of the  $0^{\circ}\text{C}$  isotherm.

b) Of course it has been known for many years that in the tropics at least, showers often fall from clouds with tops many thousands of feet beneath the  $0^{\circ}\text{C}$  level and in recent years careful visual and radar observations have shown beyond all doubt that in tropical regions heavy rain may fall from clouds which are entirely beneath the  $0^{\circ}\text{C}$  level.

We must conclude then that at least for the tropics, Bergeron and Findeisen are wrong and that some sort of coalescence process

most effectively produces precipitation in the tropics.

Three parameters having an important bearing on which mechanism dominates in releasing precipitation from a particular cloud or cloud system are:

- 1) temperature of cloud base,
- 2) cloud thickness - together these two largely control the liquid water content of the cloud and whether or not raindrops may be produced by coalescence,
- 3) temperature of cloud top - indicating the likely presence or absence of ice crystals.

Not merely is there good evidence that drop growth by coalescence is the predominant mechanism for releasing showers from tropical clouds but by using radar, researchers found in the central United States that in 60 percent of midsummer clouds reaching the  $-20^{\circ}\text{C}$  level an initial precipitation echo was received from regions beneath the  $0^{\circ}\text{C}$  level. These echoes must have returned from raindrops formed by the coalescence process.

In order for the coalescence process to be effective, the growing droplet must remain within the cloud long enough to reach the size of a raindrop. Time lapse photos of tropical cumulus and measurements within tradewind cumulus show these clouds growing in a succession of bubble-like spurts, mostly observed to occur in a central cloud column protected by surrounding cloud from evaporation or entrainment erosion by unsaturated cloud-free air.

For a cloud particle to become a precipitation element it must reach some rather critical size during the time taken for cloud air to rise from the base to the summits, such that it shall have settled some hundreds of feet relative to the air, gained a fall speed about equal to that of the updrafts near the cloud top (approx.  $1 \text{ m sec}^{-1}$ ), and have the capacity for falling with insignificant shrinking through several hundred of feet of unsaturated air and hence the chance to survive even if caught in the general evaporation of a cloud turret - and so resume its growth by settling into a newly rising mass of air within the cloud bulk. The critical drop size seems to be about 150 microns. Whether this size is reached depends on depth of cloud traversed, updraft speed and liquid concentration which is largely determined by the temperature of the cloud base and the degree of mixing of the cloudy air with the drier environment. If the entire cloud is small, its life may be only a little longer than the time taken for particles to reach the critical size - thus they are prevented from growing into precipitation elements - if the cloud is large, a shower is almost certain to develop, although a strong wind shear may intervene both by reducing the life of the cloud and by causing large particles settling out of the cloud tops to fall into clear air rather than into succeeding bubbles where they may continue their growth. Fig 7-1 follows two cumulus cloud particles through a 20-minute sequence. One particle grows to a precipitation

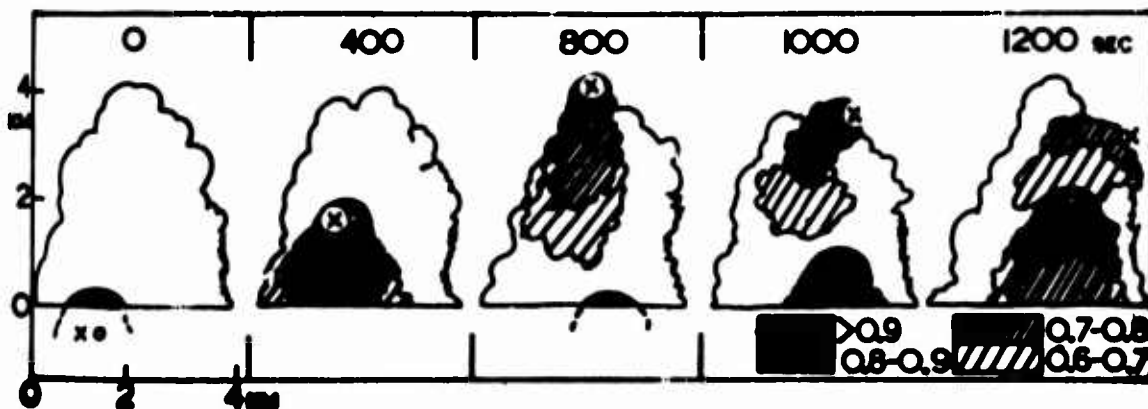


Figure 7-1. Schematic representation of the structure of cumulus. The approximation of the liquid water content (in  $\text{gm m}^{-3}$ ) to that in air rising from the base unmixed is indicated for two successive rising "bubbles" of cloud air. The successive positions of two cloud particles, one of which (white dot) grows into a precipitation element are also shown. (From "The production of showers by the growth of ice particles" by F. H. Ludlam in Q. J. Roy. Meteor. Soc., 78, 543-555. 1952).

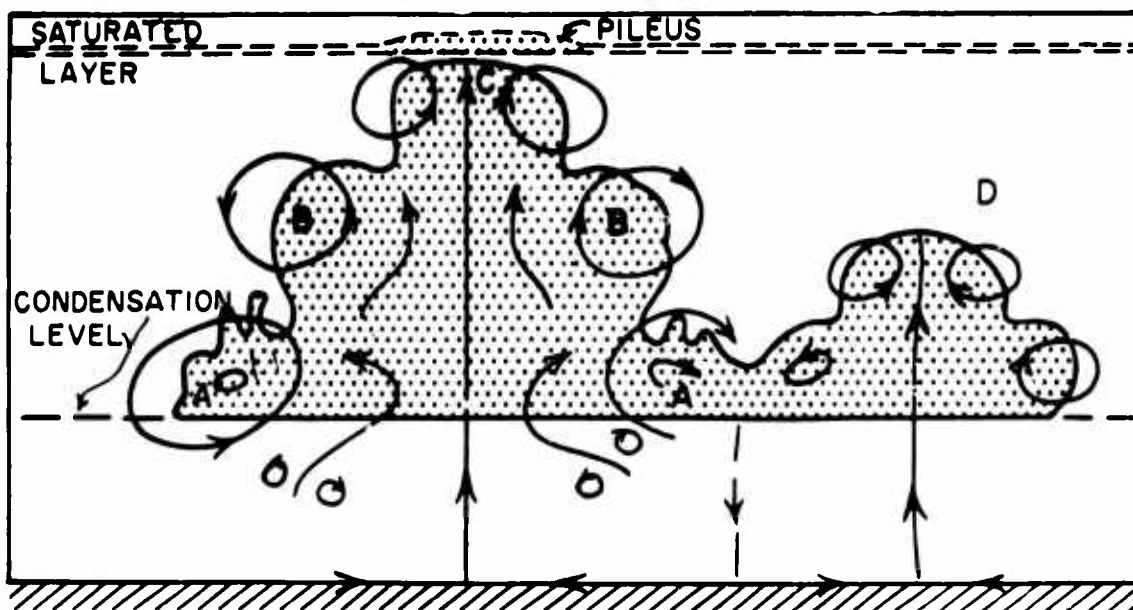


Figure 7-2. Various stages in the formation of cumulus.  
 A--old ring of original cloud elements greatly expanded and added to minor eddies.  
 B--decaying ring.  
 C--active ring of the growing top.  
 D--neighboring primitive cloud element, with secondary eddy just passing through.  
 (From "An indirect aerology of the tropical Pacific" by C. E. Palmer et al, U. of California, Inst. of Geophys., 131 pp. 1956).

**BLANK PAGE**

element, the other does not.

For a cloud bubble to move upward it must be less dense than its environment. However, at least in the trade winds, cloudy areas are colder than surrounding clear areas. Malkus explains this apparent anomaly by pointing out that "A cloudy area is composed of a small fraction of actively buoyant rapidly rising updrafts, a comparable small fraction of strongly sinking, negatively buoyant downdrafts and a great predominance, area-wise of decaying cloud matter and weakly subsiding, slightly negatively buoyant air."

Although many laboratory experiments have been designed to determine coalescence efficiencies, results to date are somewhat contradictory. We can be sure, however, that coalescence, especially in the tropics is a much more effective precipitation initiator than Bergeron imagined.

Palmer has suggested that tropical cumulus grow as a succession of ring vortices instead of bubbles (fig 7-2), and certainly time lapse photos lend as much support to this theory as to the bubble theory. For our purpose, either seems to fit the observations pretty well and to account adequately for the very short life cycle (a few minutes) of individual cloud elements, the prime importance of the central ascending column protected from entrainment, and the inhibiting effect of vertical shear on precipitation.

There is little doubt that the longer a droplet remains in a cloud, the larger it should become before precipitating. Hence we find a close connection between deep clouds with strong upcurrents, and large raindrops. However, often in tropical maritime regions an extremely small cumulus cloud precipitates a few drops of quite enormous size. These most probably have formed around giant hygroscopic salt nuclei which originated as sea spray. These nuclei have masses exceeding  $10^{-10}$  gm (or 100,000 times as heavy as the average hygroscopic nuclei) and have radii exceeding 20 microns. Even in small clouds such nuclei can very rapidly grow to considerable size. However since their concentrations are low ( $10^{-3}$  cm<sup>-3</sup>) the number of large raindrops forming on them is small.

Since very few measurements have been made in tropical middle and high clouds, any discussion of their physical properties would be largely conjectural.

##### 5. Bibliography

Malkus, J. S., 1958: On the structure of the trade wind moist layer. Pap. in Phys. Ocean. and Meteor., 13, 2, 47 pp.

Mason, B. J., 1957: The Physics of Clouds. Oxford, Clarendon Press, 481 pp.

Palmer, C. E., J. R. Nicholson and B. M. Shimaura, 1956: An indirect aerology of the tropical Pacific. Los Angeles, U. of California, Inst. of Geophys. 131 pp.

## LOCAL EFFECTS

### 1. Introduction

The discussion in Chapter 3 of PA provides an excellent basis for further consideration of the local effects of topography on the meteorological elements.

Synoptic meteorologists must work with observations. In the tropics, as elsewhere, these observations are made in centers of population and not usually where local effects are least and where conditions are typical of a wide area.

In one respect tropical synoptic meteorologists are better off than their high latitude colleagues. A good number of ocean observing stations are sited on tiny coral islands which rise only a few feet above the surrounding ocean. It is reasonable to assume that local effects in these spots do not significantly distort the overall picture.

In the tropical Pacific the island spectrum ranges from coral specks a foot or two above sea level to the great rugged masses of Borneo and New Guinea. The smallest coral islets exert no measurable effect on any meteorological element; islets large enough for an airstrip do affect temperature. On Eniwetok which has a lagoon 24 miles long and 18 miles wide, the diurnal range of temperature in a standard shelter standing on coral amounts to 10°F whereas the range over the center of the lagoon is only 5°F. Temperatures of inshore lagoon waters are often 1°F higher than those in the central lagoon which are never more than 1/2°F higher than the open ocean temperatures. Large low-lying coral islands, exemplified by Christmas Island with 160 square miles of exposed coral, produce correspondingly greater local temperature distortions.

Somewhat larger islands with peaks below 1000 ft such as Tinian and Yap, distort surface winds as well as temperatures but appear to have no appreciable effect on clouds or rainfall.

Larger and more mountainous islands about the size of Guam and the main Hawaiian Islands distort winds up to considerable heights and sharply modify the distributions of clouds and rainfall.

The very large islands of the Philippines and Indonesia besides causing sharply defined local variations, so modify the large scale distribution of meteorological elements over a wide area that the effects are easily recognizable on small scale synoptic charts.

### 2. Temperatures

By ignoring the effects of precipitation, well covered in PA, improved representativeness may be obtained by using the dew point as an air mass indicator. Of course its value is limited to fair weather, for it becomes quite unrepresentative if moisture

has been extracted by up-wind precipitation or added by evaporation from local precipitation.

### 3. Winds

Surface winds in the tropics, except over low-lying coral islands are notoriously unrepresentative. At any one time, the observed surface wind is the vector resultant of the synoptic wind, the local orographic wind and the local thermally induced wind. The proportions are never the same from hour to hour or even on either side of an airfield. Except when the synoptic wind is far stronger than the other components, as is often the case in a typhoon circulation, a meteorologist despairs of discovering it among the mess of local wind components. Nevertheless, at least for major stations, one should have sufficient appreciation of the effects of local winds and their diurnal variations to notice those shifts in the surface wind which can only betoken significant changes in the synoptic wind.

Upper winds, especially when measured at stations on rugged coasts, often show diurnal variations in both speed and direction to appreciable heights. For example, in Hong Kong where hills are from 2000 to 3000 ft high, mean 5000 ft resultant winds for the summer months show increasing offshore directions between morning and afternoon as follows:

<u>May</u>	<u>June</u>	<u>July</u>	<u>August</u>
036°	024°	060°	088°

One expects the sea breeze circulation to cause surface wind distortions while often completely ignoring the upper branch of the cell. As these figures show, the return flow may be far from negligible. Although generalization is dangerous, a fair rule would indicate that low-level observed winds are likely to be least distorted by local effects an hour or two after dawn and an hour or two after sunset. Thus, over the western Pacific, synoptic situations should be better reflected by the 00 and 12 GCT observations than by the 06 and 18 GCT observations.

### 4. Clouds and rain

Since local variations in the distribution of clouds and rain are usually closely connected to wind anomalies, we are faced with the same problem posed by the winds - how to deduce the synoptic large scale picture from the distorted local picture? The problem can be most successfully attacked by first determining the distribution of winds and weather under different synoptic situations using either aerial reconnaissance, time lapse cloud photography, radar scanning, or a dense station network. Figs 7-1 and 7-2 are examples of this method.

### 5. Diurnal curves

The diurnal variation of pressure at all tropical stations and the diurnal variations of temperature, wind, cloud, and rain

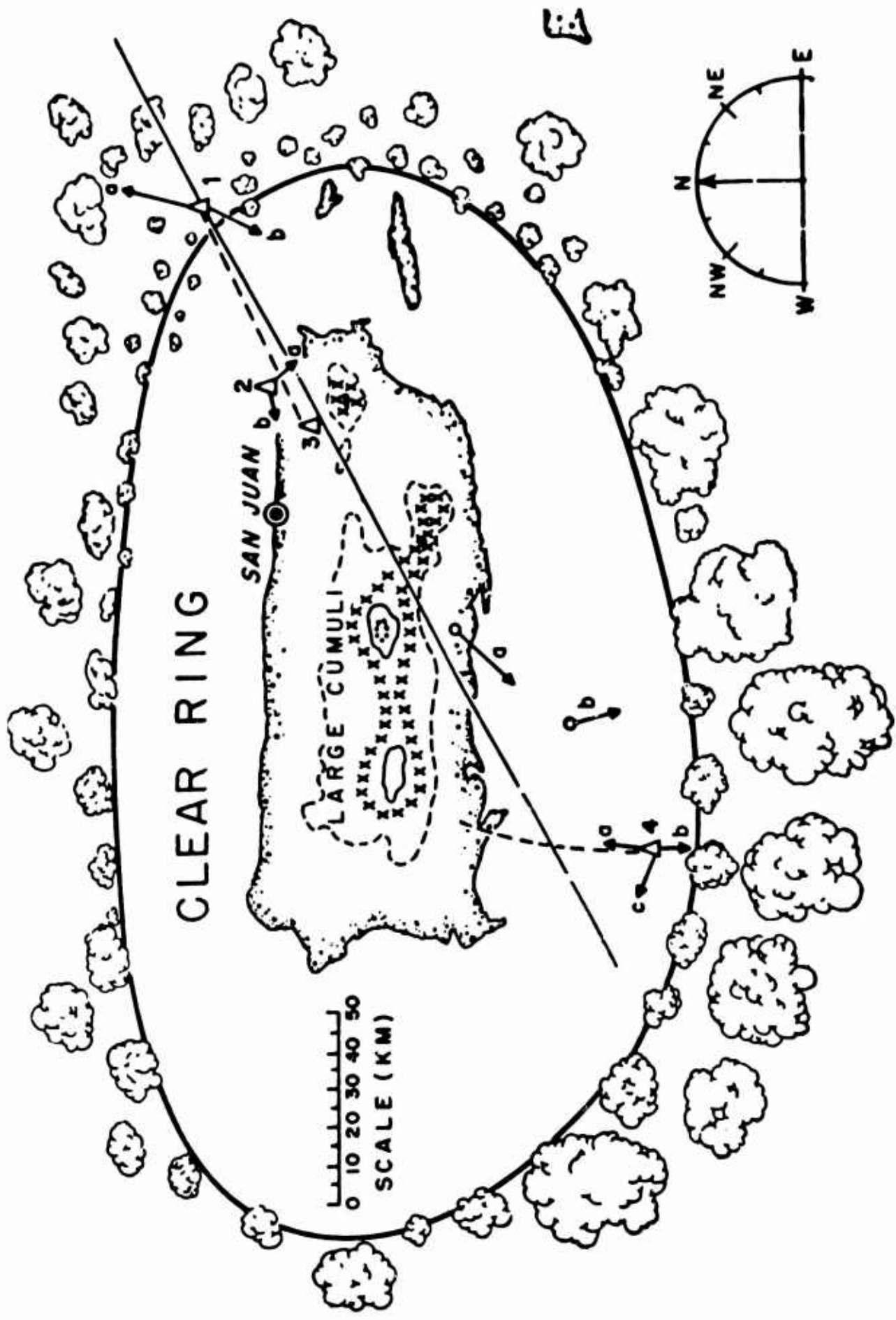
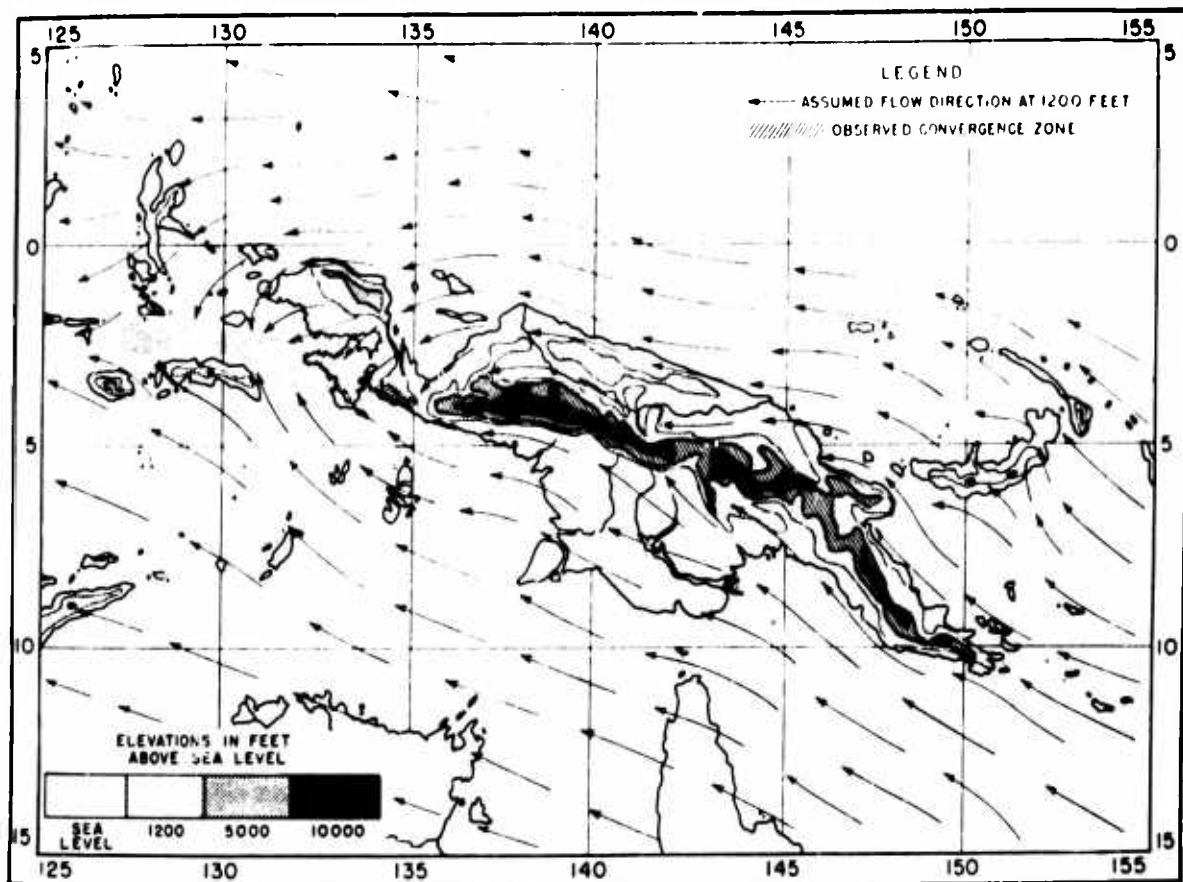


Figure 8-1. Topography and cloud distribution over and around Puerto Rico near noon on 25 June 1952. A fairly symmetric orographic convection cell with ascent over the island and compensating subsidence in the surrounding ring. (From "The effects of a large island upon the tradewind airstream" by J. S. Alkus in Q. J. Roy. Meteor. Soc., 81, 538-550, 1955.)





**Figure 8-2.** The zone of convergence which was observed in the Ceram sea and MacCleur Gulf when an easterly stream flowed around the mountain chain of New Guinea. Also shown are the assumed winds at 1200 ft under conditions of eastsoutheasterly flow. This convergence zone was observed to be of greatest intensity when the direction of the stream was eastsoutheast and the speed was 15 kn or more, conditions which obtained most often from April to October. The zone extends about 300 mi in an east-west direction and the cumulus and cumulonimbus clouds which build up in it reach maximum development shortly before dawn. The early morning cloud structure usually dissipated during the day in phase with the normal cumulus cycle of the region, the afternoon infrequently having more than scattered cumulus. (From "Examples of topographic convergence in the equatorial zone between 95°E and 160°E" by A. H. Glenn in Bull. Amer. Meteor. Soc., 30, 50-55. 1949).

over all but very small islands generally exceed all synoptic variations except those produced by tropical cyclones. In order then to deduce the synoptic picture from the observations, a meteorologist must be able to refer to the following diurnal curves for each important station:

- a) Surface pressure.
- b) Wind speed and direction - surface and aloft.
- c) Rainfall frequency, amount and duration.
- d) Low cloud bases, amounts and possibly types.
- e) Visibility and frequencies of visibilities below operating limits.

Near the equator, one or two sets of curves would probably suffice to describe the whole year. Further from the equator where seasonal influences become significant, at least four sets of curves (one for each season) would be needed.

Marked deviations of an observation from normal curves, indicate corresponding deviations of the synoptic situation from normal. For example, along the southeast China coast summer rainfall possesses a sharp morning maximum (fig V-1). Thus rain in the morning is usually less likely to persist than rain in the afternoon. Spring sea fog in this region also shows a pronounced morning maximum. In a stagnant synoptic situation, a meteorologist would be most foolhardy to forecast that a fog which developed in the afternoon would dissipate before the following afternoon.

## WEATHER RECONNAISSANCE

### 1. Introduction

Aerial weather reconnaissance has been conducted on the present scale since 1944 when the 55th Reconnaissance Squadron was established to support the 20th Air Force in the western Pacific area. Since that time many weather missions have been flown over most of the North Pacific to reconnoiter potential storm areas, track hundreds of typhoons and help fill in vast oceanic gaps in the world-wide weather observational network. For example, since the first typhoon penetration made in October 1947, the 54th Weather Reconnaissance Squadron has flown some 1000 typhoon missions on 200 or more different storms.

In recent years there has been an increasing trend toward flexibility in reconnaissance tracks and altitudes flown. This trend is in part due to a desire to cover larger areas of the Pacific Ocean with fewer aircraft of the WB-50 type. In recent years, meteorologists believing that the mechanisms which "trigger" depressions into typhoons may be readily identified at high levels (30,000-40,000 ft), have placed greater emphasis on reconnaissance at these levels.

### 2. Areas of reconnaissance

The majority of reconnaissance conducted in the Pacific area is done by squadrons of the Air Weather Service, USAF, The U. S. Navy usually undertakes reconnaissance on request.

Australia and perhaps Russia may also conduct weather reconnaissance in the Pacific. Australia has undertaken reconnaissance in the Timor Sea near northwestern Australia on a research basis. However, a more practical area for reconnaissance would be the ocean expanse between New Caledonia and the Queensland coast. Economy considerations restrict any extensive programs.

### 3. Tracks

Fig 9-1 illustrates the routine reconnaissance tracks for 1959. These tracks are generally defined by agreement between Air Weather Service meteorologists and reconnaissance squadron commanders. The tracks are changed from time to time. Missions to explore suspicious areas and missions to reconnoiter known typhoons hold precedence over missions conducted along the routine tracks.

As a matter of interest, the reconnaissance tracks are named after birds native to the area. Petrel and Loon flights are based on Hawaii, Buzzard flights on Japan and Vulture flights on Guam.

Most of the AWS reconnaissance flights are made either at 700 or 500 mb. However, flights which are aimed at initial detection of typhoons are flown entirely at 700 mb every day during the typhoon season. Several flights are now being flown

at 250-200 mb level from Japan and McClellan AFB.

Dropsondes and weather observations are made at regular intervals throughout the track (see fig 9-1). Weather observations are usually made at intervals of 100-200 mi but most commonly at 150 mi intervals.

#### 4. The reconnaissance code and its application to the tropics

Early code forms for weather reports from aircraft were developed from codes used by surface weather observers.

The fact that the observation taken from an aircraft differs markedly in scope from the surface observation prompted reconnaissance representatives to develop new codes taking into account the basic differences between surface and aircraft weather reports. Fig 9-2 describes the reconnaissance code tables in their present form (1959).

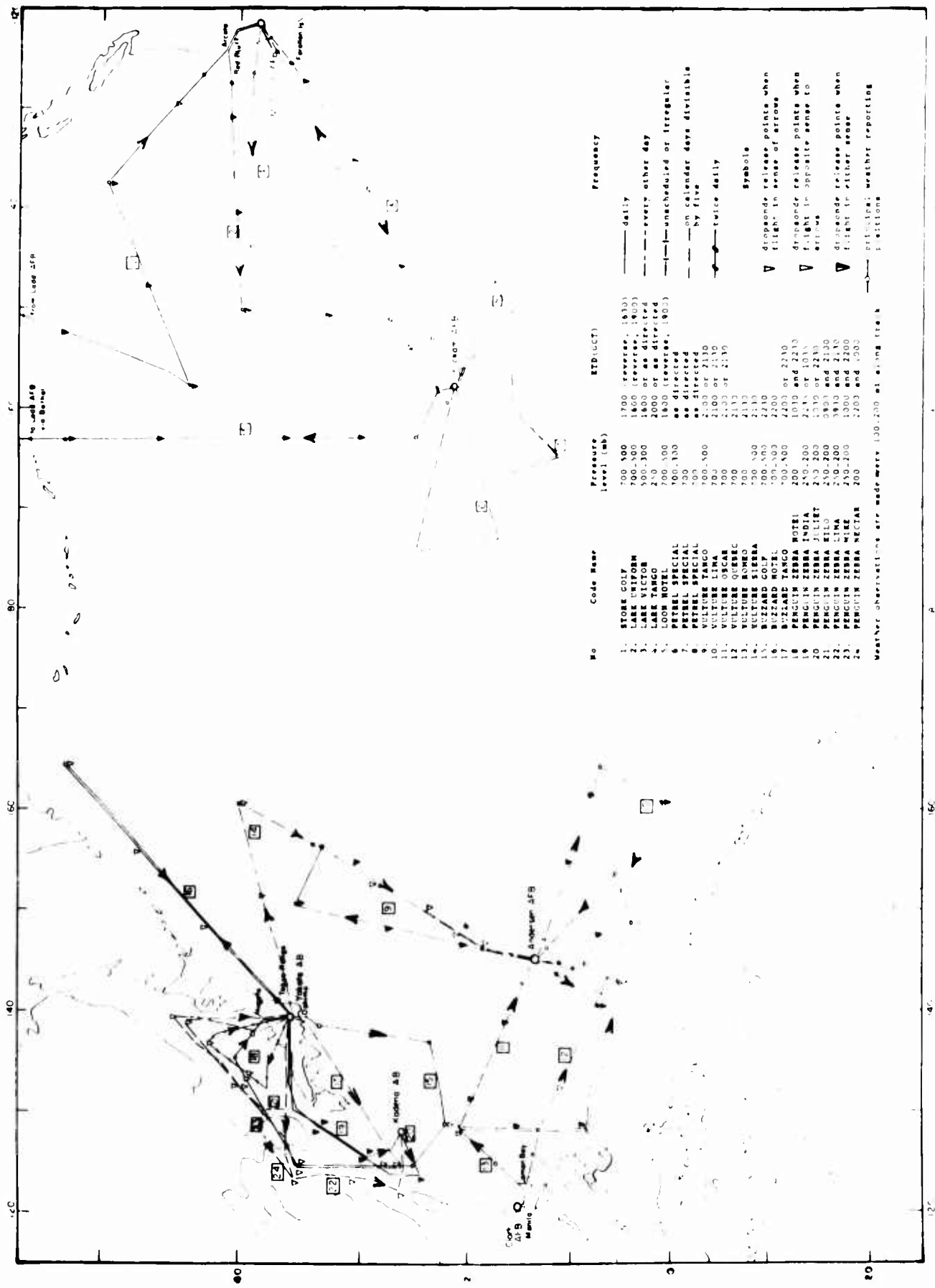
In the RECCO code, the aircraft is considered to be located at the center of a cylinder of air 30 nautical mi in radius. From this position, present weather, cloud types and amounts, flight conditions, and other observational elements are observed and reported as occurring within the cylinder.

Outside the cylinder, the quadrantal concept has been introduced to report prevailing conditions in the four major quadrants. In the event that a phenomenon of importance exists but is not predominant in a quadrant, it is reported as weather off-course. As a further extension of the observational range two groups are included for reporting radar echoes. Fig 9-3 illustrates the basic observational concept of the RECCO code.

The present reconnaissance squadrons now have the capability of covering any area in the Pacific in which tropical cyclone activity is suspected. However, there is some difficulty in applying the RECCO code to tropical regions. This is a result of the code originally being developed for mid- and high-latitude regions. Evidently some disagreements in encoding and decoding the data have developed. It may be worthwhile to point out those parts of the RECCO code inappropriate for tropical weather reconnaissance.

Present weather (W) and past weather (w). The greatest difficulty here lies in encoding weather conditions typical of the tropics. This is one section where special weather codes, which are more applicable to the tropics, would be desirable. In some cases it would be desirable to encourage weather reconnaissance observers to use the remarks section more frequently where the encoded weather group does not adequately describe existing conditions.

These same statements also apply to quadrant weather ( $Q_N$ ,  $Q_E$ ,  $Q_S$ ,  $Q_W$ ). Quadrant weather reported accurately is very important to the tropical meteorologist because through such reports the analyst can often determine the extent or intensity of a weather



No	Code Name	Pressure level (mb)	RTD(UCT)	Frequency
1.	STORE GOLF	700-500	1700 (reverse, 1830)	— daily
2.	LARK VICTOR	700-500	1800 (reverse, 1800)	— every other day
3.	LARK VICTOR	500-300	1800 or as directed	— unscheduled or irregular
4.	LARK TANGO	250	2000 or as directed	— on calendar days divisible by five
5.	LOON HOTEL	700-500	1800 (reverse, 1800)	— twice daily
6.	PETREL SPECIAL	700-300	as directed	—
7.	PETREL SPECIAL	700	as directed	—
8.	PETREL SPECIAL	500-300	as directed	—
9.	PETREL SPECIAL	700-500	2100 or 2130	—
10.	VULTURE LIMA	700	2100 or 2130	—
11.	VULTURE OSCAR	700	2100 or 2130	—
12.	VULTURE QUEBEC	700	2130	—
13.	VULTURE ROMEO	700	2130	—
14.	VULTURE SIERRA	700-500	2130	—
15.	VULTURE SIERRA	500-300	2130	—
16.	BUZZARD GOLF	700-500	2200	—
17.	BUZZARD TANGO	700-500	2200 or 2230	—
18.	PENGUIN ZEBRA HOTEL	200	1030 and 2230	—
19.	PENGUIN ZEBRA INDIA	250-200	2130 or 2135	—
20.	PENGUIN ZEBRA JULIET	250-200	2130 or 2230	—
21.	PENGUIN ZEBRA Kilo	250-200	2130 and 2230	—
22.	PENGUIN ZEBRA LIMA	250-200	2130 and 2230	—
23.	PENGUIN ZEBRA MIKE	250-200	2130 and 2200	—
24.	PENGUIN ZEBRA NECTAR	200	2200 and 2300	—

Weather observations are made every 130-200 mi along track.

Symbols:  
 ▽ drupeonde release points when flight in sense of arrow  
 ▽ drupeonde release points when flight in opposite sense to arrow  
 ▽ drupeonde release points when flight in either sense  
 — drupeonde weather reporting stations

Figure 9-1. Reconnaissance tracks. 1959.



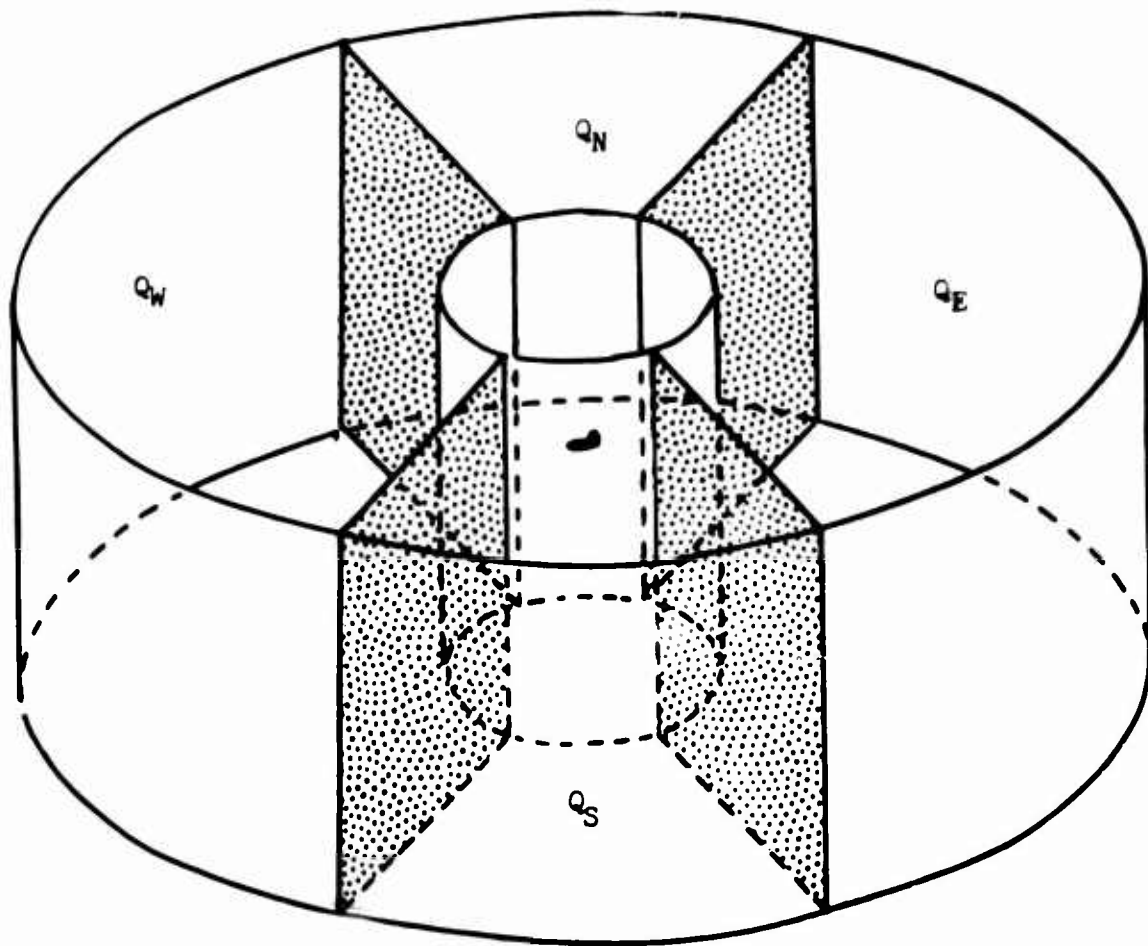


Figure 9-3. Reconnaissance observational concept. (From "Recco code" (AWSM 105-34), Air Weather Service, 55 pp. 1953).

condition. For example, the fact that a line of convergence accompanied by cumulus congestus lies along the track and regions to the right and left are relatively clear, can only be conveyed properly through accurate reporting of quadrant weather.

Cloud groups (C, hh, HH). There is very little difficulty in reporting cloud bases and tops provided the observer can properly measure or estimate them. However, in the tropical Pacific, cloud formations are often complex and many layers and types may co-exist in the same area.

It is often difficult for the analyst to picture cloud formations from the encoded message in the same way that they are observed. The difficulty usually lies in the procedures for encoding outlined in AWSM 105-34, RECCO code 1 August 1953, which were designed to fit general conditions in higher latitudes. It is impossible for the aerial observer to encode such features as shear in clouds, orientation of cloud lines or "streets" and whether stratiform clouds are dependent or independent, unless he makes liberal use of the remarks column. Quite frequently the aerial observer reports chaotic sky conditions when several layers and types of clouds are observed. This technique is little help to the weather analyst.

Significant weather changes ( $W_s$ ) and weather off course ( $W_c$ ).

These codes could be modified and amplified to report tropical conditions more accurately and completely.

Radar groups ( $O_e$ ,  $C_e$ ,  $I_e$ ). Unfortunately these reports are difficult to interpret and difficult to encode with the present code. Radar information can be of great value to the analyst if he can picture cloud formations through radar reports. A great deal more work should be done in both encoding and interpretation of weather data. The new APS-23 radar (3 cm) equipment is excellent for receiving reflections from significant cloud lines and formations for distances up to 200 mi and even greater during normal tropical weather. However, the effectiveness of this radar is questioned whenever it is used to scan heavy rainfall associated with intense storms. Heavy rain-bands nearest the radar may attenuate the beam energy to the extent that inaccurate representations may be given of other rain-bands a greater distance from the radar.

Wind data ( $hhhd_t d_a, ddfff$ ). Flight level winds are reported as either a spot or average wind. The symbol  $d_t$  indicates the distance over which the wind is computed to get an average reading. The reliability of the wind observation and the method used in obtaining it are given by code through symbol  $d_a$ .

Spot winds are obtained by the AN/APN-32 Automatic Navigator now standard equipment on WB-50's. The AN/APN-32 while primarily a navigational instrument can give accurate spot winds at any altitude when the sea surface is rough enough to reflect the radar beam. Not only does it provide accurate winds, but its precise navigational capabilities allow observers to pin-point the position of a typhoon regardless of poor radio reception conditions



or lack of visual check points.

Average winds are obtained by several navigational methods of varying degrees of reliability. Multiple drift methods have greater reliability than other methods, such as, fixing, single drift or LOPs (three lines of position).

The analyst should always consider the  $d_t$  and  $d_a$  data when analyzing wind reports. In fact, the data should be plotted on the map for reference.

Interpretation of the ddiff groups is straightforward and will not be discussed.

Summary. Since it is unlikely that the RECCO code will be changed to meet the requirements for accurately reporting tropical weather, it would be worthwhile for aerial observers to:

1. Use the remarks section of RECCO form frequently.
2. Make up detailed flight cross-sections enroute and put remarks on sections.
3. Make a complete debriefing for the duty forecaster on interpretation of reports and unusual weather along route.
4. Disseminate a summary of important weather information on a specific reconnaissance mission to other forecast units via teletype.

5. Typhoon reconnaissance

Flight procedure and altitude limitation. If conditions appear too hazardous for an aircraft to reconnoiter a storm, modifications in the reconnaissance request are submitted to the warning center.

Reconnaissance missions are not planned for altitudes below the 700 mb level. However exceptions are allowed only if the following restrictions are adhered to: in no case will reconnaissance be conducted below 1500 ft radar altitude; whenever excessive turbulence or winds of 50 kn or greater are encountered a climb to the 700 mb level will be initiated; in no case will penetration of a typhoon be attempted at an altitude below the 700 mb level; all flights near land areas are to be avoided if data can be secured from other sources.

En route weather observations. Complete weather observations are taken at 150 mi intervals en route to, and returning from tropical cyclone and suspect areas. Observations are made at 30-minute intervals when the aircraft is within 300 mi of the actual or forecast position of the cyclone center, or the center of the suspect area. Additional observations may be made at any time at the discretion of the aerial weather observer.

En route weather observations, particularly of the distances

middle and high clouds radiate out from the storm center, the number of lines of convergence encountered as well as their orientation and width, and the intensity and frequency of rain and shower activity in various quadrants can all give clues to the size and intensity of a typhoon.

Penetration of eye. Methods of locating a typhoon or hurricane eye vary. When the winds of a storm are relatively weak, low-level penetration is sometimes employed, especially in the eastern Pacific. With this type of penetration the aircraft flies at an altitude between 500 and 1500 ft. It crabs across the wind toward the center of surface wind rotation while continuous estimates of the surface wind velocities are made until the eye is reached. The low-level method is perhaps the simplest one, but can be very dangerous in well-developed storms with severe turbulence and low visibilities. For this reason its use is limited. However, the automatic navigator AN/APN-82 makes it possible to follow the same "eye-seeking" procedure at higher altitudes where there is less danger from turbulence; in this case, low visibilities are no longer an obstacle because the presence of clouds does not decrease the wind-measuring capability of the navigational equipment.

For aircraft which are not equipped with the automatic navigator, the principal method of finding a storm center is by techniques which employ the radio altimeter. Usually the aircraft is flown at 700 or 500 mb by the aid of the pressure altimeter; i.e., the aircraft is maintained at a pressure-altitude of 9880 or 18,280 ft and the radio altimeter provides the geometric heights of the pressure surface. Since the aircraft does not remain precisely on the selected pressure surface at all times, the difference between the pressure-altimeter reading and the radio-altimeter reading, or "D" value, is used as the primary parameter for pressure measurement by flight personnel. For all practical purposes the gradients of "D" are equal to the height-gradients on the pressure surface. When a definite rise of "D" is noted the course of the aircraft is altered 135° to the left (in the Northern Hemisphere) until another rise is noted, and the procedure is repeated until the aircraft enters the eye. This type of penetration requires more time than the type in which the aircraft crabs across the wind, but it can be used in darkness and without radar. Nevertheless, there are occasions when it is very difficult to locate an eye because of gently sloping height gradients. Radar is then especially useful in directing the aircraft into the eye.

Quite frequently in the Pacific, "Loran" is used to locate storm centers. This type of locating device depends upon fixed radar beacons situated on island or mainland coasts. Whenever a navigator or radar operator desires his location he dials his receiver to the frequency of a set of stations. The strong pulses of radio energy sent out by the master station trigger the transmitter of the slave station and the radar operator receives two transmitted pulses at different times. The radar operator locates his position on a Loran line by noting the difference in arrival times of the master signal and slave signal. By switching his receiver to another set of Loran stations at a different frequency

and repeating the procedure he fixes his location by the intersection of two Loran lines or by referring to Loran charts.

Other location methods such as dead-reckoning, and astro-navigation can be utilized when Loran facilities are unavailable.

Weather information within eye. Once in the eye a dropsonde observation is made and the following information is transmitted in plain language: coordinates, time, navigational method and estimated reliability in miles of center fix, diameter and description of eye, location and velocity of maximum flight level wind, location and velocity of estimated surface wind, minimum height of pressure surface flown and flight level temperature and dew point. If available, preliminary minimum sea level pressure is included in the eye data report; information regarding the diameter and shape of the eye and changes in eye shape between two fixes can give a measure of the intensity of the storm.

Maximum surface winds. The condition of the ocean surface serves as an indicator of surface wind speeds. The following categories are utilized when the flight altitude is at the 700 mb level:

<u>Wind Speed (kn)</u>	<u>Appearance of Water</u>
Calm.....	Glassy smooth.
12 .....	First detect white caps.
40 to 50 .....	First detect green patches.
65 .....	Numerous green patches and large white caps.
100 .....	Large areas of green; large white sheets.
130 .....	50 to 75 percent of surface white and green.
150 .....	Entire surface white and green but white sheet still distinguishable.
Greater than 150 .....	Solid white-green churning appearance; foam-like.

A more elaborate breakdown of the categories below 100 kn is given in AWSM 105-34 RECCO CODE 1 August 1953.

The subjectivity inherent in surface wind estimations may possibly be the reason for such wide fluctuations in reported maximum winds in typhoons or hurricanes. Especially it appears very possible that considerable errors could occur when the surface wind is above 100 kn.

Circumnavigating a typhoon. To determine the distributions

of wind and weather about a major cyclonic circulation such as a typhoon, reconnaissance aircraft may circumnavigate the disturbance. This is usually done near the outer limit of the strongest winds and is a means of determining the extent of 50 kn winds and region of maximum winds.

Circumnavigation also provides information regarding "false" or "open" eyes which could be mistaken for the true eye.

Often the quadrant of maximum rain can be observed and reported; some meteorologists believe this can give an indication of the general direction of typhoon movement.

Reports on the orientation and number of marked convergence lines (radar or verbal reports) are useful to the analyst in delineating streamlines and forecasting the movement of the lines toward the station.

Pressure and wind data collected in a circuit about the storm center can be used for an estimate of the location of the storm center. The accuracy of this estimate depends upon the degree of circular symmetry of wind and pressure around the center. Normally, this procedure does not lead to excessive errors, since typhoons or hurricanes are fairly circular in their inner portions.

The use of radar permits aircraft to remain outside the strong-wind regions of a storm and still provide position fixes of the eye. Radar-equipped flights can be of the circumnavigational type, but more often the aircraft flies back and forth near a known land area to keep navigational errors to a minimum. Locating the eye is often difficult, especially in the case of "false" or "open" eyes. There is a rather considerable short-period variability in the positions of hurricanes determined by this method. Therefore the motions derived from successive fixes determined in this manner are of greatest value only when the fixes are very frequent. As better methods are developed for interpreting radar-scope information, such fixes will no doubt increase in value.

Another type of peripheral reconnaissance is the so-called "large-scale synoptic reconnaissance," in which aircraft are flown over a large area around the storm. Flights of this type are aimed at providing reliable data for large-scale flow-pattern analysis. As no single flight can possibly provide the large-area coverage desired, the typhoon forecasters select the areas where aircraft data are most needed.

#### Normal reconnaissance requirements.

a. Suspect area: One investigative flight per day, planned so that search is conducted during the hours of daylight.

b. Tropical depressions: One fix per day, normally at 0200 GCT on tropical depressions which are not forecast to develop into tropical storms within 24 hours of fix time. If the

depression is forecast to develop into a tropical storm within 24 hours of fix time, the requirements for tropical storms will apply (see c).

c. Tropical storms: Two fixes per day, normally at 2000 GCT (first priority) and 0800 GCT (second priority) on tropical storms not forecast to develop within 12 hours of fix time, in which case the requirements for typhoons will apply.

d. Typhoons and hurricanes: Four fixes per day, normally at 2000 GCT (first priority), 0800 GCT (second priority), 0200 GCT (third priority) and 1400 GCT (fourth priority).

#### 6. Future reconnaissance plans

High level (50-60,000 ft or more) reconnaissance of weather systems is just in a budding stage. Recent examples of this type of observing technique were described in two articles in WEATHERWISE, June 1958 and April 1959. A high altitude U-2 jet aircraft fitted with a Perkin-Elmer Model-501 tracking camera was flown by the Air Weather Service over three typhoons in order to photograph the cloud patterns of the centers in addition to getting high-altitude meteorological data. One of the main purposes of this research is to gather photographic data on storms which will aid in solving some of the future weather satellite photographic problems.

#### 7. Bibliography

Air Weather Service, 1953: Recco code (AWSM 105-34). Washington, Air Weather Service, 55 pp.

\_\_\_\_\_, 1959: Synoptic weather reconnaissance (AWSR 55-12). Scott AFB, Illinois, Air Weather Service, 47 pp.

American Meteorological Society, 1959: Weather reconnaissance system AN/AMQ-15. Bull. Amer. Meteor. Soc., 40, 84.

Bundgaard, R. C., 1958: The first flyover of a tropical cyclone. Weatherwise, 11, 79-83.

\_\_\_\_\_, R. D. Fletcher and J. R. Smith, 1959: Typhoon-eye cloud patterns as viewed from above. Weatherwise, 12, 64-66.

First Weather Wing, 1958: Typhoon warning service (1WWM 55-10). APO 915, 1st Weather Wing, 34 pp.

\_\_\_\_\_, 1959: Typhoon warning service (1WWM 55-10). APO 915, 1st Weather Wing, 17 pp.

Fletcher, R. D., 1956: Aircraft reconnaissance of tropical cyclones by the Air Weather Service. Proc. Trop. Cyclone Symp., Brisbane, 371-377.

Rutherford, G. T. and F. T. Hannan, 1956: Aircraft weather reconnaissance in Australian waters. Proc. Trop. Cyclone Symp., Brisbane, 379-390.

A P P E N D I C E S

## RELATIONSHIP OF GENERAL CIRCULATION TO NORMAL WEATHER OVER SOUTHERN ASIA AND THE WESTERN PACIFIC DURING THE COOL SEASON

By *C. S. Ramage*

Royal Observatory, Hong Kong

(Original manuscript received 27 June 1952; revised manuscript received 17 August 1952)

### ABSTRACT

As a first step in a study of cool-season (November through April) weather over southern Asia and the western Pacific, an analysis of the relationship of the general circulation to normal weather has been attempted.

In October, a jet stream suddenly appears along the southern edge of the Himalayas. Thereafter it varies little in position until April, when it begins to waver prior to disappearance in early summer. This sequence, and also the fact that no comparable jet is found north of the Himalayan-Tibetan massif, are explained in terms of mechanical lifting and the effect of snow cover on insolation. Nearly all extra-tropical depressions form in and move along the jet stream, while even rapidly moving cold-fronts are temporarily, though strongly, intensified as they pass beneath it. The increasing velocity of the jet stream after it leaves the mountains seems due to confluence, over northeast India, between the westerlies and upper south-westerlies of the Bay of Bengal.

Vigorous convergence in the southwesterlies over Burma, and between the southwesterlies and the westerlies of the jet stream over northeast India, probably results in the intense subsidence and aridity observed downstream. The subtropical ridge is displaced northward and becomes nearly vertical, and south of it deep baroclinic easterlies prevail.

East of the Philippines this distribution, and over the southwest Bay of Bengal a combination of low-level trough and high-level divergence, are thought to favor the formation of tropical storms.

### 1. Introduction

The purpose of this study is to explore the major factors controlling normal weather-sequences and -distributions over the subtropical and tropical regions of Asia and the western Pacific during the cool season (November through April). In a later paper, an explanation of exceptional distributions will be attempted.

Since the war, the now well-known concept of the jet stream has formed the basis of a number of papers on the winter weather of North America. Recently Chaudhury (1950) and Yeh (1950), using cross sections, have investigated the character of the jet stream over southern Asia and the western Pacific during winter, while Yin (1949) has correlated its movements in early summer with onset of the monsoon over India. Bolin (1950) and Thompson (1951) have also touched on the same subject in more general studies. All emphasize the importance of the relationship between the jet stream and weather in this region.

In general, these writers agree with Yeh's contention that two belts of maximum westerlies exist, one flowing around the southern and the other around the northern edge of the Tibetan plateau. The position of the southern and stronger jet-stream (November through January) remains almost stationary. Its onset is abrupt, first becoming evident over northwest India in late September or early October, and then advancing

down-stream at about 3 deg long per day. The fact that its speed increases downstream, beyond the China coast, is attributed by Bolin to the effect of a reunification with the northern jet-stream. This, according to the "confluence theory" (Namias and Clapp, 1949), results in acceleration of the flow. Yeh, however, considers the two jet-streams to remain separate. He and Chaudhury demonstrate coincidence between the southern jet and the mean winter precipitation-maximum over India and China, deducing from this that the inter-annual variation in position of the jet is slight. Yin associates the surge of the summer monsoon across India and Burma with the sudden movement of the southern jet north of the Tibetan plateau.

These papers comprise a valuable introduction to a study of the general circulation of the region. However, some questions are left unanswered, and divergence of views exists on others.

In the remaining sections of this paper, an attempt is made to explain the peculiar nature of the general circulation of the region and its influence on weather.

### 2. The southern jet-stream

Bolin (1950), in a theoretical discussion of the effect of mountain ranges on large-scale flow, derives equations based on a homogeneous barotropic atmosphere, unaffected by surface thermal changes. From these

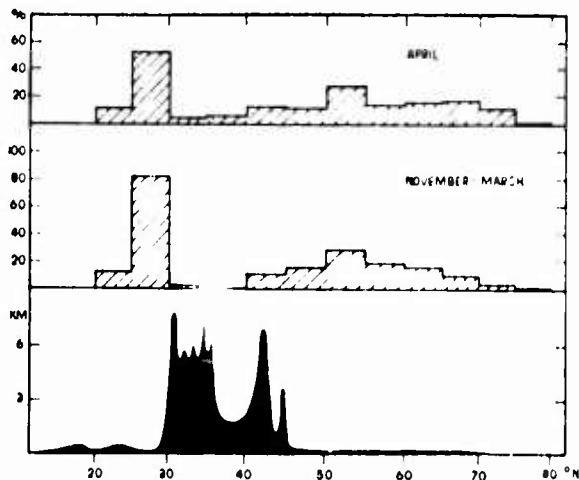


FIG. 1. Position frequency of jet streams at 500 mb (1949 and 1950) and topographical section along 80°E.

equations, he deduces that over Asia the belt of maximum westerlies is split by the Himalayan-Tibetan massif (H.T.), one branch flowing around the southern and one around the northern side. An examination of 500-mb charts (U. S. Weather Bureau, 1949) along 80°E confirms the existence of a most persistent jet usually less than 200 m. south of the ranges, but at a similar distance north of H.T. no corresponding maximum occurs (fig. 1). According to Queney (1948), the effect of horizontal thermal gradients on air flow becomes significant for mountains of the dimensions of the Himalayas, although mathematical difficulties have prevented an adequate analysis. Thus it is not surprising that Bolin's assumption of barotropy, though leading to reasonable models for smaller systems, fails when applied to the greatest mountain-range in the world.

An alternative physical theory, in harmony with the observations, can be based on the results of comparison between conditions at mountain stations and those in the free atmosphere. Many investigators (e.g., Schell, 1934; Bhatia, 1942; Eide, 1944) have found

TABLE 1. Free-air temperature over Peshawar (34°00'N, 71°37'E) minus mountain temperature at Cherat (33°50'N, 72°01'E). (Monthly means, deg. C.)

Jan.	Feb.	Mar.	Apr.	May	Jun.	Jul.	Aug.	Sep.	Oct.	Nov.	Dec.
2.6	2.2	2.1	1.1	1.2	0.0	0.6	0.8	1.0	2.2	2.0	1.9

that air temperatures measured at mountain stations are lower than temperatures in the free atmosphere at the same height. The reason given is that air lifted over mountains is cooled adiabatically at a rate greater than the free-air lapse rate. It has been found that the stronger the wind or the higher the mountain, the greater is the temperature difference, and also that insolation heating from a snow surface in winter is very much less than from an earth or rock surface in summer. The results obtained by Bhatia for Cherat (4.3 km) are characteristic (table 1).

*Establishment of the jet.*—In autumn, the zonal westerlies begin to intensify and spread equatorward. Thus, along the northwest face of H.T., lying athwart the flow, strong lifting develops. In view of the experience of glider pilots, it is probable that lifting continues to well above the mountain tops and may result in intensification and concentration to great heights of the temperature gradient between air over the mountain and that over the plains to the south. The fact that isotherms up to 14 km over northern India nearly parallel the Himalayas supports this (Venkiteswaran, 1950). Thus the normal temperature-gradient, locally intensified by adiabatic cooling from lifted air over the mountains, may lead to establishment of a jet stream, although the precise dynamic mechanism involved is not clear. An added factor in maintaining the jet is the reduction in insolation heating due to the increasing area of snow on the high country. The jet, once established in the northwest, rapidly produces conditions along the mountain barrier to the southeast which are favorable for its extension in that

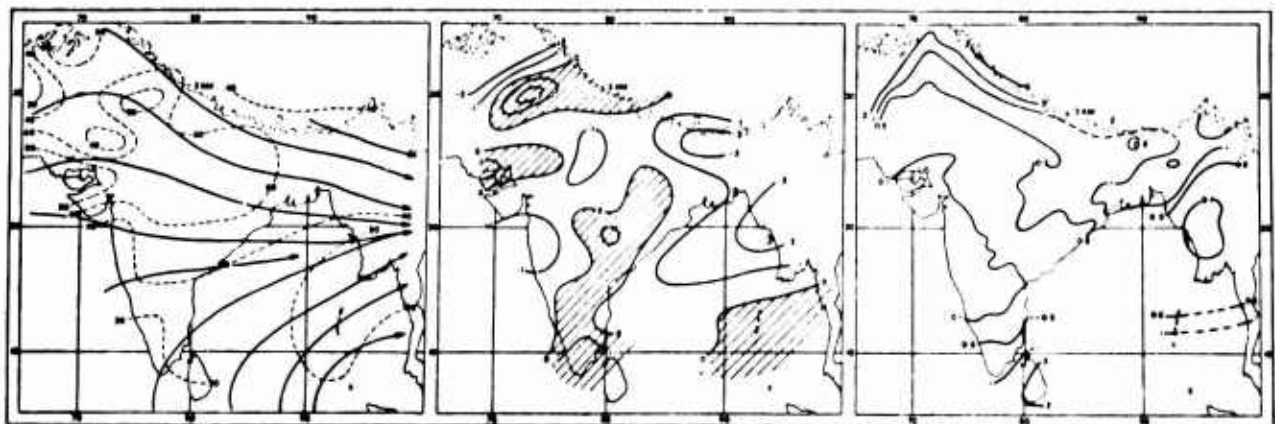


FIG. 2. Mean conditions over India for February. Left: resultant wind-flow at 12 km (after Venkiteswaran, 1950); isovels in knots. Center: divergence at 12 km in units of fractional outflow per 12 hr; Bellamy's (1949) method. Right: rainfall in inches.



direction, and it is soon firmly anchored to the southern face of H.T.

During October and November, a change is also taking place over the Indian peninsula. This rapidly cools to become colder than the Bay of Bengal, and isotherms up to at least 12 km reorient parallel to the east coast with maximum crowding at the head of the Bay. Such distribution may account for the persistent upper-level southwesterlies, increasing with height, accelerating downstream, and reaching a maximum in mid-winter. These meet the jet stream over northeast India (fig. 2, left), and the resulting vigorous high-level "confluence," should the theory be correct, could account for the marked increase in velocity of the jet stream further east. Namias and Clapp (1949) say: "The semipermanent solenoid field between the cold Asiatic continent and the Bay of Bengal and the Indian Ocean probably revitalizes the jet stream." It seems likely that this confluence, always occurring in the same restricted area, is a major factor in the immovability of the jet-stream axis as far east as 150°E.

Whereas along the southern edge of H.T. the mechanical effect of the mountains locally intensifies the normal north-south temperature gradient, along the northern edge (with air over the mountains probably colder than that over the plains) the gradient may be destroyed or even reversed, and a minimum rather than a maximum of zonal flow may result (fig. 1).

*Direct effect of the jet on weather.*—As has already been mentioned, the jet axis coincides with the axis of maximum rainfall; for not only do nearly all the extra-tropical depressions of the region form along the jet, but they also travel for most of their life along it. [See fig. 6 and also fig. 3 of Miller and Mantis (1947).] Miller and Mantis say: "There can be little doubt that the topography of the coastal region of Asia is intimately related to cyclogenesis." In fact, cyclogenesis is more directly related to the position of the jet stream, although development is favored in that

section of the jet overlying a surface with considerable moisture and temperature gradients.

Over North America, the jet accompanies the polar front in its movements north and south; over southern Asia and the western Pacific, except at times in April, it does not. Moving frontal systems intensify only temporarily as they pass through the region of the jet. This is well demonstrated in fig. 3, which shows the mean rainfalls recorded during the passage of 5 fast-moving undistorted cold-fronts. The selection was determined solely by availability of rainfall data and the requirement that preceding and succeeding weather should be fine.

*Dissolution of the jet.*—In March, the Indian peninsula begins to heat and the isotherms trend west-east. Although the jet stream maintains its strength along the Himalayas, vigorous confluence no longer occurs over northeast India; and as the jet weakens over China and the western Pacific, rainfall zones become less marked.

During April, the zonal westerlies tend to move northward but this is resisted by the mountain effect. The jet suddenly disappears and reappears south of the ranges, the disappearances becoming increasingly frequent and prolonged as the season advances (fig. 1). Each successive disappearance coincides with a surge northward of the summer monsoon (Yin, 1949). Finally the jet ceases to exist, and summer conditions prevail throughout the region.

The sudden and permanent establishment of the jet by November, in contrast to its comings and goings in April, make the weather of autumn much more stable and predictable than spring weather. In Hong Kong, in November, only stratiform clouds are observed, and precipitation accompanying cold fronts is insignificant. In April, however, stratus alternates with cumulonimbus, and cold fronts may produce anything from light drizzle to severe thunderstorms.

In India, for a great many years, there has been intense research on seasonal forecasting. Some of the factors found significant fit well in the above theory. Banerji (1950) states: "The westerly current over Northern India . . . makes its appearance at the higher levels even as early as the close of September and the beginning of October. . . . The strength of these westerly winds over Agra in the later half of September and the first fortnight of October (gives) a good indication of the coming intensity of the winter rains. . . . This factor has a correlation coefficient of 0.48 with January to March precipitation in northwest India." Again, "The first among the factors useful for the prediction of Indian rainfall was discovered about sixty years ago when it was observed that some great droughts in India appeared to be preceded by excessive winter or spring snowfalls on the mountains to the North and Northwest of India. This is to say, excessive

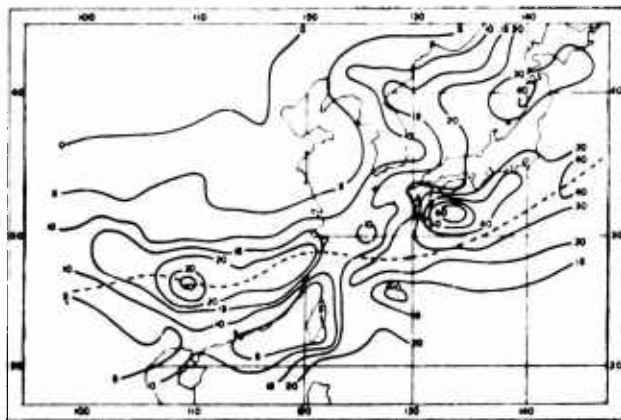


FIG. 3. Mean rainfall (mm) of five undistorted cold-fronts. Earliest 30 October, latest 21 April. Dashed line: maximum axis of mean cool-season rainfall.

snowfall on the Himalayas has on the subsequent rainfall an adverse effect which lasts for as long as four months."

### 3. Subsidence south of the jet-stream

Widespread subsidence occurs almost everywhere south of the jet stream. The explanation given for this condition in North America (University of Chicago, 1947) is that part of the air in the maximum west-wind belt is flung southward, subsides and then moves northward towards the polar front at low levels.

Over our region, subsidence is both more intense and more confined than over North America. Normal subsidence south of the jet stream occurs over northwest India, but over northeast India and Burma juxtaposition of jet stream and convergent upper south-westerlies seems to result in much more vigorous subsidence downstream (fig. 2). The excess of air at high levels, which can escape neither north nor south, must subside downstream in a zone with rather rigid latitudinal limitations.

That the southwesterlies contribute potently to subsidence is substantiated by the Hong Kong soundings. There, on 90 per cent of mid-winter days, strong subsidence inversions usually extending from 800-700 mb up to 300 mb are observed (fig. 4). Since little more than 10 per cent of the winds at either 200 or 300 mb are from directions north of west, the southwesterlies rather than the jet stream are a much more probable source. This is supported by the following.

First, subsidence is most persistent in mid-winter, when the Bay of Bengal southwesterlies are strongest. In November and April, though winds from north of west are more frequent, subsidence occurs less often (fig. 4).

Second, distances between isentropic layers over Hong Kong are less than near the jet stream (Kagoshima). Since, for corresponding points in the United States the reverse is true, Palmén and Newton (1948) were forced to postulate a solenoidal circulation extending south from the jet stream. That such an explanation is not needed for Hong Kong may indicate that the meridional circulation associated with the jet stream is rarely effective there.

The region of strong subsidence is usually confined between 17°N and 24°N, and 90°E and 150°E. Temperatures in the southern part, between the upper surface of the northeast monsoon and 300 mb, are markedly warmer than those further south. Thus the

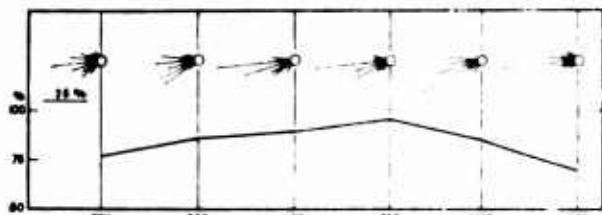


FIG. 4. Wind roses at 200 mb and percentage frequency of subsidence inversions at Hong Kong (3 years)



FIG. 5. Surface and upper wind observations made by H.M.A.S. SYDNEY on passage between Hong Kong and Singapore from 0700 GCT 9 February to 1200 GCT 12 February 1952. (Winds in knots; barb is 10 kn, solid triangle 50 kn)

subtropical ridge is well defined, lies north of its normal latitude and, as Yeh (1950) has pointed out for the Canton-Manila cross section, has a nearly vertical axis. Fig. 5, which is typical of the region south of Hong Kong, shows such a distribution; examination indicates that along 140°E a similar distribution prevails. On the other hand, mean cross-sections along 76°E (Chaudhury, 1950) and 78°E (Venkiteswaran, 1950), and sample cross-sections along about 170°E, all show the subtropical ridge in normal latitudes with normal slope.

Over the China Sea, cold fronts on the advancing edge of northeast monsoon surges can sometimes be detected as far south as 10°N. They give little precipitation in the region of subsidence (fig. 3), but may intensify as they pass south of the subtropical ridge. This is well illustrated by serial rawin soundings made by H.M.A.S. SYDNEY on passage between Hong Kong and Singapore during February 1952 (fig. 5). At the time the ship was leaving port, a weak dry cold-front was crossing Hong Kong. The front slowed thereafter, and at 0000 GCT on the 10th the ship passed through it just south of the subtropical ridge, recording appreciable precipitation and medium as well as low clouds.

### 4. Tropical storms

The only part of the tropics in which winter storms are known to form lies in the Northern Hemisphere between 70°E and 160°E. In this region, three distinct sub-areas can be distinguished (fig. 6); two where storms form (east of the Philippines and southwest

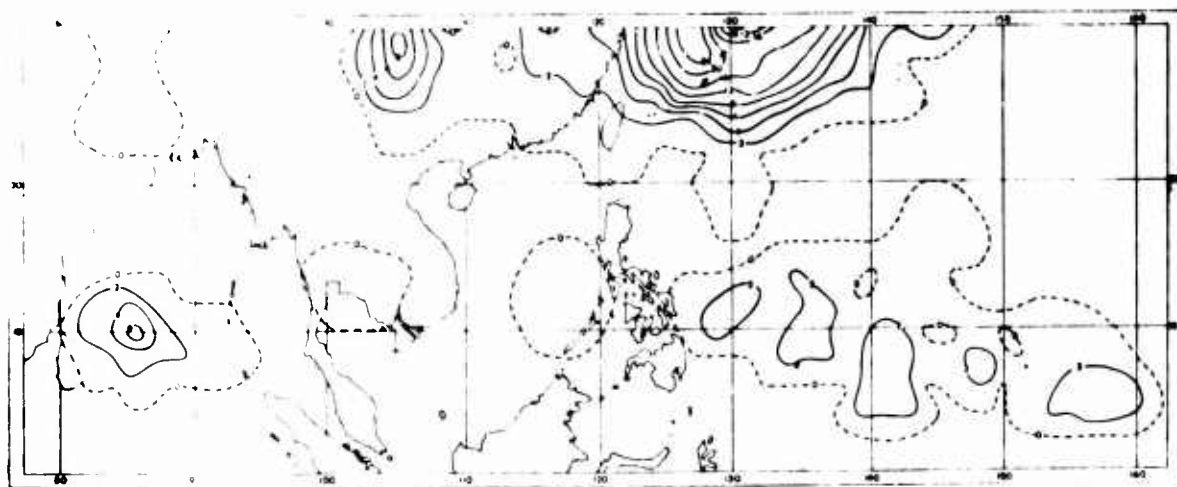


FIG. 6. Geographical frequency of formation of depressions. Value of isopleth at any point represents number of cyclones that formed within radius of 2.5 deg lat from that point in months November through April, 1932-37. [Incorporating fig. 3 of Miller and Mantis (1947).]

Bay of Bengal), separated by one where little or no development occurs.

*China Sea and western Pacific.*—Yeh (1950) suggests that the northward displacement of the subtropical ridge relative to other regions may account for the formation of winter tropical storms. Certainly, intense subsidence results in a secondary "thermal equator" associated with the ridge and favoring formation of baroclinic easterlies to the south. These often have horizontal cyclonic shear and are of sufficient latitudinal extent to allow storms to develop within them. Such a distribution between  $14^{\circ}$  and  $9^{\circ}$ N is recorded in fig. 5. Over the China Sea, however, successive surges of the winter monsoon maintain persistent, cool dry anticyclonic northeasterlies below 1.5 km. Thus, although high-level conditions are favorable, formation of tropical storms with their intense low-level circulations is impossible.

*Bay of Bengal.* As mentioned before, the slope and location of the subtropical ridge in this area are similar to other parts of the tropics, and yet the southwestern Bay shows a higher frequency of tropical-storm formation than anywhere else in the world. Probably due to the configuration of the surrounding land-masses, a weak semi-permanent trough usually exists below 3 km over the Bay, while at around 8 km over the

southern Bay the effect of southwest-northeast isotherm orientation is to produce divergence in the easterlies underlying the subtropical ridge. Fig. 7 of the paper by Chaudhury (1950) shows a layer of baroclinity centered near 400 mb at  $15^{\circ}$ N,  $78^{\circ}$ E. His analysis does not extend south of this, but it is possible that this layer becomes increasingly baroclinic towards the southeast. Rainfall distribution (fig. 2, right) tends to confirm this. Such a combination of low-level convergence and high-level divergence would make this small area a most favorable one for storm formation.

In fig. 7 are drawn curves of average monthly frequency of tropical-storm development over the western Pacific (from Starbuck, 1951) and the Bay of Bengal (from Newnham, 1922). Though for differing periods, the curves are remarkably similar, points of note being the minimum in February (when surface air of polar-continental origin extends farthest south) and the much higher frequency of storms in November and December than in April. Although sea temperatures in the latter month are higher, in early winter the Bay of Bengal southwesterlies are vigorous and persistent; but by April they are almost non-existent, conditions then more closely resembling those in other tropical regions.

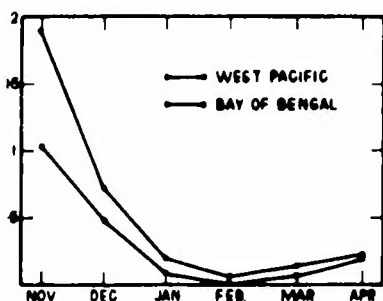


FIG. 7. Average monthly frequency of tropical-storm developments.

## 5. Conclusions

1. Over southern Asia and the western Pacific, the general-circulation patterns aloft during the cool season, and their associated weather distributions, are remarkably stable. Mean conditions are very similar to actual conditions on a high proportion of days.

2. A possible reason for this stability is found in the topography of the region, the great Himalayan-Tibetan massif and the Indian peninsula at first profoundly modifying, and then fixing the general pattern.

3. The sudden onset of winter weather with the appearance of the jet stream south of the Himalayas, as well as the more gradual disappearance of the jet in spring, are explained as effects

of mechanical lifting at the mountain face and snow on the plateau.

4. The combination of the jet stream and persistent upper southwesterlies over the Bay of Bengal may cause downstream subsidence so vigorous that the subtropical ridge is displaced northward, and may account for the south-north temperature gradient observed to the south of it.

5. The resultant deep baroclinic easterlies over the western Pacific, and high-level divergence associated with low-level convergence over the southwest Bay of Bengal, tend to favor development of tropical storms. At low levels over the China Sea, however, the persistent northeast monsoon nullifies this effect.

6. From the earlier discussion, it is possible to visualize the modification imposed in this region on the normal three-cell meridional circulation pattern. The central cell is of limited extent; over India and China it covers little more than 5 deg lat. and along 90°E much less. It operates intermittently, with the passage of depressions along the jet-stream axis, and has little direct effect south of 23°N. The equatorial cell is more vigorous than elsewhere and varies little in intensity or position. Three-dimensionally, it resembles one turn of an enormous spiral. Upper-level poleward flow takes place across the Bay of Bengal and Burma-Siam, and sinking occurs in the zone around 19°N from Burma eastward. Lower-level equatorward flow, predominantly across the China Sea, extends east of the Philippines, as well. The frequent occurrence of southerly winds between 1 and 3 km over Hong Kong indicates that some of the subsiding air north of 20°N flows into the central cell.

*Acknowledgment.*—The writer wishes to record his appreciation of the valuable observations made by Lt. Cdr. R. Fennessy and the radar staff of H.M.A.S. SYDNEY.

#### REFERENCES

- Banerji, S. K., 1950: Methods of foreshadowing monsoon and winter rainfall in India. *Indian J. Meteor. Geophys.*, **1**, 4-14.
- Bellamy, J. C., 1949: Objective calculations of divergence, vertical velocity and vorticity. *Bull. Amer. meteor. Soc.*, **30**, 45-49.
- Bhatia, K. L., 1942: A comparison of Cherat surface observations of temperature and humidity at 0800 hrs L.T. with aeroplane observations over the Peshawar plain at the same level. *India meteor. Dept., Sci. Notes*, **10**, 11-17.
- Bolin, B., 1950: On the influence of the Earth's orography on the general character of the westerlies. *Tellus*, **2**, 184-195.
- Chaudhury, A. M., 1950: On the vertical distribution of wind and temperature over Indo-Pakistan along meridian 76°E in winter. *Tellus*, **2**, 56-62.
- Eide, O., 1944: On the temperature difference between mountain peak and free atmosphere at the same level. *Meteor. Ann.*, **2**, 183-206.
- Miller, J. E., and H. E. Mantis, 1947: Extratropical cyclogenesis in the Pacific coastal region of Asia. *J. Meteor.*, **4**, 29-34.
- Namias, J., and P. F. Clapp, 1949: Confluence theory of the high tropospheric jet stream. *J. Meteor.*, **6**, 330-336.
- Newham, E. V., 1922: Hurricanes and tropical revolving storms. *Geophys. Mem.*, **2**, 213-333.
- Palmén, E., and C. W. Newton, 1948: A study of the mean wind and temperature distribution in the vicinity of the polar front in winter. *J. Meteor.*, **5**, 220-226.
- Queney, P., 1948: The problem of air flow over mountains; a summary of theoretical studies. *Bull. Amer. meteor. Soc.*, **29**, 16-26.
- Schell, I. I., 1934: Differences between temperatures, humidities and winds on the White Mountains and in the free air. *Trans. Amer. geophys. Union*, **15**, 118-124.
- Starbuck, L., 1951: A statistical survey of typhoons and tropical depressions in the western Pacific and China Sea area from observations and tracks recorded at the Royal Observatory, Hong Kong, from 1884 to 1947. *Tech. Mem. roy. Obs. Hong Kong*, No. 4, 10 pp.
- Thompson, B. W., 1951: An essay on the general circulation of the atmosphere over South-East Asia and the West Pacific. *Quart. J. r. meteor. Soc.*, **77**, 569-597.
- U. S. Weather Bureau, 1949: *Northern hemisphere sea level and 500 millibar charts with synoptic data tabulations*, Washington, U. S. Govt. Printing Office.
- University of Chicago, Staff members, 1947: On the general circulation of the atmosphere in middle latitudes. *Bull. Amer. meteor. Soc.*, **28**, 255-280.
- Venkiteswaran, S. P., 1950: Winds at 10 km and above over India and its neighbourhood. *Mem. India meteor. Dept.*, **28**, 55-120.
- Yeh, T. C., 1950: The circulation of the high troposphere over China in the winter of 1945-46. *Tellus*, **2**, 173-183.
- Yin, M. T., 1949: A synoptic-aerologic study of the onset of the summer monsoon over India and Burma. *J. Meteor.*, **6**, 393-400.

## THE COOL-SEASON TROPICAL DISTURBANCES OF SOUTHEAST ASIA

By *C. S. Ramage*

Royal Observatory, Hong Kong<sup>1</sup>

(Original manuscript received 17 May 1954; revised manuscript received 13 August 1954)

### ABSTRACT

During the cool season (November through April), two types of tropical disturbance occasionally bring rain to a normally dry part of southeast Asia. The area, enclosed approximately between 15°N and 25°N, and 95°E and 120°E, includes south China and the northern portions of Indo-China and Thailand.

In early winter, tropical storms or easterly waves, moving westward to the south of the subtropical ridge, may cause sufficient convergence north of the ridge to give rain.

In late winter and spring, tropical troughs in the high-level (above 400 mb) southwesterlies cross southern India. Moving eastward, they link in the region of Burma with the low-latitude polar westerlies further north, then intensify and become stationary over the Thailand-Indo-China region. East of the trough line, disturbances with extensive rain areas develop on the China Sea polar front.

### 1. Introduction

In an earlier article (Ramage, 1952), an analysis was made of the relationship of the general circulation to normal weather for the cool season (November through April) over southern Asia and the western Pacific. Because of great persistence of the high-level pattern, well-defined wet and dry areas can be delineated. Over an area of about  $10^6$  mi<sup>2</sup>, enclosed approximately between 15°N and 25°N, and 95°E and 120°E (fig. 1), tropospheric flow above 400 mb is usually strongly convergent. In compensation, air subsides vigorously through the middle troposphere in this area, and rain is inhibited.

On occasion, subsidence ceases and the area experiences considerable rain. This can occur during tropical-storm or easterly-wave situations, or when a "tropical

trough" moves into the area and intensifies. Ensuing sections of this article contain examples of these situations as well as tentative explanations and suggestions on forecasting procedure.

### 2. Data

U. S. Weather Bureau northern-hemisphere sea-level and 500-mb charts and synoptic tabulations comprised the basic material for the initial synoptic classification, which was made for the 1949-1950 and 1950-1951 cool seasons. Detail was provided by 6-hourly surface and upper-level charts for the Far East, plotted and analyzed at Hong Kong, and by aircraft post-flight reports. Extensive use was made of synoptic and rainfall data published by the national weather services of India, Thailand, Indo-China and Malaya. Observations from China are lacking for these years; but Chinese surface observations for the years 1929

<sup>1</sup> This work was completed at the University of Chicago during tenure of a Commonwealth Fund Fellowship.

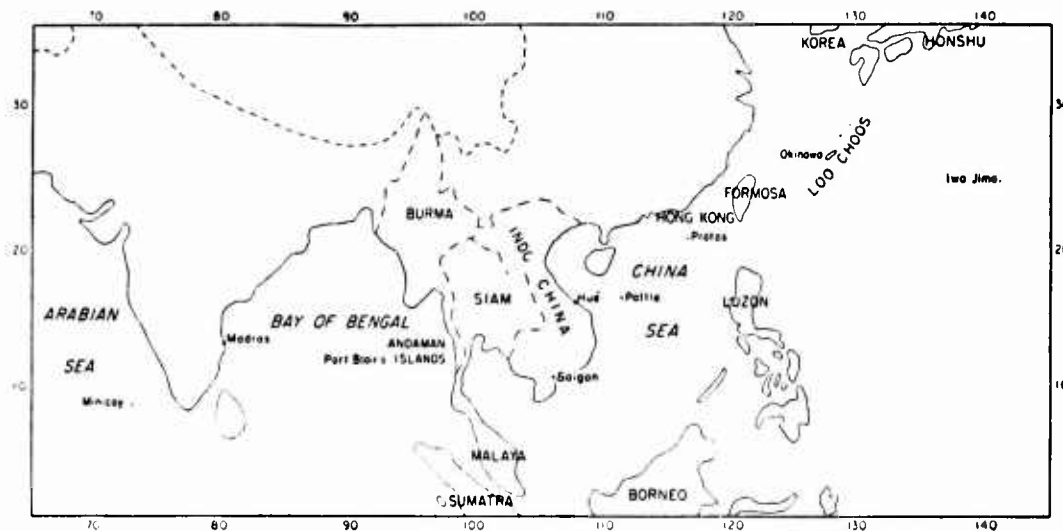


FIG. 1. Map showing places mentioned. Dashed line is 10,000-ft contour of land topography.

and 1935, and published data and analyses for 1937 (Air Ministry, Meteorological Office, 1943), helped complete the picture.

Heterogeneity of material has made impossible uniform presentation in the examples. A working rule has been to reproduce 300-mb analyses if feasible, or otherwise 700-mb or surface analyses which can be supplemented by time sections.

In the examples, normal plotting procedure has been followed. Winds are in knots, one full barb indicating 10 kn, a triangle 50 kn. On the time sections, isolines of 24-hr changes in the heights of isobaric surfaces are drawn from differences plotted in the middle of the interval over which the change was measured (López, 1948). Generally speaking, this ensures that zero isolines coincide more closely with trough or ridge positions as given by wind shifts than would be the case if changes were plotted at either end of the 24-hr interval. Values of isolines and contours on the time sections and constant-pressure charts are given in hundreds of feet. Charts show the position of surface fronts and, by means of stippling, areas in which rain was observed in the 24 hr previous to chart time. Where possible, the upper limit of air with relative humidity above 50 per cent is shown on the time sections, to give an indication of moisture distribution.

**3. Tropical storms and easterly waves**

By November, typical winter flow-patterns have been established over south and southeast Asia (Ramage, 1952). In most parts of the world, during winter, the subtropical ridge slopes equatorward with height and usually reaches to within 10 to 12 deg lat of the equator in the high troposphere. Over the China Sea and the Philippines, however, the ridge axis above 700 mb is almost vertical and is found between 15 and 17°N. South of the ridge, in the region of deep easterly flow, disturbances typical of summer continue to be observed. Tropical storms or typhoons may persist there for several days, usually dissipating when a strong monsoon surge feeds cold, dry surface air into the circulation. Waves in the easterlies are not uncommon. They propagate slowly westward, with low-level divergence and fine weather ahead, and low-level convergence and precipitation behind (Dunn, 1940). North of the vertical ridge axis, the monsoon is overlain by polar westerlies. Any effect that tropical storms or easterly waves have on regions to the north is limited to the lowest layers. Nevertheless, they often cause sufficient convergence in the relatively shallow easterlies to the north to produce rain even as far away as south China.

Riehl and Shafer (1944) show that superposition on a wave in the easterlies of a trough in the polar westerlies often results in mutual intensification. Certainly

TABLE 1. Tropical-storm days over the China Sea (1884-1896, 1905-1939 and 1946-1947).

Month:	Nov.	Dec.	Jan.	Feb.	Mar.	Apr.
Days:	99	18	3	1	3	4

when this is observed over south China more rain is experienced than would be expected from either disturbance alone.

*Monthly variation.* A tropical-storm day is defined, for present purposes, as a day when a tropical storm is centered over the China Sea between 15°N and 25°N and west of 120°E. Table 1 lists the monthly totals of tropical-storm days for a 50-yr period. From November through February, the subtropical ridge aloft shifts only slightly southward. Thus, conditions in the middle and high troposphere, south of the ridge, stay favorable for tropical-storm development. However, as the season advances, surges of the winter monsoon extend farther southward, making surface conditions more and more unfavorable to storm development or persistence. In March and April, the subtropical ridge aloft is frequently displaced south of its normal winter position. Then the belt of deep easterlies extends insufficiently far north from the equator to allow development of major circulatory systems. Easterly waves are relatively more common than storms in mid-winter, but they seldom produce rain in the region of extremely shallow low-level easterlies north of the subtropical ridge aloft.

*Example, 2 to 5 January 1951 (figs. 2 to 6).*—On 30 December 1950, a typhoon crossed southern Luzon on a west-northwest track. Weakening, which began at this stage, continued when the storm moved out across the China Sea, as surface monsoon air was injected into the system. By 1200 GCT 2 January 1951 (fig. 2), only a vestige of the circulation remained; winds near the center did not exceed 25 kn, and pressure rose over the China Sea as a fresh surge of the

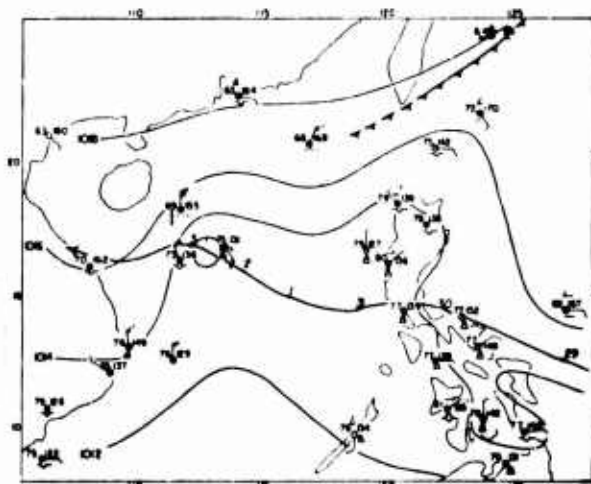


FIG. 2. Surface isobaric chart for 1200 GCT 2 January 1951. Daily positions of depression center are shown at 0000 GCT.

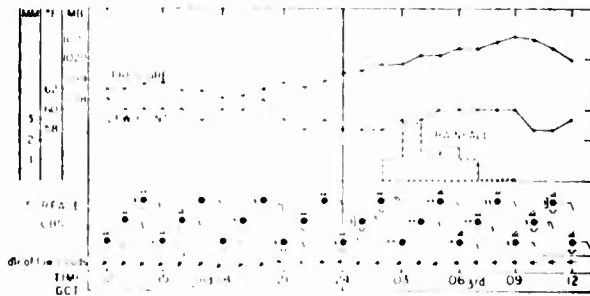


FIG. 3. Hong Kong meteorogram from 1200 GCT 2 January 1951 to 1200 GCT 3 January 1951. Pressure is adjusted for diurnal variation. Rainfall amounts are plotted for hourly intervals.

monsoon began to affect the area. Despite the weakness of the circulation, a trough extending north from the center, with characteristics of an easterly wave, was sufficiently active to give rain at Pratas on the 31st and 1st. Pattle, lying just south of the depression track, recorded 26 mm of rain; and Hué, where the disturbance entered the Indo-China coast, recorded 10 mm.

The Hong Kong surface observations (fig. 3) clearly show westward passage of the easterly trough. Direction of low-cloud movement changed from northeast to east between 2000 and 2100 GCT on the 2nd, 2 hr after minimum pressure was recorded. Shortly thereafter, measurable precipitation set in. The passage was accompanied by a veering of northeasterly winds below 800 mb and a pressure-height minimum (fig. 4).

Simultaneously with the easterly trough, a well-marked trough in the polar westerlies was approaching Hong Kong from the west. Its passage at the station is represented in fig. 4 by the portion of the zero isoline of pressure-height change above 800 mb. This isoline, and the layer of maximum wind veer in the westerlies from 800 to 650 mb between the 2nd and 3rd, indicate that by 0000 GCT on the 3rd the trough line lay over Hong Kong at about 650 mb. As is general in this

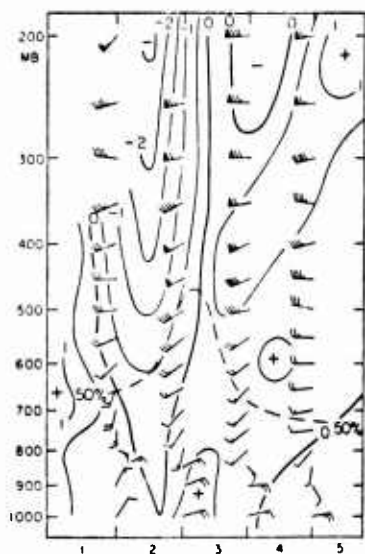


FIG. 4. Hong Kong time-section for 1 to 5 January 1951.

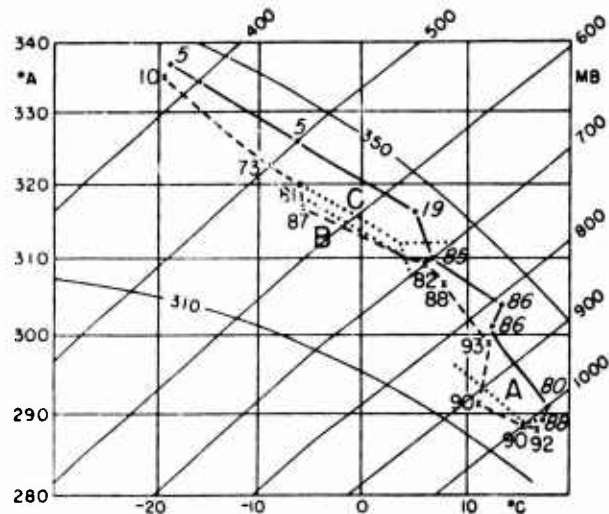


FIG. 5. Hong Kong radiosonde soundings for 0000 GCT 2 January 1951 (full line) and 0000 GCT 3 January 1951 (dashed line).

region, where normal high-level flow is from west-southwest rather than west, the trough passage produced a wind shift from south-southwest to southwest in the middle troposphere and from southwest to west in the high troposphere. Rain started as the trough in the upper troposphere was still approaching, and ceased with its passage at approximately 0900 GCT on the 3rd.

At Hong Kong in the lowest 100 to 150 mb, between the 2nd and 3rd (fig. 5), temperatures fell an average of 3°C and humidity increased. The surface dew-point at Hong Kong is very sensitive to advective temperature changes, and since it stayed steady (fig. 3) there could have been little intrusion of colder air from the

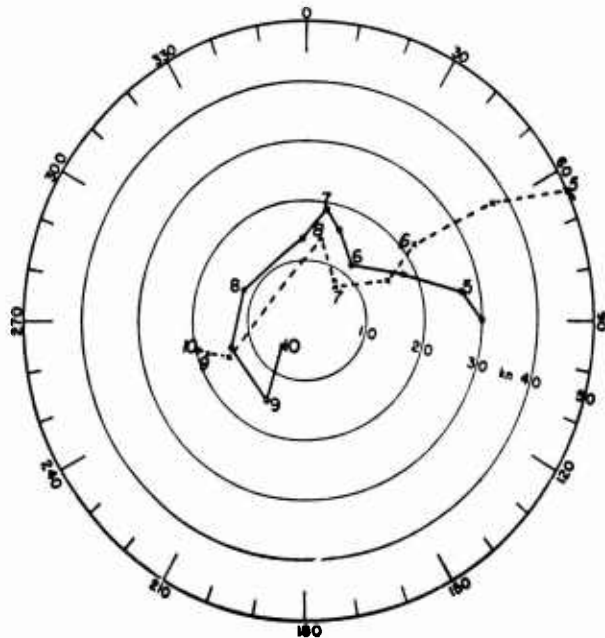


FIG. 6. Hodograph plot of Hong Kong rawinsonde soundings for 0000 GCT 2 January 1951 (full line) and 0000 GCT 3 January 1951 (dashed line). Pressure-levels are shown in hundreds of millibars.

north. The changes could have been due to ascent, for lifting of the surface air present on the 2nd would have resulted in predominantly moist-adiabatic cooling (dotted line A, fig. 5) and in an average temperature in the layer close to that observed on the 3rd.

Above the friction layer, temperature changes from the 2nd to the 3rd (fig. 5) were in accord with the westerly trough passage, but were inverse to what would be deduced from a geostrophic hodograph calculation (fig. 6). The hodograph indicates that, at 0000 GCT on the 2nd, warm air was advecting up to 450 mb. Since no geostrophic cold-air advection was present in this layer 24 hr later, an assumption that warm-air advection continued for the first 12 hr of the period leads to the conclusion that a temperature rise of at least 2C should have occurred. In fact, a fall of 2C was observed. Thus, any explanation of the change in temperature and in particular of the increased depth of the moist layer must take account of vertical motion, if non-geostrophic horizontal advection may be regarded as small. It can be seen from the dotted line B in fig. 5 that, were air from the top of the moist layer (700 mb) on the 2nd raised without entrainment, condensation would soon occur. Then, as cooling proceeded at the moist-adiabatic lapse rate, the air would arrive at 550 mb possessing the properties of the top of the moist layer on the 3rd (although containing slightly more moisture). For the 24-hr period, this gives a mean rate of ascent of about 1.5 cm/sec, which corresponds to mean convergence of only  $0.5 \times 10^{-5}$  sec<sup>-1</sup> in the layer beneath. On the other hand, one may assume warm-air advection did result in a 2C rise in temperature before lifting started. In this case, the air would have ascended as shown by dotted line C in fig. 5, and between 550 and 500 mb would have reached the same temperature as observed on the 3rd in this layer. One concludes that ascent of air above 700 mb, with or without some prior warm advection, can account for the temperature and moisture changes.

Since the air possessed no latent instability, lifting must have been continuously applied. The moist layer not only increased in depth by at least 160 mb, but penetrated 70 mb above the freezing level. It is thus possible that ice-crystal nucleation materially assisted the subsequent development of rain. The stable nature of the lifting process is reflected in the layer-type clouds and the steady rain (fig. 3). Frontal lifting cannot be postulated to explain the observed changes, because humidity tended to decrease rather than increase through the inversion located between 920 and 880 mb.

Ascending motions, as deduced in the preceding discussion, can be related to the coincidence of two factors acting to produce convergence in the lower troposphere:

1. The tropical disturbance to the south. Since mid-December, a relatively steady monsoon current had dominated south China and the northern part of the China Sea (fig. 2). This current, part of the circulation around the continental anticyclone, was of completely different origin from the mT air moving around the disturbance. Tropical air in the easterly trough never extended north of 20°N. However, the trough induced sufficient distortion in the easterly flow below 800 mb over south China appreciably to affect the weather there.

2. The trough in the westerlies. If normal distribution of convergence and divergence with respect to the trough line is assumed, high-level divergence overlaid low-level convergence as the trough approached Hong Kong. Ascent ahead of the westerly trough coincided at Hong Kong with ascent in rear of the easterly trough. Hence, moist air reached a greater depth than would have been possible had this coincidence not occurred. Although the disturbances together produced considerable rain, separately they may have given little or none. The example furnishes some insight into the means by which "superposition" brings about an increase in the depth of the moist layer, and, in many cases, an amplitude increase in the superposed disturbances.

By the 4th, weather had improved at Hong Kong. The easterly trough was no longer effective, and subsident warming behind the trough in the westerlies had rapidly depressed the top of the moist layer (fig. 4).

*Forecasting.*—Throughout the cool season, low-level flow across the China Sea has a dual character. In the north, it forms part of the circulation around the continental anticyclone; in the south, it is part of the deep easterly stream of mT air south of the subtropical ridge. In the south, weather is typically fine ahead of an easterly wave and unsettled to the rear; but in the north, particularly if a disturbance in the polar westerlies is present, weather may become unsettled some distance ahead of the trough line and worsen somewhat after its passage.

Over the China Sea, the subtropical ridge aloft seldom possesses a marked cellular structure, and storms moving westward on its southern side normally do not recurve. Should they do so, weakening is so rapid that there is little chance of their retaining destructive winds north of the ridge. Because of the generally steady movement of storms and waves, extrapolation based on previous track gives adequate results. However, storms in December or January may have their westward progress across the China Sea suddenly checked by a surge of the northeast monsoon. Movement is then slow and erratic, and filling often ensues.



#### 4. The tropical trough

In the cool season, two great airstreams dominate the upper troposphere over south and southeast Asia (Venkiteswaran, 1950; Koteswaram *et al.*, 1953). One stream, of low-latitude polar westerlies, skirts the southern rim of the Himalayas, then sweeps east-northeast across central China and Japan. The other stream appears to be equatorial in origin. It flows from the southwest or west-southwest across southern India and the Bay of Bengal, and then with little acceleration across south China and the Loochoos. The two streams converge over the northern portions of Burma, Thailand and Indo-China, and over south China. It has been suggested (Ramage, 1952) that the cool-season aridity of these countries results from compensating subsidence and low-level divergence beneath the upper convergence.

Fig. 7 for 0900 GCT 21 March 1953 typifies the normal three-dimensional distribution of temperature and wind prevailing over India and the Bay of Bengal during winter. These charts show that both contour and thickness patterns above and below 500 mb differ markedly. The trough near  $90^{\circ}\text{E}$  is in the same position as a mean trough in the low-latitude polar westerlies (Ramanathan and Ramakrishnan, 1937), which Yin (1949) considers to be a reflection of the southward bulge of the Himalayas. Since the trough has a nearly vertical axis and dies out with height, it is hard

to connect it with existence of the upper southwesterlies. The southwesterlies, at least in the Indian region, seem to be a phenomenon of the high troposphere, apparently independent of low-level temperature distribution or of surface topography. Over southern India, the lower boundary of the southwesterlies lies near 400 mb. Wind directions at that level are extremely variable (*cf.* fig. 14), alternating rapidly between southwest and directions similar to those at lower levels.

*Appearance of the tropical trough.*—An adequate explanation for the existence and maintenance of the high-tropospheric southwesterlies is lacking. However, an attempt will be made to describe their occasional abrupt breakdowns, which profoundly affect the weather of tropical southeast Asia. Breakdown occurs when a trough, which may have been stationary or have developed over the observationally blank Arabian Sea, moves eastward. Designated henceforth as a "tropical trough," its eastward movement across southern India can be traced by the change in high-level winds. Above 500 mb, there is a sharp veer from southwest to northwest. At this time the trough is too weak to have an appreciable effect either on wind or on the distribution of divergence below 500 mb, and weather remains fair. The trough continues eastward in the southwesterly stream. When it reaches the region of the orographical trough near  $90^{\circ}\text{E}$ , the two

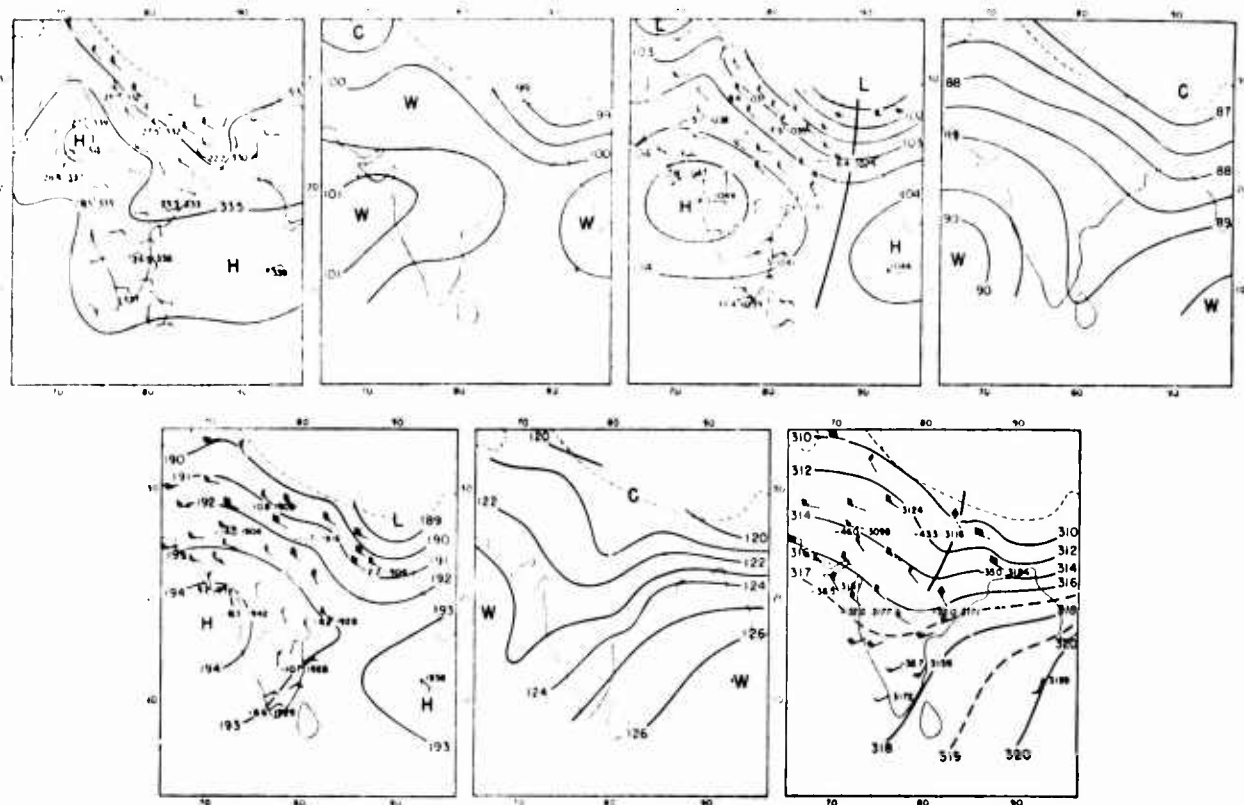


FIG. 7. Charts for 0900 GCT 21 March 1953. Top, left to right: 900-mb contours; 900- to 700-mb thickness; 700-mb contours; 700- to 500-mb thickness. Bottom, left to right: 500-mb contours; 500- to 300-mb thickness; 300-mb contours, winds at 400mb indicated by dashed arrows.

troughs seem to link. After the junction, the tropical trough is no longer confined to the relatively homogeneous southwesterlies. It receives an influx of colder air from the low-latitude polar westerlies and deepens. More important, as a result of this linkage it becomes part of the great system of westerly winds sweeping across north Africa and Arabia and to the south of the Asiatic mountain mass.

*Intensification and slowing of the trough.* As the tropical trough progresses, it usually intensifies. Ahead of the trough line, increased low-level convergence gives rain to Thailand and Indo-China. In almost all cases considered, the tropical trough intensified about two days after trough intensification in the Asia Minor-Iran region, and about one day after strengthening of the high-level ridge over India. Such a sequence of events suggests that some form of downstream energy dispersion, similar to the process outlined by Rossby (1945), might have taken place.

Once over Thailand or Indo-China, a tropical trough may remain stationary for a week or more. The reason for this may lie in the long-wave pattern of the low-latitude polar westerlies. A chart of the mean 500-mb topography for the northern hemisphere winter (Scherhag, 1948) shows a trough in the polar westerlies in the Asia Minor region, which others (Bolin, 1950; Sutcliffe, 1951) have concluded from orographical and thermal considerations is a favored location for a long-wave trough. It may be that Thailand or Indo-China lie downstream from Asia Minor at a distance which usually approximates the stationary wavelength of long-wave troughs along about latitude 20°N. Were this so, a tropical trough, once linked with the low-latitude polar westerlies over the Bay of Bengal when a long-wave trough lay across Asia Minor, would begin to slow. Recognized authorities (Haurwitz, 1940; Petterssen, 1952) disagree on the correct formula for determination of stationary wavelength in a current of finite width. Consequently, there is no point at this stage in trying to check the above conclusion by calculation.

When the tropical trough has become stationary over Thailand or Indo-China, the subtropical ridge is displaced 5 deg lat or more south of its usual position, and the polar front across the China Sea is activated. Disturbances with considerable rain areas extending to the north move east-northeast along the front, and often develop into closed surface circulations near the southern Loochoos. This activity results from the tropical trough's behavior as any deep, cold trough in the westerlies, with high-level divergence and low-level convergence east of the trough line. West of the trough line, fine weather and some surface anticyclones result from the high-level convergence and low-level divergence.

*Weakening and dissipation of the trough.*—First sign

of the eventual dissipation of the tropical trough comes with re-appearance of the upper southwesterlies over southern India. Spreading northeast, they re-establish, with the low-latitude polar westerlies, the normal pattern of high-level convergence in the region of the tropical trough. The trough weakens, and the subtropical ridge moves northward, presumably because high-level divergence east of the trough line decreases. The polar front is also displaced north, and the disturbance track then lies across south China. Coastal areas to the south experience humid, cloudy weather but little rain. The trough usually dissipates *in situ*, although it may sometimes move eastward if the low-latitude portion of an Asia Minor trough has already started east. The subtropical ridge moves north to its usual latitude, and weather returns to normal.

*Monthly variation.* This situation occurs from three to six times in a cool season, but has not been observed to develop much before mid-January. From then on, it is increasingly common, being the major rain producer for the dry belt in March and April. The monthly variation in occurrence probably results from increasingly frequent breakdowns in the upper southwesterlies to the south and west of India as the season advances. The reason for this is not known.

*Example, 21 March to 3 April 1953 (figs. 7 to 18).<sup>2</sup>*—At the start of the period, the upper southwesterlies broke down as a tropical trough moved eastward across southern India. The trough became superposed

<sup>2</sup>Over south and southeast Asia, pressure-height data are seldom sufficiently accurate or dense to enable definitive pressure-contour analyses to be made. Except for 21 March, this was true in the period of the example. Both contour and streamline analyses were made, and inconsistencies between them reduced to a minimum. The streamlines have been reproduced, since they give a more adequate idea of flow, especially south of 15°N. Data were insufficient to allow construction of charts at the 300-mb level over the whole area. The time discrepancy between the 300- and 700-mb charts is accounted for by the fact that observations over India are most frequent at 0900 GCT, but over the rest of the area between 0000 and 0300 GCT. Lack of data prevented delineation of rain areas south of 10°N and over China.

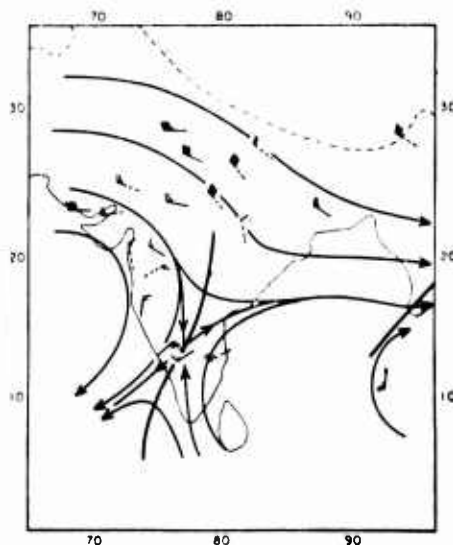


FIG. 8. 300-mb flow chart for 0900 GCT 23 March 1953.

on a disturbance in the equatorial easterlies over the Bay of Bengal. It had intensified by the time it reached Thailand, and at the same time the subtropical ridge had weakened. Over Indo-China, the tropical trough absorbed a trough which had previously retrograded near Hong Kong and soon became stationary off the Indo-China coast. East of the trough line, depressions formed on the China Sea polar front, and widespread

rain developed. The salient features of the situation are grouped under separate headings:

The upper southwesterlies. On 21 March 1953 (fig. 7, bottom right), the southwesterlies dominated southern India and the Bay of Bengal, and converged with the polar westerlies further north. The convergence zone lay above the low-level subtropical ridge. By the 23rd (fig. 8), a tropical trough had begun completely to

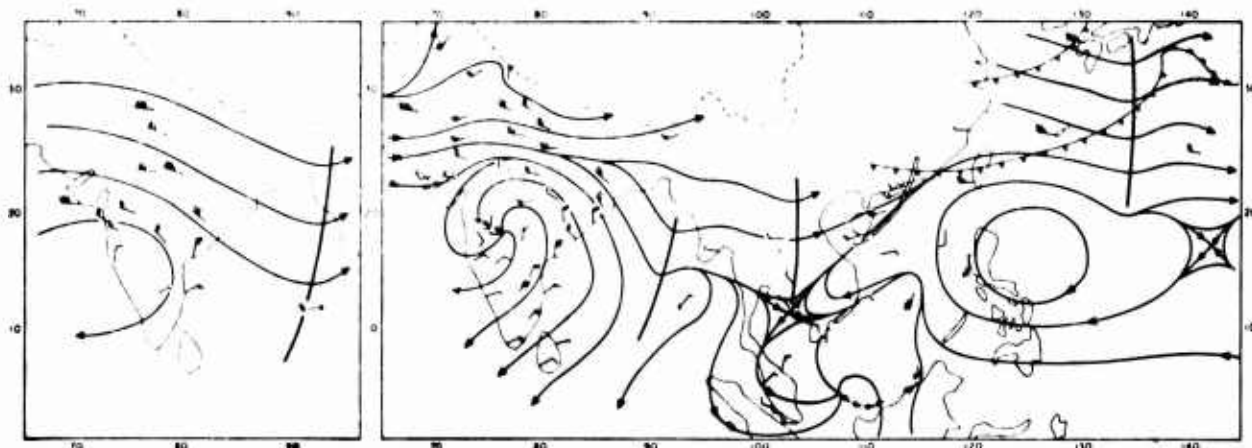


FIG. 9. Charts for 25 March 1953. Left: 300-mb flow for 0900 GCT. Right: 700-mb flow for 0000-0300 GCT. Double lines show trough positions at 300 mb, with tropical trough lying across Bay of Bengal. Dashed arrows show 48-hr movement of centers.

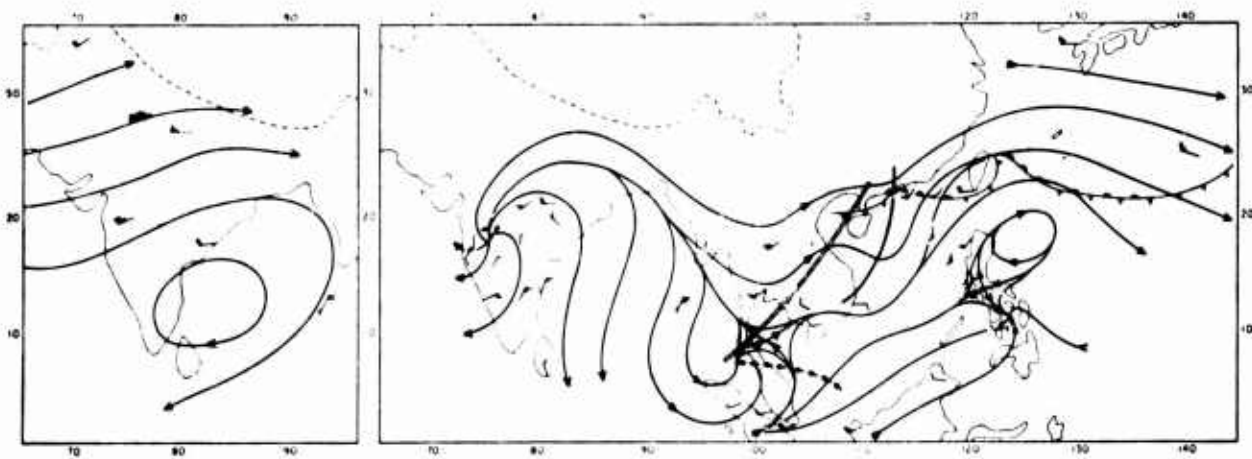


FIG. 10. Same as fig. 9, but for 27 March 1953. Tropical trough lies across Indo-China.

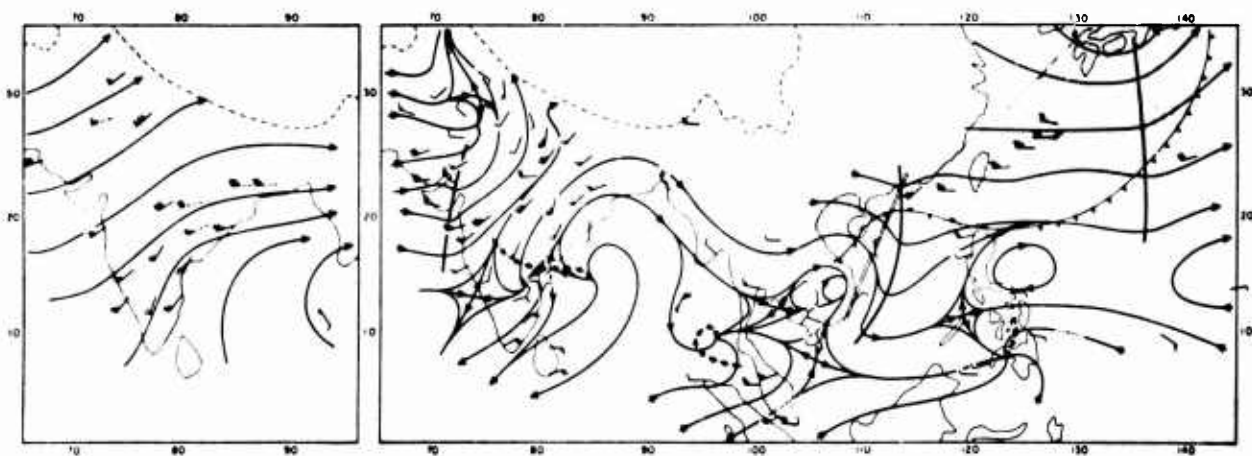


FIG. 11. Same as fig. 9, but for 29 March 1953. Tropical trough lies across western part of China Sea.

disrupt the flow, which gave way to an anticyclonic circulation west of the trough line. Not until the 29th did the southwesterlies reappear over southern India (fig. 11, left). They then extended steadily northeast, the chart for 2 April 1953 (fig. 13, left) showing them once more re-established in their usual area.

The tropical trough. The trough which moved eastward from the Arabian Sea on the 23rd (fig. 8) affected winds only above 500 mb over southern India (fig. 14). It gave rain neither over India nor at Port Blair, which it passed at 1200 GCT 25 March 1953 (fig. 15). On the 26th at Port Blair, northerly winds freshened and spread to lower levels, indicating that the trough had probably linked with the low-latitude westerlies to the north. By the 27th, extensive rain over Thailand and Indo-China (fig. 10, right), and pressure-height falls and lowering of the base of the westerlies at Saigon (fig. 16), indicated intensification of the trough. It was now moving only slowly eastward. The trough line, accompanied by a veer in wind throughout the troposphere, passed east of Hong Kong on the 27th (fig. 17).<sup>3</sup> At Saigon, its passage early on the 28th

produced a wind veer in the middle troposphere. Above 400 mb however, winds backed, then swung to east. It seems that retrogression and possible dissipation occurred in the upper troposphere there. After the 27th, the tropical trough stopped moving east and retrograded west of Hong Kong below 650 mb (fig. 17). Then it stopped again and, sloping eastward with height, lay oriented southwest-northeast from east of eastern Indo-China to the vicinity of Hong Kong. East of the trough line, the subsidence inversion disappeared. West of the trough line, there was subsidence and fine weather. At Saigon, slackening of the westerly flow (fig. 16) signified that on the 29th the trough was beginning to weaken. Weakening continued as the upper southwesterlies spread northward and the normal pattern of high-level convergence was restored (fig. 13, left). The trough finally passed east of Hong Kong on the 2nd, and weather there cleared (figs. 17 and 18).

the geostrophic advective temperature change between the 26th and 27th was computed. The temperatures so derived are incorporated in the isolines of pressure-height change in fig. 17. Since no account was taken of temperature change due to vertical motion, it is probable the trough was more sharply defined than shown.

<sup>3</sup>The radiosonde sounding at Hong Kong for 0000 GCT 27 March 1953 appears defective above 500 mb, recording improbably high temperatures (-44C at 200 mb). From the winds,

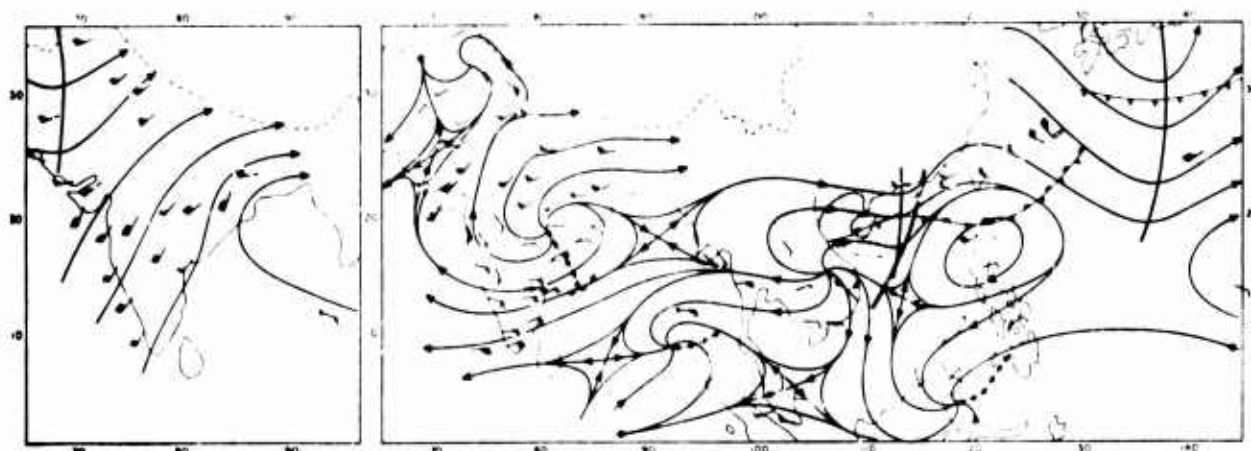


FIG. 12. Same as fig. 9, but for 31 March 1953. Tropical trough lies across western part of China Sea.

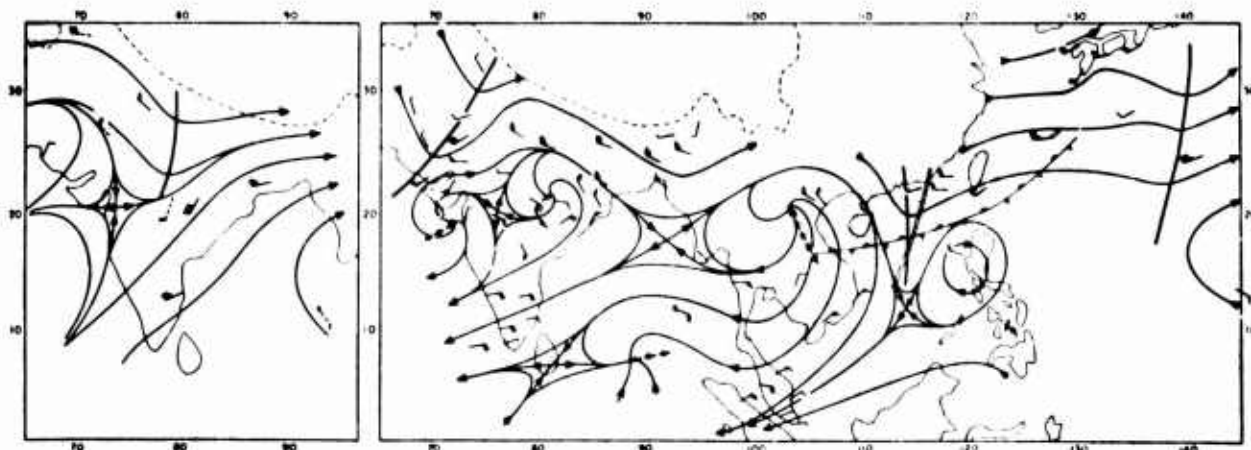


FIG. 13. Same as fig. 9, but for 2 April 1953. Tropical trough lies across central China Sea.

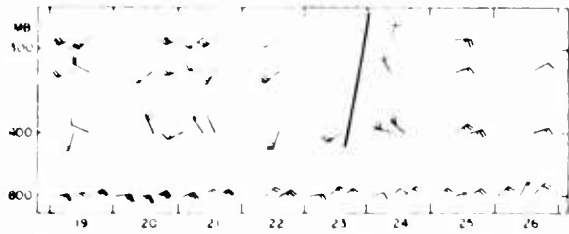


FIG. 14. Madras time-section for 19 to 26 March 1953.

Energy transmission. On the 24th, superposition of low- and middle-latitude troughs occurred along 50°E. By the 26th, the high-level ridge over northern India had built up. The following day, development of an extensive rain area east of the tropical trough line (fig. 10, right) indicated marked intensification. This sequence can be accounted for by downstream energy dispersion, resulting from trough intensification over Asia Minor due to superposition. The dispersion rate of 20 deg long per day agrees well with that calculated from the formula for 25°N (Rossby, 1945),  $c_g = u + 1.7 (L^2/360)$ , where  $c_g$  = group velocity,  $u$  = speed of basic zonal current,  $L$  = wavelength of long waves, and the distance measurement is in degrees longitude. Over western India, persistent southwesterlies at 300

mb, overlying a stationary depression (figs. 11 and 12), indicated the trough along 50°E was stationary and vigorous. On the 31st, the low-latitude portion of the western trough began moving across India (fig. 12, left). It was weakening and soon became insignificant as an energy source.

The trough in the polar westerlies. On the 21st, a weak trough in the low-latitude westerlies was moving east across northern India (fig. 7, bottom right). The southern end of the trough crossed Port Blair at about 2100 GCT 23 March 1953 (fig. 15), causing a wind shift above 500 mb but giving no rain. By the 25th, after moving eastward at about 25 kn, the trough was nearing Hong Kong. Pressure-heights there (fig. 17) first fell and then began to rise, although winds did not veer. The trough presumably had reached the zone of stable wavelength relative to the Asia Minor trough, and retrograded. It was probably absorbed later, over Indo-China, by the approaching tropical trough.

The subtropical ridge. On the 21st, the subtropical ridge at 700 mb lay along 19 to 20°N, showing negligible cellular structure. By the 25th (fig. 9, right), it had broken down into cells over India and east of the

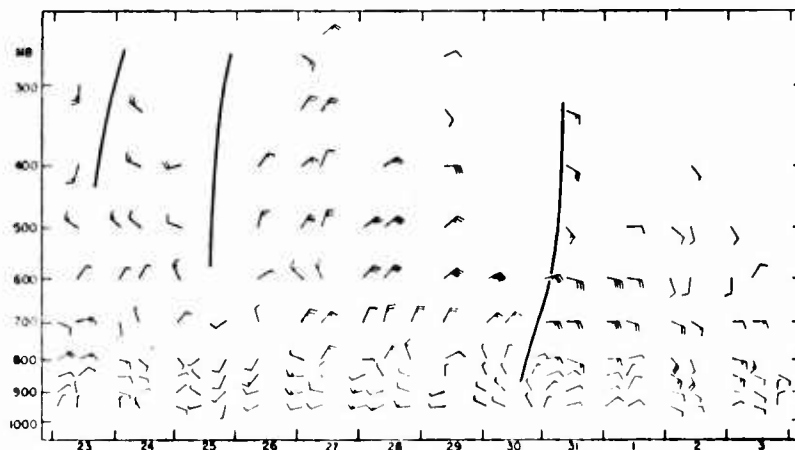


FIG. 15. Port Blair time-section for 23 March to 3 April 1953.

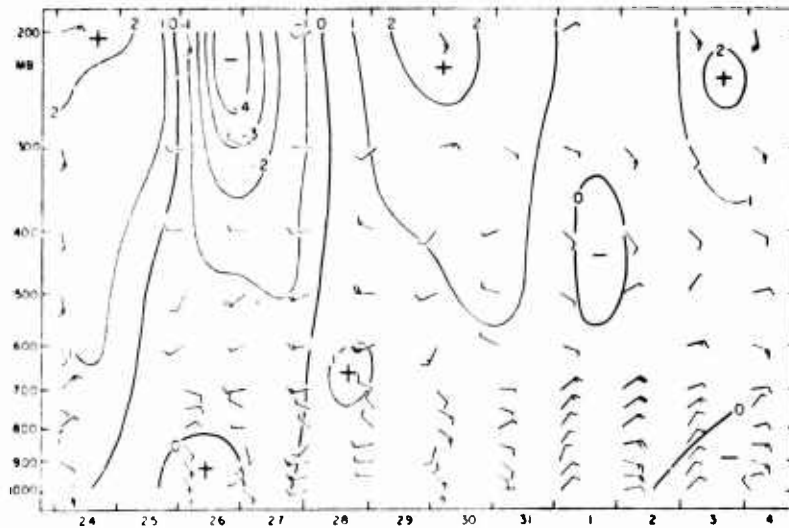


FIG. 16. Saigon time-section for 24 March to 4 April 1953.

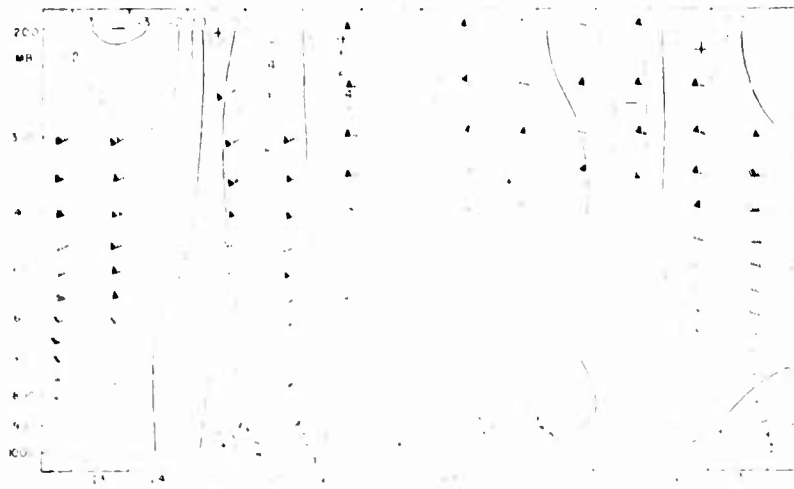


FIG. 17. Hong Kong time-section for 23 March to 4 April 1953.

Philippines. The cells moved southward and shrunk as the tropical trough intensified. First sign of recovery is found in the Saigon time-section (fig. 16). At Saigon, the pressure-height rises above 400 mb, starting on the 28th, could have been caused by weakening of the tropical trough and westward extension of a cell of the subtropical ridge. On the 29th (fig. 11, right) a third cell appeared at 700 mb over Indo-China. By the 31st (fig. 12, right) the tropical trough was no longer the dominant feature. All three cells had intensified and moved north. At the end of the series, with return of general high-level convergence, the subtropical ridge once more lay along 19 to 20° N (fig. 13, right).

The equatorial disturbance. For some days on the equatorward side of the subtropical ridge, a low-pressure area resembling an easterly wave had been moving slowly westward. On the 25th (fig. 9, right), it was centered between Borneo and Malaya. At Saigon (fig. 16), freshening and veering of the easterlies and a positive pressure-height change below 800 mb indicated the low had passed west of the station's longitude by the 26th. On the 27th (fig. 10, right),

westward progress was interrupted southeast of the Andamans. There the tropical trough, moving eastward to the north, temporarily became superposed on the low. Strengthening of the northeast winds aloft at Port Blair (fig. 15) and of the southwest winds over Malaya (figs. 10, right, and 11, right), as well as development of a rain area, are signs that superposition intensified the low between the 26th and 29th. In this case, as in the easterly-wave example, a trough in the westerlies became superposed on a disturbance in the easterlies. There was a strong east-northeast wind shear below 500 mb at Port Blair from the 27th to the 30th, indicating cold air to the southeast. Probably superposition resulted in cold air being fed into the equatorial disturbance. Then, when the tropical trough moved away eastward, an extensive pool of cold air was cut off southeast of the Andamans. On the 29th, the disturbance resumed its westward movement. The trough line crossed Port Blair between the 30th and 31st with thundershowers and a wind veer (fig. 15), while over Malaya winds decreased (fig. 12, right).

The China Sea polar front. A cold front moved southeast across China on the 24th and 25th (fig. 9,

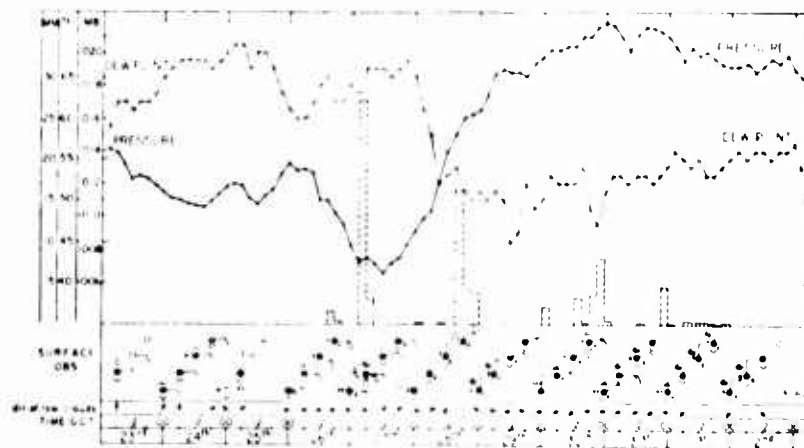


FIG. 18. Hong Kong meteorogram for 23 March to 2 April 1953. Pressure is adjusted for diurnal variation. Rainfall amounts are plotted for 3-hr intervals.

right. It had a normal passage at Hong Kong, where fair, misty weather gave way on the 25th to fresh easterlies and increased cloudiness (fig. 18). Under normal conditions, the China Sea polar front, located in a region of subsidence beneath the upper southwesterlies, is weak and inactive. In the cool air behind a fresh monsoon surge, occasional convection showers develop. Along the polar front, even when rejuvenated from the north, there is little up-slope motion or rain. This was the distribution prevailing when the tropical trough reached Indo-China. At 0600 GCT 26 March 1953, the pressure at Hong Kong began to fall, the dew point rose, and medium cloud appeared (fig. 18). The front to the south had developed a wave and was moving north, a sign that high-level divergence ahead of the approaching trough had become effective. As the wave disturbance developed (fig. 10, right) pressure continued falling at Hong Kong and rain started. The warm-front portion, preceded by a severe thunderstorm, passed over the station at 0900 GCT 27 March 1953 (fig. 18). The cold front gave little rain when it passed 12 hr later. Since at that time the station lay west of the trough line (fig. 17), high-level convergence presumably inhibited cloud development. The polar front continued active, and Hong Kong experienced three more spells of warm front rain on the 28th, 30th and 1st (fig. 18). These differed from the first spell in that the front never reached the station at the surface, the waves moving eastward to the south. The polar front was also active further east. A wave depression formed off north Formosa on the 27th (fig. 10, right) and intensified as it moved northeast. The front lapsed into quiescence after the tropical trough moved away eastward on the 2nd (fig. 17).

This example demonstrates that, although the origin of tropical troughs is unknown, they can be picked up over India, and their downstream movement and outbreak of weather can be followed. The upper southwesterlies seem to be the controlling influence; as they break down, a tropical trough appears; with their return, the trough dissipates. While a tropical trough is vigorous, it differs only in latitude from the major long-wave troughs of middle latitudes. The disturbances it initiates do not, because of the low latitude, possess the closed circulations of the northern systems, but they are potent rain producers for all that.

**Forecasting.** Premonitory signs of a tropical trough are confined to the high troposphere; an adequate 300-mb chart of the region, supplemented by time sections, is needed to detect it and follow its eastward movement. When the trough has passed east of 90°E, deepening of a trough over Asia Minor, followed by intensification of the high-level ridge over India, give about a 24-hr warning of intensification of the tropical trough.

North of the subtropical ridge, everywhere west of

the trough line, weather is brilliantly fine. East of the trough line, after the trough intensifies, rain develops in the polar-front zone. It fluctuates widely both in extent and intensity with passage of disturbances along the front. These disturbances are most readily located and tracked by their rain areas, since they may cause little distortion in the east-northeast or northeast surface flow.

Re-appearance of the upper southwesterlies over southern India presages weakening of the tropical trough. When the southwesterlies approach the polar westerlies south of the Himalayas, an increase in high-level convergence is imminent, and dissipation of the trough should be forecast.

Until World War II, Far East synoptic weather charts extended no further west than west China; subsequently, some services increased coverage to include India. Even that is not enough, for happenings in the Near East may, by means of energy dispersion, significantly modify Far Eastern weather within 48 hr.

**Acknowledgment.** The writer wishes to record his appreciation of the valuable advice and suggestions given him by Prof. H. Riehl.

#### REFERENCES

- Air Ministry, Meteorological Office, 1943: *Weather in the Indian Ocean, Land 2*. London, H.M. Stationery Off., 52 pp. and 218 pp.
- Bolin, B., 1950: On the influence of the earth's orography on the general character of the westerlies. *Tellus*, **2**, 184-195.
- Dunn, G. E., 1940: Cyclogenesis in the tropical Atlantic. *Bull. Amer. Meteor. Soc.*, **21**, 216-229.
- Haurwitz, B., 1940: Atmospheric disturbances on the rotating earth. *Trans. Amer. geophys. Union*, **21**, 262-264.
- Koteswaram, P., C. R. V. Raman, and S. Parthasarathy, 1953: The mean jet stream over India and Burma in winter. *Indian J. Meteor. Geophys.*, **4**, 111-122.
- Lopéz, M. E., 1948: A technique for detailed radiosonde analysis in the tropics. *Bull. Amer. Meteor. Soc.*, **29**, 227-236.
- Pettersen, S., 1952: On the propagation and growth of jet stream waves. *Quart. J. r. Meteor. Soc.*, **78**, 337-353.
- Ramage, C. S., 1952: Relationship of general circulation to normal weather over southern Asia and the western Pacific during the cool season. *J. Meteor.*, **9**, 403-408.
- Ramanathan, K. R., and K. P. Ramakrishnan, 1937: The general circulation of the atmosphere over India and its neighbourhood. *Mem. India Meteor. Dept.*, **26**, 189-245.
- Riehl, H., and R. J. Shafer, 1944: The recurvature of tropical storms. *J. Meteor.*, **1**, 42-54.
- Rosby, C.-G., 1945: On the propagation of frequencies and energy in certain types of oceanic and atmospheric waves. *J. Meteor.*, **2**, 187-204.
- Scherhag, R., 1948: *Wetteranalyse und Wetterprognose*. Berlin, Springer-Verlag, 424 pp.
- Sutcliffe, R. C., 1951: Mean upper contour patterns of the northern hemisphere—the thermal-synoptic viewpoint. *Quart. J. r. Meteor. Soc.*, **77**, 435-440.
- Venkiteswaran, S. P., 1950: Winds at 10 km and above over India and its neighbourhood. *Mem. India Meteor. Dept.*, **28**, 55-120.
- Yin, M. T., 1949: A synoptic-aerologic study of the onset of the summer monsoon over India and Burma. *J. Meteor.*, **6**, 393-400.

## Non-frontal Crachin and the Cool Season Clouds of the China Seas

C. S. RAMAGE

Royal Observatory, Hong Kong\*

### ABSTRACT

The *crachin* of the coastal regions of south China and northern Indochina develops during the cool season whenever relatively moist air is cooled sufficiently by contact with the cold coastal waters to lower its condensation level below the level of turbulent mixing. Inter-mensal and diurnal variation of *crachin* are discussed as well as its coincidence with low-level winds veering with height. Forecasting procedures are listed. Over the China Seas beyond the *crachin* zone, convective cloud predominates, but as sea-air temperature differences steadily decrease through the latter part of the cool season, cloud amounts also diminish.

### 1. NON-FRONTAL CRACHIN

**B**RUZON and Carton (1930) define the *crachin* of the coastal regions of northern Indochina and south China as "... a humid period of fogs and drizzle or light rain which sets in at about the time of the normal annual temperature minimum, generally toward the end of January, and interrupts the dry season. ... Then, even though temperatures rise, the *crachin* may persist into mid-April, gradually merging with the rains of the rainy season proper." *Crachin*, the most important bad weather regime of the cool season, is a low-level stratus phenomenon, most clearly marked in the arid belt between the jet stream center (28°N) and the subtropical ridge (17°N) where indeed it predominates in late winter and spring. Though there may be prolonged precipitation, the amounts recorded are small. Visibility is rapidly and seriously reduced at its onset and it constitutes the region's greatest aviation hazard. Since 1945 no fatal airline crashes in the Hong Kong area have been due to typhoons but a proportion can be attributed to *crachin*.

It has been suggested that *crachin* may develop in two ways:—(1) As the result of mixing of two nearly saturated air masses along a frontal surface. Mixing occurs only during or after passage of a cold front, and, as Pettersen (1939) points out, raises the cloud base to near the top of the cold air which is usually far from saturated. Lifting of the warm air may result in precipitation and some lowering of visibility and cloud base, but the effect is usually short-lived and weak. (2) By surface cooling of a warm moist air mass. This is almost always the cause of the worst and most persistent *crachin*.

\* This work was completed at the University of Chicago during tenure of a Commonwealth Fund Fellowship.

Either of two readily identifiable synoptic sequences may be associated with this non-frontal *crachin*. One which is most important in late winter, begins when a continental anticyclone previously consisting of polar continental air moves eastward from the mainland. Air on its eastern side follows a track across the warm waters south of Japan before swinging west to cross the cold waters along the China coast (Fig. 1). There, rapid cooling and turbulent mixing often result in *crachin* development. First, a layer of stratus forms beneath the turbulence inversion. Then, as the moisture content of the incoming air steadily increases, the stratus builds downward, drizzle sets in and eventually sea fog may

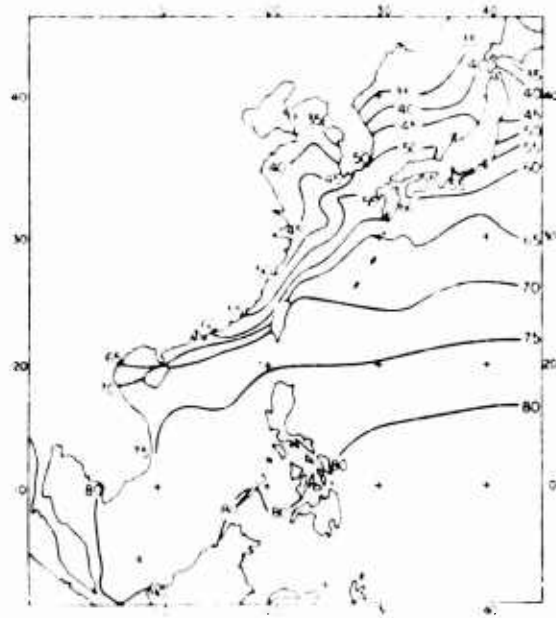


FIG. 1. Mean sea-surface temperature for February in deg. F.



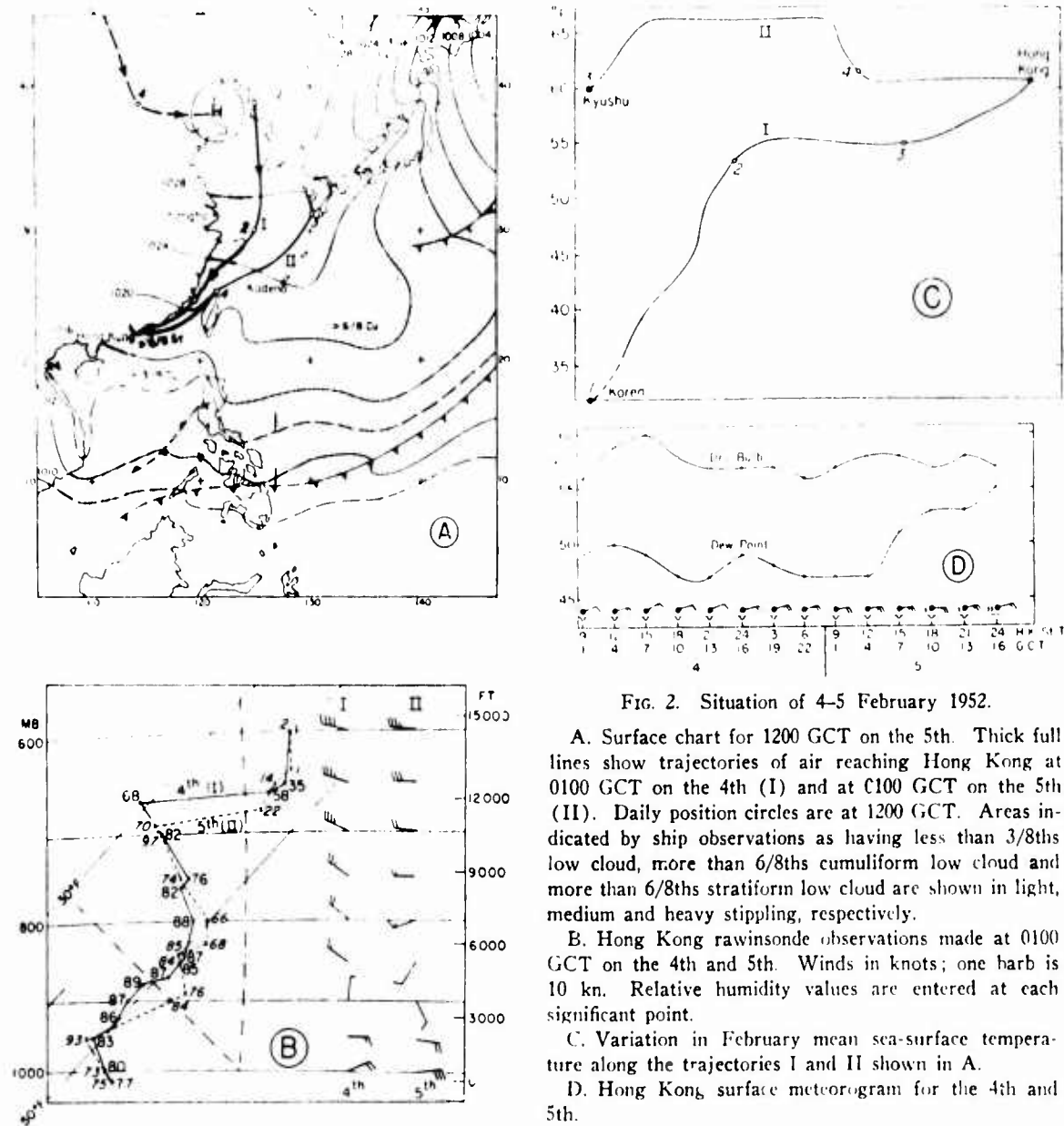


FIG. 2. Situation of 4-5 February 1952.

A. Surface chart for 1200 GCT on the 5th. Thick full lines show trajectories of air reaching Hong Kong at 0100 GCT on the 4th (I) and at 0100 GCT on the 5th (II). Daily position circles are at 1200 GCT. Areas indicated by ship observations as having less than 3/8ths low cloud, more than 6/8ths cumuliform low cloud and more than 6/8ths stratiform low cloud are shown in light, medium and heavy stippling, respectively.

B. Hong Kong rawinsonde observations made at 0100 GCT on the 4th and 5th. Winds in knots; one barb is 10 kn. Relative humidity values are entered at each significant point.

C. Variation in February mean sea-surface temperature along the trajectories I and II shown in A.

D. Hong Kong surface meteorogram for the 4th and 5th.

form. Should the anticyclone center become almost stationary to the south of Japan, intense and persistent crachin develops which can only be dispersed by a fresh surge of the monsoon. The other sequence which becomes increasingly important as spring advances, begins, when with flat pressure gradients over the mainland, a wedge of the Pacific anticyclone extends across the Philippines to China. This brings tropical maritime air to the region. Temperature contrasts between the advected air and the coastal zone are sharp and crachin often takes the form of dense sea fog. Over land, as is shown later, marked diurnal vari-

ation of crachin may occur, for when the anticyclone center lies far to the east and pressure gradients are slack, mechanical turbulence is insufficient to counteract the effect of increasing temperature during the day and the stratus cover may be temporarily dispersed.

Non-frontal crachin develops only in air which has first been strongly heated over warm seas and then cooled near the coast. As would be expected it is confined to the coastal belt of cold water (FIG. 2A) being seldom observed more than 100 miles offshore. Sverdrup (1945) and Burke (1945) have reported that air heated over the

oceans usually attains a fairly stable surface relative humidity of about 80 percent after some 500 miles of sea track, and a surface temperature but little different from the sea surface temperature. Thus, through a normal crachin period when trajectories of air reaching the coast swing progressively further southward over warmer and warmer waters, a steadily rising surface dew point is observed along the coast. At Hong Kong this rate usually amounts to about  $4F^{\circ}$  in 24 hours until the dew point approaches to within  $2F^{\circ}$  of the sea temperature. This and the fact that the dew point varies little as the air crosses the coastal waters indicates that no significant condensation occurs at the surface until the fog point is reached. Since at the same time the dry-bulb temperature reacts rapidly, falling to within a degree or two of the sea temperature, the condensation level drops, reaching the level of turbulent mixing, and crachin forms.

An example demonstrating the speed with which a synoptic situation may become favorable to crachin development is illustrated in FIGURE 2. It includes (A) the surface isobaric chart for 1200 GCT 5 February 1952, on which are shown 24-hr positions of the anticyclone center, areas of cumuliform and stratiform clouds over the sea, and the trajectories of surface air reaching Hong Kong at approximately 0100 GCT 4 February (I) and 0100 GCT 5 February (II) (based on winds observed by ships). The trajectories are timed to coincide with rawinsonde observations made at that station, results for the 4th and 5th being shown in B. In C the variation in February mean sea surface temperature along the trajectories is shown and in D the Hong Kong surface meteorogram for the 4th and 5th is plotted. (Hong Kong, situated in the middle of the crachin zone, is reckoned to be a representative station.)

By 1200 GCT 2 February, a southeastward moving cold front had crossed China and the China Seas which were dominated by a vigorous anticyclone centered near Lake Baikal. A strong monsoon was blowing along the coast. The front and the anticyclone continued southeast, the latter at 1200 GCT 4 February being centered over north China. Although ceilings at Hong Kong were relatively high at first, the air reaching there by 0100 GCT on the 4th had travelled across an increasingly warmer sea surface, relative humidities were in the eighties and there was considerable cloud. By 0100 GCT on the 5th air reaching Hong Kong possessed a different trajectory from the previous day, having first crossed the western section of the warm Kuroshio current and then

the colder waters.<sup>1</sup> This change is reflected in the Hong Kong soundings by warmer air below the subsidence inversion (700 mb) and moisture concentration below a turbulence inversion at 950 mb. As the anticyclone continued to move east conditions along the coast became more and more favorable for crachin development, drizzle setting in at Hong Kong at 0800 GCT on the 5th. By 1200 GCT on the 5th the center of the anticyclone had moved east to the Shantung peninsula with a wedge extending southeast toward the Marianas, and stratiform cloud covered Chinese coastal waters.

Simultaneous observations during aircraft meteorological ascents at Hong Kong place the upper limit of low-level turbulence at nearly the same height as the top of crachin cloud, and seldom above 4000 feet. Thus crachin has little direct connection with the persistent subsidence inversion observed throughout the cool season (Ramage, 1952), for on fewer than 14 percent of occasions does the latter drop below 5000 feet. It is usually found between 7000 and 14,000 feet and the layer beneath it and above the turbulence inversion is mostly free of cloud (see for example FIG. 2B).

*Seasonal Variation.*--Prior to 1947, detailed low-cloud observations were not made in Hong Kong. However, since drizzle almost always and fog frequently, are features of crachin, their variations are typical of crachin variations. In November, drizzle is observed on an average during 7 percent of all hourly intervals (TABLE I) and in March during 17 percent of the intervals. Similarly, on an average, fog is recorded some time during the day on 3 percent of November days but on no less than 28 percent of March days. In FIGURE 3 are plotted 5-day mean frequencies of sea temperature higher than air temperature as observed at Waglan Island, a tiny precipitous rock

TABLE I. DRIZZLE AND FOG FREQUENCY THROUGH THE COOL SEASON AT HONG KONG

Month	Nov.	Dec.	Jan.	Feb.	Mar.	Apr.
Mean percentage of hours with drizzle in each month (26 years)	7	8	10	15	17	17
Mean percentage of days with fog in each month (60 years)	3	7	13	18	28	25

<sup>1</sup> The available observations for this period indicated that the actual distribution of sea surface temperature did not differ significantly from the mean February values.

just off the Hong Kong coast (Fig. 4). One concludes that a connection exists between the increasing crachin frequency from January onward and the predominance of occasions of sea temperature below air temperature.

Since the Siberian high and the Aleutian low dominate cool season synoptic patterns, it was thought shifts in their mean monthly positions might provide a clue to this variation in crachin, but these have relatively little effect, for not only are they slight from month to month but the positions and intensities of the two centers of action are almost identical in November which has a minimum of crachin and in March which has a maximum. Analyses of variations in mean monthly storm frequencies and tracks gave similarly negative results, but on the other hand the steady westward extension of the Pacific anticyclone after February contributes to the spring increase in crachin. On a monthly basis no very



FIG. 3. 5-day mean frequencies of sea temperature higher than air temperature at Waglan Island (1947-52) at 05h and 14h Hong Kong Standard Time (GCT + 8). Air temperatures obtained by adding  $1F^{\circ}$  to the screen temperature to compensate for the 200 foot difference in height between the screen and the sea surface.

definite link between large-scale anomalies in the positions of the main centers of pressure and crachin frequency is noticeable, probably because the range of locations of the centers corresponding to crachin along the China coast is so large as to be impossible to connect with monthly anomalies.

Any adequate explanation of the inter-mensual variation must take into account two important factors. The winter monsoon established in October with its strong persistent north or northeast winds along the China coast induces a corresponding surface ocean current which flows steadily until February, transporting water from Shanghai to Hong Kong in about two months. Though the current weakens in February and by April is almost non-existent, no significant current develops in the reverse direction and the cold water brought south earlier in the season tends to remain there. The other factor, and this is probably more important in the Gulf of Tonkin,

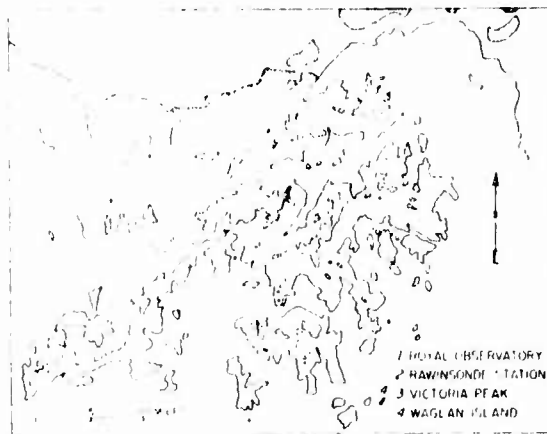


FIG. 4. Map of Hong Kong showing places mentioned in the text. Levels above 1000 feet stippled.

is the ocean's great heat capacity which causes the sea surface to possess a marked temperature lag relative to the lower atmosphere. The factors combine to the following effect. Till the end of January steadily colder monsoon bursts sweep across the area. Coastal waters cool but with a lag of almost a month. During this period surface layers of the atmosphere are usually cooler than the sea, convection develops, mixing takes place up to the subsidence inversion and low ceilings are rare. From the end of January onward, though air temperatures rise, the coastal seas cool still further before beginning slowly to warm near the end of February. As the winter monsoon weakens, the sea is more often colder than the air and crachin development is favored. In FIGURE 5 are plotted the variations of mean sea surface temperature along the same path (II of FIG. 2A) for November and March. It can be seen that identical synoptic situations in autumn and spring could produce very different coastal weather.

*Diurnal Variation.*—In the Hong Kong observations once again variation of drizzle was considered typical of crachin variation. Royal Observatory mean hourly drizzle frequencies for

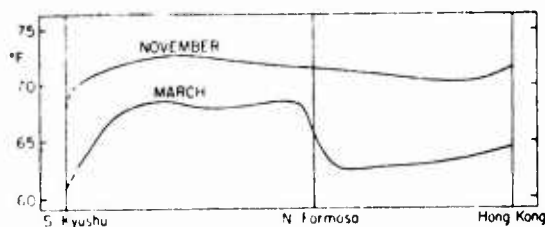


FIG. 5. Variations in March and November mean sea-surface temperatures along a path from southern Kyushu via northern Formosa to Hong Kong.

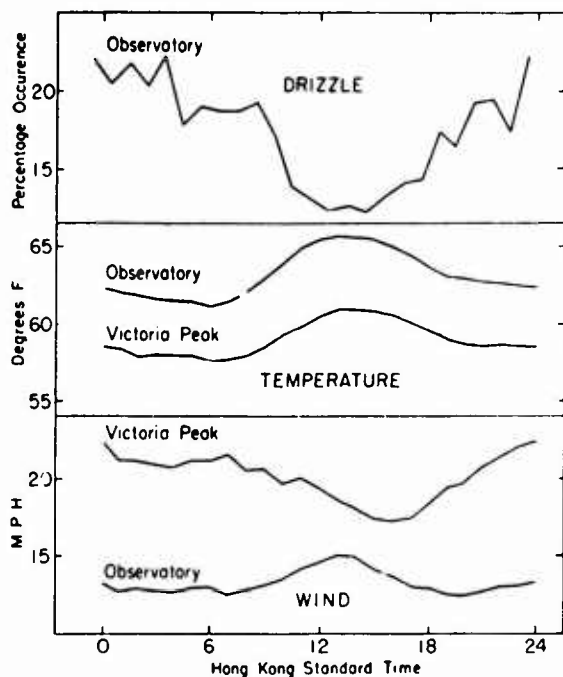


FIG. 6. Mean hourly values for March of Royal-Observatory drizzle frequency, screen temperature, and wind speed, and of Victoria Peak screen temperature and wind speed.

March, the most active crachin month are plotted in FIGURE 6 as well as means of screen temperature and wind speed for both the Observatory (100 feet above MSL) and Victoria Peak (1800 feet above MSL) (see FIG. 4). Drizzle occurs least often in the afternoon at around the temperature maximum, but although the temperature minimum is not reached until dawn, maximum drizzle frequency is reached by midnight. This is not inconsistent, for the Victoria Peak winds show that in the cloud layer itself, turbulence may also be at a maximum at midnight. Unevenness of the curve between midnight and dawn may be due to intermittent development of a land breeze with perhaps increased convection within the cloud also contributing. It is probable a sea-breeze effect also exists but the extremely uneven coastline has prevented its evaluation.

Investigation of numerous cases, besides confirming the representativeness of the mean curves, showed also that a cloud-base height curve would closely parallel the drizzle-frequency curve. Rapid clearances took place when the general wind-flow began to slacken before the temperature maximum was reached, for then the trends of mechanical turbulence and temperature both favored a decrease in cloud.

III-163

A marked diurnal variation of fog occurrence at Waglan Island with a maximum around dawn and a minimum in late afternoon, just over land, is reported by Hung (1951).

*Crachin Forecasting.*—Four years' rawin soundings made at Hong Kong showed crachin confined to those days with net veer of winds between 3000 and 7000 feet, while 6 to 8/8ths low cloud base 3000 feet or lower was observed seven times as often with veering as with backing winds. In addition, veering winds are usually associated with occasions of sea temperature lower than air temperature at Waglan Island (FIG. 7). Since crachin is usually observed on the western side of a shallow high or on the eastern side of a shallow trough, veering winds would be expected to accompany the phenomenon (FIG. 2).

At well-equipped meteorological centers, development of a crachin situation can best be forecast by the use of prognostic trajectories which depend on the accuracy and frequency of surface analyses. The insignificance of short period changes in sea temperature, stability of the dew point until near saturation is reached and the probability that air over the warm waters closely approximates the convective model, make the method a practical one. Forecasting dissipation is a matter of timing the next cold front passage.

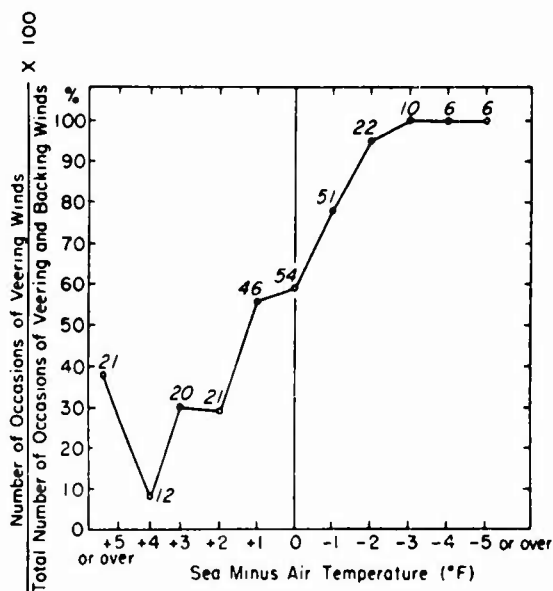


FIG. 7. Frequency of veering winds from 3000 to 7000 feet at the Hong Kong rawinsonde station as a function of sea-air temperature difference observed at Waglan Island (1949-53 cool seasons). Number of observations in each interval shown in italics.

For local forecasts, local parameters must be determined. The stable turbulent nature of the phenomenon renders it sensitive to orographic and thermal influences and in any hilly region, widely different conditions may prevail only a few miles apart. Statistical studies often provide useful information on these variations. Again, the fact of coincidence of crachin with low level veering winds may be used and to this end careful observations of cloud movement should be made at regular intervals.

On ships at sea equipped with monthly mean sea surface temperature charts, effective short-period forecasts should be possible, using these charts in conjunction with sea temperature, dry-bulb and dew-point observations. As long as sea temperature remains higher than dry-bulb temperature the risk of operationally bad weather from crachin is slight. Even without instruments some assessment of probable conditions can be made. Woodcock (1940) from observations over the North Atlantic of the flight response of herring gulls, reports that *no* continuous free soaring was observed when the sea surface temperature was lower than the air temperature or when the surface wind exceeded 25 knots. Birds accompanying a moving ship alternate between wing-flapping flight and resting on the water. He concludes soaring flight is only possible when convection produced by surface heating occurs. Considerable use can be made of these facts by mariners in the crachin zone. As long as sea birds are soaring, crachin is unlikely to be encountered for some hours but if the birds are not soaring and the ship is heading toward colder waters, crachin is likely.

## 2. COOL SEASON CLOUDS OF THE CHINA SEAS

Throughout this section, "along the coast" is taken to include the coast and a 100 miles wide strip of coastal waters extending from the region of Shanghai to the southern part of the Gulf of Tonkin, i.e., the crachin zone; while the term "at sea" embraces the remainder of the China Seas south of 30° N.

Over this second area, although sea temperatures do fall slowly as the season advances, they are never more than 1 to 2°F below air temperatures, and for much of the time, when the sea is in contact with polar air, are considerably higher.

Values of monthly mean cloud amounts at 1° latitude and longitude intersections for 1911 to 1935 are published by the Imperial Marine Observatory, Kobe (1937). Though no differentiation is made between low, middle and high clouds,

the observations are probably representative of low clouds, which predominate in these parts during the cool season. FIGURE 8 shows the change in mean amounts from December to March. There is little change along the warm Kuroshio current, positive change *along the coast* and negative change elsewhere. Clouds *at sea* are convective throughout the cool season but amounts are greater when sea-air temperature differences are greater, that is during the early part of the season or with vigorous polar outbreaks. As Sverdrup (1945) points out, where the temperature difference is small, clear skies are often observed. Only *along the coast* do the relatively lower spring sea temperatures result in more cloud, for the reasons already given.

During the crachin season, an air mass moving from the northeast quadrant is warmed *at sea* and cooled *along the coast*. One would expect the seaward limits of crachin to be sharply defined and this is confirmed by observation. Quoting from *Weather in the China Seas* (Meteorological Office, 1937), "This dividing line is often quite well marked and the state of the sky as observed on board a vessel proceeding northward in the China Sea frequently changes from perhaps less than half clouded to completely overcast in the space of a few hours when the vessel reaches a position near the 20th parallel."

*Summary of Month to Month Changes.*—In *November* at the beginning of the cool season the Siberian high is established and frequent surges of the winter monsoon pass over sea surfaces with

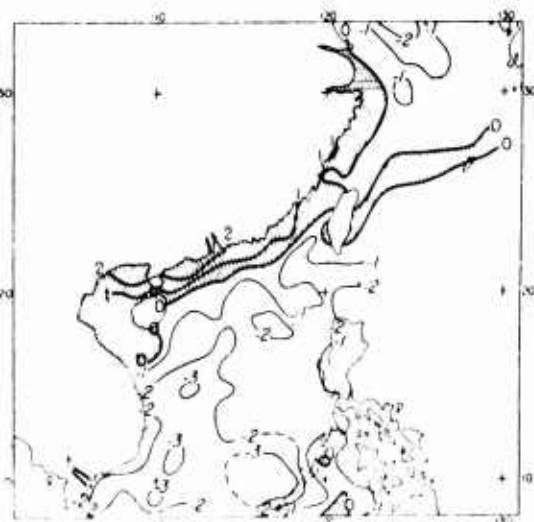


FIG. 8. Difference (March minus December) between the mean cloud amounts of spring and early winter over the China Seas (1911-35). Isolines in tenths.

temperatures rather characteristic of late summer. Heating from below is a maximum and turbulence inversions are rare. *Along the coast* polar continental outbreaks give clear skies and even modified polar continental air has little cloud. *At sea* vigorous convection and rapid addition of moisture to the air make the month a cloudy and showery one.

In *December* the Siberian high and the Aleutian low intensify and move toward each other. Frequency of polar continental outbreaks increases *along the coast* but a tendency to reduced cloudiness is counterbalanced to some extent, because with sea temperatures falling, modified polar continental air is somewhat cloudier than in the previous month. *At sea* there is little change.

In *January* the main centers of action occupy the same positions as in the previous month. *Along the coast* polar continental air is usually cloudless but with temperatures continuing to fall, turbulence cloud may form in modified polar continental air. *At sea* although the surface is still warmer than the air, the difference is not so great and hence convective addition of moisture, and cloudiness are less than in December.

In *February* the Siberian high is rather weaker and the Aleutian low further east. *Along the coast* the sea is slightly colder than in January and with reduction in the number of polar continental outbreaks and an increase in the frequency of modified polar continental incursions, crachin becomes the dominant weather type. *At sea* convective addition of moisture and hence cloudiness further decrease.

In *March* the Siberian high and the Aleutian low, still weaker, are moving further apart, while the center of the Pacific high, almost stationary since November, moves west. Thus *along the coast* not only is polar maritime air often observed but tropical maritime air also appears and the crachin intensifies. *At sea* cloud continues to decrease.

In *April* the Siberian high and the Aleutian low continue to weaken and move apart while the Pacific high continues to move west. *Along the coast*, although tropical maritime air frequently appears, conditions are not much different from March, for the increased power of the sun more often "burns off" the crachin than in the previous month. *At sea* cloudiness reaches a minimum.

### 3. CONCLUSIONS

1. Non-frontal crachin develops over the coastal areas of China and northern Indochina when rela-

tively warm moist air is advected and cooled sufficiently by contact with the surface to lower its condensation level below the level of turbulent mixing. This occurs when these areas lie under the south or southwest section of an anticyclone moving eastward to the north, or under a wedge which has extended westward from the Pacific anticyclone.

2. Favorable conditions for crachin development occur most often in late winter and spring, for during this period the cold coastal waters are warming much more slowly than the atmosphere, and the contrast between the two intensifies.

3. Over rugged coastal terrain, diurnal variation of crachin is affected by the fact that maximum turbulence at cloud level may occur around midnight and this coincides with the crachin maximum. There is a normal afternoon minimum. Over coastal waters a diurnal variation also exists with a maximum around dawn and a minimum in late afternoon.

4. The coincidence of crachin with veering winds between the subsidence inversion and the turbulence inversion can be accounted for by the fact that crachin usually occurs west of a shallow high or east of a shallow trough. If trajectories can be forecast, there is a good chance of forecasting development of a crachin situation. Local topographical and thermal influences and wind shear must also be considered, while the relationship among sea surface, dry-bulb and dew-point temperatures and even the behavior of sea birds help in making short-range crachin forecasts at sea.

5. Reports such as that of Carson (1950) confirm the belief that winter-time stratus of the lower Atlantic coast and the Gulf coast of the United States is formed by much the same processes as non-frontal crachin and any warm-front theory of its origin seems to be unjustified.

6. Over the China Seas two distinct cool-season cloud regimes can be recognized. The crachin zone has a minimum of cloud in early winter and a maximum in spring but over the remainder of the region where sea temperatures are usually higher than air temperatures, convection cloud predominates, and since the temperature contrast is greatest in early winter, cloudiness gradually decreases throughout the season.

### ACKNOWLEDGMENT

The writer wishes to record his appreciation of the advice and suggestions given him by Pro-

fessor H. Riehl, and Mr. G. S. P. Heywood, Director of the Royal Observatory, Hong Kong.

## REFERENCES

- Air Ministry, Meteorological Office, 1937: *Weather in the China Seas and in the western part of the North Pacific Ocean. II. Local information.* London, H. M. Stationery Office, 771 pp.
- Bruzon, E., and P. Carton, 1930: *Le climat de l'Indochine et les typhons de la mer de Chine.* Hanoi, Imprimerie d'Extrême-Orient, 310 pp.
- Burke, C. J., 1945: "Transformation of polar continental air to polar maritime air." *J. Meteor.*, 2: 94-112.
- Carson, R. B., 1950: "The Gulf Stream front: a cause of stratus on the lower Atlantic coast." *Mon. Wea. Rev.*, 78: 91-101.
- Hung, K. R., 1951: "Fogs at Waglan Island and their relationship to fogs in Hong Kong harbour." *Tech. Note Roy. Obs., Hong Kong No. 3*, 8 pp.
- Imperial Marine Observatory, Kobe, 1937: *The mean atmospheric pressure, cloudiness and sea surface temperature of the North Pacific Ocean and the neighbouring seas, 1911-1935.* 197 pp.
- Petterssen, S., 1939: "Some aspects of formation and dissipation of fog." *Geofys. Pub.*, 12: 10. 22 pp.
- Ramage, C. S., 1952: "Relationship of general circulation to normal weather over southern Asia and the western Pacific during the cool season." *J. Meteor.*, 9: 403-408.
- Sverdrup, H. U., 1945: "Oceanography." In: *Handb. of Meteor.*, pp. 14, 1029-1056.
- Woodcock, A. H., 1940: "Convection and soaring over the open sea." *J. Mar. Res.*, 3: 248-253.

## Variation of Rainfall Over South China Through the Wet Season

C. S. RAMAGE

Royal Observatory, Hong Kong

### ABSTRACT

Five-day means show that over south China there are certain persistent variations in the march of rainfall during the wet season (March-September). These are explained in terms of seasonal meteorological trends in the surrounding regions. The view is advanced, supported by an ancient Chinese farmers' calendar, that the rainfall pattern of south China has changed little in the past 2000 years.

### INTRODUCTION

**I**N a recent paper (Ramage, 1951), mention was made of a significant secondary minimum in Hong Kong rainfall. This usually occurs between 4 and 15 July and is revealed in the 5-day means for 60 years. The mean rainfall for the interval 10 to 14 July is 35.5 mm as compared with 70.0 mm for 30 June to 4 July and 88.5 mm for 15 to 19 July. This apparent anomaly in the middle of the wet season marks the transition between two different types of rain situation. The first, designated the "Bai-U stream," predominates during May and June when slow-moving depressions in the area bounded by Korea, the Ryukyus, the Bonins and north Honshu initiate convergence lines or surges in the prevailing upper southwesterlies of south China. The second type is associated with a maximum frequency of tropical storms in the region of south China and lasts from mid-July to the end of September.

The purpose of the present paper is (1) to discover whether this secondary minimum occurs elsewhere in south China, (2) to attempt a general explanation of the normal march of rainfall over south China during the wet season, using 5-day mean values, and (3) to make some inferences on the secular stability of the present rainfall pattern.

### DATA

Five-day means of rainfall were extracted for the following places (length of record in parenthesis): Hong Kong (60 years), Tainan, Kosyun and Hokoto (22 years), Swatow, Canton, Lungchow and Fort Bayard (15 years), and Wuchow (5 years) (see Fig. 1). To reduce or eliminate minor deviations, the values were smoothed by an overlapping method using the formula  $(A + B + C)/3 = B'$ , where the letters represent the precipitation for successive 5-day inter-

vals,  $B$  being the amount for the middle interval and  $A$  and  $C$  the amounts for the intervals next preceding and following. Values of  $B'$  for Tainan (typical of south Formosa), Hong Kong (typical

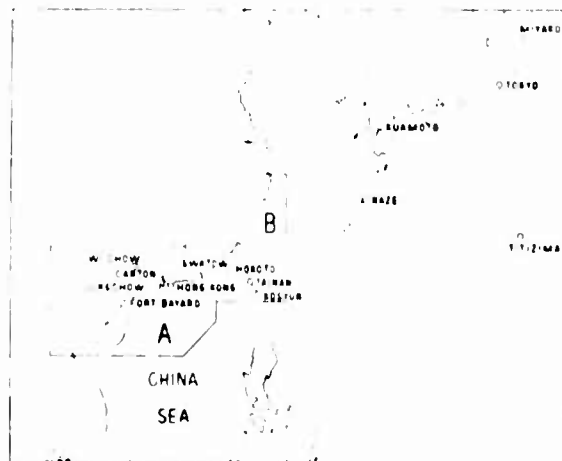


FIG. 1. General map of area showing places mentioned. Tropical storms centered in Area A usually give rain to south China. Tropical storms centered in Area B usually give rain to south Formosa.

of eastern south China) and Lungchow (typical of western south China) as well as the mean curve for all nine stations are plotted in FIGURE 2B.

Using 50 years of storm tracks showing daily positions of centers (Starbuck, 1951), the number of occasions in each 5-day interval on which storms were in a position likely to give rain either over south China (Area A, FIG. 1) or south Formosa (Area B, FIG. 1) was determined, the values smoothed and then plotted in FIGURE 2B.

Plotted in FIGURE 2A are the means of 5-day mean pressures and rainfall for five stations in the Bai-U stream initiating region—Naze, Kuamoto, Tokyo, Miyako and Titizima.

The times recommended by the ancient Chinese farming calendar, Loong Lik, as suitable for sow-



ing, planting out and harvesting of the two rice crops of south China are entered against the appropriate dates on FIGURE 2B.

DISCUSSION

(1) A secondary summer minimum of rainfall occurs throughout south China, being even more

marked in other places than in Hong Kong. It sets in earlier in the west than in the east but ends at much the same time everywhere. When one considers the differing length of records and the considerable smoothing it seems certain that the inter-annual variation in the occurrence of this dry spell must be slight.

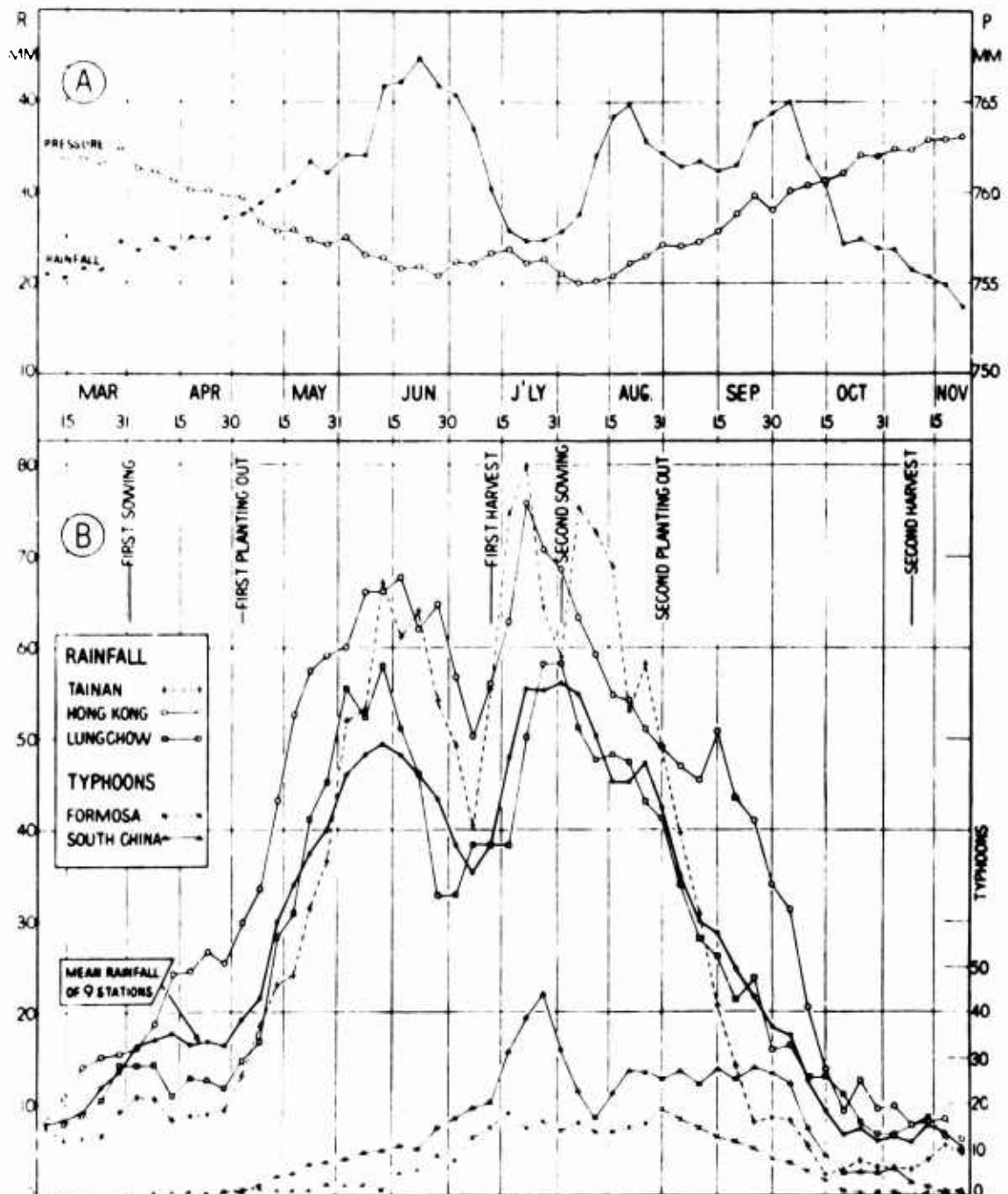


FIG. 2. (A) Mean curves of 5 day mean pressures and rainfall for Naze, Kuamoto, Tokyo, Miyako, and Titizima. (B) Smoothed curves of 5-day mean rainfall and tropical storm frequencies for south China.

(2) The wet season may be conveniently divided into the following five periods, each corresponding to a certain normal distribution of weather and pressure over southeast Asia and the western Pacific.

*First period. March and April. The dying winter monsoon.* Only at this time of the year is most of the rain of truly frontal origin, usually falling during surges of the monsoon. Early in the period, polar air replaces air of the same origin which has been modified to a slightly greater extent by a longer sea track. As the season advances and the seas to the east and south warm rapidly, air uplifted along a frontal surface is scarcely distinguishable from tropical maritime air and thus thunderstorms are more frequent and rainfall increases steadily. Since the predominant low-level flow is E or ESE, the Formosan stations are much more sheltered than those of south China and show no comparable increase.

*Second period. May and June.—The Bai-U stream.* In late April the winter high is retreating northward, frontal activity diminishes and there is a temporary drop in rainfall. This is often of some magnitude but as it varies in time from year to year, the mean curves are little affected.

In early May the summer heat-low begins to develop over south and southwest China where air mass discontinuities decrease and become insignificant. A wedge from the Pacific anticyclone extends to the China Sea and in conjunction with the heat-low circulation maintains a broad deep southwesterly flow over south China.

Temperature gradients to the north are highly favorable to cyclogenesis. Depressions cross the Eastern Sea and Japan and if one of these shows up or becomes stationary and the Pacific wedge retreats eastward, zones of convergence develop in a broad low-pressure trough in the southwesterly stream and move upstream, accompanied by heavy rain. These disturbances are usually upper level, and only rarely do corresponding surface circulations comprising more than a single isobar appear. As summer advances, pressure and rainfall at the Japanese stations reflect growing depression activity in the north. This coupled with more available moisture results in steadily increasing rainfall over south China.

Tropical storms make their appearance but are, in general, ill-developed and contribute little to the total rainfall.

*Third period. Late June and the first half of July.—The mid summer dry spell.* With the advance of the sun the Pacific anticyclone has been

moving north and, interrupting the Bai-U stream, soon dominates Japan and the seas to the south where pressure rises and rainfall decreases. Depressions are forced to the north and there is a sudden and significant decrease in rain over south China. Relative to the rest of south China, rainfall in the west begins to decrease about a fortnight early. The west is directly influenced by the summer heat low which by mid June has developed sufficiently to induce a semi-permanent anticyclone aloft. Thus, over this area, surges in the upper southwesterlies may be prevented from developing or be deflected.

Although the number of tropical storms continues to increase, they by no means make up the rainfall deficiency, for their importance as producers of early summer rain is small relative to the Bai-U stream.

*Fourth period. Mid-July to early October.—The typhoon season.* The pressure systems continue advancing north, with the zone of maximum typhoon frequency (called by some the Intertropical Convergence) reaching south China at the beginning of the period. Not only does the number of tropical storms increase rapidly, but a high proportion are major typhoons which have formed over the Carolines. Earlier in the summer such storms usually recurve before reaching the China Sea, now they travel WNW to the China coast. Thus rainfall usually reaches a maximum in the second half of July.

The intertropical convergence continues northward, and in early August pressure in the Japanese area reaches its lowest point and a secondary rainfall maximum occurs. Over south China a secondary storm minimum and a sharp decrease in rainfall occur.

The intertropical convergence shortly begins to follow the sun equatorward and moving across south China in late August is accompanied by a secondary tropical storm maximum. This is reflected by the rainfall but rather less than might have been expected. By this time the heat low of southwest China has almost disappeared and tropical storms as they approach the China coast tend to initiate surface surges of cool dry polar-continental air which on entering a storm circulation invariably causes the rain to diminish.

*Fifth period. Early October to end of November.—The winter monsoon.* High pressure is now established over China and the dry NE monsoon blows with great persistence along the China coast. Tropical storms take a much more southerly track across the China Sea and rainfall decreases abruptly. Typhoons forming in the Carolines

once more recurve rapidly and passing across the Japanese area account for the secondary minimum of pressure and secondary maximum of rainfall observed there.

(5) Tradition has it that in 2254 B.C., the Chinese Emperor Yao gave orders to his astronomers to establish the solstices and equinoxes and so instruct farmers on the most favorable times for agricultural operations. In about 200 B.C. south China was conquered by the Ch'in dynasty and for the first time was made part of a united China. The existing farmers' calendar was applied to this region, and, apart from corrections of minor errors made in the 17th century to bring it into line with more accurate Western astronomical tables, has not been changed since. Its close agreement with the rainfall curves, especially the coincidence of the first harvest with the end of the mid-summer dry spell, suggests that in historical times over south China, little change has taken place not only in the march of rainfall in the growing season but also in the amount, for much variation from present values would make the growing of two crops of rice a year most difficult.

This deduction apparently contradicts Chu (1926) and Brooks (1949), who quotes Chu's figures for the dry and wet periods of China since

600 A.D. as paralleling major fluctuations in western Asia. However, since 74% of the droughts and 75% of the floods listed by Chu occurred in provinces north of the Yangtze River and observations from south China were almost non-existent, his conclusions cannot be considered valid for this region.

#### ACKNOWLEDGMENTS

The writer wishes to record his appreciation of the helpful advice given him by Mr. G. S. P. Heewood, Director of the Royal Observatory. He is also indebted to Col. V. R. Burkhardt and Mr. K. R. Hung for supplying information on the Chinese farmers' calendar.

#### REFERENCES

- Brooks, C. E. P., 1949: *Climate through the Ages*. London, Ernest Benn, 395 pp.
- Chu, Co-Ching, 1926: Climate pulsations during historic time in China. *Geogr. Rev.*, 16: 274-282.
- Ramage, C. S., 1951: Analysis and forecasting of summer weather over and in the neighborhood of south China. *J. Meteor.*, 8: 289-299.
- Starbuck, L., 1951: A statistical survey of typhoons and tropical depressions in the western Pacific and China Sea area from observations and tracks recorded at the Royal Observatory, Hong Kong, from 1884 to 1947. *Tech. Mem. Roy. Obs., Hong Kong*, No. 4, 10 pp.

## DIURNAL VARIATION OF SUMMER RAINFALL OVER EAST CHINA, KOREA AND JAPAN

By C. S. Ramage

Royal Observatory, Hong Kong

(Original manuscript received 11 July 1951; revised manuscript received 7 January 1952)

### ABSTRACT

Over east China, Korea and Japan, diurnal variation of rainfall during the summer months of May to August is analyzed. This region is dominated by the monsoon and is found to have a morning maximum with, if the location is favorable, an afternoon maximum as well.

The limited vertical extent of the monsoon circulation, as well as lack of turbulence, favors the advection of warm air at low levels between midnight and sunrise. This causes wide-spread over turning, convective clouds develop, radiation from the tops assists the process, and a morning rainfall maximum results. This usually occurs at or before dawn inland and in temperate coastal regions, but somewhat after dawn in tropical or subtropical coastal regions.

The afternoon maximum is due to convection produced by surface heating.

Surrounding regions show no such marked pattern.

### 1. Introduction

As far as can be determined, little attention has been given to the geographical distribution of summer diurnal rainfall patterns over east Asia. Among meteorologists a vague assumption exists that, inland, a single rainfall-pool occurs during the afternoon or early evening as a result of convection caused by intense surface heating, while on the coast the pattern tends to be more complex, with possibly a morning maximum, the cause of which is obscure.

Such a morning maximum occurs in Hong Kong, and is followed by a marked minimum in the evening (fig. 1). In the course of a general survey of summer forecasting over south China (Ramage, 1951), it was thought desirable to discover how far inland this assumed coastal effect extends. As was expected, Canton, 90 mi up the Pearl River from Hong Kong, showed both morning and afternoon maxima, the latter being larger. When, however, Hengyang, Changsha, Changteh and Wuchang, all more than 300 mi from the sea, were found to have double maxima as well, with the morning one as significant as Hong Kong's,

it became obvious that current ideas would have to be revised.

To discover, if possible, the limits of this region of morning maximum, all available hourly, three-hourly and four-hourly summer rainfall-averages for China, Korea, Japan and the surrounding islands were collected and plotted. As will be evident, significant patterns did appear, for which a possible explanation is suggested.

### 2. Data

In this investigation, summer is considered to be the months May to August, inclusive. Local standard time is used throughout.

Since few records of diurnal frequency of rainfall are available, the variation of rainfall amount was analyzed. For stations observing both hourly frequencies and amounts, curves plotted for both variables showed the same characteristics, although by using amounts the significance of the afternoon maximum at inland stations is slightly exaggerated.

The observations are of three kinds:

1. Hourly, made by first-class stations;
2. Three-hourly, made by second-class Chinese stations;
3. Four-hourly, made by second-class Japanese stations.

Whenever possible, at least five years of records were used (because of changes, not always the same five years), shorter periods being indicated by small numbers beside the stations concerned (fig. 2).

The effect of single, sharp heavy falls on the hourly values was minimized by using three-hourly running means.

In Hong Kong, a single daily mean maximum of rainfall occurs between 0800 and 1100, and is of an

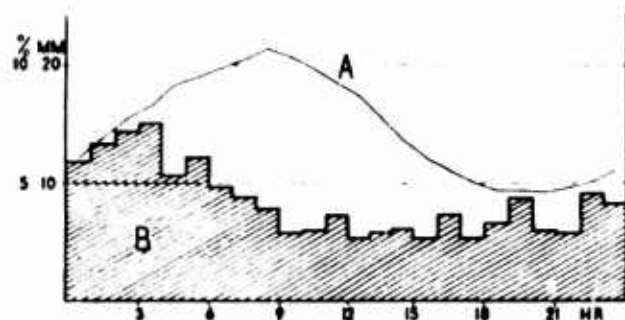


FIG. 1. A: diurnal variation of mean monthly summer rainfall at Hong Kong; B: percentage distribution of rain periods beginning in a given hour at Hong Kong.

amount 2.3 times that of the minimum (fig. 1). This is no mere statistical effect, but a real and noticeable feature of the to-day summer weather. On this basis, a station is considered to have a significant diurnal rainfall maximum if the value of the maximum is at least twice that of the lower minimum for hourly observations, and at least 1.9 times for three- and four-hourly observations. A less significant maximum is classified as having a value between 1.6 and 2.0 times the minimum for hourly, and between 1.5 and 1.9 times for three- or four-hourly observations. Stations with maximum/minimum ratios below these limits are classified as having no significant maximum. The factors for three- and four-hourly observations were deduced from plots of hourly, three-hourly and four-hourly values of stations observing hourly. As would be expected, curves are flatter for greater intervals.

In fig. 2, rainfall records are analyzed according to this classification, with a further distinction being made between morning and afternoon maxima. Noon and midnight conveniently divide the afternoon and early evening convective precipitation from precipitation initiated by nocturnal processes. Thus, for the purposes of the discussion, "morning" is defined as the 12 hr period from 0000 to 1200, and "afternoon" as that from 1200 to 2400.

### 3. Discussion

In fig. 2, certain broad geographical patterns of distribution are apparent.

- 1 *East China, the Yellow Sea coastline and Kyushu.* Significant morning maximum; significant afternoon maximum inland and at some coastal stations.
- 2 *Korea (excluding the west coast), Honshu and Shikoku.* Less significant morning maximum; less significant afternoon maximum inland.
- 3 *Manchuria and north Japan.* Little diurnal variation.
- 4 *Islands to the east and south of China and Japan.* Less significant variations, random pattern.
- 5 *Part of the east coast of Korea, southeast Honshu and northern Formosa.* Sub-areas with a greater tendency towards an afternoon maximum than their surroundings.

*Areas 1 and 2.* The stations in area 1, and to a less marked degree those in area 2 (except for sub-areas A and B, fig. 2), have a morning maximum of rainfall, irrespective of whether they are on the coast or inland. Since considerable doubt has been cast on the validity of the once popularly held concept that radiation from the top of a cloud layer at night increases the lapse rate and so promotes convection (Means, 1944), it is necessary to seek some other cause for this distribution. It seems reasonable to suppose that such uniformity springs from a large scale, persistent cause with limits probably coinciding with those of these areas. This immediately suggests the

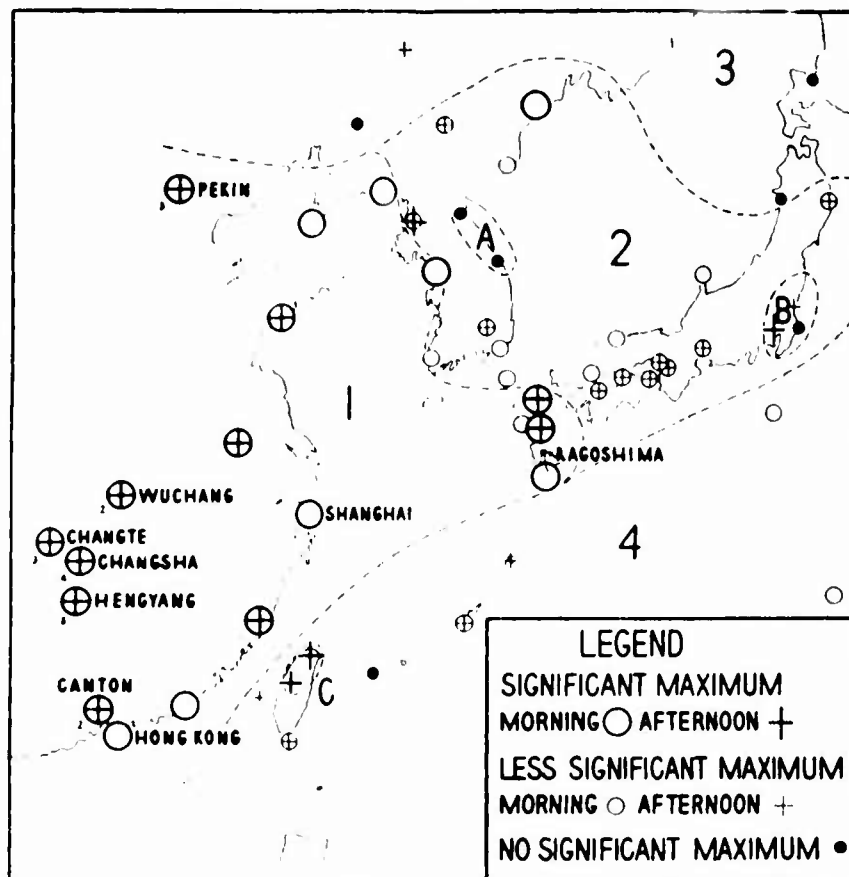


FIG. 2. Geographical distribution of various types of summer diurnal rainfall-patterns, together with stations mentioned in text.

dominating summer-monsoon of the region, particularly since distribution of diurnal-variation patterns for the other seasons was found to be completely haphazard. Significantly, 5000- and 10,000-ft daily flow charts for the Far East indicate that the boundary between areas 1 and 2 and area 4 lies in a transitional zone, with southerly or southwesterly monsoon to the north and the western portion of the North Pacific anticyclone to the south. There are, of course, day-to-day fluctuations, but the monsoon rarely extends as far as Formosa and the Loochoos, and when the Pacific high intensifies sufficiently to dominate south China and Japan, subsidence inhibits precipitation.

Bleeker and Andre (1951), discussing the nocturnal maximum of precipitation over the midwestern United States, aver that topography is important. They suggest that cooling and heating processes during the night and day, caused by the distribution of mountains and plains, set up a large-scale circulation system east of the Rockies, resulting in convergence over the plains at night and divergence during the day. Their argument is well developed and seems to account adequately for summer conditions. However, it would be equally applicable to other seasons when this particular geographical distribution of precipitation does not obtain.

Means (1944), dealing with the same topic, thinks that increased advection of warm air between 2000 and 8000 ft can result in nocturnal showers over the midwestern United States. Though producing no detailed argument, he considers that the western mountains and plateau region of America and the Arizona heat-low play a significant part in causing such advection. It is noteworthy that areas 1 and 2 occupy the same position relative to a more intense heat low and to the vast mountain and plateau expanse of west China and Tibet. To check the applicability of Means' theory to this region, upper-air soundings are necessary. Unfortunately, in area 1, where the morning maximum is most pronounced, data are available from only Hong Kong and Kagoshima. Despite the broken nature of the records, it appears that at both places advection of warm air below 10,000 ft occurs more frequently in the early morning than in the afternoon.

A heat low and the monsoon circulation it produces are of limited vertical extent and may, especially when turbulence is at a minimum, restrict warm-air advection to the lower layers. The fact that area 2, further from the main heat low than area 1, shows similar but less marked diurnal variations, supports this view. German meteorologists (*e.g.*, Sprung, 1885) have long recognized the trend towards night rains during the summer monsoon. More recently, Indian authors (Iyer and Dass, 1946; Iyer and Zafar, 1946; Narasimham and Zafar, 1947; Ramaswamy and Suryanarayana, 1950) have remarked that in their country the well-defined afternoon rainfall peak of the pre-monsoon hot period becomes very much less pronounced, or is even

replaced by a morning maximum (Ramaswamy and Suryanarayana, 1950) during the summer monsoon. For example, Narasimham and Zafar (1947), analyzing the rainfall of Poona, say:

The characteristic feature of the diurnal variation of rainfall is a marked increase in the afternoon hours of both the rainfall amounts and occasions of rainfall in all the months except July and August when the monsoon is strong.

The idea that the summer-monsoon circulation is the main contributory cause of the rain distribution observed in areas 1 and 2 is not inconsistent with Means' or with Bleeker and Andre's theories.

Comparison of fig. 4 (typical of the tropical or subtropical coastal stations of areas 1 and 2) with the corresponding curves for Omaha (Means, 1944) reveals that, although the percentage distributions of rain/thunderstorm periods beginning in a given hour for the two stations are significantly similar, maximum precipitation occurs 4 to 5 hr later at Hong Kong than at Omaha. Similarly, 10 of the 16 tropical and subtropical coastal stations of southeast China and south Japan have maxima between 0700 and 1000. On the other hand, none of the 21 other stations in areas 1 and 2 have maxima later than 0700, and 14 of them have pre-dawn maxima.

Braak (1924) and Palmer (1949) state that, in Indonesia and the Solomon Islands, a post-dawn increase in precipitation occurs along the coast, especially if the hinterland is rugged. Palmer gives the following explanation:

At night the land breeze causes the clouds to build offshore and particularly in the channels. A slight shift in the wind direction around dawn or even the sea breeze may bring the cloud inland producing morning showers along the coasts.

It is most unlikely, in view of the high frequency of rain periods commencing well before dawn, that this mechanism is the prime cause of the morning maximum in the coastal regions under consideration, but it is probable that onset of the sea-breeze convergence, occurring when the air is already unstable and highly charged with moisture, results in intensification of the rain and its prolongation for some time after the nocturnal effect has diminished.

Most probably, the afternoon maximum is due to normal convectional development as a result of intense surface-heating over land. The more marked maxima of area 1 relative to area 2 can thus be explained in terms of its greater continentality.

Near the coast, afternoon showers seem to form inland first and then drift seaward. For instance, when afternoon showers occur at Hong Kong, they fall from clouds which have drifted over from further inland. The base is usually above 5000 ft. The extremely irregular coast line of the colony makes detection of a surface sea-breeze component impossible, but nevertheless there must be a considerable landward flow

during the afternoon. Heywood (1938) found that, over the years 1933 to 1935 at Hong Kong, mean resultant winds at 5000 ft for the summer months showed increasing offshore direction between morning and afternoon as follows: May, 36°; June, 24°; July, 60°; August, 88°. These changes are sufficient, on most summer days, to replace a morning onshore by an afternoon offshore flow at 5000 ft. This probably happens along all the coasts of the two areas, and thus the upper level offshore component of the sea breeze circulation may be sufficiently marked, if conditions are favorable, to carry to the coast showers which have formed some distance inland as a result of afternoon convection. If this return drift does not develop sufficiently, then morning showers having once ceased, there is little chance of precipitation along the coast until the following morning.

From this discussion, a diurnal rainfall-variation model is suggested for areas 1 and 2.

1. Around midnight, when the turbulent effects of afternoon heating have died down, warm moist inflow tends to become channelled between the surface and the upper limit of the monsoon circulation. Instability and widespread steady vertical motion develop. Clouds form, usually in turbulent layers, and at this point radiational cooling from the tops may start and accelerate development. If the air above is conditionally unstable, occasional C break through and, if sufficient moisture is available, later C<sub>1</sub> and C<sub>2</sub> form rapidly. Rain sets in (see by D), often becoming continuous and widespread and usually reaching a maximum at or before dawn inland and in the north, but not until 3 or 4 hr after dawn along tropical or subtropical coasts.
2. With sunrise, the expanse of layered cloud absorbs radiation, stability spreads downwards, the cloud "burns off," and the rain diminishes.
3. *Inland.* After the cloud break, the surface heats rapidly and normal afternoon convection culminates in a second rainfall maximum between 1500 and 1900. After sunset, clouds disperse once more, and a second minimum occurs around midnight. *On the coast:* If no off-shore drift sets in, the cloud continues to dissipate throughout the afternoon, and rainfall reaches a minimum in early evening.

The dominant feature is the morning maximum. The afternoon maximum, although in places giving more rain, is an effect superimposed by location and topography.

*Area 3.* The diurnal variation is typical of temperate latitudes and requires no comment.

*Area 4.* The diurnal variation pattern is insignificant and confused. It has the same position relative to the North Pacific anticyclone as the southeastern United States to the North Atlantic anticyclone, and similarly demonstrates the small value of the nocturnal radiation theory as applied to tropical or subtropical oceans in general.

*Sub-area 5.* To the windward of each of these sub-areas lies a massive mountain barrier, effectively cutting off any moist warm air advection in the early

morning, but acting as an ideal source of afternoon showers which have little trouble moving seawards under the combined influence of the general flow and the upper returning sea-breeze component. It is obvious that a denser network of observations could well result in the discovery of other small, anomalous regions to the leeward of mountain ranges.

#### 4. Conclusions

1. The diurnal variation of summer rainfall over east China, Korea and Japan seems to be determined by the monsoonal circulation of the region. This probably results in increased nocturnal low-level advection of warm air which, combined with radiational cooling (and, on the coast, with the movement inshore of the sea-breeze convergence), produces a morning precipitation-maximum. An afternoon maximum develops inland in the normal way. The converse is not necessarily true, since morning maxima do occur in extra-monsoonal regions. It may be that in many of these cases (as Neumann (1951) has shown for the eastern Mediterranean) local topography is an important factor.

2. No explanation has been found for what must be a considerable diurnal variation in both the speed of flow and effectiveness of channelling of the warm air. Micro-synoptic investigations undertaken either in India or the United States may provide a solution.

3. Diurnal distribution over the sea areas to the south and east suggests that, although nocturnal radiation from cloud tops may assist in intensifying convection once started, a prior and dominating agency must operate to produce the initial instability and cloud cover.

*Acknowledgment.*—The writer wishes to record his appreciation of the helpful advice given him by Mr. L. Starbuck, Assistant Director of the Royal Observatory.

#### REFERENCES

- Bleeker, W., and M. J. Andre, 1951: On the diurnal variation of precipitation, particularly over central U. S. A. *Quart. J. r. meteor. Soc.*, **77**, 260-271.
- Braak, C., 1924: Het climat van Nederlandsch-Indie. *Kon. Mag. Meteor. Obs. Batavia*, **8**, 417-497.
- Heywood, G. S. P., 1938: *The diurnal variation of upper winds at Hong Kong*. Roy. Obs., Hong Kong. (Unpublished paper.)
- Iyer, V. D., and I. Dass, 1946: Diurnal variation of rainfall at Mahabulshwar. *India meteor. Dep., Sci. Notes*, **9**, 37-42.
- Iyer, V. D., and M. Zafar, 1946: Diurnal variation of rainfall at Simla. *India meteor. Dep., Sci. Notes*, **9**, 33-36.
- Means, L. L., 1944: The nocturnal maximum occurrence of thunderstorms in the midwestern states. *Dep. Meteor. Univ. Chicago, Misc. Rep.*, No. 16, 38 pp.
- Narasimham, V. L., and M. Zafar, 1947: An analysis of the hourly rainfall records at Poona. *India meteor. Dep., Sci. Notes*, **9**, 94-110.
- Neumann, J., 1951: Land breezes and nocturnal thunderstorms. *J. Meteor.*, **8**, 60-67.
- Palmer, C. E., 1949: Notes on tropical meteorology. *Tech. Bull. 2113rd Wea. Wing*, **1**, No. 2, 1-49.
- Ramage, C. S., 1951: Analysis and forecasting of summer weather over and in the neighborhood of south China. *J. Meteor.*, **8**, 289-299.
- Ramaswamy, C., and N. Suryanarayana, 1950: Rainfall at Peshawar. *Mem. India meteor. Dep.*, **28**, Part III, 121-137.
- Sprung, V., 1885: *Lehrbuch der Meteorologie*. Hamburg, Hoffmann und Campe, 407 pp.

## AIR FORCE SURVEYS IN GEOPHYSICS

- No. 1. (Classified Title), *W. K. Widger, Jr., Mar 1952. (SECRET/RESTRICTED DATA Report)*
- No. 2. Methods of Weather Presentation for Air Defense Operations (U), *W. K. Widger, Jr., Jun 1952. (CONFIDENTIAL Report)*
- No. 3. Some Aspects of Thermal Radiation From the Atomic Bomb (U), *R. M. Chapman, Jun 1952. (SECRET Report)*
- No. 4. Final Report on Project 8-52M-1 Tropopause (U), *S. Coroniti, Jul 1952. (SECRET Report)*
- No. 5. Infrared as a Means of Identification (U), *N. Oliver and J. W. Chamberlain, Jul 1952. (SECRET Report)*
- No. 6. Heights of Atomic Bomb Results Relative to Basic Thermal Effects Produced on the Ground (U), *R. M. Chapman and G. W. Wares, Jul 1952. (SECRET/RESTRICTED DATA Report)*
- No. 7. Peak Over-Pressure at Ground Zero From High Altitude Bursts (U), *N. A. Haskell, Jul 1952. (SECRET Report)*
- No. 8. Preliminary Data From Parachute Pressure Gauges, Operation Snapper. Project 1.1 Shots No. 5 and 8 (U), *N. A. Haskell, Jul 1952. (SECRET, RESTRICTED DATA Report)*
- No. 9. Determination of the Horizontal (U), *R. M. Chapman and M. H. Seavey, Sep 1952. (SECRET Report)*
- No. 10. Soil Stabilization Report, *C. Molineux, Sep 1952.*
- No. 11. Geodesy and Gravimetry, Preliminary Report (U), *R. J. Ford, Sep 1952. (SECRET Report)*
- No. 12. The Application of Weather Modification Techniques to Problems of Special Interest to the Strategic Air Command (U), *C. E. Anderson, Sep 1952. (SECRET Report)*
- No. 13. Efficiency of Precipitation as a Scavenger (U), *C. E. Anderson, Aug 1952. (SECRET/RESTRICTED DATA Report)*
- No. 14. Forecasting Diffusion in the Lower Layers of the Atmosphere (U), *B. Davidson, Sep 1952. (CONFIDENTIAL Report)*
- No. 15. Forecasting the Mountain Wave, *C. F. Jenkins, Sep 1952.*
- No. 16. A Preliminary Estimate of the Effect of Fog and Rain on the Peak Shock Pressure From an Atomic Bomb (U), *H. P. Gauvin and J. H. Healy, Sep 1952. (SECRET/RESTRICTED DATA Report)*
- No. 17. Operation Tumbler-Snapper Project 1.1A. Thermal Radiation Measurements With a Vacuum Capacitor Microphone (U), *M. O'Day, J. L. Bohn, F. H. Nadig and R. J. Cowie, Jr., Sep 1952. (CONFIDENTIAL/RESTRICTED DATA Report)*
- No. 18. Operation Snapper Project 1.1. The Measurement of Free Air Atomic Blast Pressures (U), *J. O. Vunn and N. A. Haskell, Sep 1952. (SECRET, RESTRICTED DATA Report)*
- No. 19. The Construction and Application of Contingency Tables in Weather Forecasting, *E. W. Wahl, R. M. White and H. A. Salmela, Nov 1952.*
- No. 20. Peak Overpressure in Air Due to a Deep Underwater Explosion (U), *N. A. Haskell, Nov 1952. (SECRET Report)*
- No. 21. Slant Visibility, *R. Penndorf, B. Goldberg and D. Lufkin, Dec 1952.*
- No. 22. Geodesy and Gravimetry (U), *R. J. Ford, Dec 1952. (SECRET Report)*
- No. 23. Weather Effects on Radar, *D. Atlas et al, Dec 1952.*
- No. 24. A Survey of Available Information on Winds Above 30,000 Ft., *C. F. Jenkins, Dec 1952.*
- No. 25. A Survey of Available Information on the Wind Fields Between the Surface and the Lower Stratosphere, *W. K. Widger, Jr., Dec 1952.*
- No. 26. (Classified Title), *A. L. Aden and L. Katz, Dec 1952. (SECRET Report)*
- No. 27. (Classified Title), *N. A. Haskell, Dec 1952 (SECRET Report)*
- No. 28. A-Bomb Thermal Radiation Damage Envelopes for Aircraft (U), *R. H. Chapman, G. W. Wares and M. H. Seavey, Dec 1952, (SECRET, RESTRICTED DATA Report)*
- No. 29. A Note on High Level Turbulence Encountered by a Glider, *J. Kuettnner, Dec 1952.*



AIR FORCE SURVEYS IN GEOPHYSICS (Continued)

- No. 30. Results of Controlled-Altitude Balloon Flights at 50,000 to 70,000 Feet During September 1952, *edited by L. O. Jung and R. A. Craig, Feb 1953.*
- No. 31. Conference: Weather Effects on Nuclear Detonations (U), *edited by B. Grossman, Feb 1953. (SECRET RESTRICTED DATA Report)*
- No. 32. Operation IVY Project 6.11. Free Air Atomic Blast Pressure and Thermal Measurements (U), *N. A. Haskell and P. R. Gast, Mar 1953. (SECRET RESTRICTED DATA Report)*
- No. 33. Variability of Subjective Cloud Observations - I, *A. M. Galligan, Mar 1953.*
- No. 34. Feasibility of Detecting Atmospheric Inversions by Electromagnetic Probing, *A. L. Aden, Mar 1953.*
- No. 35. Flight Aspects of the Mountain Wave, *C. F. Jenkins and J. Kuettnner, Apr 1953.*
- No. 36. Report on Particle Precipitation Measurements Performed During the Buster Tests at Nevada (U), *A. L. Purcell, Apr 1953. (SECRET RESTRICTED DATA Report)*
- No. 37. Critical Envelope Study for the XB-63, B-52A, and F-89 (U), *N. A. Haskell, R. M. Chapman and M. H. Seavey, Apr 1953. (SECRET Report)*
- No. 38. Notes on the Prediction of Overpressures From Very Large Thermo-Nuclear Bombs (U), *N. A. Haskell, Apr 1953. (SECRET Report)*
- No. 39. Atmospheric Attenuation of Infrared Oxygen 3-Mergerlow Emission (U), *N. J. Oliver and J. W. Chamberlain, Apr 1953. (SECRET Report)*
- No. 40. (Classified Title), *R. E. Hanson, May 1953. (SECRET Report)*
- No. 41. The Silent Area Forecasting Problem (U), *W. K. Widger, Jr., May 1953. (SECRET Report)*
- No. 42. An Analysis of the Contrail Problem (U), *R. A. Craig, Jun 1953. (CONFIDENTIAL Report)*
- No. 43. Sodium in the Upper Atmosphere, *L. E. Miller, Jun 1953.*
- No. 44. Silver Iodide Diffusion Experiments Conducted at Camp Wellfleet, Mass., During July-August 1952, *P. Goldberg et al, Jun 1953.*
- No. 45. The Vertical Distribution of Water Vapor in the Stratosphere and the Upper Atmosphere, *L. E. Miller, Sep 1953.*
- No. 46. Operation IVY Project 6.11. (Final Report). Free Air Atomic Blast Pressure and Thermal Measurements (U), *N. A. Haskell, J. O. Vann and P. R. Gast, Sep 1953 (SECRET/RESTRICTED DATA Report)*
- No. 47. Critical Envelope Study for the B61-A (U), *N. A. Haskell, R. M. Chapman and M. H. Seavey, Sep 1953. (SECRET Report)*
- No. 48. Operation Upshot-Knothole Project L3. Free Air Atomic Blast Pressure Measurements. Revised Report (U), *N. A. Haskell and R. M. Brubaker, Nov 1953. (SECRET/RESTRICTED DATA Report)*
- No. 49. Maximum Humidity in Engineering Design, *N. Sissenevine, Oct 1953.*
- No. 50. Probable Ice Island Locations in the Arctic Basin, January 1954, *A. P. Crary and I. Browne, May 1954.*
- No. 51. Investigation of TRAC for Active Air Defense Purposes (U), *G. W. Wares, R. Penndorf, V. G. Plank and B. H. Grossman, Dec 1953. (SECRET RESTRICTED DATA Report)*
- No. 52. Radio Noise Emissions During Thermonuclear Reactions (U), *T. J. Keneshea, Jun 1954. (CONFIDENTIAL Report)*
- No. 53. A Method of Correcting Tabulated Rawinsonde Wind Speeds for Curvature of the Earth, *R. Leviton, Jun 1954.*
- No. 54. A Proposed Radar Storm Warning Service For Army Combat Operations, *M. G. H. Ligda, Aug 1954.*
- No. 55. A Comparison of Altitude Corrections for Blast Overpressure (U), *N. A. Haskell, Sep 1954. (SECRET Report)*
- No. 56. Attenuating Effects of Atmospheric Liquid Water on Peak Overpressures from Blast Waves (U), *H. P. Gauvin, J. H. Healy and M. A. Bennett, Oct 1954. (SECRET Report)*

AIR FORCE SURVEYS IN GEOPHYSICS (Continued)

- No. 57. Windspeed Profile, Windshear, and Gusts for Design of Guidance Systems for Vertical Rising Air Vehicles, *N. Sissenwine, Nov 1954.*
- No. 58. The Suppression of Aircraft Exhaust Trails, *C. E. Anderson, Nov 1954.*
- No. 59. Preliminary Report on the Attenuation of Thermal Radiation From Atomic or Thermonuclear Weapons (U), *R. M. Chapman and M. H. Seavey, Nov 1954. (SECRET RESTRICTED DATA Report)*
- No. 60. Height Errors in a Rawin System, *R. Leviton, Dec 1954.*
- No. 61. Meteorological Aspects of Constant Level Balloon Operations (U), *B. K. Widger, Jr. et al, Dec 1954. (SECRET Report)*
- No. 62. Variations in Geometric Height of 30 to 60 Thousand Foot Pressure-Altitudes (U), *N. Sissenwine, A. E. Cole and W. Baginsky, Dec 1954. (CONFIDENTIAL Report)*
- No. 63. Review of Time and Space Wind Fluctuations Applicable to Conventional Ballistic Determinations, *W. Baginsky, N. Sissenwine, B. Davidson and H. Lettau, Dec 1954.*
- No. 64. Cloudiness Above 20,000 Feet for Certain Stellar Navigation Problems (U), *A. E. Cole, Jan 1955. (SECRET Report)*
- No. 65. The Feasibility of the Identification of Hail and Severe Storms, *D. Atlas and R. Donaldson, Jan 1955.*
- No. 66. Rate of Rainfall Frequencies Over Selected Air Routes and Destinations (U), *A. E. Cole and N. Sissenwine, Mar 1955. (SECRET Report)*
- No. 67. Some Considerations on the Modeling of Cratering Phenomena in Earth (U), *N. A. Haskell, Apr 1955. (SECRET RESTRICTED DATA Report)*
- No. 68. The Preparation of Extended Forecasts of the Pressure Height Distribution in the Free Atmosphere Over North America by Use of Empirical Influence Functions, *R. M. White, May 1955.*
- No. 69. Cold Weather Effect on B-62 Launching Personnel (U), *N. Sissenwine, Jun 1955. (SECRET Report)*
- No. 70. Atmospheric Pressure Pulse Measurements, Operation Castle (U), *E. A. Flauraud, Aug 1955. (SECRET/RESTRICTED DATA Report)*
- No. 71. Refraction of Shock Waves in the Atmosphere (U), *N. A. Haskell, Aug 1955. (SECRET Report)*
- No. 72. Wind Variability as a Function of Time at Muroc, California, *B. Singer, Sep 1955.*
- No. 73. The Atmosphere, *N. C. Gerson, Sep 1955.*
- No. 74. Areal Variation of Ceiling Height (U), *W. Baginsky and A. E. Cole, Oct 1955. (CONFIDENTIAL Report)*
- No. 75. An Objective System for Preparing Operational Weather Forecasts, *I. A. Lund and E. W. Wahl, Nov 1955.*
- No. 76. The Practical Aspects of Tropical Meteorology, *C. E. Palmer, C. W. Wise, L. J. Stempson and G. H. Duncan, Sep 1955.*
- No. 77. Remote Determination of Soil Trafficability by Aerial Penetrometer, *C. Molineux, Oct 1955.*
- No. 78. Effects of the Primary Cosmic Radiation on Matter, *H. O. Curtis, Jan 1956.*
- No. 79. Tropospheric Variations of Refractive Index at Microwave Frequencies, *C. F. Campen and A. E. Cole, Oct 1955.*
- No. 80. A Program to Test Skill in Terminal Forecasting, *I. I. Gringorten, I. A. Lund and M. A. Miller, Jun 1955.*
- No. 81. Extreme Atmospheres and Ballistic Densities, *N. Sissenwine and A. E. Cole, Jul 1955.*
- No. 82. Rotational Frequencies and Absorption Coefficients of Atmospheric Gases, *S. N. Ghosh and H. D. Edwards, Mar 1956.*
- No. 83. Ionospheric Effects on Positioning of Vehicles at High Altitudes, *W. Pfister and T. J. Keneshea, Mar 1956.*
- No. 84. Pre-Trough Winter Precipitation Forecasting, *P. W. Funke, Feb 1957.*

AIR FORCE SURVEYS IN GEOPHYSICS (Continued)

- No. 85. Geomagnetic Field Extrapolation Techniques — An Evaluation of the Poisson Integral for a Plane (U), *J. I. McClay and P. Fougere, Feb 1957. (SECRET Report)*
- No. 86. The ARDC Model Atmosphere, 1956, *R. A. Minzner and W. S. Ripley, Dec 1956.*
- No. 87. An Estimate of the Maximum Range of Detectability of Seismic Signals, *A. A. Haskell, Mar 1957.*
- No. 88. Some Concepts for Predicting Nuclear Crater Size (U), *F. A. Crowley, Feb 1957. (SECRET RESTRICTED DATA Report)*
- No. 89. Upper Wind Representation and Flight Planning, *I. I. Gringorten, Mar 1957*
- No. 90. Reflection of Point Source Radiation From a Lambert Plane Onto a Plane Receiver, *A. W. Guess, Jul 1957.*
- No. 91. The Variations of Atmospheric Transmissivity and Cloud Height at Newark, *T. O. Haig, and W. C. Morton, III, Jan 1958.*
- No. 92. Collection of Aeromagnetic Information For Guidance and Navigation (U), *R. Hutchinson, B. Shuman, R. Brereton and J. McClay, Aug 1957. (SECRET Report)*
- No. 93. The Accuracy of Wind Determination From the Track of a Falling Object, *V. Lally and R. Leviton, Mar 1958.*
- No. 94. Estimating Soil Moisture and Tractionability Conditions for Strategic Planning (U), Part 1 - General method, and Part 2 - Applications and interpretations, *C. W. Thornthwaite, J. R. Mather, D. B. Carter and C. E. Molineux, Mar 1958 (Unclassified Report)*. Part 3 - Average soil moisture and tractionability conditions in Poland (U), *D. B. Carter and C. E. Molineux, Aug 1958 (CONFIDENTIAL Report)*. Part 4 - Average soil moisture and tractionability conditions in Yugoslavia (U), *D. B. Carter and C. E. Molineux, Mar 1959 (CONFIDENTIAL Report)*
- No. 95. Wind Speeds at 50,000 to 1000,000 Feet and a Related Balloon Platform Design Problem (U), *N. Dvoskin and N. Sissenuwine, Jul 1957. (SECRET Report)*
- No. 96. Development of Missile Design Wind Profiles for Patrick AFB, *N. Sissenuwine, Mar 1958.*
- No. 97. Cloud Base Detection by Airborne Radar, *R. J. Donaldson, Jr., Mar 1958.*
- No. 98. Mean Free Air Gravity Anomalies, Geoid Contour Curves, and the Average Deflections of the Vertical (U), *W. A. Heiskanen, U. A. Uotila and O. W. Williams, Mar 1958. (CONFIDENTIAL Report)*
- No. 99. Evaluation of AN GMD-2 Wind Shear Data for Development of Missile Design Criteria, *N. Dvoskin and N. Sissenuwine, Apr 1958.*
- No.100. A Phenomenological Theory of the Scaling of Fireball Minimum Radiant Intensity with Yield and Altitude (U), *H. K. Sen, Apr 1958. (SECRET Report)*
- No.101. Evaluation of Satellite Observing Network for Project "Space Track", *G. R. Miczaika and H. O. Curtis, Jun 1958.*
- No.102. An Operational System to Measure, Compute, and Present Approach Visibility Information, *T. O. Haig and W. C. Morton, III, Jun 1958.*
- No.103. Hazards of Lightning Discharge to Aircraft, *G. A. Faucher and H. O. Curtis, Aug 1958.*
- No.104. Contrail Prediction and Prevention (U), *C. S. Downie, C. E. Anderson, S. J. Birstein and B. A. Silverman, Aug 1958. (SECRET Report)*
- No.105. Methods of Artificial Fog Dispersal and Their Evaluation, *C. E. Junge, Sep 1958.*
- No.106. Thermal Techniques for Dissipating Fog From Aircraft Runways, *C. S. Downie and R. B. Smith, Sep 1958.*
- No.107. Accuracy of RDF Position Fixes in Tracking Constant-Level Balloons, *K. C. Giles and R. E. Peterson, edited by W. K. Widger, Jr., Oct 1958.*
- No.108. The Effect of Wind Errors on SAGE-Guided Intercepts (U), *E. M. Darling, Jr. and C. D. Kern, Oct 1958 (CONFIDENTIAL Report)*
- No.109. Behavior of Atmospheric Density Profiles, *N. Sissenuwine, W. S. Ripley and A. E. Cole, Dec 1958.*

AIR FORCE SURVEYS IN GEOPHYSICS (Continued)

- No.110. Magnetic Determination of Space Vehicle Attitude (U), J. F. McClay and P. L. Longene, Mar 1959. (SECRET Report)
- No.111. Final Report on Exhaust Trail Physics: Project 7630, Task 76303 (U), M. W. M. Senna, and H. O. Curtis, Jul 1959. (SECRET Report)
- No.112. Accuracy of Mean Monthly Geostrophic Wind Vectors as a Function of Station Network Density, H. A. Salmela, Jun 1959.
- No.113. An Estimate of the Strength of the Acoustic Signal Generated by an ICBM Noise Cone Reentry (U), V. A. Haskell, Aug 1959. (CONFIDENTIAL Report)
- No.114. The Role of Radiation in Shock Propagation with Applications to Vertical and Yield Scaling of Nuclear Fireballs (U), H. K. Sen and E. W. Guess, Sep 1959. (SECRET Report)
- No.115. ARDC Model Atmosphere, 1959, R. A. Manabe, K. S. B. Chandra, and F. L. Brant, Dec 1959.
- No.116. Refinements in Utilization of Contour Charts for Climatologically Significant Areas, P. L. Cole, Oct 1959.
- No.117. Design Wind Profiles From Japanese Relay Sounding Data, V. S. Sankaranarayanan, and H. A. Salmela, Dec 1959.
- No.118. Military Applications of Supercooled Cloud and Fog Dissipation, G. S. Silverman, Dec 1959.
- No.119. Factor Analysis and Stepwise Regression Applied to the 24-Hour Prediction of 500-mb Winds, Temperatures, and Heights Over a Silent Area (U), E. J. Aubert, L. A. Fiedler, J. Thomason, Jr., and J. J. Pazniokas, Feb 1960. (CONFIDENTIAL Report)
- No.120. An Estimate of Precipitable Water Along High-Altitude Ray Paths, Meteor. Centre, Mar 1960.
- No.121. Analyzing and Forecasting Meteorological Conditions in the Upper Troposphere and Lower Stratosphere, R. M. Endlich and G. S. McLean, Apr 1960.
- No.122. Analysis and Prediction of the 500-mb Surface in a Silent Area, (U), E. J. Aubert, May 1960. (CONFIDENTIAL Report).
- No.123. A Diffusion-Deposition Model for In-Flight Release of Fission Fragments, M. L. Boral, D. A. Hagen, and J. J. Fuquay, Jun 1960.
- No.124. Research and Development in the Field of Geodetic Science, C. E. Fung, (to be published).
- No.125. Extreme Value Statistics -- A Method of Application, L. I. Gringorten, (to be published).